Spinor Bose Gases in Cubic Optical Lattice

im Fachbereich Physik der

Freien Universität Berlin

eingereichte Dissertation

von

Mohamed Saidan Sayed Mohamed Mobarak

Dezember 2013

Die in vorliegender Dissertation dargestellte Arbeit wurde in der Zeit zwischen Dezember 2009 und Dezember 2013 im Fachbereich Physik an der Freien Universität Berlin unter Betreuung von Prof. Dr. Dr. h.c. mult. Hagen Kleinert und Priv.-Doz. Dr. Axel Pelster durchgeführt.

Erstgutachter: Prof. Dr. Dr. h.c. mult. Hagen Kleinert

Zweitgutachter: Priv.-Doz. Dr. Axel Pelster

Abgabe: 5.12.2013
Disputation: 27.1.2014

Abstract

In recent years the quantum simulation of condensed-matter physics problems has resulted from exciting experimental progress in the realm of ultracold atoms and molecules in optical lattices. In this thesis we analyze theoretically a spinor Bose gas loaded into a three-dimensional cubic optical lattice. In order to account for different superfluid phases of spin-1 bosons with a linear Zeeman effect, we work out a Ginzburg-Landau theory for the underlying spin-1 Bose-Hubbard model. To this end we add artificial symmetry-breaking currents to the spin-1 Bose-Hubbard Hamiltonian in order to break the global $U(1)$ symmetry. With this we determine a diagrammatic expansion of the grand-canonical free energy up to fourth order in the symmetry-breaking currents and up to the leading non-trivial order in the hopping strength which is of first order. As a cross-check we demonstrate that the resulting grand-canonical free energy allows to recover the mean-field theory. Applying a Legendre transformation to the grand-canonical free energy, where the symmetry-breaking currents are transformed to order parameters, we obtain the effective Ginzburg-Landau action. With this we calculate in detail at zero temperature the Mott insulator-superfluid quantum phase boundary as well as condensate and particle number density in the superfluid phase.

We find that both mean-field and Ginzburg-Landau theory yield the same quantum phase transition between the Mott insulator and superfluid phases, but the range of validity of the mean-field theory turns out to be smaller than that of the Ginzburg-Landau theory. Due to this finding we expect that the Ginzburg-Landau theory gives better results for the superfluid phase and, thus, we restrict ourselves to extremize only the effective Ginzburg-Landau action with respect to the order parameters. Without external magnetic field the superfluid phase is a polar (ferromagnetic) state for anti-ferromagnetic (ferromagnetic) interactions, i.e. only the hyperfine spin 0 (1) is macroscopically occupied, in accordance with previous mean-field results. On the other hand, in the presence of the external magnetic field for ferromagnetic interaction, the superfluid phase does not change as the minimization of the energy implies the maximal spin value. However, when an anti-ferromagnetic interaction competes with the linear Zeeman effect, we can distinguish various ferromagnetic and anti-ferromagnetic superfluid phases within the range of validity of the Ginzburg-Landau theory. Increasing the external magnetic field yields a breaking of spin singlet pairs and a subsequent alignment of spins, thus anti-ferromagnetic phases decrease until only a ferromagnetic superfluid phase prevails. In addition, we find that the superfluid-Mott insulator phase transition is always of second order for both ferromagnetic and anti-ferromagnetic interactions. However, the transitions between different superfluid phases for an anti-ferromagnetic interaction can be both of first and second order depending on whether the respective macroscopic occupation of hyperfine spin states changes discontinuously or continuously.

The established Ginzburg-Landau theory for spin-1 bosons in optical lattices will certainly be the basis for many further applications as, for instance, time-of-flight absorption pictures or collective excitations, which are of experimental importance.

Kurzzusammenfassung

In den letzten Jahren ist die Quantensimulation von Problemen der Physik der kondensierten Materie aus spannenden experimentellen Fortschritten auf dem Gebiet der ultrakalten Atome und Moleküle in optischen Gittern hervorgegangen. In dieser Arbeit untersuchen wir theoretisch ein Spinor-Bose-Gas, das in ein dreidimensionales kubisches optisches Gitter geladen wird. Um die verschiedenen superfluiden Phasen von Spin-1 Bosonen mit linearem Zeeman-Effekt zu untersuchen, erarbeiten wir eine Ginzburg-Landau-Theorie für das zu Grunde liegende Spin-1 Bose-Hubbard-Modell. Zu diesem Zweck fügen wir künstliche symmetriebrechende Ströme zum Spin-1 Bose-Hubbard-Hamiltonian, um die globale U(1)-Symmetrie zu brechen. Dann bestimmen wir eine diagrammatische Entwicklung der großkanonischen freien Energie bis zur vierten Ordnung in den symmetriebrechenden Strömen und bis zu der führenden nicht-trivialen Ordnung im Tunnelmatrixelement, die von erster Ordnung ist. Zur Kontrolle zeigen wir, dass die resultierende großkanonische freie Energie in der Lage ist, die Molekularfeld-Theorie zu reproduzieren. Eine Legendre-Transformation der großkanonischen freien Energie, wo die symmetriebrechenden Ströme in Ordnungsparameter umgewandelt werden, führt auf die effektive Ginzburg-Landau-Wirkung. Damit berechnen wir im Detail am absoluten Temperaturnullpunkt die Mott-Isolator-Superfluid-Quantenphasengrenze sowie Kondensat- und Teilchenzahldichte in der superfluiden Phase.

Wir finden, dass sowohl Molekularfeld- als auch Ginzburg-Landau-Theorie denselben Quantenphasenübergang zwischen Mott-Isolator und superfluider Phasen erhalten, aber der Gültigkeitsbereich der Molekularfeld-Theorie stellt sich als kleiner als der der Ginzburg-Landau-Theorie heraus. Aufgrund dieser Erkenntnis erwarten wir, dass die Ginzburg-Landau-Theorie zu besseren Ergebnissen in der superfluiden Phase führen wird und beschränken uns daher darauf, die effektive Ginzburg-Landau Wirkung bezüglich der Ordnungsparameter zu extremalisieren. Ohne äußeres Magnetfeld ist die superfluide Phase ein polarer (ferromagnetischer) Zustand für anti-ferromagnetische (ferromagnetische) Wechselwirkung, d.h. nur der Hyperfeinspin 0 (1) ist makroskopisch besetzt in Übereinstimmung mit früheren Molekularfeld-Ergebnissen. In der Anwesenheit des externen Magnetfeldes für ferromagnetische Wechselwirkung ändert sich die superfluide Phase nicht, da eine Minimierung der Energie zu einem maximalen Spin führt. Wenn jedoch eine anti-ferromagnetische Wechselwirkung mit dem linearen Zeeman-Effekt konkurriert, können wir verschiedene ferromagnetische und anti-ferromagnetische superfluide Phasen im Gültigkeitbereich der Ginzburg-Landau-Theorie unterscheiden. Eine Erhöhung des externen Magnetfeldes bricht Singulett-Paare auf und führt anschließend zu einer Ausrichtung der Spins, also verringern sich die anti-ferromagnetischen Phasen, bis nur noch eine ferromagnetische superfluide Phase übrig bleibt. Darüber hinaus finden wir, dass der Superfluid-Mott-Isolator Phasenübergang sowohl für ferromagnetische als auch für anti-ferromagnetische Wechselwirkungen von zweiter Ordnung ist. Jedoch können die Übergänge zwischen verschiedenen superfluiden Phasen für eine anti-ferromagnetische Wechselwirkung sowohl von erster als auch von zweiter Ordnung sein,

abhängig davon, ob sich die jeweilige makroskopische Besetzung von Hyperfeinspin-Zuständen diskontinuierlich oder kontinuierlich ändert.

Die etablierte Ginzburg-Landau-Theorie für Spin-1-Bosonen in optischen Gittern wird sicherlich die Grundlage für viele weitere Anwendungen sein, wie zum Beispiel Flugzeit-Absorptionsbilder oder kollektive Anregungen, die von experimenteller Bedeutung sind.

Selbstständigkeitserklärung

Hiermit versichere ich, die vorliegende Arbeit ohne unzulässige Hilfe Dritter und ohne Benutzung anderer als der angegebenen Hilfsmittel angefertigt zu haben. Die aus fremden Quellen direkt oder indirekt übernommenen Gedanken sind als solche kenntlich gemacht. Die Arbeit wurde bisher weder im In- noch im Ausland in gleicher oder ähnlicher Form einer anderen Prüfungsbehörde vorgelegt.

Berlin, 5.12.2013

Mohamed Saidan Sayed Mohamed Mobarak

Contents

1. Introduction

The observation of Bose-Einstein condensation (BEC) started in 1995 by its first experimental realization in dilute atomic gases which opened a new era in the study of many-body quantum physics and was, thus, honored with the Nobel prize in 2001. This experimental demonstration produced by the group of Cornell and Wieman as well as that of Ketterle, achieved BEC of dilute gases of alkali metal atoms by using lasers and magnetic fields.

In this chapter, we present a brief summary of the history, recent experiments, and the theoretical description of Bose-Einstein condensation. Furthermore, we study Bose gases in optical lattices.

1.1. History of Bose Einstein Condensation

In three dimensions all identical atoms are either fermions or bosons, i.e. they are characterized by half-integer or integer spin. Fermions obey the Fermi-Dirac statistics which includes the Pauli exclusion principle that the two identical fermions cannot occupy the same quantum state. On the other hand, bosons obey the Bose-Einstein statistics where they can collapse into the same quantum ground state in order to form a Bose-Einstein condensate. In 1925 Einstein [1] predicted this phenomenon by extending the original work of Bose for photons [2] to massive particles. At a critical temperature, Einstein predicted that a macroscopic particle number of an ideal gas condenses into a single quantum state of lowest energy. The mean occupation number of atoms in quantum state s with the energy ϵ_s in equilibrium at temperature T is given by Bose-Einstein distribution:

$$n_s = \frac{1}{e^{\beta(\epsilon_s-\mu)}-1}, \tag{1.1}$$

where μ denotes the chemical potential, $\beta = 1/(k_{\mathrm{B}}T)$ represents the reciprocal temperature, and k_{B} is the Boltzmann constant. Once a macroscopic number of particles occupies the ground state, the phase transition to a Bose-Einstein condensate has happened, which is characterized by a "giant matter wave". The occurrence of this phase transition can be described by the de Broglie wavelength

$$\lambda_{\mathrm{dB}} = \sqrt{\frac{2\pi\hbar^2}{mk_{\mathrm{B}}T}}, \tag{1.2}$$

where $\hbar$ is Planck's constant and m is the atomic mass. At room temperature the inter-particle distance of the atoms, which is of order of $n^{-1/3}$, is much greater than the de Broglie wavelength λ_{dB}, where n denotes the particle density. When the temperature of the gas decreases, but is still larger than the critical temperature, the atoms of the gas represent "wave packets" with the extension λ_{dB}. If the temperature equals the critical temperature, the atomic wave functions begin to overlap i.e. the thermal de Broglie wavelength equals the inter-particle distance of the atoms and a Bose-Einstein

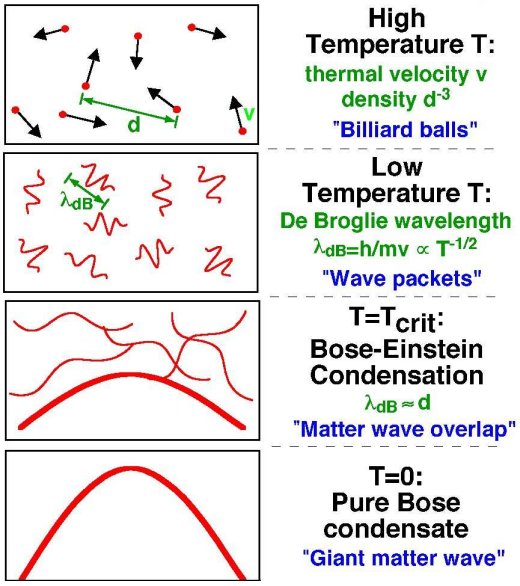

Figure 1.1.: Occurrence of Bose-Einstein condensation [3]. At high temperature, the atoms of the gas behave like point particles (top). When the temperature is decreased, the wave nature of the particles is clearer visible. When the critical temperature of BEC is reached, the atomic wave functions overlap and the de Broglie wavelength (1.2) equals the average distance $d = n^{-1/3}$ between the atoms. When the temperature is nearly close to zero, a pure Bose condensate is obtained.

condensate forms as shown in Fig. 1.1. When the temperature is lowered near to zero, all individual atomic wave functions form a single macroscopic matter wave. However, in order to get BEC, the phase space density of the gas $\rho = n\lambda_{\mathrm{dB}}^3$ should be one.

In 1938 Kapitza [4] as well as Allen and Misener [5] discovered the superfluidity in liquid helium. In the same year, London showed the connection between Bose-Einstein condensation and the phenomenon of superfluidity in ^{4}He, despite the strong interactions in this system [6]. Tisza, initiated by London, came up with the two-fluid model, which describes the character of liquid helium by two parts, a normal component, that moves with friction, and a superfluid component that moves without friction, where the superfluid component is interpreted in terms of Bose condensed ^{4}He atoms [7]. The model was further developed by Landau based on the novel idea of "weakly interacting quasi-particles" [8]. In 1947 Bogoliubov suggested a microscopic theory of superfluidity in terms of a weakly interacting Bose gas [9]. He explained the effect of the interaction between bosons upon the properties of a Bose gas in terms of Landau quasi-particles with a characteristic excitation spectrum. Nonetheless, further theoretical progress was achieved by Penrose and Onsager in 1956 [10], who showed that Bose-Einstein condensation is related to the existence of off-diagonal long-range order in the single-particle density matrix. The equation of motion for the macroscopic wave function of the condensate atoms, which defines the mean-field order parameter, was independently deduced by both Gross [11] and Pitaevskii [12]. This Gross-Pitaevskii equation played a principal role to describe a pure Bose-Einstein condensate at temperatures near absolute zero.

It took 75 years since the theoretical prediction of Bose-Einstein condensate before its experimental realization was achieved in 1995 by Cornell, Wiemann at JILA [20] in a rubidium vapor and by Ketterle

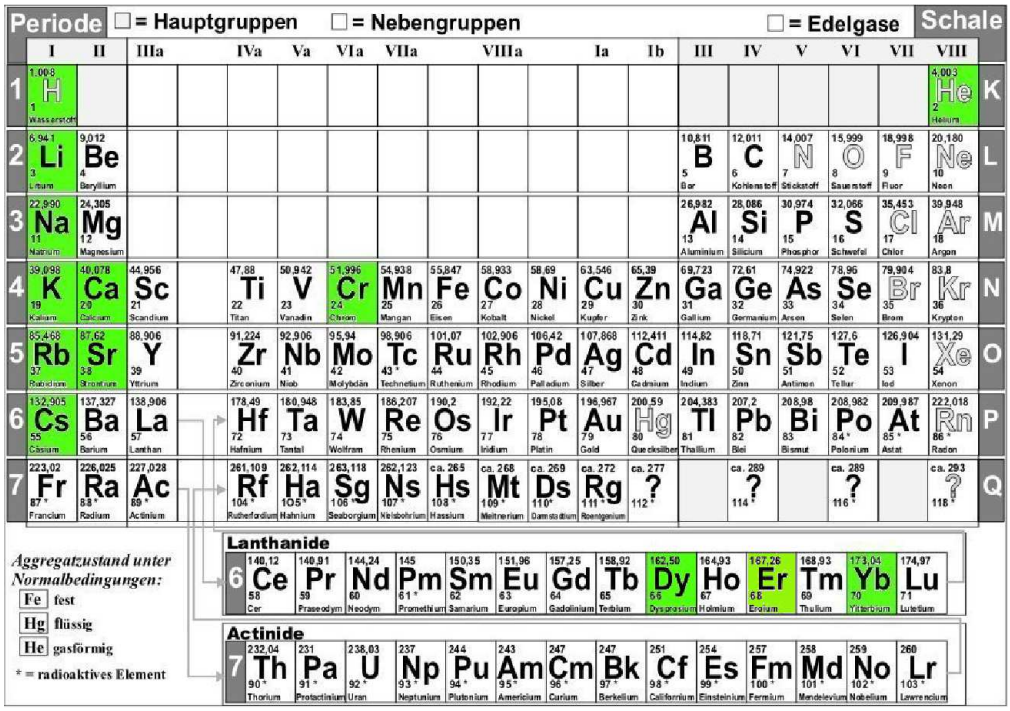

Figure 1.2.: Periodic table where all elements, which are high-lighted in green, have been Bose-Einstein condensed.

at MIT [13] in a sodium vapor by using the advances made in laser cooling techniques. The reason for this long period lies in the experimental difficulty to cool down the atoms to temperatures in the nK regime and to catch them in a trap. These experiments use a magneto-optical trap (MOT), where a particular arrangement of laser beams and magnetic fields allows to cool the atoms in order to produce samples of cold, trapped, neutral atoms at micro-Kelvin temperatures using laser cooling techniques [14]. Then, these atoms are transferred to a magnetic trap in order to cool them at nano-Kelvin temperatures using evaporative cooling [15]. Finally, we mention that Bose-Einstein condensates have so far been produced with thirteen chemical elements as shown in the periodic table of Fig. 1.2. The first column in the periodic table includes hydrogen [16], lithium [17], sodium [13], potassium [18], rubidium [19, 20], and cesium [21]. Bose-Einstein condensation for rare-earth element like ytterbium atoms in optical trap is done in 2003 [22]. In 2009 Bose-Einstein condensation was achieved for the alkaline earth metals calcium [23] and strontium [24, 25]. Bose-Einstein condensation in a dilute gas of helium was observed in 2001 [26, 27]. Furthermore, strong dipolar BECs were observed in chromium [28], erbium [29], and dysprosium [30].

1.2. Ultracold Spinor Atomic Gases

Spinor ultracold gases are those comprised of atoms with non-zero internal angular momentum, where all orientations of the atomic spin may be realized. The Zeeman hyperfine energy levels are described by the total atomic angular momentum F which is the sum of nuclear I and electronic angular momenta J, where the latter is the sum of the orbital angular momentum L and the spin of the outer electrons S. Each ground-state subspace is defined by manifolds of Zeeman states which are charcterized by

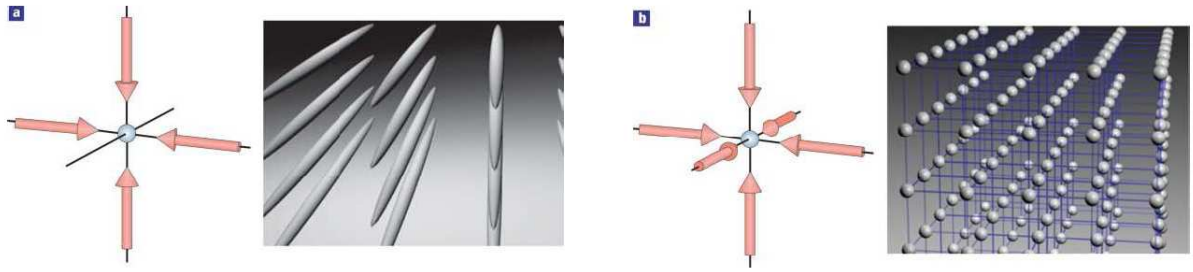

Figure 1.3.: Counter-propagating laser beams produce an optical lattice in two (**a**) or three (**b**) dimensions [55].

$\{|F, m_F\rangle\}$, where m_F is the magnetic quantum number which can take values from $-F$ to F [31].

Spinor condensates, which are Bose-Einstein condensates with atomic spin internal degrees of freedom, allow to study the magnetization in the quantum gas. The first theoretical discussion of a BEC with spin degrees of freedom was performed in Refs. [32, 33]. There the Hamiltonian of a spinor Bose-Einstein condensate and the mean-field condensate wave function were determined. This ansatz was verified experimentally by the Ketterle group by studying the ground state of the spin-1 system consisting of ^{23}Na atoms [34]. Furthermore, the MIT group succeeded to transfer a spin-polarized ^{23}Na condensate, which was produced in a traditional magneto-optical trap in one hyperfine state, into a dipole trap formed by the focus of a far-off-resonant laser [35]. Such an optical lattice confines neutral atoms due to the interaction between the electric field of the laser light and the induced electric dipole moment of the atoms. Therefore, in contrast to the magneto-optical trap, a dipole trap allows to trap the atoms in all hyperfine spin states [36]. With this, spinor condensates opened a new area to study various aspects of the quantum magnetism such as spin dynamics [37–40], spin waves [41, 42], or spin mixing [43, 44]. These examples result from coherent collisional processes between two atoms, where the total magnetization is constant but the spins of the individual particles can change.

1.3. Optical Lattice

An optical lattice is a periodic potential produced by the interference of counter-propagating laser beams. Its realization has opened a new era in atomic physics in the context of atom diffraction [45, 46]. Hemmerich et al. [47–49] and Grynberg et al. [50] have succeeded in cooling the atoms to the micro-Kelvin regime in a two and three-dimensional optical lattices. Before the production of BEC, the band structure in the optical lattice played a principal role in the gases under the effect of external forces which induce non-adiabatic transitions between Bloch bands at micro-Kelvin temperature where Landau-Zener tunneling is achieved [51, 52]. Anderson and Kasevich observed Bose-Einstein condensates, Bloch oscillation and Landau-Zener tunneling between different energy bands in an optical lattice by using the gravitational force of the earth on a vertically oriented lattice in one-dimension [53]. Afterwards, Josephson junction arrays and Josephson oscillations were achieved with a Bose-Einstein condensate [54].

The advantages of optical lattices are the following. Firstly, the height of the lattice can be used to control the strength of atom-atom interactions by changing the intensity of the laser field. However, using a Feshbach resonance the interaction strength, symmetry and sign for repulsive or attractive can be changed without modifying the lattice height [56]. Secondly, lattice site filling factor and lattice geometry has been controlled. Thirdly, the dimension of the quantum gas can be changed from 3D to 1D or 2D in an optical lattice as shown in Fig. 1.3. Fourthly, the optical lattice is free of defects, and so the atoms undergo no scattering due to imperfections in the crystal.

The physics of optical lattices is that the interaction between the neutral atoms and the laser light is carried out in both a conservative and a dissipative way. The interaction between the light and the induced dipole moment of the atom is called conservative interaction. This interaction leads to a shift in the potential energy called ac-Stark shift. The dissipative interaction results from the absorption of photons due to spontaneous emission in which the net effect is a dissipative force on the atoms. It stems from the transfer of momentum to the atom by the absorbed or spontaneously emitted photons.

In Ref. [57] it was suggested to load a BEC in a periodic potential, so the atoms of the system are condensed in the weakly interacting regime. As the lattice potential is increased, the band gap between the first and second Bloch bands increases. Therefore, all atoms are assumed to reside in the lowest Bloch band and the system can be described by a single-band Bose-Hubbard model that describes the physics of strongly interacting bosons by the competition between kinetic and interaction energy. It has been studied analytically and numerically with different techniques like mean-field approximations [58–60] and quantum Monte Carlo methods [61–64].

Fisher *et. al.* [65] predicted theoretically within the Bose-Hubbard model the phase transition between the superfluid and Mott insulator phase, which was later on realized experimentally by Greiner *et. al.* [66]. Fig. 1.4 shows that the superfluid-Mott insulator transition is obtained by changing the lattice depths. When the lattice depth is small, the uncertainty of momenta is small and then a huge spatial uncertainty is achieved due to the Heisenberg uncertainty principle. Thus, the ground state is a superfluid as the bosons are delocalized and the phase is coherent over the entire lattice. On the contrary, a huge uncertainty of momenta results from a large lattice depth and thus the spatial uncertainty will be small. Then, the ground state is a Mott insulator, where the bosons are localized in one of the respective minima and can no longer tunnel to the neighboring minima. The location of the quantum phase transition can be more precisely determined from slightly tilting the optical lattice. The Mott insulator is characterized by gapped excitations and, thus, a slight tilt does not lead to a motion of bosons. Contrary to that the superfluid phase is characterized by a gapless Goldstone mode and, thus, a slight tilt initiates a motion of bosons. Furthermore, extensions of the Bose-Hubbard model have been investigated, which cover for instance, superlattices [67], Bose-Fermi mixtures [68–71], quantum simulations like entanglement of atoms or quantum teleportation [72], and disorder [73–75].

1.4. Spinor Gases in Optical Lattice

Preparing experimentally a spin-1 BEC of ^{23}Na or ^{87}Rb atoms in an optical trap the atomic spin degrees of freedom are not frozen due to the electric dipole force between atoms and the electric field of a laser beam [34, 76]. This experimental realization of an optically trapped BEC opened a new window to

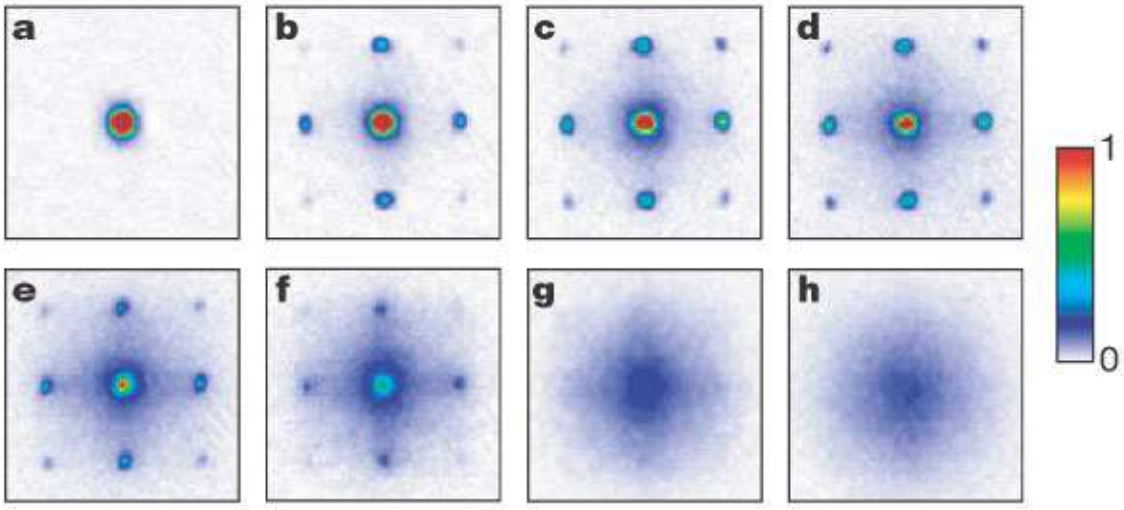

Figure 1.4.: Superfluid to Mott insulator transition in an optical lattice for different lattice depths: (a) 0 E_{R}, (b) 3 E_{R}, (c) 7E_{R}, (d) 10 E_{R}, (e) 13 E_{R}, (f) 14 E_{R}, (g) 16 E_{R}, (h) 20 E_{R} where $E_{\mathrm{R}} = \pi^2\hbar^2/(2ma^2)$ is the recoil energy (m is the mass of a single atom and a is the lattice constant) [66].

study also various phenomena of spinor Bose gases loaded in an optical lattice. For instance, they offer the possibility of studying strongly correlated states, for example the coherent collisional spin dynamics in an optical lattice was measured in Ref. [77] and the ^{87}Rb scattering lengths for $F = 1$ and $F = 2$ were determined in Ref. [78]. In particular, combining the spin degree of freedom with various types of interactions and with different lattice geometries offers the prospect to realize a plethora of superfluid phases with magnetic properties. A first tentative step in this direction was the loading of ^{87}Rb in a frustrated triangular lattice [79]. Despite these initial promising investigations, spinor Bose gases in optical lattice seem experimentally to be so challenging that no further detailed experiments have been performed.

On the other hand, the properties of spin-1 Bose gases in an optical lattice were investigated in detail some time ago theoretically in Refs. [80,81]. Several unique MI and SF phases for spin-1 bosons were determined without external magnetic field at zero temperature in case of an anti-ferromagnetic interaction in an optical lattice [80]. For instance, the MI phase with an even number of atoms is more strongly stabilized than that with an odd number because of the formation of singlet pairs [81]. Moreover, the SF phase represents a polar spin-0 state with zero spin expectation value [80, 81]. On the other side, the influence of the linear Zeeman effect with a non-vanishing external magnetic field upon the MI-SF phase boundary was determined within a mean-field approximation in Refs. [82, 83]. In addition, it was also shown in Ref. [82, 83] that the superfluid transition occurs into either a polar spin-1 or a polar spin-(-1) state, but it was not investigated, which magnetic phases may emerge deeper in the superfluid.

1.5. Outline of Thesis

In this thesis, we follow Refs. [84,85] and study the effect of an external magnetic field on the emergence of superfluid phases for anti-ferromagnetic spin-1 bosons in a three-dimensional cubic optical lattice at zero temperature. To this end, we extend the Ginzburg-Landau theory developed in Refs. [86,87] from the spin-0 to the spin-1 Bose-Hubbard model. Thus, we calculate the effective action which allows us to obtain the different superfluid phases and to determine the respective order of the transitions between them. To this end, we organize the thesis as follows:

In **Chapter 2**, bosons in a cubic optical lattice are considered with spin degrees of freedom. In addition, we focus on particles with effective spin $F = 1$. We describe theoretically the behavior of the spin-1 Bose-Hubbard model at zero temperature. Furthermore, at zero temperature and no hopping, we explain the properties of a spin-1 system without or with magnetization. In addition, we show the effect of the critical external magnetic field on the ground state in the Mott insulator phase for a fixed spin-dependent interaction.

We discuss in **Chapter 3** the classification of phase transitions and the properties of a second-order phase transition and the underlying symmetry-breaking mechanism. Furthermore, the principle role of the order parameter is explained. Additionally, at zero temperature, we calculate the superfluid-Mott insulator quantum phase transition without and with magnetization in case of ferromagnetic and anti-ferromagnetic interactions by generalizing the mean-field approximation which is used to describe spinless bosons. To this end, it is necessary to calculate various matrix elements which is done recursively in **Appendix A**.

In **Chapter 4**, we determine the partition function of the system in the Dirac interaction picture. Within the Ginzburg-Landau theory the additional source currents are added to the Bose-Hubbard model in order to break the global $U(1)$ symmetry. Furthermore, a strong-coupling perturbation theory will be developed by taking into account diagrammatic rules which treat the bosons in a cubic optical lattice. Thus, we get a diagrammatic expansion of the grand-canonical free energy in the first order of the hopping parameter and in the fourth order of the symmetry-breaking currents. We reproduce the mean-field free energy in order to estimate the accuracy of our calculation and investigate the range of validity.

The corresponding spin-dependent order parameters in **Chapter 5** are introduced via a Legendre transformation with respect to the currents and calculate the resulting hopping expansion of the effective action up to first order. With this we study the quantum phase transition between the superfluid phase and the Mott insulator. In addition, we determine the range of validity of the Ginzburg-Landau theory, which turns out to be limited due to a sharp increase of the condensate density in the superfluid phase and is larger than that of mean-field theory. By extremising the effective Ginzburg-Landau action we show that, in particular at zero temperature, our theory can distinguish between various ferromagnetic and anti-ferromagnetic superfluid phases for an anti-ferromagnetic interaction and a non-vanishing external magnetic field. Furthermore, we show for a vanishing external magnetic field that the superfluid phase is a polar state, where all the atoms condense in the spin-0 state [81]. Moreover, we study whether the superfluid-Mott insulator phase transition and the transitions between the various superfluid phases for a non-vanishing external magnetic field are of first or second order.

In **Chapter 6**, finally, we summarize our thesis and present the outlook.

2. Spinor Bose Gases in Optical Lattice

After having discussed general properties of optical lattices in the previous chapter, we start this chapter with introducing the spinor interaction potential between atoms of spinor Bose gases. Subsequently, the Bose-Hubbard model for spin-1 atoms in a cubic optical lattice is derived by using a tight-binding approximation. Additionally, the properties of Mott insulator phases are investigated in the atomic limit, i.e. with zero hopping between the nearest neighbor sites, without and with magnetization. To this end we observe how the ground-state energy changes both with the external magnetic field and the chemical potential.

2.1. Spinor Interaction Potential

The interactions between two atoms are the workhorse for ultracold quantum gases in optical lattices. In the scalar case, the ultracold atomic interactions are characterized by a single parameter a_s, the three-dimensional s-wave scattering length [88,89]. Therefore, this interaction can be described by the pseudopotential [90] which is defined as

$$V_{\text{int}}(\mathbf{r},\mathbf{r}') = g\delta(\mathbf{r}-\mathbf{r}'), \tag{2.1}$$

where

$$g = \frac{4\pi\hbar^2 a_s}{M} \tag{2.2}$$

is the interaction strength and M is the particle mass.

In the spinor case, we note that the knowledge of the interaction potential between two atoms with spin degree of freedom is more difficult than that of the spinless case. In order to determine the spinor interaction potential we generalize the pseudopotential (2.1) to a system of of two identical bosons of spin f yielding the total spin F [32,33]:

$$V_{\text{int}}(\mathbf{r},\mathbf{r}') \;=\; \delta(\mathbf{r}-\mathbf{r}')\sum_{F=0}^{2f} g_F \mathbf{P}_F. \tag{2.3}$$

The respective coupling strengths g_F are given by

$$g_F \;=\; \frac{4\pi\hbar^2 a_F}{M}, \tag{2.4}$$

where a_F denotes the s-wave scattering length for two colliding atoms with total hyperfine spin F.

The corresponding projection operator $\mathbf{P}_F$ is defined according to

$$\mathbf{P}_F = \sum_{m_F=-F}^{F} |F, m_F\rangle \langle F, m_F| . \tag{2.5}$$

Note that Eq. (2.3) is valid for low energies when all other relevant length scales of the system, i.e. the de Broglie wavelength of the atoms and the average interatomic spacing, are much larger than the range of the two-body scattering potential.
For identical bosons, the allowed total spins F must be even [81, 91], and the normalization condition of projection operators reads

$$1 = \sum_{F=0}^{2f} \mathbf{P}_F. \tag{2.6}$$

However, the spin-spin coupling of two spin-f bosons can be found from using the identity

$$\mathbf{f}_1 \cdot \mathbf{f}_2 = \frac{\mathbf{F}^2 - \mathbf{f}_1^2 - \mathbf{f}_2^2}{2} = \frac{F(F+1) - 2f(f+1)}{2}. \tag{2.7}$$

Combining Eqs. (2.6) and (2.7) we get

$$\mathbf{f}_1 \cdot \mathbf{f}_2 = (\mathbf{f}_1 \cdot \mathbf{f}_2)\, \mathbf{1} = \sum_{F=0}^{2f} \mathbf{f}_1 \cdot \mathbf{f}_2 \mathbf{P}_F = \sum_{F=0}^{2f} \lambda_F \mathbf{P}_F, \tag{2.8}$$

with the abbreviation

$$\lambda_F = \frac{F(F+1) - 2f(f+1)}{2}.$$

For spin-1 condensates, for instance, we have from (2.6)

$$1 = \mathbf{P}_0 + \mathbf{P}_2, \tag{2.9}$$

and from (2.8)

$$\mathbf{f}_1 \cdot \mathbf{f}_2 = \mathbf{P}_2 - 2\mathbf{P}_0, \tag{2.10}$$

so we yield for the projection operators

$$\mathbf{P}_0 = \frac{1 - \mathbf{f}_1 \cdot \mathbf{f}_2}{3}, \qquad \mathbf{P}_2 = \frac{2 + \mathbf{f}_1 \cdot \mathbf{f}_2}{3}. \tag{2.11}$$

From Eqs. (2.3) and (2.11), we then get

$$V_{\text{int}}(\mathbf{r}, \mathbf{r}') \;\; = \;\; \delta(\mathbf{r} - \mathbf{r}')(c_0 + c_2 \mathbf{f}_1 \cdot \mathbf{f}_2), \tag{2.12}$$

with

$$c_0 = \frac{g_0 + 2g_2}{3} \quad , \qquad c_2 = \frac{g_2 - g_0}{3} \tag{2.13}$$

representing the spin-independent and spin-dependent interaction coefficients, respectively.

2.2. Spin-1 Bose-Hubbard Hamiltonian

The spinor Bose Hubbard model describes the low-energy spin-1 bosons loaded in a deep optical lattice. In order to derive this model, we start from the second quantized Hamiltonian for a spin-1 Bose gas in the grand-canonical ensemble [32, 33, 80, 81, 92–95] by neglecting the effect of any additional harmonic trapping potential which is given by

$$\hat{H} = \sum_{\alpha} \int d^3x \hat{\Psi}^{\dagger}_{\alpha}(\mathbf{x}) \left[-\frac{\hbar^2}{2M}\nabla^2 + V(\mathbf{x}) - \mu \right] \hat{\Psi}_{\alpha}(\mathbf{x}) - \eta \sum_{\alpha,\beta} \int d^3x \hat{\Psi}^{\dagger}_{\alpha}(\mathbf{x}) F^z_{\alpha\beta} \hat{\Psi}_{\beta}(\mathbf{x})$$
$$+ \frac{c_0}{2} \sum_{\alpha,\beta} \int d^3x \hat{\Psi}^{\dagger}_{\alpha}(\mathbf{x}) \Psi^{\dagger}_{\beta}(\mathbf{x}) \hat{\Psi}_{\beta}(\mathbf{x}) \hat{\Psi}_{\alpha}(\mathbf{x}) + \frac{c_2}{2} \sum_{\alpha,\beta,\gamma,\delta} \int d^3x \hat{\Psi}^{\dagger}_{\alpha}(\mathbf{x}) \Psi^{\dagger}_{\gamma}(\mathbf{x}) \mathbf{F}_{\alpha\beta} \cdot \mathbf{F}_{\gamma\delta} \hat{\Psi}_{\delta}(\mathbf{x}) \hat{\Psi}_{\beta}(\mathbf{x}). \quad (2.14)$$

Here μ is the chemical potential and η stands for the external magnetic field. Furthermore, $V(\mathbf{x}) = V_0 \sum_{\nu=1}^{3} \sin^2(k_L x_\nu)$ is the periodic potential of a 3-dimensional cubic optical lattice with a lattice period $a = \lambda_L/2$, where the lattice depth is measured in units of the recoil energy $E_R = \hbar^2 k_L^2/2M$, where $k_L = 2\pi/\lambda_L$. We note that the potential decomposes in three one-dimensional parts, which is a special property of the cubic lattice. In addition, $\hat{\Psi}_{\alpha}(\mathbf{x})$ is a field operator that annihilates a particle in a hyperfine state $|F = 1, m_F = -1, 0, 1\rangle$. Because of the bosonic nature of the particles, the field operators fullfill the standard commutator relations:

$$\left[\hat{\Psi}_{\alpha}(\mathbf{x}), \hat{\Psi}_{\beta}(\mathbf{x}')\right] = 0 \quad , \quad \left[\hat{\Psi}^{\dagger}_{\alpha}(\mathbf{x}), \hat{\Psi}^{\dagger}_{\beta}(\mathbf{x}')\right] = 0 \quad , \quad \left[\hat{\Psi}_{\alpha}(\mathbf{x}), \hat{\Psi}^{\dagger}_{\beta}(\mathbf{x}')\right] = \delta_{\alpha,\beta}\delta(\mathbf{x} - \mathbf{x}'). \quad (2.15)$$

Here $\mathbf{F}_{\alpha\beta}$ are the spin-1 matrices

$$F_x = \frac{1}{\sqrt{2}} \begin{pmatrix} 0 & 1 & 0 \\ 1 & 0 & 1 \\ 0 & 1 & 0 \end{pmatrix}, \qquad F_y = \frac{i}{\sqrt{2}} \begin{pmatrix} 0 & -1 & 0 \\ 1 & 0 & -1 \\ 0 & 1 & 0 \end{pmatrix}, \qquad F_z = \begin{pmatrix} 1 & 0 & 0 \\ 0 & 0 & 0 \\ 0 & 0 & -1 \end{pmatrix}, \quad (2.16)$$

which fullfill the commutator relations $\left[F_\alpha, F_\beta\right] = i \sum_\gamma \epsilon_{\alpha\beta\gamma} F_\gamma$ of an angular momentum algebra. The first term in (2.14) results from the one-particle Hamiltonian, the second one denotes the Zeeman energy in the external magnetic field, the third one describes the spin-independent interaction, and the last one the spin-dependent interaction. The spin-dependent interaction is ferromagnetic (anti-ferromagnetic) when $c_2 < 0$, i.e., $a_2 < a_0$ ($c_2 > 0$, i.e., $a_2 > a_0$) where a_F is the s-wave scattering length with total spin F for $F = 0, 2$. We remark that the scattering of total spin $F = 1$ is forbidden due to the bosonic parity [81]. In the case of ^{23}Na atoms the interaction is anti-ferromagnetic where its scattering lengths are $a_0 = (46 \pm 5)a_B$ and $a_2 = (52 \pm 5)a_B$, where a_B is the Bohr radius [96]. For ^{87}Rb, we have instead $a_0 = (110 \pm 4)a_B$ and $a_2 = (107 \pm 4)a_B$, so the interaction is ferromagnetic [32].

It is important to show that in a periodic potential Bloch wave functions are the energy eigenstates of a single atom. These states can be written as a set of Wannier functions which are localized on the lattice sites through the tight-binding limit [97]. Thus, we can expand a field operator by the Wannier functions of the lowest energy band for low enough temperatures as then the energy gap between the

first and the second band $E_{\rm gap}$ is much larger than $k_{\rm B}T$:

$$\hat{\Psi}_\alpha(\mathbf{x}) \;=\; \sum_i \hat{a}_{i\alpha} w(\mathbf{x}-\mathbf{x}_i) \qquad , \qquad \hat{\Psi}^\dagger_\alpha(\mathbf{x}) = \sum_i \hat{a}^\dagger_{i\alpha} w^*(\mathbf{x}-\mathbf{x}_i), \tag{2.17}$$

where $\hat{a}^\dagger_{i\alpha}$ ($\hat{a}_{i\alpha}$) is the creation (annihilation) operator for an atom at site i with hyperfine spin $m_F = \alpha$. Using orthonormality conditions, we obtain the commutation relations for the lattice operator

$$\left[\hat{a}_{i\alpha}, \hat{a}_{j\beta}\right] = 0 \quad , \quad \left[\hat{a}^\dagger_{i\alpha}, \hat{a}^\dagger_{j\beta}\right] = 0 \quad , \quad \left[\hat{a}_{i\alpha}, \hat{a}^\dagger_{j\beta}\right] = \delta_{\alpha,\beta}\delta_{i,j}. \tag{2.18}$$

Inserting Eq. (1.2) into (2.14), and using the approximation that the overlap of Wannier functions at different sites can be neglected for a deep enough lattice potential, the Bose-Hubbard model for spin-1 bosons in a cubic optical lattice becomes

$$\begin{aligned}\hat{H} = \sum_i \Bigg[&\frac{U_0}{2}\sum_{\alpha,\beta} \hat{a}^\dagger_{i\alpha}\hat{a}^\dagger_{i\beta}\hat{a}_{i\alpha}\hat{a}_{i\beta} + \frac{U_2}{2}\sum_{\alpha,\beta,\gamma,\delta} \hat{a}^\dagger_{i\alpha}\hat{a}^\dagger_{i\gamma}\mathbf{F}_{\alpha\beta}\cdot\mathbf{F}_{\gamma\delta}\hat{a}_{i\delta}\hat{a}_{i\beta} \\ &-\mu\sum_\alpha \hat{a}^\dagger_{i\alpha}\hat{a}_{i\alpha} - \eta\sum_{\alpha,\beta}\hat{a}^\dagger_{i\alpha}F^z_{\alpha\beta}\hat{a}_{i\beta}\Bigg] - J\sum_{<i,j>}\sum_\alpha \hat{a}^\dagger_{i\alpha}\hat{a}_{j\alpha}.\end{aligned} \tag{2.19}$$

Here $< i,j >$ describes a summation over all sets of nearest neighbor sites. The hopping matrix element is

$$J = J_{ij} = -\int d^3x w^*(\mathbf{x}-\mathbf{x}_i)\left[-\frac{\hbar^2}{2M}\nabla^2 + V(\mathbf{x})\right] w(\mathbf{x}-\mathbf{x}_j). \tag{2.20}$$

We can drop the site indices since all J_{ij} are equal in the case of the nearest-neighbor hopping due to translational invariance. Furthermore, U_0 and U_2 represent the on-site spin-independent and spin-dependent interaction, respectively, where U_F is defined by

$$U_F \;=\; c_F\int d^3x \big|w(\mathbf{x}-\mathbf{x}_i)\big|^4, \tag{2.21}$$

which is proportional to the parameter c_F defined in (2.13). Therefore, we have a ferromagnetic (antiferromagnetic) when $U_2 < 0$ ($U_2 > 0$). Note that we have neglected in (2.19) a physically irrelevant energy shift, which is of the form (2.20) with $i = j$.
We can rearrange the spin dependent term in (2.19) by using this identity

$$\sum_{\alpha,\beta,\gamma,\delta} \hat{a}^\dagger_{i\alpha}\hat{a}^\dagger_{i\gamma}\mathbf{F}_{\alpha\beta}\cdot\mathbf{F}_{\gamma\delta}\hat{a}_{i\delta}\hat{a}_{i\beta} = \sum_{\alpha,\beta,\gamma,\delta,\nu}\big(\hat{a}^\dagger_{i\alpha}F^\nu_{\alpha\beta}\hat{a}_{i\beta}\big)\big(\hat{a}^\dagger_{i\gamma}F^\nu_{\gamma\delta}\hat{a}_{i\delta}\big) - \sum_{\alpha,\beta,\delta,\nu} F^\nu_{\alpha\beta}F^\nu_{\beta\delta}\hat{a}^\dagger_{i\alpha}\hat{a}_{i\delta}. \tag{2.22}$$

Here, we define the spin operator $\hat{\mathbf{S}}_i = \sum_{\alpha,\beta}\hat{a}^\dagger_{i\alpha}\,\mathbf{F}_{\alpha\beta}\,\hat{a}_{i\beta}$, the number operator for each spin component

$\hat{n}_{i\alpha} = \hat{a}^\dagger_{i\alpha}\hat{a}_{i\alpha}$, and $\hat{n}_i = \sum_\alpha \hat{n}_{i\alpha}$ is the total atom number operator. Therefore, Eq. (2.19) becomes

$$\hat{H} = \sum_i \left[\frac{U_0}{2}\hat{n}_i(\hat{n}_i - 1) + \frac{U_2}{2}(\hat{\mathbf{S}}_i^2 - 2\hat{n}_i) - \mu\hat{n}_i - \eta\hat{S}_{iz} \right] - J \sum_{<i,j>} \sum_\alpha \hat{a}^\dagger_{i\alpha}\hat{a}_{j\alpha}. \tag{2.23}$$

In order to derive that the operator $\hat{\mathbf{S}}$ behaves like an angular momentum or spin operator, we write down explicitly each component of the spin operator

$$\hat{S}_{ix} = \frac{1}{\sqrt{2}}(\hat{a}^\dagger_{i1}\hat{a}_{i0} + \hat{a}^\dagger_{i0}\hat{a}_{i1} + \hat{a}^\dagger_{i0}\hat{a}_{i-1} + \hat{a}^\dagger_{i-1}\hat{a}_{i0}), \tag{2.24}$$

$$\hat{S}_{iy} = \frac{i}{\sqrt{2}}(-\hat{a}^\dagger_{i1}\hat{a}_{i0} + \hat{a}^\dagger_{i0}\hat{a}_{i1} - \hat{a}^\dagger_{i0}\hat{a}_{i-1} + \hat{a}^\dagger_{i-1}\hat{a}_{i0}), \tag{2.25}$$

$$\hat{S}_{iz} = \hat{n}_{i1} - \hat{n}_{i-1}. \tag{2.26}$$

With this one can show that the operators $\hat{S}_{i\sigma}$with $\sigma = x, y, z$ obey the usual angular momentum commutation relation $\left[\hat{S}_i, \hat{S}_j\right] = i\sum_k \epsilon_{ijk}\hat{S}_k$. Using Eqs. (2.24)–(2.26), we get furthermore

$$\hat{\mathbf{S}}_i^2 = 2\hat{n}_{i1}\hat{n}_{i0} + 2\hat{n}_{i0}\hat{n}_{i-1} + \hat{n}_{i1} + 2\hat{n}_{i0} + \hat{n}_{i-1} + \hat{n}_{i1}^2 - 2\hat{n}_{i1}\hat{n}_{i-1} + \hat{n}_{i-1}^2 + 2\hat{a}^\dagger_{i1}\hat{a}^\dagger_{i-1}\hat{a}^2_{i0} + 2\hat{a}^\dagger_{i0}\hat{a}^\dagger_{i0}\hat{a}_{i1}\hat{a}_{i-1}. \tag{2.27}$$

The spin-1 Bose-Hubbard Hamiltonian (2.23) represents the starting point for the following analysis.

2.3. Thermodynamic Properties

In this section, we provide a brief introduction into thermodynamic quantities which are needed throughout the thesis. Here, we use the grand-canonical ensemble by assuming that both energy and particles can be exchanged between the considered system and its environment. Therefore, the grand-canonical free energy for a magnetic system is the underlying thermodynamic potential, which is given by [90, 99]:

$$\mathcal{F}(T, V, \mu, \eta) \quad = \quad -\frac{1}{\beta}\ln \mathcal{Z}(T, V, \mu, \eta), \tag{2.28}$$

where the grand-canonical partition function $\mathcal{Z}$ reads

$$\mathcal{Z} = \mathrm{Tr}\left[e^{-\beta(\hat{H} - \mu\hat{N} - \eta\hat{M})}\right]. \tag{2.29}$$

Here V is the volume, μ refers to the chemical potential which is defined as the change in energy per particle added to the system [98] and $\beta = 1/(k_B T)$ corresponds to the reciprocal of system temperature T and k_B labels the Boltzmann constant. In addition, η denotes the external magnetic field [99] which corresponds to the Zeeman splitting between two states differing by $\Delta m_F = 1$ under the effect of an

external magnetic field [32, 82, 83, 100, 101]. Both μ and η should be adjusted in order to fix the total number of particles and the total magnetization, respectively.
In quantum statistics, the thermal average of an arbitrary operator $\hat{O}$ can be obtained by

$$< \hat{O} >= \frac{1}{\mathcal{Z}} \mathrm{Tr}\Big[\hat{O}\, e^{-\beta(\hat{H}-\mu\hat{N}-\eta\hat{M})}\Big] \quad . \tag{2.30}$$

Thus, the total particle number is given by

$$N = \left\langle \hat{N} \right\rangle = -\frac{\partial \mathcal{F}}{\partial \mu}, \tag{2.31}$$

and the magnetization of the system follows from

$$M \;\; = \left\langle \hat{M} \right\rangle = \;\; -\frac{\partial \mathcal{F}}{\partial \eta}\,. \tag{2.32}$$

2.4. System Properties With Zero Hopping

In this section, we study the properties of the system with no hopping, i.e. $J = 0$. In this atomic limit, the Bose-Hubbard Hamiltonian (2.23) reduces to a sum of single-site Hamiltonians

$$\hat{H} \;\; = \;\; \sum_i \hat{H}_i^{(0)}, \tag{2.33}$$

where

$$\hat{H}_i^{(0)} = -\mu\hat{n}_i + \frac{U_0}{2}\hat{n}_i(\hat{n}_i - 1) + \frac{U_2}{2}(\hat{\mathbf{S}}_i^2 - 2\hat{n}_i) - \eta\hat{S}_{iz}\,. \tag{2.34}$$

We are able to drop site index i in the following since all sites are equivalent and, therefore, use the remaining part of this chapter only the local Hamiltonian

$$\hat{H}^{(0)} \;\; = \;\; -\mu\hat{n} + \frac{U_0}{2}\hat{n}(\hat{n} - 1) + \frac{U_2}{2}(\hat{\mathbf{S}}^2 - 2\hat{n}) - \eta\hat{S}_z\,. \tag{2.35}$$

We remark that the eigenstates of the Hamiltonian (2.35) can be determined by the three quantum numbers S, m, n as the operators $\hat{\mathbf{S}}^2$, $\hat{S}_z$ and $\hat{n}$ commute with each other [81]. The eigenvalue problems of these operators therefore read

$$\hat{\mathbf{S}}^2\,|S, m, n\rangle = S(S+1)\,|S, m, n\rangle\,, \tag{2.36}$$

$$\hat{S}_z\,|S, m, n\rangle = m\,|S, m, n\rangle\,, \tag{2.37}$$

$$\hat{n}\,|S, m, n\rangle = n\,|S, m, n\rangle\,. \tag{2.38}$$

We find that $S+n$ is even because S is even (odd) when n is even (odd) due to the Bose statistics [32]. Correspondingly, the eigenvalue problem of the local Hamiltonian (2.35) is given by

$$\hat{H}^{(0)} |S, m, n\rangle = E^{(0)}_{S,m,n} |S, m, n\rangle \,, \tag{2.39}$$

where, the states $|S, m, n\rangle$ are orthonormal, i.e.

$$\langle S, m, n | S', m', n' \rangle \;\; = \;\; \delta_{S,S'} \delta_{m,m'} \delta_{n,n'}. \tag{2.40}$$

With the help of Eqs. (2.36)–(2.38), the energy eigenvalues are defined as

$$E^{(0)}_{S,m,n} = -\mu n + \frac{U_0}{2} n(n-1) + \frac{U_2}{2} \big[S(S+1) - 2n \big] - \eta m. \tag{2.41}$$

In the following we investigate in detail how the resulting ground state changes with the chemical potential μ and the external magnetic field η.

2.4.1. Non-Magnetized System

In this subsection, we follow Refs. [102, 103] for an unmagnetized system $\eta = 0$ at zero temperature. Then, the magnetic quantum number m disappears from the eigenenergies (2.41):

$$E^{(0)}_{S,n} = -\mu n + \frac{U_0}{2} n(n-1) + \frac{U_2}{2} \big[S(S+1) - 2n \big]. \tag{2.42}$$

Thus, the eigenstates are $(2S+1)$-fold degenerated. In this case, the U_2 sign influences the ground state as follows [102, 103]:

- When $U_2 < 0$, the interaction is ferromagnetic. Thus, in order to minimize the energy, the spin should be maximum, i.e. $S = n$. Thus, the neighboring Mott lobes are characterized by the following condition

  $$E^{(0)}_{n-1,n-1} < E^{(0)}_{n,n} < E^{(0)}_{n+1,n+1} \tag{2.43}$$

  so we obtain from Eq. (2.42)

  $$\Big(1 + \frac{U_2}{U_0}\Big)(n-1) < \frac{\mu}{U_0} < n\Big(1 + \frac{U_2}{U_0}\Big) \quad . \tag{2.44}$$

- When $U_2 > 0$, the interaction is anti-ferromagnetic. Therefore, the minimization of the energy is obtained by the minimal spin S. This value of spin S depends on the number of atoms per site n:

  – For an even n the ground state is $|0, 0, n\rangle$ with $S = 0$. This ground state is called the "spin-singlet insulator" [80]. In this case we have to distinguish two situations. The first one is $U_2/U_0 < 0.5$ and the second one is $U_2/U_0 > 0.5$ as shown in Fig. 2.1 [102, 103].

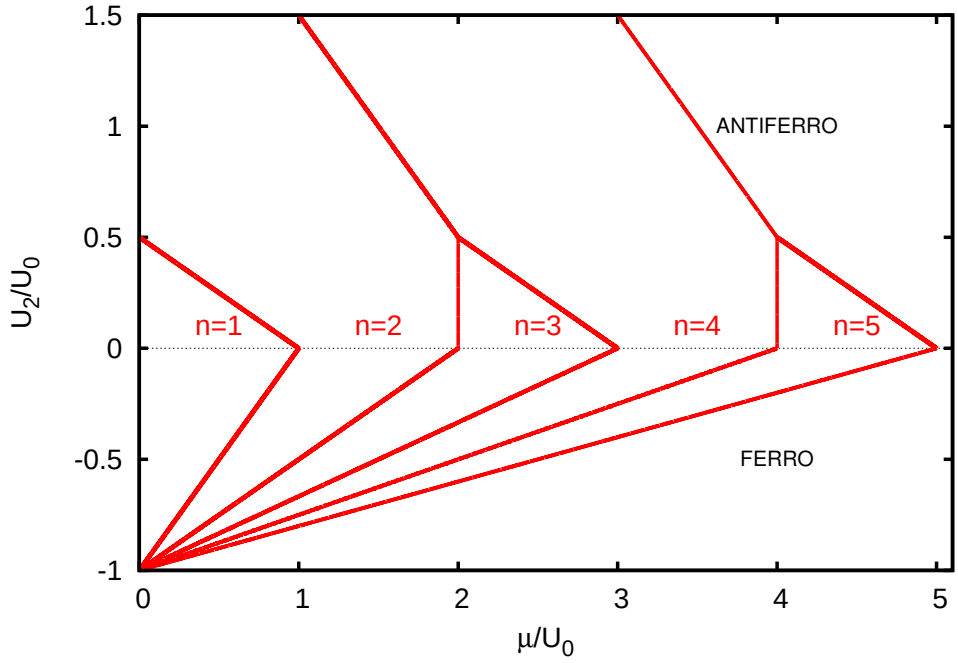

Figure 2.1.: Phase diagram of spinor $F = 1$ Bose-Hubbard model for unmagnetized system with no hopping at zero temperature. The system is ferromagnetic (anti-ferromagnetic) when $U_2/U_0 < 0$ ($U_2/U_0 > 0$) [102, 103].

∗ For $U_2/U_0 < 0.5$, we have

$$E^{(0)}_{1,n-1} < E^{(0)}_{0,n} < E^{(0)}_{1,n+1}, \tag{2.45}$$

which reduces with Eq. (2.41) to

$$(n-1) - 2\frac{U_2}{U_0} < \frac{\mu}{U_0} < n\,. \tag{2.46}$$

∗ For $U_2/U_0 > 0.5$ we have

$$E^{(0)}_{0,n-2} < E^{(0)}_{0,n} < E^{(0)}_{0,n+2}, \tag{2.47}$$

which yields accordingly

$$\left(n - \frac{1}{2}\right) - \frac{U_2}{U_0} < \frac{\mu}{U_0} < \left(n + \frac{1}{2}\right) - \frac{U_2}{U_0}\,. \tag{2.48}$$

– For an odd n the ground state is $|1, m, n\rangle$ where $m = 0, \pm 1$. The difference between the odd and even n case is that the odd lobes disappear when $U_2/U_0 > 0.5$. This means that the odd lobes exist only for the inequality $U_2/U_0 < 0.5$. This leads to

$$E^{(0)}_{0,n-1} < E^{(0)}_{1,n} < E^{(0)}_{0,n+1}, \tag{2.49}$$

which is equivalent to

$$(n-1) < \frac{\mu}{U_0} < n - 2\frac{U_2}{U_0}\,. \tag{2.50}$$

Figure 2.1 shows the resulting phase diagram in the plane spanned by the control parameters U_2/U_0 and μ/U_0 for vanishing hopping $J = 0$. In the case of anti-ferromagnetic interaction, for $0 < U_2/U_0 < 0.5$ the right boundary of even lobes does not change with the spin-dependent interaction U_2. On the other hand, when U_2/U_0 is larger than 0.5, the odd lobes disappear while even lobes continue. For ferromagnetic interaction, the even and odd lobes decrease when $|U_2|$ increases and vanish when U_2/U_0 is less than -1 [102, 103].

2.4.2. Magnetized System

In this subsection, we go beyond Refs. [82, 102, 103] for a system with external magnetic field $\eta > 0$ at zero temperature $T = 0$ and no hopping $J = 0$. Therefore, the degeneracy is lifted and the ground state of the Hamiltonian (2.35) depends on the respective value of the spin-independent interaction U_0, the spin-dependent interaction U_2, the chemical potential μ, and the external magnetic field η. In addition, the lowest energy state for given n and S is $|S, S, n\rangle$.

For the following discussion it turns out to be important to determine the degeneracy when two states have the same energy with equal particle number but with total spin differing by 2 [82, 104]. Thus, this degeneracy point describes the situation when it becomes energetically favorable to break or to form a spin-singlet pair. In order to define these degeneracy points we put

$$E^{(0)}_{S,S,n} = E^{(0)}_{S+2,S+2,n}, \tag{2.51}$$

and substituting (2.41) into (2.51) we get

$$\eta^{\text{crit}} = U_2 \left(S + \frac{3}{2}\right). \tag{2.52}$$

Note that this relation, which characterizes the critical values of η and U_2 for both even and odd lobes either to break or to form a spin-singlet pair, does not depend on the particle number n [82, 101, 104].

Now we aim at determining for a given even and odd particle number n, which spin S yields a minimal energy. To this end we investigate in detail the energy difference, which yields with (2.41), for an even n

$$\begin{aligned}\Delta E^{(0)}_{S,S,n} =& E^{(0)}_{S,S,n} - E^{(0)}_{0,0,n} \\ =& -S\eta + \frac{U_2}{2} S\,(S+1)\,,\end{aligned} \tag{2.53}$$

and for an odd n

$$\begin{aligned}\Delta E^{(0)}_{S,S,n} =& E^{(0)}_{S,S,n} - E^{(0)}_{1,1,n} \\ =& -\eta\,(S-1) + \frac{U_2}{2}\big[S\,(S+1) - 2\big].\end{aligned} \tag{2.54}$$

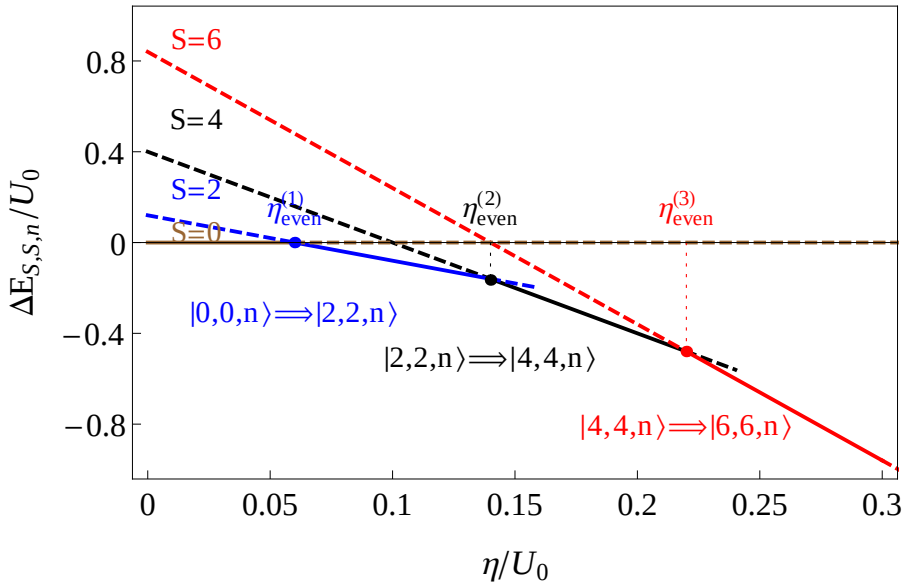

(a) For an even n.

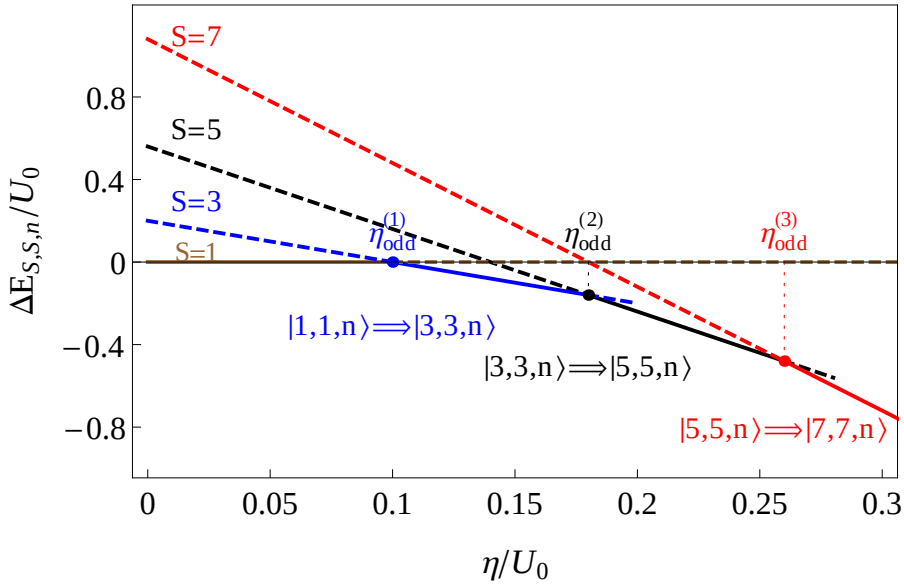

(b) For an odd n.

Figure 2.2.: Dependence of energy difference (2.53) and (2.54) on the external magnetic field for fixed spin-dependent interaction $U_2 = 0.04\,U_0$. The solid lines represent the minimal energy difference.

Let us first of all depict this energy difference (2.53) and (2.54) in Fig. 2.2 as a function of the external magnetic field η for a fixed spin-dependent interaction U_2. We observe that the spin S with minimal energy changes by 2 at the critical external magnetic field (2.52). For the case of even n, Fig. 2.2a shows three critical η values. At the first critical value the spin S and the magnetic quantum number m change from 0 to 2. Thus, the ground state becomes $|2,2,n\rangle$. Similarly, at the second critical value the ground state yields a change from $|2,2,n\rangle$ to $|4,4,n\rangle$. In the same way, the ground state is $|6,6,n\rangle$ emerges from $|4,4,n\rangle$ at the third critical value. On the other hand, for the case of odd n, Fig. 2.2b also shows three critical values of η. At the first critical η, the quantum numbers S and m change from 1 to 3. Correspondingly, the ground state changes from $|3,3,n\rangle$ to $|5,5,n\rangle$ at the second critical value. Beyond the third critical value, the ground state is given by $|7,7,n\rangle$. Thus, we observe that spin and magnetic quantum number of the ground state increase with increasing external magnetic field η for a fixed spin-dependent interaction U_2, as then the spin-singlet pairs are broken for both even and odd lobes, so all spins tend to align in the direction of the magnetic field as shown in Fig. 2.2.

On the contrary, Fig. 2.3 shows how the energy difference (2.53) and (2.54) depends on the spin-dependent interaction U_2 for a fixed external magnetic field η. The corresponding critical spin-dependent interaction values for even and odd n, where the spin S of the minimal energy changes by 2 follow from (2.52)

$$U_2^{\text{crit}} = \frac{\eta}{S+\frac{3}{2}}, \tag{2.55}$$

and can be read off from Fig. 2.3a and 2.3b, respectively. Figure 2.3a shows three critical U_2 for even lobes. Within the first critical U_2, the quantum numbers S and m changes from 6 to 4. Similarly, the ground state changes from $|4,4,n\rangle$ to $|2,2,n\rangle$ at the second critical U_2. After the third critical value the ground state becomes $|0,0,n\rangle$. Furthermore, Fig. 2.3b illustrates three critical U_2 for odd lobes. By the same way, S and m change from 7 to 5 through the first critical U_2. Similarly, the ground state changes to $|3,3,n\rangle$ and $|1,1,n\rangle$ through the second and third critical U_2, respectively. Thus, we conclude that the spin and magnetic quantum number decrease with increasing the spin-dependent interaction U_2 for a fixed external magnetic field η, Thus, the spin-singlet pairs will be formed for both even and odd lobes because this field is not able to align the spins as shown in Fig. 2.3.

After having determined the critical external magnetic field η and spin-dependent interaction U_2, where degeneracies occur, the calculation of the respective ground state yields the following results:

- In the case of the **ferromagnetic** interaction, i.e. $U_2 < 0$, there is no difference between the ground state with and without magnetization because all spins are aligned. Thus, the ground state is given by $|n,n,n\rangle$. In addition, the particle number n is then defined from the condition

$$E^{(0)}_{n-1,n-1,n-1} < E^{(0)}_{n,n,n} < E^{(0)}_{n+1,,n+1n+1} \tag{2.56}$$

  using (2.41), we get

$$\Big(1+\frac{U_2}{U_0}\Big)(n-1) < \frac{\mu+\eta}{U_0} < n\Big(1+\frac{U_2}{U_0}\Big). \tag{2.57}$$

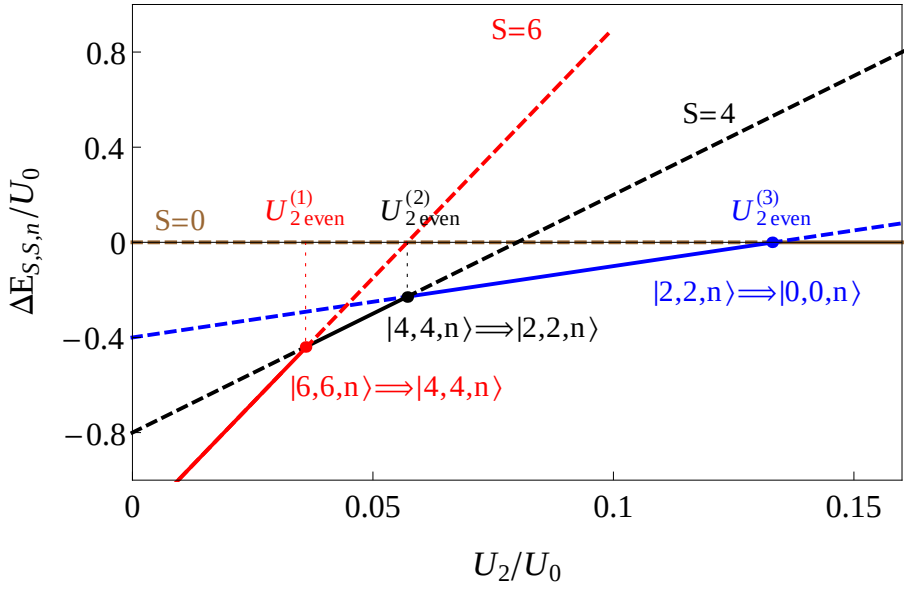

(a) For an even n.

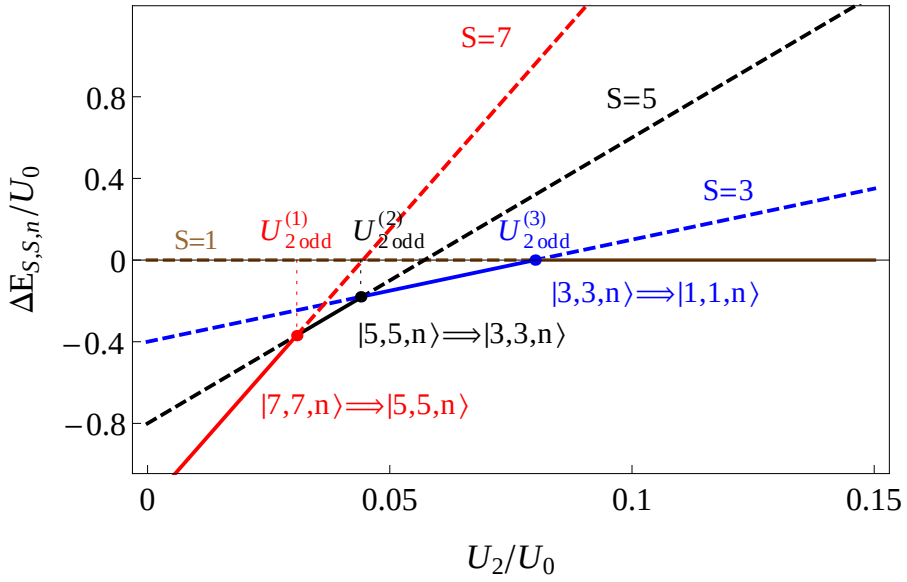

(b) For an odd n.

Figure 2.3.: Dependence of energy difference (2.53) and (2.54) on spin-dependent interaction U_2 for fixed external magnetic field $\eta = 0.2\,U_0$. The solid lines represent the minimal energy difference.

By rewriting the chemical potential as

$$\mu + \eta \to \mu \tag{2.58}$$

Eq. (2.57) reduces to

$$(n-1)\Big(1+\frac{U_2}{U_0}\Big) < \frac{\mu}{U_0} < n\Big(1+\frac{U_2}{U_0}\Big) \tag{2.59}$$

which coincides with the unmagnetized result in (2.44).

- For an **anti-ferromagnetic** system, i.e. $U_2 > 0$, the situation becomes quite complicated. It turns out that, we have the following four cases for the ground state.
  - The first case is

$$E^{(0)}_{S-1,S-1,n-1} < E^{(0)}_{S,S,n} < E^{(0)}_{S+1,S+1,n+1}, \tag{2.60}$$

    which yields with (2.41)

$$n-1+(S-1)\,\frac{U_2}{U_0} - \frac{\eta}{U_0} < \frac{\mu}{U_0} < n + S\frac{U_2}{U_0} - \frac{\eta}{U_0}. \tag{2.61}$$

  - The second case is

$$E^{(0)}_{S-1,S-1,n-1} < E^{(0)}_{S,S,n} < E^{(0)}_{S-1,S-1,n+1}, \tag{2.62}$$

    which becomes

$$n-1+(S-1)\,\frac{U_2}{U_0} - \frac{\eta}{U_0} < \frac{\mu}{U_0} < n - (S+1)\,\frac{U_2}{U_0} + \frac{\eta}{U_0}. \tag{2.63}$$

  - The third case is

$$E^{(0)}_{S+1,S+1,n-1} < E^{(0)}_{S,S,n} < E^{(0)}_{S+1,S+1,n+1}, \tag{2.64}$$

    which reduces to

$$1-n+(S+2)\,\frac{U_2}{U_0} - \frac{\eta}{U_0} < \frac{\mu}{U_0} < n + S\frac{U_2}{U_0} - \frac{\eta}{U_0}. \tag{2.65}$$

  - The fourth case

$$E^{(0)}_{S,S,n-2} < E^{(0)}_{S,S,n} < E^{(0)}_{S,S,n+2}, \tag{2.66}$$

    yields with (2.41)

$$\frac{1}{2}\left(2n-3-2\frac{U_2}{U_0}\right) < \frac{\mu}{U_0} < \frac{1}{2}\left(1+2n-2\frac{U_2}{U_0}\right). \tag{2.67}$$

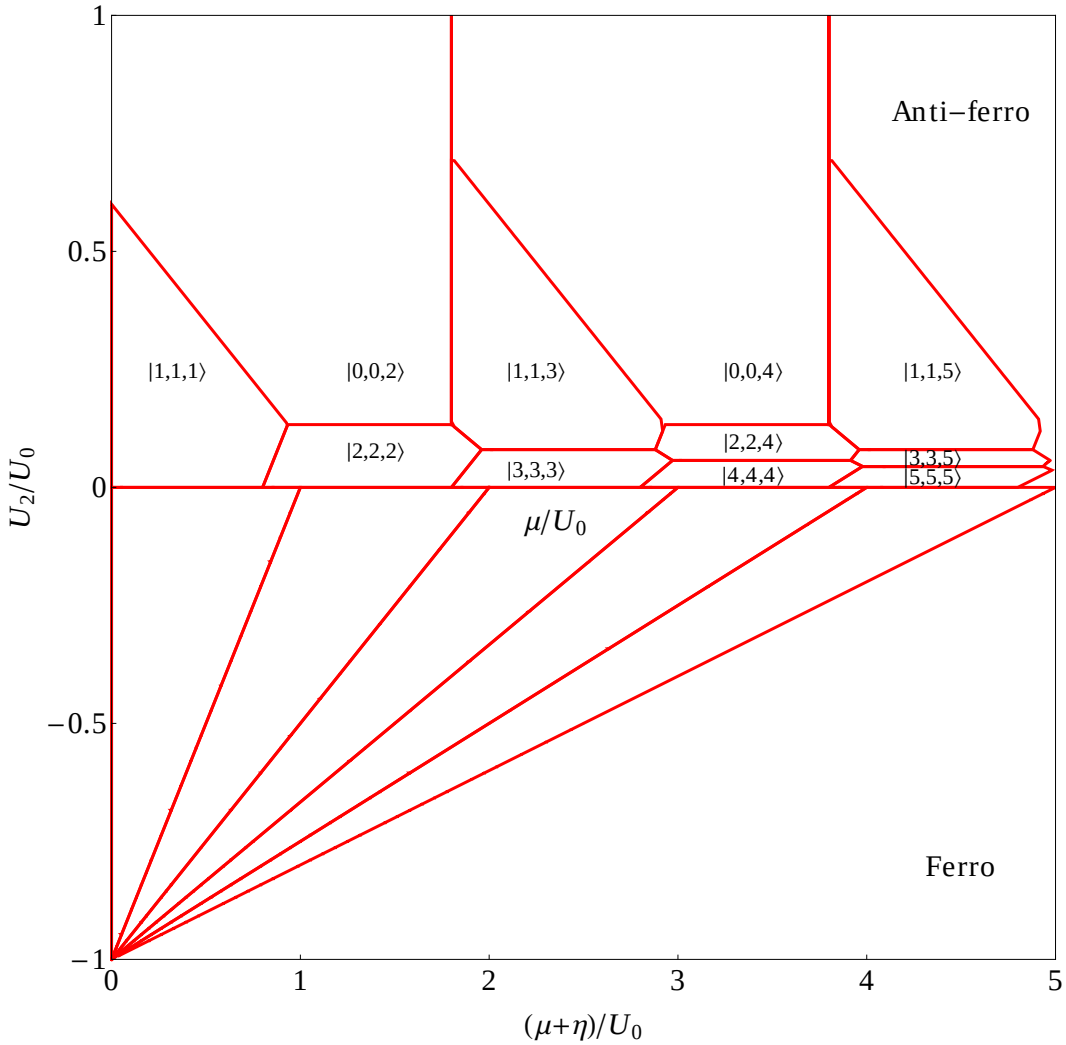

Figure 2.4.: Phase diagram of spinor $F = 1$ Bose-Hubbard model for a magnetized system with $\eta = 0.2\,U_0$ with no hopping at zero temperature. The x-axis in the anti-ferromagnetic case ($U_2 > 0$) is the chemical potential, whereas in the ferromagnetic case ($U_2 < 0$) the chemical potential is shifted according to (2.58).

Figure 2.4 shows the resulting zero hopping phase diagram of the spin $F = 1$ Bose-Hubbard model for a magnetized system at zero temperature for a fixed external magnetic field η. Note that in the anti-ferromagnetic case ($U_2 > 0$) the x-axis is the chemical potential μ, whereas in the ferromagnetic case ($U_2 < 0$) it is shifted by the external magnetic field η according to (2.58) for illustrative purposes.

In the case of anti-ferromagnetic interaction with $0 < U_2/U_0 < 0.5 + \eta/U_0$ only the first three cases can occur. At first, we remark that the right boundary of the even lobes occurs for a fixed chemical potential $\mu = 3.8\,U_0$ when $U_2 \geqslant U^{(3)}_{2\text{even}} = 2\eta/3$, where the ground state for the even lobes is $|0, 0, n\rangle$ which is known as the spin-singlet insulator [80]. When $U_2 \leq 2\eta/3$ both the spin S and the magnetic quantum number m of the odd and the even lobes increase step by step by 2. For instance, the ground state for the fourth lobe successively changes from $|0, 0, 4\rangle$ to $|4, 4, 4\rangle$ due to the respective critical values of $U^{(2)}_{2\text{even}} = 2\eta/3$ and $U^{(3)}_{2\text{even}} = 2\eta/7$, where the ground state changes from $|0, 0, 4\rangle$ via $|2, 2, 4\rangle$ to $|4, 4, 4\rangle$ according to the second case (2.63) as discussed above. Another one is the critical value

$U^{(2)}_{2\text{odd}} = 2\eta/5$, where the ground state changes from $|1,1,n\rangle$ to $|3,3,n\rangle$ which satisfies Eq. (2.65) for odd lobes. The critical value $U^{(2)}_{2\text{even}} = 2\eta/9$ is finally a value for which the ground state for the odd lobes becomes $|5,5,n\rangle$ which satisfies the first case (2.61).

On the other hand, for $U_2/U_0 \geqslant 0.5 + \eta/U_0$, the odd lobes vanish while the even lobes continue. Furthermore, the boundaries for the even lobes occur for a fixed chemical potential $\mu = 1.8\,U_0$ and $\mu = 3.8\,U_0$. The reason is that the external magnetic field can not align the spins, so then the fourth case occurs. Finally, we remark that the even and odd lobes shrink when $U_2 = 0$ as shown in Fig. 2.4.

For ferromagnetic interaction, the even and odd lobes decrease with increasing $|U_2|$ and vanish when $U_2/U_0 < -1$. Therefore, there occurs no difference between the ferromagnetic case with or without magnetization which coincides with the results of [82, 102, 103], because all spins are aligned in the same direction.

3. Mean-Field Theory for Spin-1 BH Model

As an introduction to the physics of phase transitions and critical phenomena, we explain a number of basic ideas such as the classical and quantum phase transitions. In particular, we describe the properties of a second-order phase transition and the underlying symmetry breakdown mechanism. In detail we discuss the principle role of the order parameter. As a special case we refer then to the Bose-Hubbard model for a spin-1 Bose gas at zero-temperature in a cubic optical lattice. Finally, we calculate the superfluid-Mott insulator quantum phase transition without and with magnetization in case of ferromagnetic and anti-ferromagnetic interactions within the realm of the mean-field theory.

3.1. Second-Order Quantum Phase Transition

No one can deny that phase transitions play a principal role in the materials of nature by a change of thermodynamic variables, e. g., the temperature, the pressure or the magnetic field. These phase transitions are classified as first- or second-order transitions. They depend on the behavior of the order parameter which was introduced by Landau. It is non-zero in the ordered phase and zero in the disordered phase [105]. Examples for classical phase transitions are the gas-liquid transition at the critical point, the ferromagnetic transition, and the superconducting transition.

In a first-order phase transition, the order parameter jumps at the phase boundary where the phases coexist at the transition point. In addition, the phase transition is accompanied by latent heat because of the discontinuous change in the density. It is characterized by a finite correlation length. The ice to water phase transition is an example for such a first-order phase transition, where the order parameter is the density difference. Fig. 3.1 shows the three phases solid, liquid and gaseous of water and the phase boundaries as a function of pressure and temperature. On the other hand, a second-order phase transition occurs when the transition does not involve any latent heat. Therefore, the order parameter changes continuously and the correlation length will be infinite. A prominent example of a continuous phase transition is the ferromagnetic-paramagnetic phase transition.

In contrast to classical phase transitions, quantum phase transitions are induced by varying a non-thermal parameter such as the magnetic field or the pressure at zero temperature [106]. Therefore, such transitions are driven by quantum fluctuations and the quantum phase transitions can be explained in terms of the energy spectrum of a many-body quantum system. In this spectrum there is a gap between the ground state and the first excited state, which characterizes the disorder phase [106]. The value of the physical parameter P used to induce the transition relates to this gap. As P is changed, there is a level crossing between the lowest two states at a quantum critical point (QCP) where the gap has the smallest value. In a thermodynamic system, the gap will disappear and we get a phase transition. Since the order parameter of the transition is zero on one side and non-zero on the other, the properties of the many-body ground state are different on the two sides of the transition. At

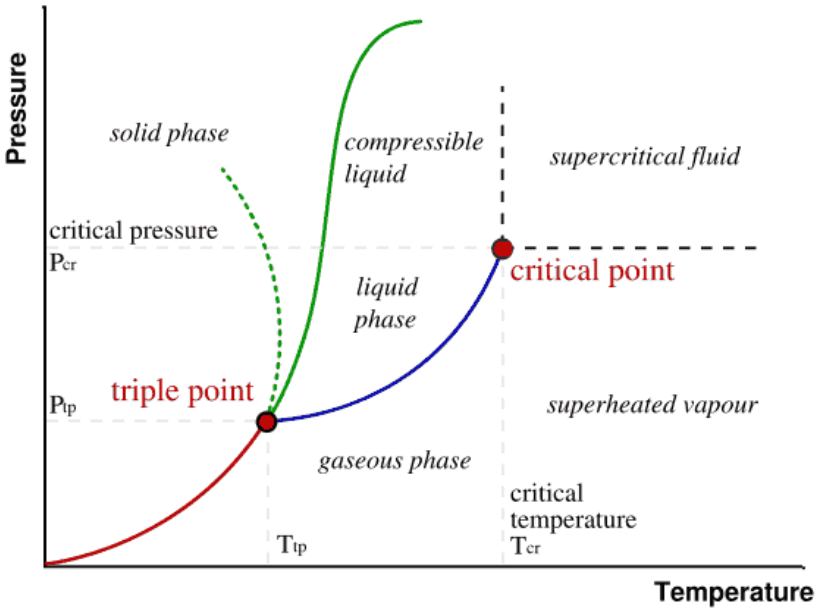

Figure 3.1.: Schematic phase diagram in pressure–temperature plane. The green dotted line refers to the anomalous behavior of water. The green and blue lines show the variation of the freezing point and the boiling point with pressure, respectively. The red line shows the boundary in which sublimation or deposition occur [105].

$T = 0$, we have a quantum critical point between the quantum disordered phase and the ordered phase as shown in Fig. 3.2. At high temperature, the ordered phase will undergo a classical phase transition to a disordered phase at a critical temperature T_c. Thus, the system is governed by classical thermal fluctuations (light blue area) as shown in Fig. 3.2. In addition, when the temperature is decreased, this region becomes narrower and turns towards the QCP [106–108]. A prominent example for such a quantum phase transition is the Mott insulator-superfluid transition in a system consisting of bosonic particles with repulsive interactions hopping through a lattice potential [65].

Landau developed a simple mean-field theory to describe thermal phase transitions by using a spatially and temporally constant order parameter. Ginzburg generalized this approach by allowing for both a spatially and temporally varying order parameter to describe the impact of thermal fluctuations. Thus, the Ginzburg-Landau theory is a general phenomenological description of the onset (or not) of different kinds of order in many-body systems [109, 110]. Within this framework it is also possible to study the effects of dimensionality on ordering. However, it is questionable whether the Ginzburg-Landau concept also applies to the Mott insulator-superfluid quantum phase transition which would have to describe the possible onset of superfluidity as a second-order phase transition. To this end, we need an effective theory involving only long-range collective fluctuations of the system in order to describe the properties near the critical point because of the infinite correlation length.

The Bose-Hubbard Hamiltonian is the simplest model which describes interacting bosons on an optical lattice in a periodic potential. Using a mean field theory the quantum phase transition from a Mott-insulator to superfluid state was theoretically predicted in 1989 by M. P. A. Fisher et al. [65]. Additionally, it underestimates by about 16% the position of the first lobe tip for three-dimensional

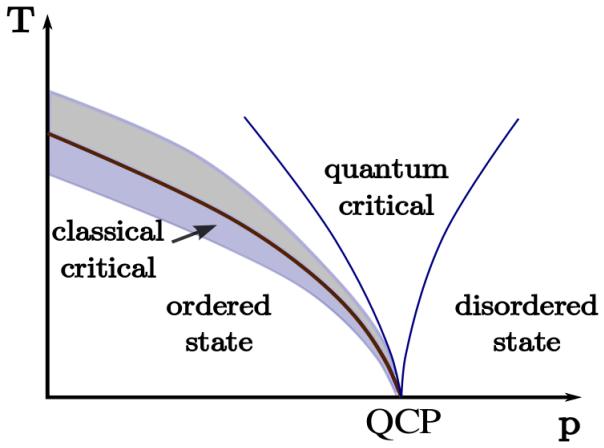

Figure 3.2.: Generic phase diagram around a quantum critical point at $T = 0$ and $P =$ QCP [106–108].

cubic lattices in comparison with recent high-precision quantum Monte-Carlo data [111]. This phase boundary at zero temperature was also calculated on the basis of a strong-coupling expansion, which overestimates the phase boundary [112]. Santos and Pelster [87] showed that the Ginzburg-Landau theory concept can also be used for describing the quantum phase transition of spinless bosons in three-dimensional optical lattices. In a three-dimensional cubic optical lattice the first-order hopping order reproduces the mean-field result, whereas the second-order hopping order improves this such that the relative error for the quantum phase boundary is less than 3 %. The research group of Martin Holthaus in Oldenburg showed that the coefficients in the expansion of the effective action method with respect to the order parameter can be computed perturbatively with the help of the process-chain approach, which allows to obtain numerically even higher hopping orders [113]. With this, the quantum phase boundary between superfluid and Mott insulator can be determined with such an accuracy, that it becomes indistinguishable from the above mentioned quantum Monte-Carlo data and even allows the calculation of critical exponents [114].

3.2. Mean-Field Theory

Here we follow Refs. [81, 104] and generalize the mean-field theory concept to spin-1 bosons in a cubic optical lattice. This will allow us to calculate the phase boundary for the transition between a Mott insulator and a superfluid phases at zero temperature with and without magnetization for ferromagnetic and anti-ferromagnetic interactions. To this end we proceed as follows. As discussed in Chapter 2, the physics of spin-1 bosons loaded in a cubic optical lattice can be described by the Bose-Hubbard Hamiltonian

$$\hat{H}_{\mathrm{BH}} = -J \sum_{<i,j>} \sum_{\alpha} \hat{a}_{i\alpha}^{\dagger} \hat{a}_{j\alpha} + \sum_{i} \left[\frac{U_0}{2} \hat{n}_i (\hat{n}_i - 1) + \frac{U_2}{2} (\hat{\mathbf{S}}_i^2 - 2\hat{n}_i) - \mu \hat{n}_i - \eta \hat{S}_{iz} \right]. \tag{3.1}$$

In contrast to a scalar Bose gas, a spin-1 Bose gas has three order parameters which are defined by

the expectation value of annihilation and creation operators

$$\Psi_\alpha \;=\; \langle \hat{a}_{i\alpha} \rangle \qquad , \qquad \Psi^*_\alpha = \left\langle \hat{a}^\dagger_{i\alpha} \right\rangle , \tag{3.2}$$

with $\alpha = -1, 0, 1$ denoting the spin index. Note that these order parameters do not depend on the site index i due to homogenity. In the case of the Mott insulator-superfluid phase transition we will be examining, the relevant symmetry is the breaking of the global $U(1)$ phase symmetry

$$\hat{a}_{i\alpha} \;\rightarrow\; \hat{a}_{i\alpha} e^{i\theta} \qquad , \qquad \hat{a}^\dagger_{i\alpha} \rightarrow \hat{a}^\dagger_{i\alpha} e^{-i\theta} \qquad , \tag{3.3}$$

in the superfluid ground state [110]. Due to (3.2) the expectation value of the creation and annihilation operators must not depend on the phase angle θ, which is only possible when

$$\langle \hat{a}_{i\alpha} \rangle \;=\; \left\langle \hat{a}^\dagger_{i\alpha} \right\rangle = 0 \quad . \tag{3.4}$$

Clearly, from Eq. (3.1), this represents the symmetry of the underlying Hamiltonian, so that the breaking of it by the ground state of the system is referred to as spontaneous symmetry breaking.

Here we review the mean-field theory for the Bose-Hubbard model of spin-1 bosons with which we can describe the superfluid-Mott insulator quantum phase transition [81, 104]. To study this, we consider the Bose-Hubbard model in the strong-coupling limit. The unperturbed Hamiltonian

$$\hat{H}^{(0)} = \sum_i \left[-\mu \hat{n}_i + \frac{U_0}{2} \hat{n}_i (\hat{n}_i - 1) + \frac{U_2}{2} (\hat{\mathbf{S}}_i^2 - 2\hat{n}_i) - \eta \hat{S}_i^z \right] \tag{3.5}$$

is then local, while the perturbation

$$\hat{H}^{(1)} = -J \sum_{\langle i,j \rangle} \sum_\alpha \hat{a}^\dagger_{i\alpha} \hat{a}_{j\alpha} \tag{3.6}$$

is bilocal as it couples different lattice sites. In mean field theory, the idea is to rewrite the field operators as a sum of their mean values, and their fluctuations, i.e,

$$\hat{a}_{j\alpha} = \langle \hat{a}_{j\alpha} \rangle + \delta \hat{a}_{j\alpha} \qquad , \qquad \hat{a}^\dagger_{i\alpha} = \left\langle \hat{a}^\dagger_{i\alpha} \right\rangle + \delta \hat{a}^\dagger_{i\alpha}. \tag{3.7}$$

Thus we obtain for the square of fluctuations

$$\delta \hat{a}^\dagger_{i\alpha} \delta \hat{a}_{j\alpha} = \hat{a}^\dagger_{i\alpha} \hat{a}_{j\alpha} - \langle \hat{a}_{j\alpha} \rangle \, \hat{a}^\dagger_{i\alpha} - \left\langle \hat{a}^\dagger_{i\alpha} \right\rangle \hat{a}_{j\alpha} + \left\langle \hat{a}^\dagger_{i\alpha} \right\rangle \langle \hat{a}_{j\alpha} \rangle \, . \tag{3.8}$$

The mean-field approximation is achieved by neglecting products of such fluctuations, i.e., neglecting the term $\delta \hat{a}^\dagger_{i\alpha} \delta \hat{a}_{j\alpha}$ in Eq. (3.8), which results in the mean-field approximation

$$\hat{a}^\dagger_{i\alpha} \hat{a}_{j\alpha} \approx \langle \hat{a}_{j\alpha} \rangle \, \hat{a}^\dagger_{i\alpha} + \left\langle \hat{a}^\dagger_{i\alpha} \right\rangle \hat{a}_{j\alpha} - \left\langle \hat{a}^\dagger_{i\alpha} \right\rangle \langle \hat{a}_{j\alpha} \rangle \, . \tag{3.9}$$

Since our system is translationally invariant, the expectation value of the operators must not depend on the site index i. Therefore, introducing the order parameters according to (3.2), Eq. (3.9) reduces

to

$$\hat{a}_{i\alpha}^{\dagger}\hat{a}_{j\alpha} \approx \Psi_{\alpha}\hat{a}_{i\alpha}^{\dagger} + \Psi_{\alpha}^{*}\hat{a}_{j\alpha} - \Psi_{\alpha}^{*}\Psi_{\alpha}. \tag{3.10}$$

Using this approximation in (3.1), the Bose-Hubbard mean-field Hamiltonian becomes local

$$\hat{H}_{\mathrm{MF}} = \sum_{i}\left[\hat{H}_{i}^{(0)} + \hat{H}_{i\mathrm{MF}}^{(1)}\right], \tag{3.11}$$

where the localized hopping term reads

$$\hat{H}_{i\mathrm{MF}}^{(1)} = -zJ\sum_{\alpha}\left(\Psi_{\alpha}\hat{a}_{i\alpha}^{\dagger} + \Psi_{\alpha}^{*}\hat{a}_{i\alpha} - |\Psi_{\alpha}|^{2}\right). \tag{3.12}$$

Note that the original summation $\langle i,j\rangle$ in (3.6) reduced here to $z\sum_{i}$, where z denotes the number of nearest-neighbor sites. This coordination number in a three-dimensional cubic lattice is given by $z = 6$.

Now we show that the order parameter (3.2) is determined from extremising the free energy

$$\mathcal{F}_{\mathrm{MF}} \;=\; -\frac{1}{\beta}\ln\mathcal{Z}_{\mathrm{MF}}, \tag{3.13}$$

where the grand-canonical partition function is defined by

$$\mathcal{Z}_{\mathrm{MF}} \;=\; \mathrm{Tr}\left[e^{-\beta\hat{H}_{\mathrm{MF}}}\right]. \tag{3.14}$$

This yields at first

$$\frac{\partial\mathcal{F}_{\mathrm{MF}}}{\partial\Psi_{\alpha}} = -\frac{1}{\beta}\frac{1}{\mathcal{Z}_{\mathrm{MF}}}\mathrm{Tr}\left[\frac{\partial}{\partial\Psi_{\alpha}}e^{-\beta\hat{H}_{\mathrm{MF}}}\right] = 0 \tag{3.15}$$

with the three different hyperfine states $\alpha = 0, \pm 1$. Therefore, we get

$$\begin{aligned}\frac{\partial\mathcal{F}_{\mathrm{MF}}}{\partial\Psi_{\alpha}} &= \frac{1}{\mathcal{Z}_{\mathrm{MF}}}\mathrm{Tr}\left[\frac{\partial\hat{H}_{\mathrm{MF}}}{\partial\Psi_{\alpha}}e^{-\beta\hat{H}_{\mathrm{MF}}}\right]\\ &= \frac{-zJ}{\mathcal{Z}_{\mathrm{MF}}}\sum_{i}\sum_{\alpha}\mathrm{Tr}\left[\left(a_{i\alpha}^{\dagger} - \Psi_{\alpha}^{*}\right)e^{-\beta\hat{H}_{\mathrm{MF}}}\right] = 0.\end{aligned} \tag{3.16}$$

Here condition (3.16) reduces to

$$\sum_{i}\left(\left\langle a_{i\alpha}^{\dagger}\right\rangle - \Psi_{\alpha}^{*}\right) = 0 \tag{3.17}$$

because of the thermal expectation value

$$\langle\bullet\rangle = \frac{1}{\mathcal{Z}_{\mathrm{MF}}}\mathrm{Tr}\left[\bullet e^{-\beta\hat{H}_{\mathrm{MF}}}\right]. \tag{3.18}$$

Since the thermal expectation value $\left\langle a_{i\alpha}^{\dagger}\right\rangle$ does not depend on the site i due to the translational

invariance, Eq. (3.17) becomes

$$N_s \left(\left\langle a_{i\alpha}^{\dagger} \right\rangle - \Psi_{\alpha}^{*} \right) = 0, \tag{3.19}$$

where N_s denotes the number of lattice sites. Therefore, (3.19) coincides with the self-consistency condition (3.2).

Thus, the free energy of the mean-field system represents a function of the order parameter which can be calculated perturbatively in the vicinity of the phase transition. This means that, near the quantum phase boundary, the free energy can be expanded in a power series of the order parameter Ψ_α. Due to the above mentioned $U(1)$-symmetry the lowest order term must be a function of $|\Psi_\alpha|^2$:

$$\frac{\mathcal{F}_{\mathrm{MF}}}{N_S} = a_0 + \sum_{\alpha} a_{2\alpha} |\Psi_\alpha|^2 + \cdots , \tag{3.20}$$

where the Landau coefficients $a_{2\alpha}$ will now be calculated. At zero temperature the zeroth-order Landau coefficient a_0 coincides with the lowest eigenvalue (2.41) of the unperturbed Hamiltonian (3.5):

$$a_0 = E_{S,m,n}^{(0)} = -\mu n + \frac{U_0}{2} n(n-1) + \frac{U_2}{2} \big[S(S+1) - 2n \big] - \eta m. \tag{3.21}$$

For fixed parameter values of U_0, U_2, μ, η the minimization of (3.21) yields the quantum numbers S, m, n, which characterize the ground state, as discussed in detail in Section 2.4.

3.3. Mean-Field Perturbation Theory

In order to determine the Landau coefficient $a_{2\alpha}$, we use the on-site mean-field perturbation theory which was developed in Refs. [81, 104] for the Bose-Hubbard model of spin-1 bosons. The on-site mean-field perturbation Hamiltonian

$$\hat{H}_{\mathrm{MF}}^{(1)} = -zJ \sum_{\alpha} \left(\Psi_\alpha \hat{a}_\alpha^{\dagger} + \Psi_\alpha^{*} \hat{a}_\alpha - |\Psi_\alpha|^2 \right) \tag{3.22}$$

acts on an eigenstate $|S,m,n\rangle$ of the unperturbed Hamiltonian (3.5). Thus, we need to calculate $\hat{a}_\alpha^{\dagger} \mid S,m,n \rangle$ and $\hat{a}_\alpha \mid S,m,n \rangle$ as the order parameters Ψ_α and Ψ_α^{*} are not operators. It is possible to show that a spin-1 particle with its spin orientation specified by α can be produced by the creation operator $\hat{a}_\alpha^{\dagger}$. We find that $\hat{a}_\alpha^{\dagger} \mid S,m,n \rangle$ is directly proportional to $|S \pm 1, m+\alpha, n+1\rangle$ due to the conservation of the z-component of the magnetic moment and of the spin. As a result of adding one spin-1 particle, the quantum number of the total spin will be changed by ± 1. Similarly, $\hat{a}_\alpha \mid S,m,n \rangle$ is directly proportional to $|S \pm 1, m-\alpha, n-1\rangle$ since a spin-1 particle is annihilated. Thus, these results can be written in the following form [81, 104]:

$$\hat{a}_\alpha^{\dagger} |S,m,n\rangle = M_{\alpha,S,m,n} |S+1, m+\alpha, n+1\rangle + N_{\alpha,S,m,n} |S-1, m+\alpha, n+1\rangle , \tag{3.23}$$

$$\hat{a}_\alpha |S,m,n\rangle = O_{\alpha,S,m,n} |S+1, m-\alpha, n-1\rangle + P_{\alpha,S,m,n} |S-1, m-\alpha, n-1\rangle , \tag{3.24}$$

where $M_{\alpha,S,m,n}$ and $N_{\alpha,S,m,n}$ are the matrix elements of creation and correspondingly, $O_{\alpha,S,m,n}$ and $P_{\alpha,S,m,n}$ are the matrix elements of annihilation. These matrix elements are calculated recursively in Appendix A.

As discussed in Subsection 2.4.2, with finite external magnetic field all ground states turn out to be of the form $|S,S,n\rangle$ with $0 \leq S \leq n$. To calculate the first-order correction in $\hat{H}^{(1)}_{\mathrm{MF}}$, we treat the mean-field hopping term (3.22) as a perturbation. From Eqs. (2.40), and (3.22)–(3.24), we obtain

$$E^{(1)}_{S,S,n} = \left|\left\langle S,S,n \left| \hat{H}^{(1)}_{\mathrm{MF}} \right| S,S,n \right\rangle\right| = zJ \sum_{\alpha} |\Psi_\alpha|^2 \,. \tag{3.25}$$

Correspondingly, the second-order correction to the ground-state energy reads

$$E^{(2)}_{S,S,n} = \sum_{S',m',n' \neq S,S,n} \frac{\left|\left\langle S',m',n' \left| \hat{H}^{(1)}_{\mathrm{MF}} \right| S,S,n \right\rangle\right|^2}{E_{S',m',n'} - E_{S,S,n}}. \tag{3.26}$$

Inserting Eqs. (3.22)–(3.24) into (3.26), we get

$$\begin{aligned} E^{(2)}_{S,S,n} = (zJ)^2 \sum_{\alpha} |\Psi_\alpha|^2 \Bigg[& \frac{M^2_{\alpha,S,S,n}}{E^{(0)}_{S+1,S+\alpha,n+1} - E^{(0)}_{S,S,n}} + \frac{N^2_{\alpha,S,S,n}}{E^{(0)}_{S-1,S+\alpha,n+1} - E^{(0)}_{S,S,n}} \\ & + \frac{O^2_{\alpha,S,S,n}}{E^{(0)}_{S+1,S-\alpha,n-1} - E^{(0)}_{S,S,n}} + \frac{P^2_{\alpha,S,S,n}}{E^{(0)}_{S-1,S-\alpha,n-1} - E^{(0)}_{S,S,n}} \Bigg] . \end{aligned} \tag{3.27}$$

From a comparison with Eq. (3.20), we then obtain the Landau coefficients:

$$\begin{aligned} a_{2\alpha} = (zJ)^2 \Bigg[& \frac{M^2_{\alpha,S,S,n}}{E^{(0)}_{S+1,S+\alpha,n+1} - E^{(0)}_{S,S,n}} + \frac{N^2_{\alpha,S,S,n}}{E^{(0)}_{S-1,S+\alpha,n+1} - E^{(0)}_{S,S,n}} \\ & + \frac{O^2_{\alpha,S,S,n}}{E^{(0)}_{S+1,S-\alpha,n-1} - E^{(0)}_{S,S,n}} + \frac{P^2_{\alpha,S,S,n}}{E^{(0)}_{S-1,S-\alpha,n-1} - E^{(0)}_{S,S,n}} \Bigg] + zJ. \end{aligned} \tag{3.28}$$

In the next section, we plot the resulting Mott insulator-superfluid phase boundary without and with magnetization by using these Landau coefficients.

3.4. Phase Boundary at Zero Temperature

In this section, we calculate the Mott insulator-superfluid phase transition. To do this, we know that extremising of the free energy (3.20) yields the value of the order parameter

$$\boldsymbol{\Psi} = (\Psi_1, \Psi_0, \Psi_{-1}) \,, \tag{3.29}$$

where the Mott insulator phase is the ground state with $\mathbf{\Psi} = 0$ and the superfluid phase corresponds to $\mathbf{\Psi} \neq 0$. In order to be able to determine this quantum phase boundary, we set

$$a_{2\alpha} = 0 \qquad . \tag{3.30}$$

In Chapter 4 we will calculate a_4 and only then we will be able to determine that the quantum phase transition is of a second-order phase transition, which leads to the condition (3.30). For the transition from the Mott insulator to the superfluid phase the critical hopping parameter with a spin index α follows from (3.28) and (3.30):

$$\begin{aligned} zJ_{c,\alpha} = \Bigg[& \frac{M^2_{\alpha,S,S,n}}{E^{(0)}_{S+1,S+\alpha,n+1} - E^{(0)}_{S,S,n}} + \frac{N^2_{\alpha,S,S,n}}{E^{(0)}_{S-1,S+\alpha,n+1} - E^{(0)}_{S,S,n}} \\ & + \frac{O^2_{\alpha,S,S,n}}{E^{(0)}_{S+1,S-\alpha,n-1} - E^{(0)}_{S,S,n}} + \frac{P^2_{\alpha,S,m,n}}{E^{(0)}_{S-1,S-\alpha,n-1} - E^{(0)}_{S,S,n}} \Bigg]^{-1} . \end{aligned} \tag{3.31}$$

In order to obtain the location of the quantum phase transition, we have to take the minimum of Eq. (3.31) with respect to the spin index α [81, 104]:

$$zJ_c = \min_{\alpha} J_{c,\alpha}. \tag{3.32}$$

3.4.1. No Magnetization

At first we discuss the quantum phase boundary in the case of **ferromagnetic interaction** $U_2 < 0$ with vanishing magnetization, i.e. $\eta = 0$. In this situation, all states with the same total spin quantum number S are degenerated with respect to their magnetic quantum number m, thus we can use here the short-hand notation $E^{(0)}_{S,n} = E^{(0)}_{S,m,n}$ for the unperturbed energy eigenvalues. In addition, the ferromagnetic interaction yields a minimal energy when the spin is maximal, i.e. $S = n$. Therefore, the ground state becomes $|n, n, n\rangle$ [31, 81]. From Appendix A, we obtain the required coefficients as follows:

$$M_{1,n,n,n} = \sqrt{n+1}, \quad M_{-1,n,n,n} = \sqrt{\frac{1}{2n+1}}, \tag{3.33}$$

$$M_{0,n,n,n} = 1, \quad N_{1,n,n,n} = 0, \tag{3.34}$$

$$N_{-1,n,n,n} = -\sqrt{\frac{2n}{2n+1}}, \quad N_{0,n,n,n} = 0, \tag{3.35}$$

$$P_{1,n,n,n} = \sqrt{n}, \quad P_{0,n,n,n} = P_{-1,n,n,n} = 0, \tag{3.36}$$

$$O_{\alpha,n,n,n} = 0, \quad \alpha = 0, \pm 1. \tag{3.37}$$

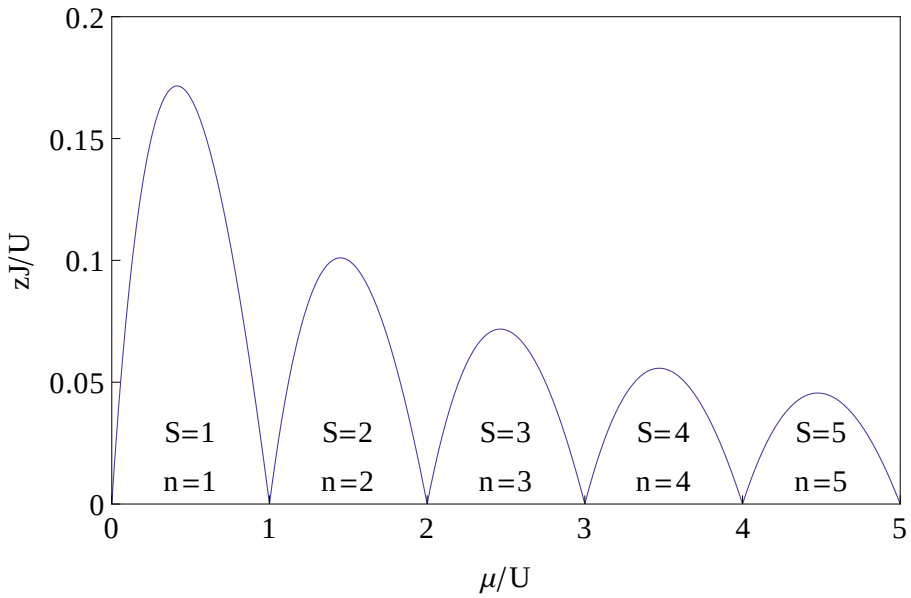

Figure 3.3.: Quantum phase boundary between a Mott insulator and a superfluid phase for ferromagnetic interaction $U_2 < 0$ with $\eta = 0$.

In order to simplify the notation we also define the effective interaction strength $U = U_0 + U_2$. Inserting Eqs. (3.33)–(3.37) into (3.31), we get

$$\frac{zJ_{c,1}}{U} = \left(\frac{n+1}{n-\mu/U} + \frac{n}{1-n+\mu/U} \right)^{-1} . \tag{3.38}$$

When we calculate $zJ_{c,0}$ and $zJ_{c,-1}$, we find that both are larger than $zJ_{c,1}$. Therefore, due to(3.32), the resulting quantum phase boundary is exactly the mean-field result of the scalar Bose-Hubbard model in Ref. [65] as shown in Fig. 3.3.

On the other side, for **anti-ferromagnetic interaction** $U_2 > 0$ with $\eta = 0$, the minimization of the energy implies a minimum of the spin value which depends on the number of atoms per site. The ground state of the nonperturbative Hamiltonian is $|0, 0, n\rangle$ for even n [80] and $|1, m, n\rangle$ for odd particle number n [31, 81] as was already discussed in Section 2.4. In the latter case we have to determine the value of m to get the minimum of the critical hopping. This means that we have to find this minimum with respect to both α and m in order to determine the phase boundary. The result is that the component with $m = 0$ forms the superfluid, i.e. $\Psi_0 \neq 0$, so the SF phase is a polar state with $\Psi_1 = \Psi_{-1} = 0$ in agreement with previous results in the literature [80, 81]. Thus, using the matrix elements from Appendix A and Eq. (2.41), Eq. (3.31) reduces to

- **Mott insulator with an even number of atoms**

$$zJ_{c,0} = \left(\frac{M^2_{0,0,0,n}}{E^{(0)}_{1,n+1} - E^{(0)}_{0,n}} + \frac{O^2_{0,0,0,n}}{E^{(0)}_{1,n-1} - E^{(0)}_{0,n}} \right)^{-1} , \tag{3.39}$$

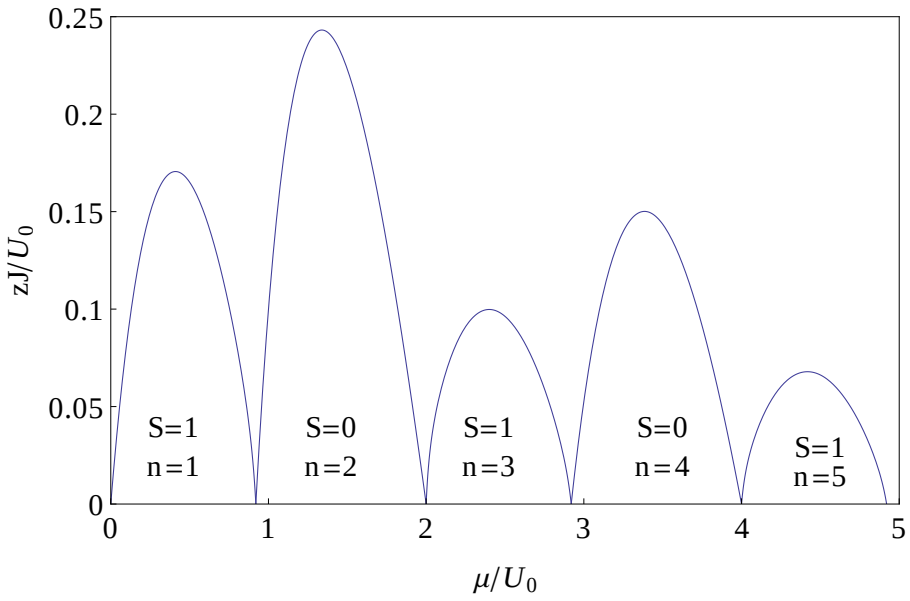

Figure 3.4.: Quantum phase boundary between a Mott insulator and a superfluid phase for antiferromagnetic interaction $U_2 > 0$ with $U_2/U_0 = 0.04$ and $\eta = 0$ [81, 104].

where the non-vanishing matrix elements are given by

$$M_{0,0,0,n} = \sqrt{\frac{n+1}{3}}, \qquad O_{0,0,0,n} = \sqrt{\frac{n}{3}}. \tag{3.40}$$

- **Mott insulator with an odd number of atoms**

$$zJ_{c,0} = \left(\frac{M^2_{0,1,0,n}}{E^{(0)}_{2,n+1} - E^{(0)}_{1,n}} + \frac{N^2_{0,1,0,n}}{E^{(0)}_{0,n+1} - E^{(0)}_{1,n}} + \frac{O^2_{0,1,0,n}}{E^{(0)}_{2,n-1} - E^{(0)}_{1,n}} + \frac{P^2_{0,1,0,n}}{E^{(0)}_{0,n-1} - E^{(0)}_{1,n}} \right)^{-1}, \tag{3.41}$$

where the non-vanishing matrix elements read

$$M_{0,1,0,n} = 2\sqrt{\frac{n+4}{15}} \quad , \quad N_{0,1,0,n} = \sqrt{\frac{n+1}{3}}, \tag{3.42}$$

$$O_{0,1,0,n} = 2\sqrt{\frac{n-1}{15}} \quad , \quad P_{0,1,0,n} = \sqrt{\frac{n+2}{3}}. \tag{3.43}$$

There are several aspects of the spin-1 Bose-Hubbard model which already appear at $J = 0$. The ground-state energy for an odd and even number is $E^{(0)}_{1,n} = -\mu n + \frac{U_0}{2} n(n-1) + U_2 (1-n)$ and $E^{(0)}_{0,n} = -\mu n + \frac{U_0}{2} n(n-1) - U_2 n$, respectively. If the system goes from the nth to the $(n+1)$th Mott lobe, the chemical potential results from the conditions $\triangle E^{(0)} [n_{\text{odd}} \to (n_{\text{odd}} + 1)] = 0$ and $\triangle E^{(0)} [n_{\text{even}} \to (n_{\text{even}} + 1)] = 0$, respectively [115]. Thus, the values $\mu [n_{\text{odd}} \to (n_{\text{odd}} + 1)] = n_{\text{odd}} U_0 - 2U_2$ and $\mu [n_{\text{even}} \to (n_{\text{even}} + 1)] = n_{\text{even}} U_0$ become the lobe boundaries. Therefore, in the **antiferromagnetic case**, i.e. $U_2 > 0$, the even Mott lobes expand and the odd Mott lobes shrink as shown in Fig. 3.4.

We remark that the even Mott lobes are strongly stabilized against the superfluid phase in comparison with the odd Mott lobes as shown in Fig. 3.4 [81]. The reason is that all atoms in an even Mott lobe,

which have total spin 0, form singlet pairs at each lattice site. Therefore, the bosons are not able to hop to the nearest neighbor sites. On the other hand, one single atom in an odd Mott lobes can not make a singlet pair on each site. Thus, it has the total spin 1 and can hop easier to neighboring site.

3.4.2. With magnetization

In this section, we will study the effect of the external magnetic field η on the phase boundary. To this end we assume without loss of generality that $\eta > 0$. In Subsection 2.4.2, we found many different ground states for the even and odd lobes and discussed how they depend on η. To this end we note that the general ground state can be taken as $|S, S, n\rangle$.

For a **ferromagnetic interaction**, there is no change as the minimization of the energy implies the maximum of spin value as it is in the case without η except the degeneracy with respect to m is lifted, so the ground state becomes $|n, n, n\rangle$. Thus, the quantum phase boundary with η is the same as that without it as shown in Fig. 3.3.

For an **anti-ferromagnetic interaction**, the situation is more complicated. If η is large compared with U_2, all spins will be aligned in the z-direction, so the ground state will be a high spin state $|n, n, n\rangle$ as seen in Fig. 3.5f. In the opposite limit that η is small in comparison with U_2, the ground state will be $|0, 0, n\rangle$ for even n and $|1, 1, n\rangle$ for odd n as seen in Fig. 3.5a. In between the ground state can be $|S, S, n\rangle$ with $0 \leq S \leq n$ as discussed in detail in Subsection 2.4.2. Using the matrix elements from Appendix A and Eqs. (2.41) and (3.32), we get

- **Mott insulator with an even number of atoms**

$$zJ_{c,\alpha} = \left(\frac{M^2_{\alpha,0,0,n}}{E^{(0)}_{1,\alpha,n+1} - E^{(0)}_{0,0,n}} + \frac{O^2_{\alpha,0,0,n}}{E^{(0)}_{1,-\alpha,n-1} - E^{(0)}_{0,0,n}} \right)^{-1}, \tag{3.44}$$

  where

$$M_{\alpha,0,0,n} = \sqrt{\frac{n+1}{3}}, \qquad O_{\alpha,0,0,n} = \sqrt{\frac{n}{3}}, \tag{3.45}$$

- **Mott insulator with an odd number of atoms**

$$zJ_{c,\alpha} = \left[\frac{M^2_{\alpha,1,1,n}}{E^{(0)}_{2,1+\alpha,n+1} - E^{(0)}_{1,1,n}} + \frac{N^2_{\alpha,1,1,n}}{E^{(0)}_{0,1+\alpha,n+1} - E^{(0)}_{1,1,n}} + \frac{O^2_{\alpha,1,1,n}}{E^{(0)}_{2,1-\alpha,n-1} - E^{(0)}_{1,1,n}} + \frac{P^2_{\alpha,1,1,n}}{E^{(0)}_{0,1-\alpha,n-1} - E^{(0)}_{1,1,n}} \right]^{-1}, \tag{3.46}$$

  where the matrix elements are determined by Appendix A. Both for an even and odd number of atoms it still remains to determine the minimum of (3.44) and (3.46) with respect to α.

In the next two sections, we show in more detail how η and U_2 affect the quantum phase boundary.

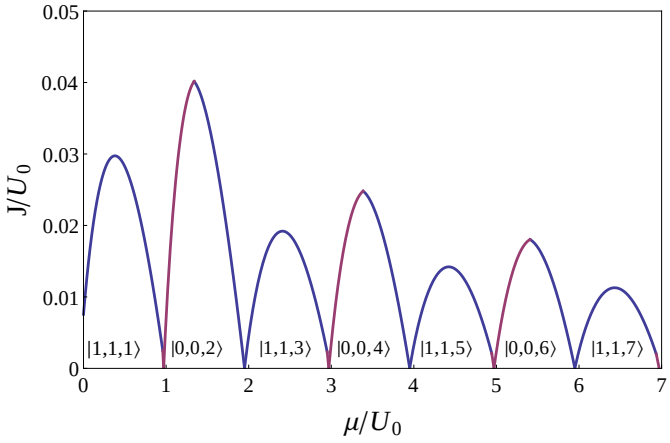

(a) $\eta/U_0 = 0.05$ [104].

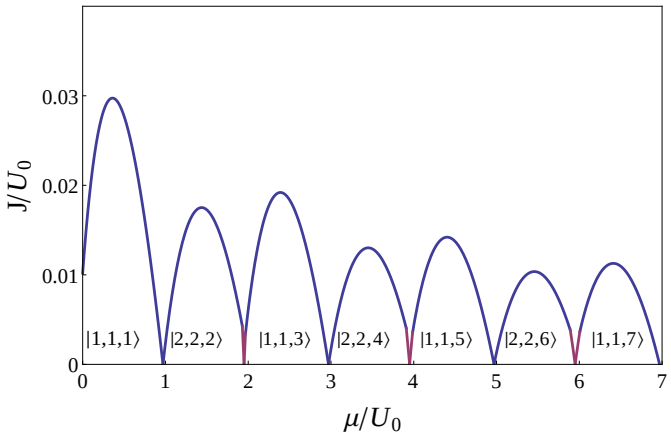

(b) $\eta/U_0 = 0.07$.

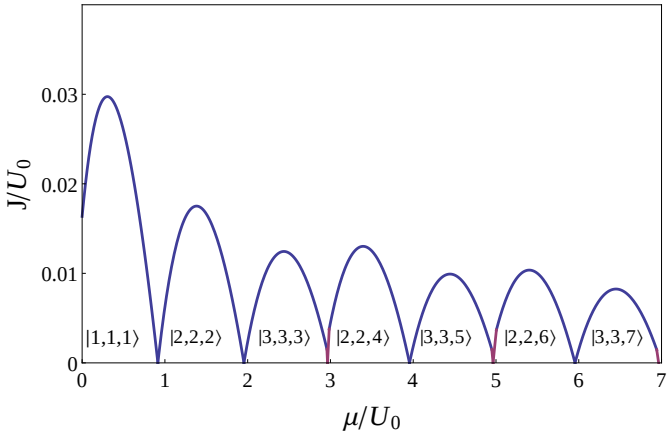

(c) $\eta/U_0 = 0.125$.

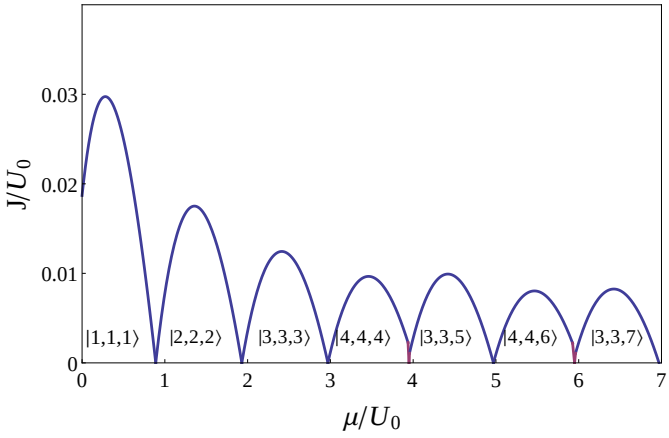

(d) $\eta/U_0 = 0.15$.

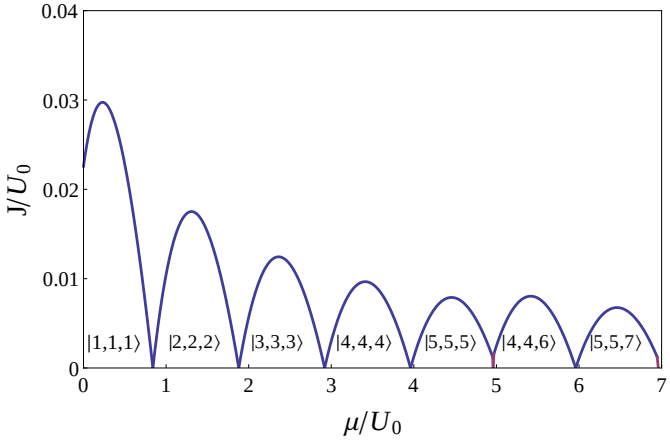

(e) $\eta/U_0 = 0.2$.

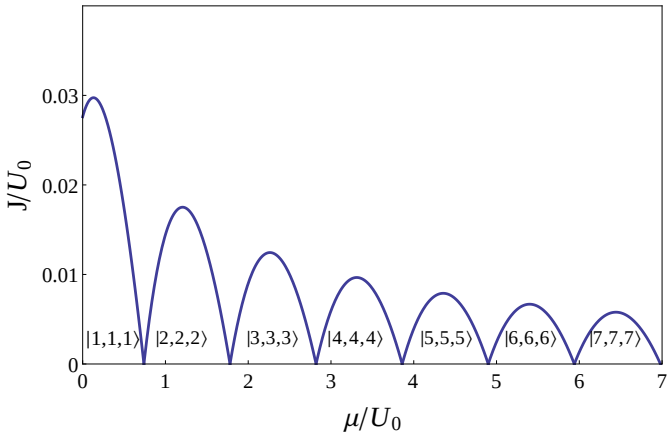

(f) $\eta/U_0 = 0.3$.

Figure 3.5.: Quantum phase boundary between Mott insulator and superfluid phase for antiferromagnetic interaction with $U_2/U_0 = 0.04$. The blue and red line correspond to an instability of the spin-1 and spin-(-1) component, respectively.

3.5. Effect of Magnetization on Quantum Phase Boundary

In this subsection we explain the effect of the external magnetic field η on the phase boundary between superfluid phase and Mott insulator phases with the fixed value $U_2 = 0.04\ U_0$, which corresponds to ^{23}Na atoms, as shown in Fig. 3.5:

- As discussed above, when the external magnetic field η is small in comparison with U_2, the ground state is $|0,0,n\rangle$ ($|1,1,n\rangle$) for even (odd) n. The minimization of (3.44) and (3.46) for spin index α yields that the components of spin-1 and spin-(-1) lead to the quantum phase boundary, whereas the spin-0 component has no effect [82, 104] as shown in Fig. 3.5a.

- When the external magnetic field η is increased above the critical $\eta^{(1)}_{\text{even}} = 0.06\,U_0$, which has been determined discussed in Subsection 2.4.2, the ground states change from $|0,0,n\rangle$ to $|2,2,n\rangle$ for even lobes as shown in Fig. 3.5b. Thus, the Mott insulator phases for the even lobes are decreased. The components of spin-1 and spin-(-1) still lead to the phase boundary for all lobes except for the first lobe, where the phase boundary is only determined by the spin-1 component.

- When η is increased further beyond the critical value $\eta^{(1)}_{\text{odd}} = 0.1U_0$, the quantum number S and m for the odd lobes change from $|1,1,n\rangle$ to $|3,3,n\rangle$ as shown in Fig. 3.5c. The phase boundary for the first and second lobe is only determined by the spin-1 component, but all other lobes stem from the spin-1 and spin-(-1) component.

- When η increases beyond $\eta^{(2)}_{\text{even}} = 0.14\,U_0$, S and m for the even lobes change from $|2,2,n\rangle$ to $|4,4,n\rangle$ as shown in Fig. 3.5d. Similarly, the phase boundary for the first three lobes are only determined by spin-1 component, but the other lobes stem from the spin-1 and spin-(-1) components.

- Beyond the critical value $\eta^{(2)}_{\text{odd}} = 0.18\,U_0$, S and m for the even lobes change from $|3,3,n\rangle$ to $|5,5,n\rangle$ as shown in Fig. 3.5e. The component of spin-1 affects the phase boundary for the first four lobes but the spin-1 and spin-(-1) component determine the other lobes.

- When η increases to 0.3 U_0 beyond the critical values $\eta^{(3)}_{\text{even}} = 0.22\,U_0$ and $\eta^{(3)}_{\text{odd}} = 0.26\,U_0$, S and m changes from $|4,4,n\rangle$ to $|6,6,n\rangle$ for the even lobes and from $|5,5,n\rangle$ to $|7,7,n\rangle$ for the odd lobes as shown in Fig. 3.5f, so all seven lobes have now $S = m = n$. Therefore, the ground state corresponds to one of a ferromagnetic interaction and only the spin-1 component determines the phase boundary.

3.6. Effect of Spin-Dependent Interaction on Quantum Phase Boundary

In this subsection we explain the effect of spin-dependent interaction U_2 on the phase boundary between superfluid phase and Mott insulator phases for a fixed external magnetic field $\eta = 0.2\,U_0$ as shown in Fig. 3.6.

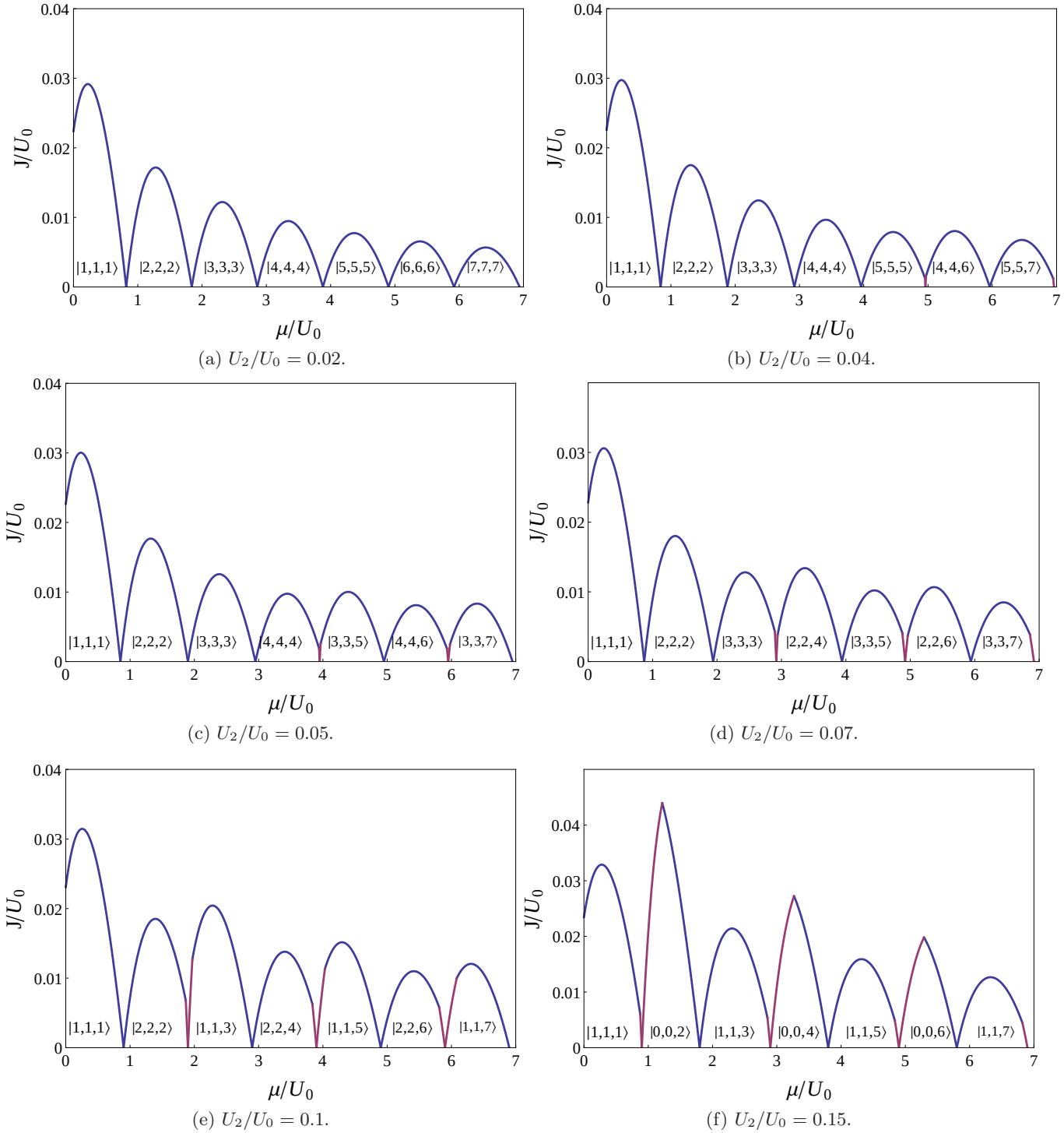

(a) $U_2/U_0 = 0.02$. (b) $U_2/U_0 = 0.04$.

(c) $U_2/U_0 = 0.05$. (d) $U_2/U_0 = 0.07$.

(e) $U_2/U_0 = 0.1$. (f) $U_2/U_0 = 0.15$.

Figure 3.6.: Quantum phase boundary between Mott insulator and superfluid phase for antiferromagnetic interaction with $\eta = 0.2$. The blue and red line correspond to an instability of the spin-1 and spin-(-1) component, respectively.

- If U_2 is 0.02 U_0, the phase boundary is only determined by spin-1 component. Therefore, the ground state $|n, n, n\rangle$ is ferromagnetic with maximum spin for all six lobes as shown in Fig. 3.6a. So, the phase boundaries for all lobes are only determined by the spin-1 component.

- When U_2 is increased above the critical values $U_{2\text{odd}}^{(1)} = 0.0308\,U_0$ and $U_{2\text{even}}^{(1)} = 0.036\,U_0$ as discussed in Subsection 2.4.2, both the spin S and the magnetic quantum numbers m change from $|7, 7, n\rangle$ to $|5, 5, n\rangle$ for odd lobes and from $|7, 7, n\rangle$ to $|5, 5, n\rangle$ for even lobes, respectively as shown in Fig. 3.6b. When spin-dependent interaction is increased, the effect of magnetic field is decreased. Therefore, the Mott lobes will be increased and the phase boundary for the fifth, sixth and seventh lobe is determined by spin-1 and spin-(-1) components but that of the other lobes is still determined by the spin-1 component.

- Beyond the critical value $U_{2\text{odd}}^{(2)} = 0.044\,U_0$, the S and m for the odd lobes change from $|5, 5, n\rangle$ to $|3, 3, n\rangle$ as shown in Fig. 3.6c. The spin-1 and spin-(-1) components determine the phase boundary for the last four lobes. However, the phase boundary for the other lobes stem from the spin-1 component.

- After the critical value $U_{2\text{even}}^{(2)} = 0.05714U_0$, the quantum numbers S and m change from $|4, 4, n\rangle$ to $|2, 2, n\rangle$ for the even lobes as shown in Fig. 3.6d and the Mott lobes continue to increase. The phase boundary for the last five lobes stem from spin-1 and spin-(-1) components, but the phase boundary for the first and second lobe is only effected by the spin-1 component.

- Beyond the critical value $U_{2\text{odd}}^{(3)} = 0.08\,U_0$, the quantum numbers S and m change from $|3, 3, n\rangle$ to $|1, 1, n\rangle$ for the odd lobes as shown in Fig. 3.6e. Similarly, the phase boundary for all lobes except the first lobe is determined by spin-1 and spin-(-1) component.

- If U_2 reaches to 0.15 U_0 beyond the critical value $U_{2\text{even}}^{(3)} = 0.133\,U_0$, the quantum numbers S and m change from $|2, 2, n\rangle$ to $|0, 0, n\rangle$ for the even lobes as shown in Fig. 3.6f. When the value of η is close to U_2, the effect of the magnetic field becomes negligible. Therefore, the ground state becomes anti-ferromagnetic with $|0, 0, n\rangle$ for an even n and $|1, 1, n\rangle$ for an odd n. Therefore, the phase boundary for all lobes is now determined by both the spin-1 and the spin-(-1) component.

4. Free Energy

In the previous chapter, we calculated the Mott insulator-superfluid phase boundary by working out a mean-field theory for the spin-1 Bose-Hubbard model at zero-temperature. In this chapter we follow Refs. [84, 85] and develop an alternative field-theoretic approach to determine the quantum phase boundary in terms of a Ginzburg-Landau theory, where additional source currents are added to the spin-1 Bose-Hubbard model in order to break the global $U(1)$ symmetry. To this end a strong-coupling perturbation theory will be developed by taking into account diagrammatic rules which treat the bosons in a cubic optical lattices. Thus, we get a diagrammatic expansion of the grand-canonical free energy in the first order of the hopping parameter and in the fourth order of the symmetry-breaking currents. As a cross-check we demonstrate that the resulting grand-canonical free energy allows to recover the mean-field theory. Furthermore, we determine the validity range of the mean-field theory for the spin-1 Bose-Hubbard model.

4.1. Ginzburg-Landau Theory

We introduce site, imaginary-time and spin-dependent sources to deal with the spin-dependent order parameters of systems which exhibit spontaneous symmetry breaking [116,117]. With this, the general Hamiltonian reads as follows:

$$\hat{H}_{\mathrm{BH}}(\tau) = \hat{H}_{\mathrm{BH}} + \sum_{i} \sum_{\alpha} \left[j^{*}_{i\alpha}(\tau)\hat{a}_{i\alpha} + j_{i\alpha}(\tau)\hat{a}^{\dagger}_{i\alpha} \right]. \tag{4.1}$$

The imaginary-time evolution operator with $\tau = it$ is defined with $\hbar = 1$ by the differential equation

$$-\frac{\partial \hat{U}(\tau,\tau_0)}{\partial \tau} = \hat{H}_{\mathrm{BH}}(\tau)\hat{U}(\tau,\tau_0). \tag{4.2}$$

Its solution with the initial condition

$$\hat{U}(\tau_0,\tau_0) = 1 \tag{4.3}$$

can be written as

$$\hat{U}(\tau,\tau_0) = \hat{T} e^{-\int_{\tau_0}^{\tau} d\tau' \hat{H}_{\mathrm{BH}}(\tau')}, \tag{4.4}$$

where $\hat{T}$ denotes the imaginary-time ordering operator which is defined as

$$\hat{T}\left[\hat{A}(\tau_1)\hat{A}(\tau_2)\right] = \Theta(\tau_1-\tau_2)\,\hat{A}(\tau_1)\hat{A}(\tau_2) + \Theta(\tau_2-\tau_1)\,\hat{A}(\tau_2)\hat{A}(\tau_1), \tag{4.5}$$

with Θ being the Heaviside step function. The partition function

$$\mathcal{Z}\left[j, j^*\right] = \mathrm{Tr}\ \hat{U}(\beta, 0) \tag{4.6}$$

can then be written as

$$\mathcal{Z}\left[j, j^*\right] = \mathcal{Z}_{\mathrm{BH}} \left\langle \hat{U}(\beta, 0) \right\rangle_{\mathrm{BH}}, \tag{4.7}$$

where the expectation value is defined according to

$$\langle \bullet \rangle = \frac{1}{\mathcal{Z}_{\mathrm{BH}}} \mathrm{Tr}\left[\bullet\ \exp\left\{ -\beta \hat{H}_{\mathrm{BH}} \right\} \right] \tag{4.8}$$

with the partition function of the unperturbed system being given by

$$\mathcal{Z}_{\mathrm{BH}} = \mathrm{Tr}\left[\exp\left\{ -\beta \hat{H}_{\mathrm{BH}} \right\} \right]. \tag{4.9}$$

Successive functional derivatives with respect to the currents yield Green functions of the Bose-Hubbard system. Here we do not work out further this source formalism, but consider instead the free energy which also becomes a generating functional

$$\mathcal{F}\left[j, j^*\right] = -\frac{1}{\beta} \ln \mathcal{Z}\left[j, j^*\right]. \tag{4.10}$$

We investigate the expectation value of the creation and annihilation operator

$$\psi^*_{i\alpha}(\tau) = \left\langle \hat{a}^\dagger_{i\alpha}(\tau) \right\rangle, \qquad \psi_{i\alpha}(\tau) = \left\langle \hat{a}_{i\alpha}(\tau) \right\rangle, \tag{4.11}$$

which may turn out to be non-zero in the thermodynamic limit and follows from

$$\psi_{i\alpha}(\tau) = \beta \frac{\delta \mathcal{F}}{\delta j^*_{i\alpha}(\tau)}, \qquad \psi^*_{i\alpha}(\tau) = \beta \frac{\delta \mathcal{F}}{\delta j_{i\alpha}(\tau)}. \tag{4.12}$$

We consider Eq. (4.12) as a motivation to perform a functional Legendre transformation and define the effective action according to

$$\Gamma\left[\Psi_{i\alpha}, \Psi^*_{i\alpha}\right] = \mathcal{F}\left[j, j^*\right] - \frac{1}{\beta} \sum_i \sum_\alpha \int_0^\beta d\tau \left[\Psi_{i\alpha}(\tau) j^*_{i\alpha}(\tau) + \Psi^*_{i\alpha}(\tau) j_{i\alpha}(\tau) \right]. \tag{4.13}$$

The Legendre identities complementary to Eq. (4.12) read

$$j_{i\alpha}(\tau) = -\beta \frac{\delta \Gamma\left[\Psi_{i\alpha}, \Psi^*_{i\alpha}\right]}{\delta \Psi^*_{i\alpha}(\tau)}, \qquad j^*_{i\alpha}(\tau) = -\beta \frac{\delta \Gamma\left[\Psi_{i\alpha}, \Psi^*_{i\alpha}\right]}{\delta \Psi_{i\alpha}(\tau)}. \tag{4.14}$$

To obtain the physical value of the order parameter, we put the currents in Eq. (4.14) to zero

$$\left. \frac{\delta \Gamma\left[\Psi_{i\alpha}, \Psi^*_{i\alpha}\right]}{\delta \Psi^*_{i\alpha}(\tau)} \right|_{j_{i\alpha}=0}^{j^*_{i\alpha}=0} = 0, \qquad \left. \frac{\delta \Gamma\left[\Psi_{i\alpha}, \Psi^*_{i\alpha}\right]}{\delta \Psi_{i\alpha}(\tau)} \right|_{j_{i\alpha}=0}^{j^*_{i\alpha}=0} = 0. \tag{4.15}$$

Therefore, the order parameter is determined from extremising the effective action. Furthermore, we read off from (4.13) that evaluating the effective action for the equilibrium field Ψ_{eq} yields the physical grand-canonical free energy:

$$\Gamma\Big|_{\Psi_{i\alpha}=\Psi_{\mathrm{eq}}}^{\Psi^*_{i\alpha}=\Psi^*_{\mathrm{eq}}} = \mathcal{F}\Big|_{j_{i\alpha}=0}^{j^*_{i\alpha}=0}. \tag{4.16}$$

4.2. Dirac Interaction Picture

In order to split the Hamiltonian into an unperturbed part and a perturbed part we switch to the imaginary-time Dirac interaction picture. Thus, the partition function will be expressed as a perturbation series. The Schrödinger picture, the Heisenberg picture, and the Dirac picture are the pictures which are most popular in quantum mechanics. Each picture has a different way to treat the time evolution of the system which is divided between the states and the operators. In the Schrödinger picture, the state vectors are time-dependent and the operators are constant in time. On the contrary, in the Heisenberg picture, the operators depend on time and the state vectors are independent of time. In the Dirac picture, however, both states and operators carry a time-dependence where the dynamics of the operators is determined the unperturbed part of the Hamiltonian and the states follow the perturbed part. This means that we split the Hamiltonian into a free part $\hat{H}^{(0)}$, which can be solved, and a perturbative term $\hat{H}^{(1)}$ according to $\hat{H}(\tau) = \hat{H}^{(0)}(\tau) + \hat{H}^{(1)}(\tau)$. In this picture, we use the Wick rotation [118, 119] $t \to -i\tau$ to determine the time evolution of both operators and states. The time evolution of the states and the operators in the interaction picture in imaginary time τ with $\hbar = 1$ are defined by

$$|\Psi_I(\tau)\rangle = \hat{U}_I(\tau, \tau') \left|\Psi_I(\tau')\right\rangle \tag{4.17}$$

and

$$A_I(\tau) = \hat{U}^{(0)-1}(\tau, \tau_0) A\, \hat{U}^{(0)}(\tau, \tau_0), \tag{4.18}$$

where the imaginary-time evolution operator in the Dirac interaction picture is given by

$$\hat{U}_I(\tau, \tau') = \hat{U}^{(0)-1}(\tau, \tau_0)\hat{U}(\tau, \tau')\hat{U}^{(0)}(\tau', \tau_0), \tag{4.19}$$

with the unperturbed imaginary-time evolution operator

$$\hat{U}^{(0)}(\tau, \tau_0) = e^{-\hat{H}^{(0)}(\tau - \tau_0)}. \tag{4.20}$$

The equation of motion for the state vector is

$$\frac{\partial \left|\Psi(\tau)\right\rangle_I}{\partial \tau} = -\hat{H}_I(\tau) \left|\Psi(\tau)\right\rangle_I, \tag{4.21}$$

where

$$\hat{H}_I(\tau) = \hat{U}^{(0)-1}(\tau, 0)\hat{H}^{(1)}(\tau)\hat{U}^{(0)}(\tau, 0). \tag{4.22}$$

Substituting (4.17) into (4.21), we get

$$\frac{\partial}{\partial\tau}\hat{U}_I(\tau,\tau_0) = -\hat{H}_I(\tau)\hat{U}_I(\tau,\tau_0). \tag{4.23}$$

Using the initial condition

$$\hat{U}_I(\tau_0,\tau_0) = 1 \tag{4.24}$$

Eq. (4.23) is formally solved by

$$\hat{U}_I(\tau,\tau_0) \;=\; 1 - \int_{\tau_0}^{\tau} d\tau' \hat{H}_I(\tau')\hat{U}_I(\tau',\tau_0). \tag{4.25}$$

By solving this integral equation iteratively we obtain the Dyson series as follows:

$$\hat{U}_I(\tau,\tau_0) \;=\; 1 + \sum_{n=1}^{\infty}(-1)^n \int_{\tau_0}^{\tau} d\tau_1 \int_{\tau_0}^{\tau_1} d\tau_2 \cdots \int_{\tau_0}^{\tau_{n-1}} d\tau_n \, \hat{H}_I(\tau_1)\hat{H}_I(\tau_2)\cdots\hat{H}_I(\tau_n). \tag{4.26}$$

Thus, taking into account the imaginary-time ordering operator (4.5), Eq. (4.26) becomes

$$\hat{U}_I(\tau,\tau_0) = 1 + \sum_{n=1}^{\infty}(-1)^n \frac{1}{n!} \int_{\tau_0}^{\tau} d\tau_1 \int_{\tau_0}^{\tau} d\tau_2 \cdots \int_{\tau_0}^{\tau} d\tau_n \, \hat{T}\left[\hat{H}_I(\tau_1)\hat{H}_I(\tau_2)\cdots\hat{H}_I(\tau_n)\right]. \tag{4.27}$$

Note that we haver added the factor $1/n!$ due to all the possible imaginary-time variable permutations generated by the time ordering operator. We remark that Eq. (4.27) can be transformed to

$$\hat{U}_I(\tau,\tau_0) = \hat{T}\exp\left[-\int_{\tau_0}^{\tau} d\tau' \hat{H}_I(\tau')\right]. \tag{4.28}$$

The partition function (4.6) in the imaginary Dirac picture can be derived by the following manipulation

$$\mathcal{Z} = \mathrm{Tr}\Big[\exp\left\{-\beta\hat{H}^{(0)}\right\}\exp\left\{\beta\hat{H}^{(0)}\right\}\hat{U}(\beta,0)\exp\left\{-\hat{H}^{(0)}\cdot 0\right\}\Big], \tag{4.29}$$

which can be written due to (4.19) and (4.20) as

$$\mathcal{Z} = \mathrm{Tr}\Big[\exp\left\{-\beta\hat{H}^{(0)}\right\}\hat{U}_I(\beta,0)\Big]. \tag{4.30}$$

This equation allows to determine the partition function perturbatively in terms of the Dyson series (4.27). To this end, using the thermal average definition with respect to the unperturbed system

$$\langle\bullet\rangle^{(0)} = \frac{1}{\mathcal{Z}^{(0)}}\mathrm{Tr}\Big[\bullet\,\exp\left\{-\beta\hat{H}^{(0)}\right\}\Big], \tag{4.31}$$

we get the grand-canonical partition function

$$\mathcal{Z} = \mathcal{Z}^{(0)}\left\langle\hat{U}_I(\beta,0)\right\rangle^{(0)}, \tag{4.32}$$

where

$$\mathcal{Z}^{(0)} = \mathrm{Tr}\left[\exp\left\{-\beta\hat{H}^{(0)}\right\}\right]. \tag{4.33}$$

The resulting expression of the partition function is

$$\mathcal{Z} = \mathcal{Z}^{(0)}\left[1+\sum_{n=1}^{\infty}(-1)^n\frac{1}{n!}\int_0^\beta d\tau_1\int_0^\beta d\tau_2\cdots\int_0^\beta d\tau_n\,\left\langle\hat{T}\left[\hat{H}_I(\tau_1)\hat{H}_I(\tau_2)\cdots\hat{H}_I(\tau_n)\right]\right\rangle^{(0)}\right]. \tag{4.34}$$

Thus, the grand-canonical partition function can be determined by the unperturbed system partition function $\mathcal{Z}^{(0)}$ and a thermal average with respect to the unperturbed system over a power series of the perturbative Hamiltonian in the Dirac interaction picture.

4.3. Perturbation Theory

We have introduced in Eq. (4.1) additional source currents $j_{i\alpha}(\tau), j^*_{i\alpha}(\tau)$ in the Bose-Hubbard Hamiltonian to break the global U (1) symmetry [116, 117]. Therefore, this approach leads to a Ginzburg-Landau theory, where the order parameter depends on space and the imaginary time. To this end, we first decompose the generalized Bose-Hubbard Hamiltonian (4.1) as follows:

$$\hat{H}_{\mathrm{BH}}(\tau) = \hat{H}^{(0)} + \hat{H}^{(1)}(\tau), \tag{4.35}$$

where we assume that $\hat{H}^{(0)}$ is the unperturbed Hamiltonian (2.34). The perturbative Hamiltonian in the imaginary-time Dirac interaction picture is then

$$\hat{H}_I^{(1)}(\tau)\,[j,j^*] = -\sum_{ij}\sum_{\alpha}J_{ij}\hat{a}^\dagger_{i\alpha}(\tau)\hat{a}_{i\alpha}(\tau) + \sum_{i}\sum_{\alpha}\left[j^*_{i\alpha}(\tau)\hat{a}_{i\alpha}(\tau) + j_{i\alpha}(\tau)\hat{a}^\dagger_{i\alpha}(\tau)\right]. \tag{4.36}$$

We rewrite the hopping constant in the form

$$J_{ij} = \begin{cases} J, & \text{if } i;j \text{ are next neigbors} \\ 0, & \text{otherwise} \end{cases}. \tag{4.37}$$

Inserting (4.36) into (4.34) yields the partition function $\mathcal{Z}\,[j,j^*]$ as a functional of the currents $j_{i\alpha}(\tau)$, $j^*_{i\alpha}(\tau)$. It can be expressed as

$$\mathcal{Z}\,[j,j^*] = \mathcal{Z}^{(0)} + \mathcal{Z}^{(0)}\sum_{n=1}^{\infty}\mathcal{Z}^{(n)}\,[j,j^*]\,, \tag{4.38}$$

where the respective perturbative terms read

$$\mathcal{Z}^{(n)}\,[j,j^*] = (-1)^n\frac{1}{n!}\int_0^\beta d\tau_1\int_0^\beta d\tau_2\cdots\int_0^\beta d\tau_n\left\langle\hat{T}\left[\hat{H}_I^{(1)}(\tau_1)\,[j,j^*]\cdots\hat{H}_I^{(1)}(\tau_n)\,[j,j^*]\right]\right\rangle^{(0)}. \tag{4.39}$$

The grand-canonical free energy (4.10) is then given by

$$\mathcal{F}[j,j^*] = \mathcal{F}_0 - \frac{1}{\beta}\ln\left\{1 + \sum_{n=1}^{\infty} \mathcal{Z}^{(n)}[j,j^*]\right\}, \tag{4.40}$$

where the unperturbed term reads

$$\mathcal{F}_0 = -\frac{1}{\beta}\ln \mathcal{Z}^{(0)}. \tag{4.41}$$

Using the Taylor series of the logarithm

$$\ln(1+x) = \sum_{n=1}^{\infty} \frac{(-1)^{n+1}}{n} x^n, \tag{4.42}$$

Eq. (4.40) becomes

$$\mathcal{F}[j,j^*] = \mathcal{F}_0 - \frac{1}{\beta}\left\{\sum_{n=1}^{\infty} \mathcal{Z}^{(n)}[j,j^*] + \cdots\right\}. \tag{4.43}$$

The respective perturbative contributions in (4.43) contain different orders of the hopping matrix element J and the currents j and j^*. As we aim at working out a Ginzburg-Landau theory, we restrict ourselves to the fourth order in the currents. Furthermore, we focus on the leading non-trivial order in the hopping which is of first order. Therefore, we only need the terms

$$\begin{aligned}
\sum_{n=1}^{5} \mathcal{Z}^{(n)}[j,j^*] = &-\int_0^\beta d\tau_1 \langle \hat{H}_I^{(1)}(\tau_1)\rangle^{(0)} + \frac{1}{2}\int_0^\beta d\tau_1 \int_0^\beta d\tau_2 \left\{ \left\langle \hat{T}\left[\hat{H}_I^{(1)}(\tau_1)\hat{H}_I^{(1)}(\tau_2)\right]\right\rangle^{(0)} \right. \\
&- \frac{1}{6}\int_0^\beta d\tau_3 \left\langle \hat{T}\left[\hat{H}_I^{(1)}(\tau_1)\hat{H}_I^{(1)}(\tau_2)\hat{H}_I^{(1)}(\tau_3)\right]\right\rangle^{(0)} \\
&+ \frac{1}{24}\int_0^\beta d\tau_3 \int_0^\beta d\tau_4 \left\langle \hat{T}\left[\hat{H}_I^{(1)}(\tau_1)\hat{H}_I^{(1)}(\tau_2)\hat{H}_I^{(1)}(\tau_3)\hat{H}_I^{(1)}(\tau_4)\right]\right\rangle^{(0)} \\
&\left. - \frac{1}{120}\int_0^\beta d\tau_3 \int_0^\beta d\tau_4 \int_0^\beta d\tau_5 \left\langle \hat{T}\left[\hat{H}_I^{(1)}(\tau_1)\hat{H}_I^{(1)}(\tau_2)\hat{H}_I^{(1)}(\tau_3)\hat{H}_I^{(1)}(\tau_4)\hat{H}_I^{(1)}(\tau_5)\right]\right\rangle^{(0)} \right\}.
\end{aligned} \tag{4.44}$$

Inserting the perturbative Hamiltonian (4.36) in Eq. (4.44), we get up to fourth order in the currents and the first order in the hopping

$$\begin{aligned}
\sum_{n=1}^{5} \mathcal{Z}^{(n)}[j,j^*] = &\sum_{i_1,i_2}\sum_{\alpha_1,\alpha_2}\int_0^\beta d\tau_1 \int_0^\beta d\tau_2 \left\{ j_{i_1\alpha_1}(\tau_1) j^*_{i_2\alpha_2}(\tau_2) \left\langle \hat{T}\left[\hat{a}^\dagger_{i_1\alpha_1}(\tau_1)\hat{a}_{i_2\alpha_2}(\tau_2)\right]\right\rangle^{(0)} \right. \\
&+ \sum_{i_3,j_3}\sum_{\alpha_3} J_{i_3 j_3} \int_0^\beta d\tau_3 j_{i_1\alpha_1}(\tau_1) j^*_{i_2\alpha_2}(\tau_2) \left\langle \hat{T}\left[\hat{a}^\dagger_{i_1\alpha_1}(\tau_1)\hat{a}_{i_2\alpha_2}(\tau_2)\hat{a}^\dagger_{i_3\alpha_3}(\tau_3)\hat{a}_{j_3\alpha_3}(\tau_3)\right]\right\rangle^{(0)} + \frac{1}{4}\sum_{i_3,i_4}\sum_{\alpha_3,\alpha_4} \\
&\times \int_0^\beta d\tau_3 \int_0^\beta d\tau_4 j_{i_1\alpha_1}(\tau_1) j_{i_2\alpha_2}(\tau_2) j^*_{i_3\alpha_3}(\tau_3) j^*_{i_4\alpha_4}(\tau_4) \left\langle \hat{T}\left[\hat{a}^\dagger_{i_1\alpha_1}(\tau_1)\hat{a}_{i_3\alpha_3}(\tau_3)\hat{a}^\dagger_{i_2\alpha_2}(\tau_2)\hat{a}_{i_4\alpha_4}(\tau_4)\right]\right\rangle^{(0)} \\
&+ \frac{1}{4}\sum_{i_3,i_4}\sum_{i_5,j_5}\sum_{\alpha_3,\alpha_4}\sum_{\alpha_5} J_{i_5 j_5} \int_0^\beta d\tau_3 \int_0^\beta d\tau_4 \int_0^\beta d\tau_5 j_{i_1\alpha_1}(\tau_1) j_{i_2\alpha_2}(\tau_2) j^*_{i_3\alpha_3}(\tau_3) j^*_{i_4\alpha_4}(\tau_4) \\
&\left. \times \left\langle \hat{T}\left[\hat{a}^\dagger_{i_1\alpha_1}(\tau_1)\hat{a}_{i_3\alpha_3}(\tau_3)\hat{a}^\dagger_{i_2\alpha_2}(\tau_2)\hat{a}_{i_4\alpha_4}(\tau_4)\hat{a}^\dagger_{i_5\alpha_5}(\tau_5)\hat{a}_{j_5\alpha_5}(\tau_5)\right]\right\rangle^{(0)} \right\}.
\end{aligned} \tag{4.45}$$

We see that the thermal averages in Eq. (4.45) can be expressed in terms of n-particle Green functions of the unperturbed system

$$G_n^{(0)}(i_1'\alpha_1',\tau_1';\ldots;i_n'\alpha_n',\tau_n'|i_1\alpha_1,\tau_1;\ldots;i_n\alpha_n,\tau_n)=\left\langle \hat{T}\left[\hat{a}^\dagger_{i_1'\alpha_1'}(\tau_1')\hat{a}_{i_1\alpha_1}(\tau_1)\ldots\hat{a}^\dagger_{i_n'\alpha_n'}(\tau_n')\hat{a}_{i_n\alpha_n}(\tau_n)\right]\right\rangle^{(0)}. \tag{4.46}$$

Substituting (4.45) in (4.43), we thus get the free energy

$$\begin{aligned}\mathcal{F}[j,j^*]=\mathcal{F}_0-\frac{1}{\beta}\sum_{i_1,i_2}\sum_{\alpha_1,\alpha_2}\int_0^\beta d\tau_1\int_0^\beta d\tau_2\Bigg\{ j_{i_1\alpha_1}(\tau_1)j^*_{i_2\alpha_2}(\tau_2)\Big[a_2^{(0)}(i_1\alpha_1,\tau_1|i_2\alpha_2,\tau_2) \\ +\sum_{i_3,j_3}J_{i_3j_3}a_2^{(1)}(i_1\alpha_1,\tau_1;i_3|i_2\alpha_2,\tau_2;j_3)\Big]+\frac{1}{4}\sum_{i_3,i_4}\sum_{\alpha_3,\alpha_4}\int_0^\beta d\tau_3\int_0^\beta d\tau_4\Big[j_{i_1\alpha_1}(\tau_1)j_{i_2\alpha_2}(\tau_2)j^*_{i_3\alpha_3}(\tau_3)j^*_{i_4\alpha_4}(\tau_4) \\ \times a_4^{(0)}(i_1\alpha_1,\tau_1;i_2\alpha_2,\tau_2|i_3\alpha_3,\tau_3;i_4\alpha_4,\tau_4)+\sum_{i_5,j_5}J_{i_5j_5}a_4^{(1)}(i_1\alpha_1,\tau_1;i_2\alpha_2,\tau_2;i_5|i_3\alpha_3,\tau_3;i_4\alpha_4;j_5)\Big]\Bigg\},\end{aligned} \tag{4.47}$$

where we have introduced the abbreviations

$$a_2^{(0)}(i_1\alpha_1,\tau_1|i_2\alpha_2,\tau_2)=G_1^{(0)}(i_1\alpha_1,\tau_1|i_2\alpha_2,\tau_2), \tag{4.48}$$

$$a_2^{(1)}(i_1\alpha_1,\tau_1;i_3|i_2\alpha_2,\tau_2;j_3)=\sum_{\alpha_3}\int_0^\beta d\tau_3 G_2^{(0)}(i_1\alpha_1,\tau_1;i_3\alpha_3,\tau_3|i_2\alpha_2,\tau_2;j_3\alpha_3,\tau_3), \tag{4.49}$$

$$\begin{aligned}a_4^{(0)}(i_1\alpha_1,\tau_1;i_2\alpha_2,\tau_2|i_3\alpha_3,\tau_3;i_4\alpha_4,\tau_4)=G_2^{(0)}(i_1\alpha_1,\tau_1;i_2\alpha_2,\tau_2|i_3\alpha_3,\tau_3;i_4\alpha_4,\tau_4) \\ -G_1^{(0)}(i_1\alpha_1,\tau_1|i_3\alpha_3,\tau_3)G_1^{(0)}(i_2\alpha_2,\tau_2|i_4\alpha_4,\tau_4)-G_1^{(0)}(i_1\alpha_1,\tau_1|i_4\alpha_4,\tau_4)G_1^{(0)}(i_2\alpha_2,\tau_2|i_3\alpha_3,\tau_3),\end{aligned} \tag{4.50}$$

$$\begin{aligned}a_4^{(1)}(i_1\alpha_1,\tau_1;i_2\alpha_2,\tau_2;i_5|i_3\alpha_3,\tau_3;i_4\alpha_4;j_5)=\sum_{\alpha_5}\int_0^\beta d\tau_5 \\ \Big[G_3^{(0)}(i_1\alpha_1,\tau_1;i_2\alpha_2,\tau_2;i_5\alpha_5,\tau_5|i_3\alpha_3,\tau_3;i_4\alpha_4;j_5\alpha_5,\tau_5)-G_2^{(0)}(i_1\alpha_1,\tau_1;i_5\alpha_5,\tau_5|i_3\alpha_3,\tau_3;j_5\alpha_5,\tau_5) \\ \times G_1^{(0)}(i_2\alpha_2,\tau_2|i_4\alpha_4,\tau_4)-G_2^{(0)}(i_2\alpha_2,\tau_2;i_5\alpha_5,\tau_5|i_4\alpha_4,\tau_4;j_5\alpha_5,\tau_5)G_1^{(0)}(i_1\alpha_1,\tau_1|i_3\alpha_3,\tau_3)\Big].\end{aligned} \tag{4.51}$$

Note that the upper (lower) index of these abbreviations refers to the order in the hopping parameter (the symmetry-breaking currents). If the order of the thermal Green function increases, the calculation will be more complex because the number of space- and time-index permutations increases. Thus, in order to simplify this calculation, we decompose the thermal Green functions in the next section into cumulants.

4.4. Cumulant Expansion

In this section, we use the approach proposed in Refs. [86, 87] to expand the thermal Green functions of the unperturbed system diagrammatically in terms of cumulants. To this end we show that each Green function consists of a sum of products of cumulants which can be defined in terms of Feynman diagrams. Therefore, by formulating certain diagrammatic rules, every Green function can be expressed in terms of cumulants without any calculation. In order to define a generating functional for them we couple the creation and annihilation operators to external currents [117, 121, 122] and consider the Hamiltonian

$$\hat{H}(\tau)\left[j, j^*\right] = \hat{H}^{(0)} + \sum_i \sum_\alpha \left[j^*_{i\alpha}(\tau)\hat{a}_{i\alpha} + j_{i\alpha}(\tau)\hat{a}^\dagger_{i\alpha} \right], \tag{4.52}$$

where the unperturbed Hamiltonian (2.35) is local according to

$$\hat{H}^{(0)} = \sum_i \hat{H}^{(0)}_i. \tag{4.53}$$

We remark that, since the functional depends on the current fields $j_{i\alpha}(\tau)$ and $j^*_{i\alpha}(\tau)$ on each lattice site, the Hamiltonian (4.52) is time dependent. Therefore, in the Dirac picture the perturbed Hamiltonian in Eq. (4.52) becomes

$$\hat{H}^{(1)}_I(\tau) = \sum_i \sum_\alpha \left[j^*_{i\alpha}(\tau)\hat{a}_{i\alpha}(\tau) + j_{i\alpha}(\tau)\hat{a}^\dagger_{i\alpha}(\tau) \right]. \tag{4.54}$$

Substituting Eq. (4.54) into (4.28), yields

$$\hat{U}_I\left[j, j^*\right](\tau, \tau_0) = \hat{T} \exp\left\{ -\int_{\tau_0}^{\tau} d\tau' \sum_i \sum_\alpha \left[j_{i\alpha}(\tau')\hat{a}^\dagger_{i\alpha}(\tau') + j^*_{i\alpha}(\tau')\hat{a}_{i\alpha}(\tau') \right] \right\}. \tag{4.55}$$

Then, the partition function (4.32) is

$$\mathcal{Z}^{(0)}\left[j, j^*\right] = \mathcal{Z}^{(0)} \left\langle \hat{T} \exp\left[-\int_0^\beta d\tau \sum_i \sum_\alpha \left[j_{i\alpha}(\tau)\hat{a}^\dagger_{i\alpha}(\tau) + j^*_{i\alpha}(\tau)\hat{a}_{i\alpha}(\tau) \right] \right] \right\rangle^{(0)}. \tag{4.56}$$

Using functional derivatives of the above equation with respect to the currents, we get

$$\begin{aligned} \frac{1}{\mathcal{Z}^{(0)}} \frac{\delta^2 \mathcal{Z}^{(0)}\left[j, j^*\right]}{\delta j_{n'\alpha'}(\tau')\delta j^*_{n\alpha}(\tau)}\bigg|_{j=j^*=0} &= \Bigg\langle \hat{T} \Bigg\{ \hat{a}^\dagger_{n'\alpha'}(\tau')\hat{a}_{n\alpha}(\tau) \\ &\times \exp\left[-\int_0^\beta d\tau'' \sum_i \sum_{\alpha''} \left[j_{i\alpha''}(\tau'')\hat{a}^\dagger_{i\alpha''}(\tau'') + j^*_{i\alpha''}(\tau'')\hat{a}_{i\alpha''}(\tau'') \right] \right] \Bigg\} \Bigg\rangle^{(0)}. \end{aligned} \tag{4.57}$$

In the case of vanishing currents we obtain the one-point thermal Green function of the unperturbed system

$$\frac{1}{\mathcal{Z}^{(0)}} \frac{\delta^2 \mathcal{Z}^{(0)}\left[j, j^*\right]}{\delta j_{n'\alpha'}(\tau')\delta j^*_{n\alpha}(\tau)}\bigg|_{j=j^*=0} = \left\langle \hat{T}\left[\hat{a}^\dagger_{n'\alpha'}(\tau')\hat{a}_{n\alpha}(\tau) \right] \right\rangle^{(0)}. \tag{4.58}$$

Therefore, in view of higher Green functions, we do the same procedure and find that a general thermal n-point Green functions can be obtained from (4.56) by performing $2n$ functional derivatives with respect to the source currents. Thus, the thermal Green functions can be expressed by

$$\begin{aligned} &G_n^{(0)}(\tau_1', i_1'\alpha_1'; \ldots; \tau_n', i_n'\alpha_n' | \tau_1, i_1\alpha_1; \ldots; \tau_n, i_n\alpha_n) \\ &= \frac{1}{\mathcal{Z}^{(0)}} \frac{\delta^{2n} \mathcal{Z}^{(0)}[j, j^*]}{\delta j_{i_1'\alpha_1'}(\tau_1') \delta j^*_{i_1\alpha_1}(\tau_1) \ldots \delta j_{i_n'\alpha_n'}(\tau_n') \delta j^*_{i_n\alpha_n}(\tau_n)} \Bigg|_{j=j^*=0}. \end{aligned} \tag{4.59}$$

Now, in order to calculate the correlation functions in many-body theory, we usually use the Wick theorem which allows to decompose the n-point correlation function (4.59) into sums of products of one-point correlation functions [118, 119]. This theorem is not valid for the considered system here because the unperturbed Bose-Hubbard Hamiltonian (2.35) contains parts which are of fourth order in the creation and annihilation operators. Therefore, instead, we use the linked cluster theorem [120], which states that the sum of all connected Green functions is defined by the logarithm of the partition function, whereas Eq. (4.59) represents the decomposition into connected and disconnected diagrams. Thus, in order to remove these disconnected diagrams we use the generating functional of the cumulants

$$C_0^{(0)}[j, j^*] = \ln \frac{\mathcal{Z}^{(0)}[j, j^*]}{\mathcal{Z}^{(0)}}, \tag{4.60}$$

which yields with (4.56)

$$C_0^{(0)}[j, j^*] = \ln \left\langle \hat{T} \exp \left[- \int_0^\beta d\tau \sum_i \sum_\alpha \left[j_{i\alpha}(\tau) \hat{a}^\dagger_{i\alpha}(\tau) + j^*_{i\alpha}(\tau) \hat{a}_{i\alpha}(\tau) \right] \right] \right\rangle^{(0)}. \tag{4.61}$$

We note that according to (4.53) the unperturbed Hamiltonian (2.35) decomposes into a sum over local contributions. For this reason, the generating functional decomposes into a sum over local terms as

$$C_0^{(0)}[j, j^*] = \sum_i {}_iC_0^{(0)}[j, j^*], \tag{4.62}$$

where

$${}_iC_0^{(0)}[j, j^*] = \ln \left\langle \hat{T} \exp \left[- \int_0^\beta d\tau \sum_\alpha \left[j_{i\alpha}(\tau) \hat{a}^\dagger_{i\alpha}(\tau) + j^*_{i\alpha}(\tau) \hat{a}_{i\alpha}(\tau) \right] \right] \right\rangle^{(0)}. \tag{4.63}$$

In order to obtain higher order cumulants, we calculate the functional derivatives with respect to the symmetry breaking currents $j_{i\alpha}(\tau)$:

$$C_n^{(0)}(\tau_1', i_1'\alpha_1'; \ldots; \tau_n', i_n'\alpha_n' | \tau_1, i_1\alpha_1; \ldots; \tau_n, i_n\alpha_n) = \frac{\delta^{2n} C_0^{(0)}[j, j^*]}{\delta j_{i_1'\alpha'}(\tau') \delta j^*_{i_1\alpha_1}(\tau) \ldots \delta j_{i_n'\alpha_n'}(\tau_n') \delta j^*_{i_n\alpha_n}(\tau_n)} \Bigg|_{j=j^*=0}. \tag{4.64}$$

From (4.62) and (4.64) we read off that the cumulants are local quantities i.e., the n-th order cumulant is given by

$$C_n^{(0)}(\tau_1', i_1'\alpha_1'; \ldots; \tau_n', i_n'\alpha_n' | \tau_1, i_1\alpha_1; \ldots; \tau_n, i_n\alpha_n) = {}_{i_1}C_n^{(0)}(\tau_1', \alpha_1'; \ldots; \tau_n', \alpha_n' | \tau_1, \alpha_1; \ldots; \tau_n, \alpha_n) \times \delta_{i_1,i_2} \cdots \delta_{i_{n-1},i_n} \delta_{i_1',i_n}\, \delta_{i_1',i_2'} \cdots \delta_{i_{n-1}',i_n'}. \quad (4.65)$$

It is important to know that the cumulants represent the keystone for constructing the Green functions. To see this, we calculate the unperturbed one- and the two-point Green functions with the above formulas and obtain:

$$G_1^{(0)}(i_1\alpha_1, \tau_1 | i_2\alpha_2, \tau_2) = \delta_{i_1,i_2}\, {}_{i_1}C_1^{(0)}(\tau_1, \alpha_1 | \tau_2, \alpha_2), \quad (4.66)$$

and

$$\begin{aligned} G_2^{(0)}(i_1\alpha_1, \tau_1; i_2\alpha_2, \tau_2 | i_3\alpha_3, \tau_3; i_4\alpha_4, \tau_4) = {} & \delta_{i_1,i_3}\delta_{i_2,i_4}\delta_{i_3,i_4}\, {}_{i_1}C_1^{(0)}(\tau_1, \alpha_1; \tau_2, \alpha_2 | \tau_3, \alpha_3; \tau_4, \alpha_4) \\ & + \delta_{i_1,i_3}\delta_{i_2,i_4}\, {}_{i_1}C_1^{(0)}(\tau_1, \alpha_1 | \tau_3, \alpha_3)\, {}_{i_2}C_1^{(0)}(\tau_2, \alpha_2 | \tau_4, \alpha_4) \\ & + \delta_{i_1,i_4}\delta_{i_2,i_3}\, {}_{i_1}C_1^{(0)}(\tau_1, \alpha_1 | \tau_4, \alpha_4)\, {}_{i_2}C_1^{(0)}(\tau_2, \alpha_2 | \tau_3, \alpha_3). \end{aligned} \quad (4.67)$$

In principle, one would also need the 3-point Green function $G_3^{(0)}$ as it appears in Eq. (4.51). However, we do not mention it explicitly because it turns out during the following calculation that $a_4^{(1)}$ is not needed in the end.

Now the expansion of the free energy (4.47) and the abbreviations (4.48)–(4.51) can be expressed in terms of these cumulants. Thus, the grand-canonical free energy is a sum over cumulants which represent only the connected Green functions because the disconnected diagrams of the thermal Green functions would be cancelled due to the expansion of the logarithm. In the next section, we introduce a graphical notation which shows the basic diagrammatic rules for this expansion.

4.5. Basic Diagrammatic Calculations

In this section, we define the diagrammatic rules which yield a much simpler calculation for the perturbative contributions of the free energy. These rules show the representation of the partition function with the cumulant decomposition of Green functions.

4.5.1. Diagrammatic Rules

We obtain the diagrammatic expansion according to the following rules [86, 104, 123]:

1. At a lattice site a n-point cumulant is represented by a vertex with n entering and n leaving lines.

2. Each line is labelled with both an imaginary-time and a spin index.

3. The currents $j_{i\alpha}^*(\tau)$ ($j_{i\alpha}(\tau)$) are described by entering (leaving) lines.

4. Each line, which connects two vertices, is associated with a factor of the hopping matrix element J.

5. For a connected Green function of a given order draw all inequivalent connected diagrams.

6. Sum over all site and spin indices and integrate over all time variables.

4.5.2. Diagram Weights

The diagrammatic rules stated in Subsection 4.5.1 are not sufficient for the diagrammatic expansion of the grand-canonical free energy. The goal of this subsection is to calculate the weights of the emerging diagrams in order to find the correct decomposition. Therefore, we need to introduce the symmetry factor which allows us to calculate these weights. For a given diagram the weight has two contributions. The first contribution is that there are $n!$ possible permutations of equal imaginary-time and spin variables, where the Green function $G_n^{(0)}$ consists of a sum of products of cumulants. The second contribution is that not all of these permutations describe the cumulant decomposition in the higher hopping orders. Therefore, we keep in mind the symmetry factor. This factor gives the possible permutations of the imaginary-time, the spin variables, and the vertex indices. So, the weight of a diagram is given by

$$\text{weight} \quad = \quad \frac{1}{n!}\frac{n!}{\text{symmetry factor}}, \tag{4.68}$$

where $1/n!$ is the prefactor from the Taylor expansion in (4.39).

With this, we can express the expansion coefficients of the free energy defined in (4.48)–(4.51) graphically as follows:

$$\begin{aligned} a_2^{(0)}(i_1\alpha_1,\tau_1|i_2\alpha_2,\tau_2) &= \delta_{i_1,i_2} \quad \tau_1,\alpha_1 \xrightarrow{\qquad i_1 \qquad} \tau_2,\alpha_2 \\ &= \delta_{i_1,i_2} \quad {}_{i_1}C_1^{(0)}(\tau_1,\alpha_1|\tau_2,\alpha_2), \end{aligned} \tag{4.69}$$

$$\begin{aligned} J_{i_3j_3}a_2^{(1)}(i_1\alpha_1,\tau_1;i_3|i_2\alpha_2,\tau_2;j_3) &= \delta_{i_1,i_3}\delta_{i_2,j_3} \quad \tau_1,\alpha_1 \xrightarrow{\quad i_3 \quad j_3 \quad} \tau_2,\alpha_2 \\ &= \sum_{\alpha_3}\delta_{i_1,i_3}\delta_{i_2,j_3}J_{i_3j_3}\int_0^\beta \mathrm{d}\tau_3 \, {}_{i_3}C_1^{(0)}(\tau_1,\alpha_1|\tau_3,\alpha_3)_{j_3}C_1^{(0)}(\tau_3,\alpha_3|\tau_2,\alpha_2), \end{aligned} \tag{4.70}$$

$$a_4^{(0)}(i_1\alpha_1,\tau_1;i_2\alpha_2,\tau_2|i_3\alpha_3,\tau_3;i_4\alpha_4,\tau_4) = \delta_{i_1,i_2}\delta_{i_2,i_3}\delta_{i_3,i_4}$$

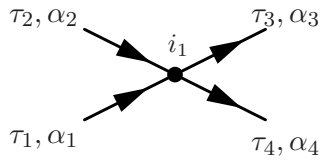

$$= \delta_{i_1,i_2}\delta_{i_2,i_3}\delta_{i_3,i_4} \, {}_{i_1}C_2^{(0)}(\tau_1,\alpha_1;\tau_2,\alpha_2|\tau_3,\alpha_3;\tau_4,\alpha_4), \tag{4.71}$$

$$
\begin{aligned}
&a_4^{(1)}(i_1\alpha_1,\tau_1;i_2\alpha_2,\tau_2;i_5|i_3\alpha_3,\tau_3;i_4\alpha_4,\tau_4;j_5)\\
&= \delta_{i_3,j_5}\delta_{i_1,i_2}\delta_{i_2,i_5}\delta_{i_4,i_5}
\end{aligned}
$$

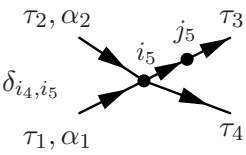

$$
+\,\delta_{i_2,j_5}\delta_{i_1,i_5}\delta_{i_3,i_5}\delta_{i_3,i_4}
$$

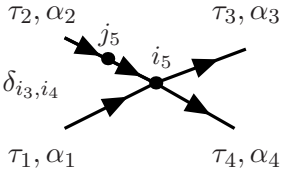

$$
\begin{aligned}
&= \sum_{\alpha_5} J_{i_5 j_5}\Big[\delta_{i_3,j_5}\delta_{i_1,i_2}\delta_{i_2,i_5}\delta_{i_4,i_5}\int_0^\beta \mathrm{d}\tau_5\; {}_{i_5}C_2^{(0)}(\tau_1,\alpha_1;\tau_2,\alpha_2|\tau_5,\alpha_5;\tau_4,\alpha_4)_{j_5}C_1^{(0)}(\tau_5,\alpha_5|\tau_3,\alpha_3)\\
&\quad + \;\delta_{i_2,j_5}\delta_{i_1,i_5}\delta_{i_3,i_5}\delta_{i_3,i_4}\int_0^\beta \mathrm{d}\tau_5\; {}_{i_5}C_2^{(0)}(\tau_1,\alpha_1;\tau_5,\alpha_5|\tau_3,\alpha_3;\tau_4,\alpha_4)_{j_5}C_1^{(0)}(\tau_2,\alpha_2|\tau_5,\alpha_5)\Big]. \qquad (4.72)
\end{aligned}
$$

4.5.3. Diagrammatic Series for Free energy

Using the weights discussed in the previous subsection, the diagrammatic expansion of the grand-canonical free energy up to first order in the hopping parameter and the fourth order in the symmetry-breaking currents is given by

$$
\mathcal{F}[j,j^*] = \quad \mathcal{F}^{(0)} +
$$

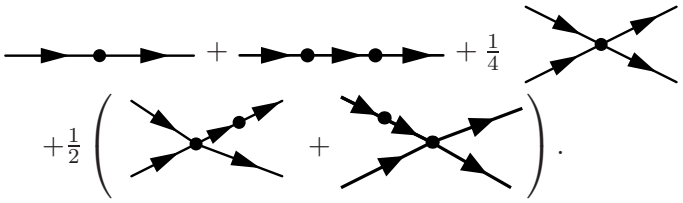

$$
+\tfrac{1}{4}
$$

$$
+\tfrac{1}{2}\Bigg(
$$

$$
+
$$

$$
\Bigg). \qquad (4.73)
$$

We remark that all imaginary time, spin and vertex indices can be dropped in order to show that all variables have been integrated out as is demanded by rule 6 in Subsection 4.5.1. As discussed in the Subsection 4.5.2, the pre-factors show the symmetry factors of the respective diagrams. Converting the Feynman diagrams into explicit expressions, the grand-canonical free energy (4.73) reads

$$
\begin{aligned}
\mathcal{F}[j,j^*] \;=\; & \mathcal{F}_0 - \frac{1}{\beta}\sum_{i_1,i_2}\sum_{\alpha_1,\alpha_2}\int_0^\beta d\tau_1\int_0^\beta d\tau_2\Big\{ j_{i_1\alpha_1}(\tau_1)j^*_{i_2\alpha_2}(\tau_2)W_2(i_1\alpha_1,\tau_1|i_2\alpha_2,\tau_2)\\
& +\frac{1}{4}\sum_{i_3,i_4}\sum_{\alpha_3,\alpha_4}\int_0^\beta d\tau_3\int_0^\beta d\tau_4 j_{i_1\alpha_1}(\tau_1)j_{i_2\alpha_2}(\tau_2)j^*_{i_3\alpha_3}(\tau_3)j^*_{i_4\alpha_4}(\tau_4)\\
& \times W_4(i_1\alpha_1,\tau_1;i_2\alpha_2,\tau_2|i_3\alpha_3,\tau_3;i_4\alpha_4,\tau_4)\Big\}. \qquad (4.74)
\end{aligned}
$$

Here we have introduced the abbreviations

$$
W_2(i_1\alpha_1,\tau_1|i_2\alpha_2,\tau_2) = a_2^{(0)}(i_1\alpha_1,\tau_1|i_2\alpha_2,\tau_2) + \sum_{i_3,j_3} J_{i_3 j_3}a_2^{(1)}(i_1\alpha_1,\tau_1;i_3|i_2\alpha_2,\tau_2;j_3), \qquad (4.75)
$$

and

$$W_4(i_1\alpha_1,\tau_1;i_2\alpha_2,\tau_2|i_3\alpha_3,\tau_3;i_4\alpha_4,\tau_4) = a_4^{(0)}(i_1\alpha_1,\tau_1;i_2\alpha_2,\tau_2|i_3\alpha_3,\tau_3;i_4\alpha_4,\tau_4) + \sum_{i_5,j_5} J_{i_5 j_5} a_4^{(1)}(i_1\alpha_1,\tau_1;i_2\alpha_2,\tau_2;i_5|i_3\alpha_3,\tau_3;i_4\alpha_4;j_5), \tag{4.76}$$

which are determined by respective cumulants. From (4.66) and (4.67) as well as (4.46), we get for the relevant cumulants the following explicit expressions

$$\begin{aligned} {}_iC_1^{(0)}(\tau_1,\alpha_1|\tau_2,\alpha_2) &= \left\langle \hat{T}\left[\hat{a}^\dagger_{i\alpha_1}(\tau_1)\hat{a}_{i\alpha_2}(\tau_2)\right]\right\rangle^{(0)} \\ &= \frac{1}{\mathcal{Z}^{(0)}}\mathrm{Tr}\left\{ e^{-\beta\hat{H}_0}\hat{T}\left[\hat{a}^\dagger_{i\alpha_1}(\tau_1)\hat{a}_{i\alpha_2}(\tau_2)\right]\right\}, \end{aligned} \tag{4.77}$$

$$\begin{aligned} {}_iC_2^{(0)}(\tau_1,\alpha_1;\tau_2,\alpha_2|\tau_3,\alpha_3;\tau_4,\alpha_4) = \left\langle \hat{T}\left[\hat{a}^\dagger_{i\alpha_1}(\tau_1)\hat{a}^\dagger_{i\alpha_2}(\tau_2)\hat{a}_{i\alpha_3}(\tau_3)\hat{a}_{i\alpha_4}(\tau_4)\right]\right\rangle^{(0)} - {}_iC_1^{(0)}(\tau_1,\alpha_1|\tau_3,\alpha_3) \\ \times {}_iC_1^{(0)}(\tau_2,\alpha_2|\tau_4,\alpha_4) - {}_iC_1^{(0)}(\tau_1,\alpha_1|\tau_4,\alpha_4){}_iC_1^{(0)}(\tau_2,\alpha_2|\tau_3,\alpha_3). \end{aligned} \tag{4.78}$$

We can simplify the calculation of these expressions by converting them into frequency space. Therefore, we need the Matsubara transformation which is defined in the next subsection.

4.5.4. Matsubara Transformation

Here we go into the frequency space instead of using the imaginary-time in order to simplify our calculations. Thus, we use the Matsubara transformation where the imaginary-time variable runs from 0 to β. The Matsubara transformation is given by

$$f(\omega_m) = \frac{1}{\sqrt{\beta}}\int_0^\beta d\tau e^{i\omega_m\tau} f(\tau). \tag{4.79}$$

where the Matsubara frequencies are defined according to

$$\omega_m = \frac{2\pi m}{\beta}, \qquad m \in \mathbb{Z} \tag{4.80}$$

The inverse Matsubara transformation yields

$$f(\tau) = \frac{1}{\sqrt{\beta}}\sum_{m=-\infty}^{\infty} e^{-i\omega_m\tau} f(\omega_m). \tag{4.81}$$

Now we can express the bosonic annihilation and creation operators in Matsubara space

$$\hat{a}^\dagger_\alpha(\omega_m) = \frac{1}{\sqrt{\beta}}\int_0^\beta d\tau e^{-i\omega_m\tau}\hat{a}^\dagger_\alpha(\tau), \tag{4.82}$$

and

$$\hat{a}_\alpha(\omega_m) = \frac{1}{\sqrt{\beta}} \int_0^\beta d\tau e^{i\omega_m \tau} \hat{a}_\alpha(\tau). \tag{4.83}$$

Using Eqs. (4.82) and (4.83) in the further considerations the cumulants in the free energy expansion (4.77) and (4.78) can be calculated in Matsubara space.

4.6. Second Order in Currents

In this section, we calculate $a_2^{(0)}(i_1\alpha_1, \omega_{m1}|i_2\alpha_2, \omega_{m2})$ in Matsubara space. Because of the locality of the cumulants and the conservation of frequency, we can use Eqs. (4.69) and (4.77) by applying the Matsubara transformation according to Eqs. (4.82) and (4.83) and get the following relation

$$a_2^{(0)}(i_1\alpha_1, \omega_{m1}|i_2\alpha_2, \omega_{m2}) = a_2^{(0)}(i_1\alpha_1, \omega_{m1})\delta_{i_1,i_2}\delta_{\alpha_1,\alpha_2}\delta_{\omega_{m1},\omega_{m2}}. \tag{4.84}$$

With this, we obtain at first

$$\begin{aligned}
a_2^{(0)}(i_1\alpha_1, \omega_{m1}) =& \frac{1}{\beta}\int_0^\beta d\tau_1 \int_0^\beta d\tau_2 a_2^{(0)}(i_1\alpha_1, \tau_1|i_1\alpha_1, \tau_2) e^{-i\omega_{m1}(\tau_1-\tau_2)} \\
=& \frac{1}{\beta}\int_0^\beta d\tau_1 \int_0^\beta d\tau_2 \left\langle \hat{T}\left[\hat{a}^\dagger_{\alpha_1}(\tau_1)\hat{a}_{\alpha_1}(\tau_2)\right]\right\rangle^{(0)} e^{-i\omega_{m1}(\tau_1-\tau_2)} \\
=& \frac{1}{\mathcal{Z}^{(0)}}\frac{1}{\beta}\int_0^\beta d\tau_1 \int_0^\beta d\tau_2 \mathrm{Tr}\left\{ e^{-\beta\hat{H}_0}\hat{T}\left[\hat{a}^\dagger_{\alpha_1}(\tau_1)\hat{a}_{\alpha_1}(\tau_2)\right]\right\} e^{-i\omega_{m1}(\tau_1-\tau_2)} \\
=& \sum_{S_{i_1},m_{i_1},n_{i_1}} e^{-\beta E^{(0)}_{S_{i_1},m_{i_1},n_{i_1}}} \int_0^\beta d\tau_1 \int_0^\beta d\tau_2 \frac{e^{-i\omega_{m1}(\tau_1-\tau_2)}}{\beta\mathcal{Z}^{(0)}} \Big\langle S_{i_1}, m_{i_1}, n_{i_1}|\Theta(\tau_1-\tau_2) \\
& \times e^{(\tau_1-\tau_2)\hat{H}^{(0)}}\hat{a}^\dagger_{\alpha_1}e^{(\tau_2-\tau_1)\hat{H}_0}\hat{a}_{\alpha_1} + \Theta(\tau_2-\tau_1)e^{(\tau_2-\tau_1)\hat{H}_0}\hat{a}_{\alpha_1}e^{(\tau_1-\tau_2)\hat{H}_0}\hat{a}^\dagger_{\alpha_1}|S_{i_1}, m_{i_1}, n_{i_1}\Big\rangle.
\end{aligned} \tag{4.85}$$

With the help of Eqs. (3.23) and (3.24), we get

$$\begin{aligned}
a_2^{(0)}(i_1\alpha_1, \omega_{m1}) =& \frac{1}{\beta\mathcal{Z}^{(0)}} \sum_{S_{i_1},m_{i_1},n_{i_1}} e^{-\beta E^{(0)}_{S_{i_1},m_{i_1},n_{i_1}}} \int_0^\beta d\tau_1 \int_0^\beta d\tau_2 \Big\{ e^{(\tau_1-\tau_2)E^{(0)}_{S_{i_1},m_{i_1},n_{i_1}}}\Theta(\tau_1-\tau_2) \\
& \times \left[O^2_{\alpha_1,S_{i_1},m_{i_1},n_{i_1}}\, e^{-(\tau_1-\tau_2)E^{(0)}_{S_{i_1}+1,m_{i_1}-\alpha_1,n_{i_1}-1}} + P^2_{\alpha_1,S_{i_1},m_{i_1},n_{i_1}} e^{-(\tau_1-\tau_2)E^{(0)}_{S_{i_1}-1,m_{i_1}-\alpha_1,n_{i_1}-1}}\right] \\
& + e^{(\tau_2-\tau_1)E^{(0)}_{S_{i_1},m_{i_1},n_{i_1}}}\Theta(\tau_2-\tau_1)\left[M^2_{\alpha_1,S_{i_1},m_{i_1},n_{i_1}} e^{-(\tau_2-\tau_1)E^{(0)}_{S_{i_1}+1,m_{i_1}+\alpha_1,n_{i_1}+1}}\right. \\
& \left. + N^2_{\alpha_1,S_{i_1},m_{i_1},n_{i_1}} e^{-(\tau_2-\tau_1)E^{(0)}_{S_{i_1}-1,m_{i_1}+\alpha_1,n_{i_1}+1}}\right]\Big\} e^{-i\omega_{m1}(\tau_1-\tau_2)}.
\end{aligned} \tag{4.86}$$

Note that the Heaviside step function changes the integration limits. With this Eq. (4.86) becomes

$$a_2^{(0)}(i_1\alpha_1, \omega_{m1}) = \frac{1}{\beta\mathcal{Z}^{(0)}} \sum_{S_{i_1},m_{i_1},n_{i_1}} e^{-\beta E^{(0)}_{S_{i_1},m_{i_1},n_{i_1}}} \left\{ \int_0^\beta d\tau_1 \int_0^{\tau_1} d\tau_2 e^{(\tau_1-\tau_2)E^{(0)}_{S_{i_1},m_{i_1},n_{i_1}}}\right.$$

$$\times \left[O^2_{\alpha_1,S_{i_1},m_{i_1},n_{i_1}} \; e^{-(\tau_1-\tau_2)E^{(0)}_{S_{i_1}+1,m_{i_1}-\alpha_1,n_{i_1}-1}} + P^2_{\alpha_1,S_{i_1},m_{i_1},n_{i_1}} e^{-(\tau_1-\tau_2)E^{(0)}_{S_{i_1}-1,m_{i_1}-\alpha_1,n_{i_1}-1}} \right]$$
$$+ \int_0^\beta d\tau_2 \int_0^{\tau_2} d\tau_1 e^{(\tau_2-\tau_1)E^{(0)}_{S_{i_1},m_{i_1},n_{i_1}}} \left[M^2_{\alpha_1,S_{i_1},m_{i_1},n_{i_1}} e^{-(\tau_2-\tau_1)E^{(0)}_{S_{i_1}+1,m_{i_1}+\alpha_1,n_{i_1}+1}} \right.$$
$$\left. + \; N^2_{\alpha_1,S_{i_1},m_{i_1},n_{i_1}} e^{-(\tau_2-\tau_1)E^{(0)}_{S_{i_1}-1,m_{i_1}+\alpha_1,n_{i_1}+1}} \right] \Big\} e^{-i\omega_{m1}(\tau_1-\tau_2)}. \tag{4.87}$$

This expression contains integrals of the form

$$\mathcal{I} \;=\; \int_0^\beta d\tau_1 \int_0^{\tau_1} d\tau_2 e^{a\tau_1} e^{b\tau_2} = \frac{1-e^{a\beta}}{ab} + \frac{e^{(a+b)\beta}-1}{(a+b)b}, \tag{4.88}$$

whose special case $a+b \to 0$ needs to apply the L'Hospital rule:

$$\lim_{a+b\to 0} \quad \tfrac{e^{(a+b)\beta}-1}{(a+b)b} \quad = \frac{\beta}{b}\,. \tag{4.89}$$

Therefore, we get

$$\mathcal{I}_{a^\dagger_{\alpha_1} a_{\alpha_1}} = O^2_{\alpha_1,S_{i_1},m_{i_1},n_{i_1}} \left[\frac{-1+e^{(E^{(0)}_{S_{i_1},m_{i_1},n_{i_1}} - E^{(0)}_{S_{i_1}+1,m_{i_1}-\alpha_1,n_{i_1}-1} - i\omega_{m1})\beta}}{(E^{(0)}_{S_{i_1},m_{i_1},n_{i_1}} - E^{(0)}_{S_{i_1}+1,m_{i_1}-\alpha_1,n_{i_1}-1} - i\omega_{m1})^2} \right.$$
$$\left. - \frac{\beta}{E^{(0)}_{S_{i_1},m_{i_1},n_{i_1}} - E^{(0)}_{S_{i_1}+1,m_{i_1}-\alpha_1,n_{i_1}-1} - i\omega_{m1}} \right] + P^2_{\alpha_1,S_{i_1},m_{i_1},n_{i_1}}$$
$$\times \left[\frac{-1+e^{(E^{(0)}_{S_{i_1},m_{i_1},n_{i_1}} - E^{(0)}_{S_{i_1}-1,m_{i_1}-\alpha_1,n_{i_1}-1} - i\omega_{m1})\beta}}{(E^{(0)}_{S_{i_1},m_{i_1},n_{i_1}} - E^{(0)}_{S_{i_1}-1,m_{i_1}-\alpha_1,n_{i_1}-1} - i\omega_{m1})^2} - \frac{\beta}{E^{(0)}_{S_{i_1},m_{i_1},n_{i_1}} - E^{(0)}_{S_{i_1}-1,m_{i_1}-\alpha_1,n_{i_1}-1} - i\omega_{m1}} \right], \tag{4.90}$$

and correspondingly

$$\mathcal{I}_{a_{\alpha_1} a^\dagger_{\alpha_1}} = M^2_{\alpha_1,S_{i_1},m_{i_1},n_{i_1}} \left[\frac{-1+e^{(E^{(0)}_{S_{i_1},m_{i_1},n_{i_1}} - E^{(0)}_{S_{i_1}+1,m_{i_1}+\alpha_1,n_{i_1}+1} + i\omega_{m1})\beta}}{(E^{(0)}_{S_{i_1}+1,m_{i_1}+\alpha_1,n_{i_1}+1} - E^{(0)}_{S_{i_1},m_{i_1},n_{i_1}} - i\omega_{m1})^2} \right.$$
$$\left. - \frac{\beta}{E^{(0)}_{S_{i_1},m_{i_1},n_{i_1}} - E^{(0)}_{S_{i_1}+1,m_{i_1}+\alpha_1,n_{i_1}+1} + i\omega_{m1}} \right]$$
$$+ N^2_{\alpha_1,S_{i_1},m_{i_1},n_{i_1}} \left[\frac{-1+e^{(E^{(0)}_{S_{i_1},m_{i_1},n_{i_1}} - E^{(0)}_{S_{i_1}-1,m_{i_1}-\alpha_1,n_{i_1}-1} + i\omega_{m1})\beta}}{(E^{(0)}_{S_{i_1},m_{i_1},n_{i_1}} - E^{(0)}_{S_{i_1}-1,m_{i_1}-\alpha_1,n_{i_1}-1} - i\omega_{m1})^2} \right.$$
$$\left. - \frac{\beta}{E^{(0)}_{S_{i_1},m_{i_1},n_{i_1}} - E^{(0)}_{S_{i_1}-1,m_{i_1}+\alpha_1,n_{i_1}+1} + i\omega_{m1}} \right]. \tag{4.91}$$

Thus, Eq. (4.87) reduces to

$$a^{(0)}_2(i_1\alpha_1,\omega_{m1}) = \frac{1}{\beta\mathcal{Z}^{(0)}} \sum_{S_{i_1},m_{i_1},n_{i_1}} e^{-\beta E^{(0)}_{S_{i_1},m_{i_1},n_{i_1}}} \left(\mathcal{I}_{a^\dagger_{\alpha_1} a_{\alpha_1}} + \mathcal{I}_{a_{\alpha_1} a^\dagger_{\alpha_1}} \right). \tag{4.92}$$

The terms in Eq. (4.92) without β-factor can be summarized as:

$$\sum_{S_{i_1}=0}^{\infty}\sum_{n_{i_1}=1}^{\infty}\sum_{m_{i_1}=-S}^{S} O^2_{\alpha_1,S_{i_1},m_{i_1},n_{i_1}} \frac{-e^{-\beta E^{(0)}_{S_{i_1},m_{i_1},n_{i_1}}} + e^{-\beta E^{(0)}_{S_{i_1}+1,m_{i_1}-\alpha_1,n_{i_1}-1}}}{(E^{(0)}_{S_{i_1},m_{i_1},n_{i_1}} - E^{(0)}_{S_{i_1}+1,m_{i_1}-\alpha_1,n_{i_1}-1} - i\omega_{m1})^2}$$
$$+ \sum_{S_{i_1}=1}^{\infty}\sum_{n_{i_1}=1}^{\infty}\sum_{m_{i_1}=-S}^{S} P^2_{\alpha_1,S_{i_1},m_{i_1},n_{i_1}} \frac{-e^{-\beta E^{(0)}_{S_{i_1},m_{i_1},n_{i_1}}} + e^{-\beta E^{(0)}_{S_{i_1}-1,m_{i_1}-\alpha_1,n_{i_1}-1}}}{(E^{(0)}_{S_{i_1},m_{i_1},n_{i_1}} - E^{(0)}_{S_{i_1}-1,m_{i_1}-\alpha_1,n_{i_1}-1} - i\omega_{m1})^2}$$
$$+ \sum_{S_{i_1}=0}^{\infty}\sum_{n_{i_1}=0}^{\infty}\sum_{m_{i_1}=-S}^{S} M^2_{\alpha_1,S_{i_1},m_{i_1},n_{i_1}} \frac{-e^{-\beta E^{(0)}_{S_{i_1},m_{i_1},n_{i_1}}} + e^{-\beta E^{(0)}_{S_{i_1}+1,m_{i_1}+\alpha_1,n_{i_1}+1}}}{(E^{(0)}_{S_{i_1},m_{i_1},n_{i_1}} - E^{(0)}_{S_{i_1}+1,m_{i_1}+\alpha_1,n_{i_1}+1} + i\omega_{m1})^2}$$
$$+ \sum_{S_{i_1}=1}^{\infty}\sum_{n_{i_1}=0}^{\infty}\sum_{m_{i_1}=-S}^{S} N^2_{\alpha_1,S_{i_1},m_{i_1},n_{i_1}} \frac{-e^{-\beta E^{(0)}_{S_{i_1},m_{i_1},n_{i_1}}} + e^{-\beta E^{(0)}_{S_{i_1}-1,m_{i_1}+\alpha_1,n_{i_1}+1}}}{(E^{(0)}_{S_{i_1},m_{i_1},n_{i_1}} - E^{(0)}_{S_{i_1}-1,m_{i_1}+\alpha_1,n_{i_1}+1} + i\omega_{m1})^2}, \tag{4.93}$$

By shifting the summation index, we obtain:

$$\sum_{S_{i_1}=1}^{\infty}\sum_{n_{i_1}=0}^{\infty}\sum_{m_{i_1}=-S}^{S} O^2_{\alpha_1,S_{i_1}-1,m_{i_1}+\alpha_1,n_{i_1}+1} \frac{-e^{-\beta E^{(0)}_{S_{i_1}-1,m_{i_1}+\alpha_1,n_{i_1}+1}} + e^{-\beta E^{(0)}_{S_{i_1},m_{i_1},n_{i_1}}}}{(E^{(0)}_{S_{i_1}-1,m_{i_1}+\alpha_1,n_{i_1}+1} - E^{(0)}_{S_{i_1},m_{i_1},n_{i_1}} - i\omega_{m1})^2}$$
$$+ \sum_{S_{i_1}=0}^{\infty}\sum_{n_{i_1}=0}^{\infty}\sum_{m_{i_1}=-S}^{S} P^2_{\alpha_1,S_{i_1}+1,m_{i_1}+\alpha_1,n_{i_1}+1} \frac{-e^{-\beta E^{(0)}_{S_{i_1}+1,m_{i_1}+\alpha_1,n_{i_1}+1}} + e^{-\beta E^{(0)}_{S_{i_1},m_{i_1},n_{i_1}}}}{(E^{(0)}_{S_{i_1}+1,m_{i_1}+\alpha_1,n_{i_1}+1} - E^{(0)}_{S_{i_1},m_{i_1},n_{i_1}} - i\omega_{m1})^2}$$
$$+ \sum_{S_{i_1}=0}^{\infty}\sum_{n_{i_1}=0}^{\infty}\sum_{m_{i_1}=-S}^{S} M^2_{\alpha_1,S_{i_1},m_{i_1},n_{i_1}} \frac{-e^{-\beta E^{(0)}_{S_{i_1},m_{i_1},n_{i_1}}} + e^{-\beta E^{(0)}_{S_{i_1}+1,m_{i_1}+\alpha_1,n_{i_1}+1}}}{(E^{(0)}_{S_{i_1},m_{i_1},n_{i_1}} - E^{(0)}_{S_{i_1}+1,m_{i_1}+\alpha_1,n_{i_1}+1} + i\omega_{m1})^2}$$
$$+ \sum_{S_{i_1}=1}^{\infty}\sum_{n_{i_1}=0}^{\infty}\sum_{m_{i_1}=-S}^{S} N^2_{\alpha_1,S_{i_1},m_{i_1},n_{i_1}} \frac{-e^{-\beta E^{(0)}_{S_{i_1},m_{i_1},n_{i_1}}} + e^{-\beta E^{(0)}_{S_{i_1}-1,m_{i_1}+\alpha_1,n_{i_1}+1}}}{(E^{(0)}_{S_{i_1},m_{i_1},n_{i_1}} - E^{(0)}_{S_{i_1}-1,m_{i_1}+\alpha_1,n_{i_1}+1} + i\omega_{m1})^2} = 0, \tag{4.94}$$

where we have used the identity $e^{-i\beta\omega_m} = 1$ following from (4.80) and the fact $P^2_{\alpha_1,S_{i_1}+1,m_{i_1}+\alpha_1,n_{i_1}+1} = M^2_{\alpha_1,S_{i_1},m_{i_1},n_{i_1}}$ and $O^2_{\alpha_1,S_{i_1}-1,m_{i_1}+\alpha_1,n_{i_1}+1} = N^2_{\alpha_1,S_{i_1},m_{i_1},n_{i_1}}$ as is shown in Eqs. (A.27) and (A.29). Therefore Eq. (4.92) reduces to

$$a^{(0)}_2(i_1\alpha_1,\omega_{m1}) = \frac{1}{\mathcal{Z}^{(0)}} \sum_{S_{i_1},m_{i_1},n_{i_1}} e^{-\beta E^{(0)}_{S_{i_1},m_{i_1},n_{i_1}}} \left[\frac{M^2_{\alpha_1,S_{i_1},m_{i_1},n_{i_1}}}{E^{(0)}_{S_{i_1}+1,m_{i_1}+\alpha_1,n_{i_1}+1} - E^{(0)}_{S_{i_1},m_{i_1},n_{i_1}} - i\omega_{m1}} \right.$$
$$+ \frac{N^2_{\alpha_1,S_{i_1},m_{i_1},n_{i_1}}}{E^{(0)}_{S_{i_1}-1,m_{i_1}+\alpha_1,n_{i_1}+1} - E^{(0)}_{S_{i_1},m_{i_1},n_{i_1}} - i\omega_{m1}} - \frac{O^2_{\alpha_1,S_{i_1},m_{i_1},n_{i_1}}}{E^{(0)}_{S_{i_1},m_{i_1},n_{i_1}} - E^{(0)}_{S_{i_1}+1,m_{i_1}-\alpha_1,n_{i_1}-1} - i\omega_{m1}}$$
$$\left. - \frac{P^2_{\alpha_1,S_{i_1},m_{i_1},n_{i_1}}}{E^{(0)}_{S_{i_1},m_{i_1},n_{i_1}} - E^{(0)}_{S_{i_1}-1,m_{i_1}-\alpha_1,n_{i_1}-1} - i\omega_{m1}} \right]. \tag{4.95}$$

In view of (4.70), we use the cumulant multiplicity properties in frequency space and frequency con-

servation, which leads to the relation

$$a_2^{(1)}(i_1\alpha_1,\omega_{m1};i_3|i_2\alpha_2,\omega_{m2};j_3) = a_2^{(0)}(i_1\alpha_1,\omega_{m1})a_2^{(0)}(j_3\alpha_2,\omega_{m2}) \times \delta_{i_1,i_3}\delta_{j_3,i_2}\delta_{\omega_{m1},\omega_{m2}}\delta_{\alpha_1,\alpha_2}, \tag{4.96}$$

we find that the expansion coefficient correction (4.70) under consideration takes on the form

$$\begin{aligned} a_2^{(1)}(i_1\alpha_1,\omega_{m1};i_3|i_2\alpha_2,\omega_{m2};j_3) &= \frac{1}{(\mathcal{Z}^{(0)})^2}\sum_{S_{i_1},m_{i_1},n_{i_1}} e^{-\beta E^{(0)}_{S_{i_1},m_{i_1},n_{i_1}}}\delta_{i_2,i_3}\delta_{j_3,i_1}\delta_{\omega_{m1},\omega_{m2}}\delta_{\alpha_1,\alpha_2} \\ &\times\left[\frac{M^2_{\alpha_1,S_i,m_i,n_i}}{E^{(0)}_{S_{i_1}+1,m_{i_1}+\alpha_1,n_{i_1}+1}-E^{(0)}_{S_{i_1},m_{i_1},n_{i_1}}-i\omega_{m1}}+\frac{N^2_{\alpha_1,S_i,m_i,n_i}}{E^{(0)}_{S_i-1,m_i+\alpha_1,n_i+1}-E^{(0)}_{S_i,m_i,n_i}-i\omega_{m1}}\right. \\ &\left.-\frac{O^2_{\alpha_1,S_i,m_i,n_i}}{E^{(0)}_{S_i,m_i,n_i}-E^{(0)}_{S_i+1,m_i-\alpha_1,n_i-1}-i\omega_{m1}}-\frac{P^2_{\alpha_1,S_i,m_i,n_i}}{E^{(0)}_{S_i,m_i,n_i}-E^{(0)}_{S_i-1,m_i-\alpha_1,n_i-1}-i\omega_{m1}}\right] \\ &\times\left[\frac{M^2_{\alpha_2,S_{j_3},m_{j_3},n_{j_3}}}{E^{(0)}_{S_{j_3}+1,m_{j_3}+\alpha_2,n_{j_3}+1}-E^{(0)}_{S_{j_3},m_{j_3},n_{j_3}}-i\omega_{m2}}+\frac{N^2_{\alpha_2,S_{j_3},m_{j_3},n_{j_3}}}{E^{(0)}_{S_{j_3}-1,m_{j_3}+\alpha_2,n_{j_3}+1}-E^{(0)}_{S_{j_3},m_{j_3},n_{j_3}}-i\omega_{m2}}\right. \\ &\left.-\frac{O^2_{\alpha_2,S_{j_3},m_{j_3},n_{j_3}}}{E^{(0)}_{S_{j_3},m_{j_3},n_{j_3}}-E^{(0)}_{S_{j_3}+1,m_{j_3}-\alpha_2,n_{j_3}-1}-i\omega_{m2}}-\frac{P^2_{\alpha_2,S_{j_3},m_{j_3},n_{j_3}}}{E^{(0)}_{S_{j_3},m_{j_3},n_{j_3}}-E^{(0)}_{S_{j_3}-1,m_{j_3}-\alpha_2,n_{j_3}-1}-i\omega_{m2}}\right]. \end{aligned} \tag{4.97}$$

Thus with (4.95) and (4.97), we obtain the full expression for Eq. (4.75) in Matsubara frequency space which has the form

$$W_2(i_1\alpha_1,\omega_{m1}|i_2\alpha_2,\omega_{m2}) = \Big[a_2^{(0)}(i_1\alpha_1,\omega_{m1})\delta_{i_1,i_2} + \sum_{i_3,j_3} J_{i_3j_3}a_2^{(0)}(i_3\alpha_1,\omega_{m1}) \times a_2^{(0)}(j_3\alpha_2,\omega_{m2})\delta_{i_3,i_1}\delta_{j_3,i_2}\Big]\delta_{\omega_{m1},\omega_{m2}}\delta_{\alpha_1,\alpha_2}. \tag{4.98}$$

4.7. Fourth Order in Currents

In this section we derive the coefficient of fourth order in the currents (4.76) in Matsubara frequency. To do this, we need to consider at first the zeroth order hopping term, which we do in frequency space

$$a_4^{(0)}(i_1\alpha_1,\omega_{m1};i_2\alpha_2,\omega_{m2}|i_3\alpha_3,\omega_{m3};i_4\alpha_4,\omega_{m4}) = \frac{1}{\beta^2}\delta_{i_1,i_2}\delta_{i_3,i_4}\delta_{i_1,i_3}\int_0^\beta d\tau_1\int_0^\beta d\tau_2\int_0^\beta d\tau_3\int_0^\beta d\tau_4 \times_{i_1} C_2^{(0)}(\alpha_1,\tau_1;\alpha_2,\tau_2|\alpha_3,\tau_3;\alpha_4,\tau_4)e^{-i(\omega_{m1}\tau_1+\omega_{m2}\tau_2-\omega_{m3}\tau_3-\omega_{m4}\tau_4)}. \tag{4.99}$$

Thus, this coefficients is of the form

$$a_4^{(0)}(i_1\alpha_1,\omega_{m1};i_2\alpha_2,\omega_{m2}|i_3\alpha_3,\omega_{m3};i_4\alpha_4,\omega_{m4}) = a_4^{(0)}(\alpha_1,\omega_{m1};\alpha_2,\omega_{m2}|\alpha_3,\omega_{m3};\alpha_4,\omega_{m4};i_1)\delta_{i_1,i_2}\delta_{i_3,i_4}\delta_{i_1,i_3}. \tag{4.100}$$

Substituting Eq. (4.78) into (4.99), leads to

$$a_4^{(0)}(\alpha_1,\omega_{m1};\alpha_2,\omega_{m2}|\alpha_3,\omega_{m3};\alpha_4,\omega_{m4};i_1) = \frac{1}{\beta^2}\int_0^\beta d\tau_1\int_0^\beta d\tau_2\int_0^\beta d\tau_3\int_0^\beta d\tau_4$$
$$\times\left[\left\langle\hat{T}\left[\hat{a}^\dagger_{i_1\alpha_1}(\tau_1)\hat{a}^\dagger_{i_1\alpha_2}(\tau_2)\hat{a}_{i_1\alpha_3}(\tau_3)\hat{a}_{i_1\alpha_4}(\tau_4)\right]\right\rangle^{(0)} - {}_{i_1}C_1^{(0)}(\tau_1,\alpha_1|\tau_3,\alpha_3)\,{}_{i_1}C_1^{(0)}(\tau_2,\alpha_2|\tau_4,\alpha_4)\right.$$
$$\left. - {}_{i_1}C_1^{(0)}(\tau_1,\alpha_1|\tau_4,\alpha_4){}_{i_1}C_1^{(0)}(\tau_2,\alpha_2|\tau_3,\alpha_3)\right] e^{-i(\omega_{m1}\tau_1+\omega_{m2}\tau_2-\omega_{m3}\tau_3-\omega_{m4}\tau_4)}. \tag{4.101}$$

Using the conservation of frequency and spin index leads to the expression

$$a_4^{(0)}(\alpha_1,\omega_{m1};\alpha_2,\omega_{m2}|\alpha_3,\omega_{m3};\alpha_4,\omega_{m4};i_1) = \frac{1}{\beta^2}\delta_{\omega_{m1}+\omega_{m2},\omega_{m3}+\omega_{m4}}\left\{\int_0^\beta d\tau_1\int_0^\beta d\tau_2\right.$$
$$\int_0^\beta d\tau_3\int_0^\beta d\tau_4\left\langle\hat{T}\left[\hat{a}^\dagger_{i_1\alpha_1}(\tau_1)\hat{a}^\dagger_{i_1\alpha_2}(\tau_2)\hat{a}_{i_1\alpha_3}(\tau_3)\hat{a}_{i_1\alpha_4}(\tau_4)\right]\right\rangle e^{-i(\omega_{m1}\tau_1+\omega_{m2}\tau_2-\omega_{m3}\tau_3-\omega_{m4}\tau_4)}$$
$$- a_2^{(0)}(i_1\alpha_1,\omega_{m1}|i_1\alpha_3,\omega_{m3})a_2^{(0)}(i_1\alpha_2,\omega_{m2}|i_1\alpha_4,\omega_{m4})\left[\delta_{\alpha_1,\alpha_3}\delta_{\alpha_2,\alpha_4}\delta_{\omega_{m1},\omega_{m3}}\delta_{\omega_{m2},\omega_{m4}}\right.$$
$$\left.\left.+\delta_{\alpha_1,\alpha_4}\delta_{\alpha_2,\alpha_3}\delta_{\omega_{m1},\omega_{m4}}\delta_{\omega_{m2},\omega_{m3}}\right]\right\}\delta_{\alpha_1+\alpha_2,\alpha_3+\alpha_4}. \tag{4.102}$$

Now we calculate the integral over the time-ordered thermal average in the above expression because the last two terms have already been calculated in Eq (4.95). Note that there are six distinct permutations leading to different expectation values for the time-ordered product of the annihilation and creation operators. Each order has four time and four spin variable permutations corresponding to $\tau_1 \leftrightarrow \tau_2$, $\tau_3 \leftrightarrow \tau_4$, $\alpha_1 \leftrightarrow \alpha_2$ and $\alpha_3 \leftrightarrow \alpha_4$. Thus, we have 24 terms for the above expectation value. Fortunately, we need to determine only six different thermal averages for one specific time-ordering because, due to symmetry reasons, there are some integrals over different time-variable permutations which yield the same result. Furthermore, as these expectation values are local, we drop the site indices in the following calculations and calculate the following expressions:

$$\Theta(\tau_4-\tau_3)\Theta(\tau_3-\tau_1)\Theta(\tau_1-\tau_2)\left\langle\hat{a}_{\alpha_4}(\tau_4)\hat{a}_{\alpha_3}(\tau_3)\hat{a}^\dagger_{\alpha_1}(\tau_1)\hat{a}^\dagger_{\alpha_2}(\tau_2)\right\rangle^{(0)}, \tag{4.103}$$
$$\Theta(\tau_1-\tau_2)\Theta(\tau_2-\tau_3)\Theta(\tau_3-\tau_4)\left\langle\hat{a}^\dagger_{\alpha_1}(\tau_1)\hat{a}^\dagger_{\alpha_2}(\tau_2)\hat{a}_{\alpha_3}(\tau_3)\hat{a}_{\alpha_4}(\tau_4)\right\rangle^{(0)}, \tag{4.104}$$
$$\Theta(\tau_4-\tau_1)\Theta(\tau_1-\tau_3)\Theta(\tau_3-\tau_2)\left\langle\hat{a}_{\alpha_4}(\tau_4)\hat{a}^\dagger_{\alpha_1}(\tau_1)\hat{a}_{\alpha_3}(\tau_3)\hat{a}^\dagger_{\alpha_2}(\tau_2)\right\rangle^{(0)}, \tag{4.105}$$
$$\Theta(\tau_1-\tau_4)\Theta(\tau_4-\tau_3)\Theta(\tau_3-\tau_2)\left\langle\hat{a}^\dagger_{\alpha_1}(\tau_1)\hat{a}_{\alpha_4}(\tau_4)\hat{a}_{\alpha_3}(\tau_3)\hat{a}^\dagger_{\alpha_2}(\tau_2)\right\rangle^{(0)}, \tag{4.106}$$
$$\Theta(\tau_4-\tau_1)\Theta(\tau_1-\tau_2)\Theta(\tau_2-\tau_3)\left\langle\hat{a}_{\alpha_4}(\tau_4)\hat{a}^\dagger_{\alpha_1}(\tau_1)\hat{a}^\dagger_{\alpha_2}(\tau_2)\hat{a}_{\alpha_3}(\tau_3)\right\rangle^{(0)}, \tag{4.107}$$
$$\Theta(\tau_1-\tau_3)\Theta(\tau_3-\tau_2)\Theta(\tau_2-\tau_4)\left\langle\hat{a}^\dagger_{\alpha_1}(\tau_1)\hat{a}_{\alpha_3}(\tau_3)\hat{a}^\dagger_{\alpha_2}(\tau_2)\hat{a}_{\alpha_4}(\tau_4)\right\rangle^{(0)}. \tag{4.108}$$

First, we will define all the above expressions individually in Appendix B in Eqs. (B.1)–(B.6) without Heaviside step function before the integration. Following the same method as for the second-order expansion coefficient, we perform a Matsubara transformation according to equations (4.82) and (4.83). The details of the calculation are given in Appendix B in Eqs. (B.7)–(B.10) so that Eq. (4.102) finally

becomes

$$a_4^{(0)}(\alpha_1,\omega_{m1};\alpha_2,\omega_{m2}|\alpha_3,\omega_{m3};\alpha_4,\omega_{m4}) = \frac{1}{\beta}\frac{1}{\mathcal{Z}^{(0)}}\sum_{S,m,n} e^{-\beta E^{(0)}_{S,m,n}}\delta_{\alpha_1+\alpha_2,\alpha_3+\alpha_4}\delta_{\omega_{m1}+\omega_{m2},\omega_{m3}+\omega_{m4}}$$

$$\times\left\{\frac{M_{\alpha_2,S,m,n}M_{\alpha_4,S,m,n}M_{\alpha_3,S+1,m+\alpha_4,n+1}M_{\alpha_1,S+1,m+\alpha_2,n+1}}{\left(\triangle E^{(0)}_{S+1,m+\alpha_4,n+1}+i\omega_{m3}-i\omega_{m1}-i\omega_{m2}\right)\left(\triangle E^{(0)}_{S+2,m+\alpha_2+\alpha_1,n+2}-i\omega_{m1}-i\omega_{m2}\right)}\right.$$

$$\times\frac{1}{\left(\triangle E^{(0)}_{S+1,m+\alpha_2,n+1}-i\omega_{m2}\right)}+\frac{N_{\alpha_2,S,m,n}N_{\alpha_4,S,m,n}N_{\alpha_3,S-1,m+\alpha_4,n+1}N_{\alpha_1,S-1,m+\alpha_2,n+1}}{\left(\triangle E^{(0)}_{S-2,m+\alpha_2+\alpha_1,n+2}-i\omega_{m1}-i\omega_{m2}\right)\left(\triangle E^{(0)}_{S-1,m+\alpha_2,n+1}-i\omega_{m2}\right)}$$

$$\times\frac{1}{\left(\triangle E^{(0)}_{S-1,m+\alpha_4,n+1}+i\omega_{m3}-i\omega_{m1}-i\omega_{m2}\right)}+\frac{O_{\alpha_1,S,m,n}O_{\alpha_4,S,m,n}O_{\alpha_2,S+1,m-\alpha_1,n-1}O_{\alpha_3,S+1,m-\alpha_4,n-1}}{\left(\triangle E^{(0)}_{S+1,m-\alpha_1,n-1}+i\omega_{m3}+i\omega_{m4}-i\omega_{m2}\right)}$$

$$\times\frac{1}{\left(\triangle E^{(0)}_{S+2,m-\alpha_2-\alpha_1,n-2}+i\omega_{m3}+i\omega_{m4}\right)\left(\triangle E^{(0)}_{S+1,m-\alpha_4,n-1}+i\omega_{m4}\right)}+\frac{1}{\left(\triangle E^{(0)}_{S-1,m-\alpha_4,n-1}+i\omega_{m4}\right)}$$

$$\times\frac{P_{\alpha_1,S,m,n}P_{\alpha_4,S,m,n}P_{\alpha_2,S+1,m-\alpha_1,n-1}P_{\alpha_3,S+1,m-\alpha_4,n-1}}{\left(\triangle E^{(0)}_{S-1,m-\alpha_1,n-1}+i\omega_{m3}+i\omega_{m4}-i\omega_{m2}\right)\left(\triangle E^{(0)}_{S-2,m-\alpha_2-\alpha_1,n-2}+i\omega_{m3}+i\omega_{m4}\right)}$$

$$+\frac{1}{\left(\triangle E^{(0)}_{S,m+\alpha_3+\alpha_4,n+2}-i\omega_{m1}-i\omega_{m2}\right)}\left(\frac{M_{\alpha_4,S,m,n}N_{\alpha_3,S+1,m+\alpha_4,n+1}}{\triangle E^{(0)}_{S+1,m+\alpha_4,n+1}+i\omega_{m3}-i\omega_{m1}-i\omega_{m2}}\right.$$

$$\left.+\frac{N_{\alpha_4,S,m,n}M_{\alpha_3,S-1,m+\alpha_4,n+1}}{\triangle E^{(0)}_{S-1,m+\alpha_4,n+1}+i\omega_{m3}-i\omega_{m1}-i\omega_{m2}}\right)\left(\frac{M_{\alpha_2,S,m,n}N_{\alpha_1,S+1,m+\alpha_2,n+1}}{\triangle E^{(0)}_{S+1,m+\alpha_2,n+1}-i\omega_{m2}}\right.$$

$$\left.+\frac{N_{\alpha_2,S,m,n}M_{\alpha_1,S-1,m+\alpha_2,n+1}}{\triangle E^{(0)}_{S-1,m+\alpha_2,n+1}-i\omega_{m2}}\right)+\frac{1}{\triangle E^{(0)}_{S,m-\alpha_1-\alpha_2,n-2}+i\omega_{m3}+i\omega_{m4}}$$

$$\times\left(\frac{O_{\alpha_1,S,m,n}P_{\alpha_2,S+1,m-\alpha_1,n-1}}{\triangle E^{(0)}_{S+1,m-\alpha_1,n-1}+i\omega_{m3}+i\omega_{m4}-i\omega_{m2}}+\frac{P_{\alpha_1,S,m,n}O_{\alpha_2,S-1,m-\alpha_1,n-1}}{\triangle E^{(0)}_{S-1,m-\alpha_1,n-1}+i\omega_{m3}+i\omega_{m4}-i\omega_{m2}}\right)$$

$$\times\left(\frac{O_{\alpha_4,S,m,n}P_{\alpha_3,S+1,m-\alpha_4,n-1}}{\triangle E^{(0)}_{S+1,m-\alpha_4,n-1}+i\omega_{m4}}+\frac{P_{\alpha_4,S,m,n}O_{\alpha_3,S-1,m-\alpha_4,n-1}}{\triangle E^{(0)}_{S-1,m-\alpha_4,n-1}+i\omega_{m4}}\right)+\frac{1}{\triangle E^{(0)}_{S+2,m+\alpha_4-\alpha_1,n}-i\omega_{m2}+i\omega_{m3}}$$

$$\times\left(\frac{M_{\alpha_4,S,m,n}O_{\alpha_1,S+1,m+\alpha_4,n+1}}{\triangle E^{(0)}_{S+1,m+\alpha_4,n+1}+i\omega_{m3}-i\omega_{m1}-i\omega_{m2}}+\frac{O_{\alpha_1,S,m,n}M_{\alpha_4,S+1,m-\alpha_1,n-1}}{\triangle E^{(0)}_{S+1,m-\alpha_1,n-1}+i\omega_{m3}+i\omega_{m4}-i\omega_{m2}}\right)$$

$$\times\left(\frac{M_{\alpha_2,S,m,n}O_{\alpha_3,S+1,m+\alpha_2,n+1}}{\triangle E^{(0)}_{S+1,m+\alpha_2,n+1}-i\omega_{m2}}+\frac{O_{\alpha_3,S,m,n}M_{\alpha_2,S+1,m-\alpha_3,n-1}}{\triangle E^{(0)}_{S+1,m-\alpha_3,n-1}+i\omega_{m3}}\right)+\frac{1}{\triangle E^{(0)}_{S-2,m+\alpha_4-\alpha_1,n}-i\omega_{m2}+i\omega_{m3}}$$

$$\times\left(\frac{N_{\alpha_4,S,m,n}P_{\alpha_1,S-1,m+\alpha_4,n+1}}{\triangle E^{(0)}_{S-1,m+\alpha_4,n+1}+i\omega_{m3}-i\omega_{m1}-i\omega_{m2}}+\frac{P_{\alpha_1,S,m,n}N_{\alpha_4,S+1,m-\alpha_1,n-1}}{\triangle E^{(0)}_{S-1,m-\alpha_1,n-1}+i\omega_{m3}+i\omega_{m4}-i\omega_{m2}}\right)$$

$$\times\left(\frac{N_{\alpha_2,S,m,n}P_{\alpha_3,S-1,m+\alpha_2,n+1}}{\triangle E^{(0)}_{S-1,m+\alpha_2,n+1}-i\omega_{m2}}+\frac{P_{\alpha_3,S,m,n}N_{\alpha_2,S-1,m-\alpha_3,n-1}}{\triangle E^{(0)}_{S-1,m-\alpha_3,n-1}+i\omega_{m3}}\right)$$

$$+\ \delta_{\alpha_1,\alpha_4}\delta_{\omega_{m1},\omega_{m4}}\left(\frac{M_{\alpha_4,S,m,n}M_{\alpha_1,S,m,n}}{\triangle E^{(0)}_{S+1,m+\alpha_4,n+1}-i\omega_{m1}}+\frac{N_{\alpha_4,S,m,n}N_{\alpha_1,S,m,n}}{\triangle E^{(0)}_{S-1,m+\alpha_4,n+1}-i\omega_{m1}}+\frac{O_{\alpha_4,S,m,n}O_{\alpha_1,S,m,n}}{\triangle E^{(0)}_{S+1,m-\alpha_1,n-1}-i\omega_{m4}}\right.$$

$$
\begin{aligned}
&+\frac{P_{\alpha_4,S,m,n}P_{\alpha_1,S,m,n}}{\triangle E^{(0)}_{S-1,m-\alpha_1,n-1}-i\omega_{m4}}\Bigg)\Bigg(\frac{M_{\alpha_3,S,m,n}M_{\alpha_2,S,m,n}}{\triangle E^{(0)}_{S+1,m+\alpha_2,n+1}-i\omega_{m2}}\left(\frac{\beta}{2}-\frac{1}{\triangle E^{(0)}_{S+1,m+\alpha_2,n+1}-i\omega_{m3}}\right)\\
&+\frac{N_{\alpha_3,S,m,n}N_{\alpha_2,S,m,n}}{\triangle E^{(0)}_{S-1,m+\alpha_2,n+1}-i\omega_{m2}}\left(\frac{\beta}{2}-\frac{1}{\triangle E^{(0)}_{S-1,m+\alpha_2,n+1}-i\omega_{m3}}\right)\\
&+\frac{O_{\alpha_3,S,m,n}O_{\alpha_2,S,m,n}}{\triangle E^{(0)}_{S+1,m-\alpha_3,n-1}-i\omega_{m3}}\left(\frac{\beta}{2}-\frac{1}{\triangle E^{(0)}_{S+1,m-\alpha_3,n-1}-i\omega_{m2}}\right)\\
&+\frac{P_{\alpha_3,S,m,n}P_{\alpha_2,S,m,n}}{\triangle E^{(0)}_{S+1,m-\alpha_3,n-1}-i\omega_{m3}}\left(\frac{\beta}{2}-\frac{1}{\triangle E^{(0)}_{S+1,m-\alpha_3,n-1}-i\omega_{m2}}\right)\Bigg)\Bigg\}_{\substack{\alpha_1\leftrightarrow\alpha_2\\ \alpha_3\leftrightarrow\alpha_4\\ \omega_{m1}\leftrightarrow\omega_{m2}\\ \omega_{m3}\leftrightarrow\omega_{m4}}}\\
&-2\,\delta_{\alpha_1,\alpha_3}\delta_{\alpha_2,\alpha_4}\delta_{\omega_{m1},\omega_{m3}}\delta_{\omega_{m2},\omega_{m4}}a_2^{(0)}(\alpha_1,\omega_{m1}|\alpha_3,\omega_{m3})a_2^{(0)}(\alpha_2,\omega_{m2}|\alpha_4,\omega_{m4})\\
&-2\,\delta_{\alpha_1,\alpha_4}\delta_{\alpha_2,\alpha_3}\delta_{\omega_{m1},\omega_{m4}}\delta_{\omega_{m2},\omega_{m3}}a_2^{(0)}(\alpha_1,\omega_{m1}|\alpha_4,\omega_{m4})a_2^{(0)}(\alpha_2,\omega_{m2}|\alpha_3,\omega_{m3}),
\end{aligned}
\tag{4.109}
$$

where $\triangle E^{(0)}_{S',m',n'}=E^{(0)}_{S',m',n'}-E^{(0)}_{S,m,n}$ and $\omega_{m1}\leftrightarrow\omega_{m2}$ and $\alpha_1\leftrightarrow\alpha_2$ refer to a symmetrization with respect to the Matsubara frequencies and spin indices. Eq. (4.109) shows the expression for the fourth-order coefficient of the free energy, which we can cross-check in different ways. At first we consider the zero-temperature limit, i.e. $\beta\to\infty$, and observe that all β-divergent terms in Eq. (4.109) are cancelled by the $(a_2^{(0)})^2$-terms. In the next section, we show that Eq. (4.109) allows to recover the mean-field approach from Chapter 3 at zero-temperature.

The next quantity, which would have to be calculated, is $a_4^{(1)}$ being defined in Eq. (4.72). However, in Section 4.8 it turns out that $a_4^{(1)}$ is not needed for the mean-field theory and it will be proven in Chapter 5 that $a_4^{(1)}$ will also not appear in the effective action. Therefore, we do not have to calculate it explicitly.

4.8. Mean-Field Theory

We start with comparing the mean-field Hamiltonian (3.11) with the source Hamiltonian (4.1), which yields with (4.37) the identification

$$j_{i\alpha}(\tau)=-zJ\Psi_\alpha. \tag{4.110}$$

Inserting (4.110) into (4.74), we obtain an expansion of the mean-field free energy $\mathcal{F}_{\mathrm{MF}}$ in powers of the order parameter which reads up to fourth order as follows:

$$\mathcal{F}_{\mathrm{MF}}=\mathcal{F}_0-N_s\left(\sum_\alpha a_2^{\mathrm{MF}}(\alpha,0)\,|\Psi_\alpha|^2+\sum_{\alpha_1}\sum_{\alpha_2}\sum_{\alpha_3}\sum_{\alpha_4}a_4^{\mathrm{MF}}(\alpha_1,0;\alpha_2,0|\alpha_3,0;\alpha_4,0)\,\Psi^*_{\alpha_1}\Psi^*_{\alpha_2}\Psi_{\alpha_3}\Psi_{\alpha_4}\right), \tag{4.111}$$

where the respective mean-field Landau coefficients are only calculated up to the fourth hopping order. Thus, we get for them

$$a_2^{\mathrm{MF}}(\alpha,0)=a_2^{(0)}(\alpha,0)(zJ)^2-zJ, \tag{4.112}$$

$$a_4^{\mathrm{MF}}(\alpha_1,0;\alpha_2,0|\alpha_3,0;\alpha_4,0)=\frac{\beta}{4}\,a_4^{(0)}(\alpha_1,0;\alpha_2,0|\alpha_3,0;\alpha_4,0)(zJ)^4. \tag{4.113}$$

We note that here $a_4^{(1)}$ does not appear as it is of fifth order in the hopping.

4.8.1. Ferromagnetic Interaction

Hence, in order to check the result (4.109), we first calculate $a_4^{(0)}$ for vanishing Matsubara frequencies $\omega_{m1}=\omega_{m2}=\omega_{m3}=\omega_{m4}=0$ in the case of ferromagnetic interaction at zero temperature with spin-1 which should yield the mean-field result. As discussed in Subsection 3.4.2, for a ferromagnetic interaction there is no difference between this interaction with and without η except that the degeneracy with respect to the magnetic quantum number m is lifted. Hence, the ground state becomes $|n,n,n\rangle$. Therefore, the coefficients $a_2^{(0)}$ and $a_4^{(0)}$ are defined as

$$a_2^{(0)}(1,0)=\frac{1}{\mathcal{Z}^{(0)}}\sum_{n=0}^{\infty}e^{-\beta E^{(0)}_{n,n,n}}\left(\frac{n+1}{\triangle E^{(0)}_{n+1,n+1,n+1}}+\frac{n}{\triangle E^{(0)}_{n-1,n-1,n-1}}\right), \tag{4.114}$$

$$\begin{aligned}
a_4^{(0)}(1,0;1,0|1,0;1,0)=\frac{2}{\beta\mathcal{Z}^{(0)}}\sum_{n=0}^{\infty}e^{-\beta E^{(0)}_{n,n,n}}\Bigg\{&\frac{2n\,(n-1)}{(\triangle E^{(0)}_{n-1,n-1,n-1})^2\triangle E^{(0)}_{n-2,n-2,n-2}}\\
&+n^2\left[-\frac{2}{(\triangle E^{(0)}_{n-1,n-1,n-1})^3}+\frac{\beta}{(\triangle E^{(0)}_{n-1,n-1,n-1})^2}\right]+\frac{2\,(n+1)\,(n+2)}{(\triangle E^{(0)}_{n+1,n+1,n+1})^2\triangle E^{(0)}_{n+2,n+2,n+2}}\\
&-n\,(n+1)\left[\frac{2\left(\triangle E^{(0)}_{n+1,n+1,n+1}+\triangle E^{(0)}_{n-1,n-1,n-1}\right)}{\left(\triangle E^{(0)}_{n-1,n-1,n-1}\right)^2\left(\triangle E^{(0)}_{n+1,n+1,n+1}\right)^2}-\frac{2\beta}{\triangle E^{(0)}_{n-1,n-1,n-1}\triangle E^{(0)}_{n+1,n+1,n+1}}\right]\\
&-(n+1)^2\left[\frac{2}{(\triangle E^{(0)}_{n+1,n+1,n+1})^3}-\frac{\beta}{(\triangle E^{(0)}_{n+1,n+1,n+1})^2}\right]\Bigg\}-2\left[a_2^{(0)}(1,0)\right]^2,
\end{aligned} \tag{4.115}$$

where $\triangle E^{(0)}_{S',m',n'}=E^{(0)}_{S',m',n'}-E^{(0)}_{n,n,n}$. This result coincides with the finite-temperature finding in Ref. [64]. Note that another cross check is possible for ferromagnetic interaction at zero-temperature as then (4.114) and (4.115) reduce to the result which is obtained by Refs. [86, 123, 124].

The condensate density is obtained by minimizing the mean-field energy with the help of Eq. (3.16), we get

$$\left|\Psi_1^{\mathrm{MF}}\right|^2=-\frac{2a_2^{\mathrm{MF}}(1,0)}{a_4^{\mathrm{MF}}(1,0;1,0|1,0;1,0)}. \tag{4.116}$$

We remark that, when the chemical potential μ is fixed, the mean-field condensate density $\left|\Psi_1^{\mathrm{MF}}\right|^2$ with spin-1 is not monotonically increasing with the hopping J as shown in Fig. 4.1, see also Ref. [86]. Thus, the mean-field prediction for the condensate density is not physical provided that the hopping is too large. We use this circumstance to our advantage and define a validity range of the mean-field theory as follows. For a fixed chemical potential point we determine the hopping value at which the condensate density has its maximal value. Until this hopping value the condensate density increases

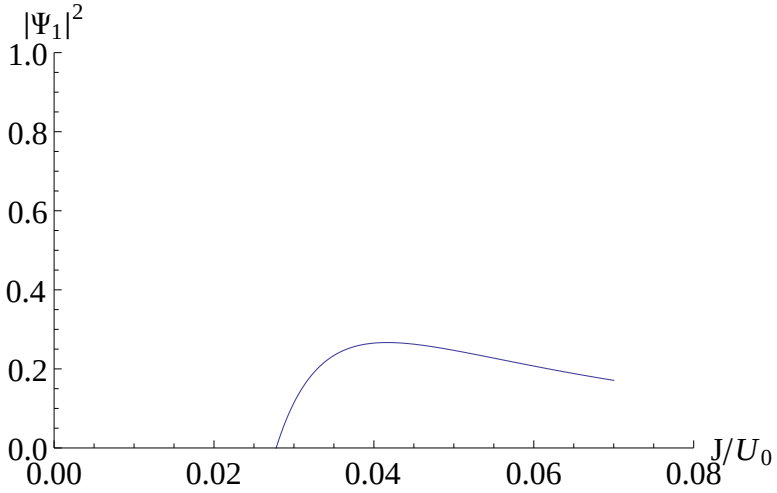

Figure 4.1.: The mean-field condensate density as a function of the tunneling parameter J/U for fixed $\mu/U = 0.5$.

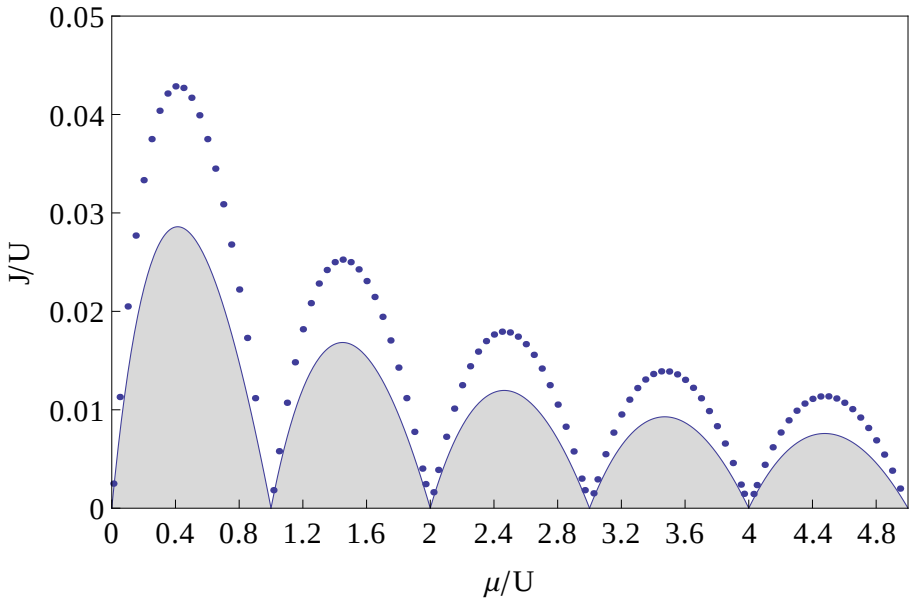

Figure 4.2.: The validity range of mean-field theory for the Bose-Hubbard model in the ferromagnetic case at zero temperature is depicted by blue dots.

with increasing hopping, so that this point defines the validity limit for a fixed μ. Beyond this hopping value, we can not use the prediction of the mean-field theory because the condensate density decreases with increasing the hopping parameter as shown in Fig. 4.1. Thus, we can expect a range of validity until a critical hopping J as shown in Fig. 4.2. Similarly, we could apply the same procedure for the anti-ferromagnetic interaction without and with magnetization.

4.8.2. Anti-ferromagnetic Interaction Without Zeeman Effect

In the previous subsection we did check the result derived for $a_4^{(0)}$ in the case of ferromagnetic interaction. Now we make another check for $a_4^{(0)}$ in the case of anti-ferromagnetic interaction with an even and an odd number of atoms at zero-temperature. To do this, we will calculate the ground state

energy of the superfluid phase by using perturbation theory at the zero-temperature limit. In order to do this, we assume that the hopping matrix element J is small. The ground state of the nonperturbative Hamiltonian $H_i^{(0)}$is $|0,0,n_i\rangle$ for even n_i and $|1,m,n_i\rangle$ for odd n_i. Since the effective Hamiltonian (2.41) is diagonal with respect to the site, we drop the site index in the following. We introduce three complex order parameters Ψ_α, which can be combined to a vector

$$\mathbf{\Psi} = (\Psi_1, \Psi_0, \Psi_{-1}). \tag{4.117}$$

We note that the order parameter has three components due to the three different hyperfine states $\alpha = 0, \pm 1$. Thus, the energy of the system is a function of the order parameter and has to be minimized. We calculate the fourth-order perturbation correction for an even and odd numbers of atoms to determine the symmetry of the order parameter.

- **Superfluid state with an even number of atoms**

Here, we define the fourth-order perturbation correction for an even number of atoms with no magnetization. Thus, the ground state will be $|0,0,n\rangle$ for even n as discussed in Subsection 3.4.1. To this end, inserting Eqs. (4.109) and (4.113) into (4.111) by using the matrix elements in Appendix A, yields

$$E_G^{(4)}(\mathbf{\Psi}) = A(n,U_0,U_2,\mu)\left||\Psi_0|^2 - 2\,|\Psi_1|\,|\Psi_{-1}|\right|^2 + B(n,U_0,U_2,\mu)(\mathbf{\Psi}^\dagger\cdot\mathbf{\Psi})^2, \tag{4.118}$$

where $(\mathbf{\Psi}^\dagger\cdot\mathbf{\Psi})$ is symmetric under the rotation in spin space. Here the coefficients $A(n,U_0,U_2,\mu)$ and $B(n,U_0,U_2,\mu)$ are given by

$$\begin{aligned} A(n,U_0,U_2,\mu) =& (zJ)^4\left[-\frac{2n(n+3)}{15\triangle E_{2,n}^{(0)}\triangle E_{1,n-1}^{(0)}\triangle E_{1,n+1}^{(0)}} - \frac{1}{15\left(\triangle E_{1,n-1}^{(0)}\right)^2\triangle E_{2,n-2}^{(0)}\triangle E_{0,n-2}^{(0)}\triangle E_{2,n}^{(0)}}\right. \\ &\times\left[6n(n+3)U_2\triangle E_{0,n-2}^{(0)} + 15n(n+1)U_2^2 + n(n+3)\left(\triangle E_{0,n-2}^{(0)}\right)^2\right] \\ &\left. - \frac{6n(n+3)U_2\triangle E_{0,n+2}^{(0)} + 15\,(n+2)\,(n+3)U_2^2 + n(n+3)\left(\triangle E_{0,n+2}^{(0)}\right)^2}{15\left(\triangle E_{1,n+1}^{(0)}\right)^2\triangle E_{2,n+2}^{(0)}\triangle E_{0,n+2}^{(0)}\triangle E_{2,n}^{(0)}}\right], \end{aligned} \tag{4.119}$$

$$\begin{aligned} B(n,U_0,U_2,\mu) = (zJ)^4&\left[\frac{1}{9}\left(\frac{n}{\triangle E_{1,n-1}^{(0)}} + \frac{n+3}{\triangle E_{1,n+1}^{(0)}}\right)\left(\frac{n}{\left(\triangle E_{1,n-1}^{(0)}\right)^2} + \frac{n+3}{\left(\triangle E_{1,n+1}^{(0)}\right)^2}\right)\right. \\ &- \frac{n\,(n+3)}{45\triangle E_{2,n}^{(0)}}\left(\frac{1}{\triangle E_{1,n-1}^{(0)}} + \frac{1}{\triangle E_{1,n+1}^{(0)}}\right)^2 - \frac{2}{15}\left(\frac{n\,(n-2)}{\left(\triangle E_{1,n-1}^{(0)}\right)^2\triangle E_{2,n-2}^{(0)}} + \frac{(n+3)\,(n+5)}{\left(\triangle E_{1,n+1}^{(0)}\right)^2\triangle E_{2,n+2}^{(0)}}\right)\Bigg]. \end{aligned} \tag{4.120}$$

where $\triangle E^{(0)}_{S',n'} = E^{(0)}_{S',n'} - E^{(0)}_{0,n}$. The result (4.118) coincides with Ref. [81], which represents another check for Eq. (4.109). The spin average in the SF phase is defined as

$$\langle \mathbf{F} \rangle \equiv \sum_{\alpha,\beta} \Psi^*_\alpha \mathbf{F}_{\alpha\beta} \Psi_\beta \qquad (\alpha, \beta = x, y, z)\,, \tag{4.121}$$

thus we have

$$\left| |\Psi_0|^2 - 2\,|\Psi_1|\,|\Psi_{-1}| \right|^2 = 1 - \langle \mathbf{F} \rangle^2\,. \tag{4.122}$$

We remark that the coefficient $A(n, U_0, U_2, \mu)$ is negative. Therefore, $\langle \mathbf{F} \rangle = \mathbf{0}$ because $\langle \mathbf{F} \rangle^2$ has the minimum value in the ground state. Thus, we obtain the polar superfluid phase [81].

- **Superfluid State with an Odd Number of Atoms**

The mean-field result for an odd number number of atoms has not been found in the literature. For the sake of completeness we derive it here within our approach. Thus, the ground state becomes $|1, m, n\rangle$ for odd n where $m = 0, \pm 1$ as discussed in Subsection 3.4.1. By the same way, inserting Eqs. (4.109) and (4.113) into (4.111) by using the matrix elements in Appendix A, we get the fourth order perturbation energy at zero-temperature as follows:

$$\begin{aligned} E^{(4)}_G(\mathbf{\Psi}) =& C(n, U_0, U_2, \mu) \left| |\Psi_0|^2 - 2\,|\Psi_1|\,|\Psi_{-1}| \right|^2 + D(n, U_0, U_2, \mu)(\mathbf{\Psi}^\dagger \cdot \mathbf{\Psi})^2 \\ &+ E(n, U_0, U_2, \mu) \left[|\Psi_1|^2 - |\Psi_{-1}|^2 \right]^2 + H(n, U_0, U_2, \mu) \left[(\Psi^*_0 \Psi_0)^2 + 2\,(\Psi^*_1 \Psi_{-1})^2 \right], \end{aligned} \tag{4.123}$$

where the coefficients of $C(n, U_0, U_2, \mu)$, $D(n, U_0, U_2, \mu)$, $E(n, U_0, U_2, \mu)$ and $H(n, U_0, U_2, \mu)$ are relegated to Appendix C in Eqs. (C.2)–(C.5). It turns out that $C(n, U_0, U_2, \mu)$ is negative. Therefore, we have again $\langle \mathbf{F} \rangle = 0$ because $\langle \mathbf{F} \rangle^2$ has then its minimal value in the ground state. Thus, we obtain again a polar superfluid phase.

4.8.3. Anti-ferromagnetic Interaction With Zeeman effect

In this subsection we calculate the fourth order perturbation energy at the zero-temperature limit for $\eta \neq 0$. As discussed in Subsections 2.4.2 and 3.4.2, the ground states for the even and odd lobes depend on the value of η and U_2. In addition, the general form of the ground state is $|S, S, n\rangle$. However, the rotational symmetry will be broken at the presence of magnetic field, e.g. SO(3) will be reduced to SO(2) symmetry. Therefore, magnetization will be induced in the minimization process [125].

- **Superfluid state with an even number of atoms**

Therefore, the fourth order perturbation energy for an even number of atoms follows as

$$\begin{aligned} E^{(4)}_G(\mathbf{\Psi}) =& F(S, S, n, U_0, U_2, \mu, \eta)\,|\Psi_1|^4 + G(S, S, n, U_0, U_2, \mu, \eta)\,|\Psi_{-1}|^4 + I(S, S, n, U_0, U_2, \mu, \eta)\,|\Psi_0|^4 \\ &+ 4L(S, S, n, U_0, U_2, \mu, \eta)\,|\Psi_1|^2\,|\Psi_{-1}|^2 + 4R(S, S, n, U_0, U_2, \mu, \eta)\,|\Psi_1|^2\,|\Psi_0|^2 + 4Q(S, S, n, U_0, U_2, \mu, \eta) \\ &\times |\Psi_{-1}|^2\,|\Psi_0|^2 + 2T(S, S, n, U_0, U_2, \mu, \eta)\left(\Psi^*_0 \Psi^*_0 \Psi_1 \Psi_{-1} + \Psi^*_1 \Psi^*_{-1} \Psi_0 \Psi_0\right), \end{aligned} \tag{4.124}$$

where

$$F(S,S,n,U_0,U_2,\mu,\eta) = a_4^{\mathrm{MF}}(1,0;1,0|1,0;1,0), \tag{4.125}$$

$$G(S,S,n,U_0,U_2,\mu,\eta) = a_4^{\mathrm{MF}}(-1,0;-1,0|-1,0;-1,0), \tag{4.126}$$

$$I(S,S,n,U_0,U_2,\mu,\eta) = a_4^{\mathrm{MF}}(0,0;0,0|0,0;0,0), \tag{4.127}$$

$$\begin{aligned} L(S,S,n,U_0,U_2,\mu,\eta) &= a_4^{\mathrm{MF}}(1,0;-1,0|1,0;-1,0) \\ &= a_4^{\mathrm{MF}}(1,0;-1,0|-1,0;1,0) \\ &= a_4^{\mathrm{MF}}(-1,0;1,0|1,0;-1,0) \\ &= a_4^{\mathrm{MF}}(-1,0;1,0|-1,0;1,0), \end{aligned} \tag{4.128}$$

$$\begin{aligned} R(S,S,n,U_0,U_2,\mu,\eta) &= a_4^{\mathrm{MF}}(1,0;0,0|1,0;0,0) \\ &= a_4^{\mathrm{MF}}(1,0;0,0|0,0;1,0) \\ &= a_4^{\mathrm{MF}}(0,0;1,0|1,0;0,0) \\ &= a_4^{\mathrm{MF}}(0,0;1,0|0,0;1,0), \end{aligned} \tag{4.129}$$

$$\begin{aligned} Q(S,S,n,U_0,U_2,\mu,\eta) &= a_4^{\mathrm{MF}}(-1,0;0,0|-1,0;0,0) \\ &= a_4^{\mathrm{MF}}(-1,0;0,0|0,0;-1,0) \\ &= a_4^{\mathrm{MF}}(0,0;-1,0|-1,0;0,0) \\ &= a_4^{\mathrm{MF}}(0,0;-1,0|0,0;-1,0), \end{aligned} \tag{4.130}$$

$$\begin{aligned} T(S,S,n,U_0,U_2,\mu,\eta) &= a_4^{\mathrm{MF}}(0,0;0,0|1,0;-1,0) \\ &= a_4^{\mathrm{MF}}(0,0;0,0|-1,0;1,0) \\ &= a_4^{\mathrm{MF}}(-1,0;1,0|0,0;0,0) \\ &= a_4^{\mathrm{MF}}(1,0;-1,0|0,0;0,0). \end{aligned} \tag{4.131}$$

The relations between the coefficients with and without magnetization are given by

$$A(n,U_0,U_2,\mu) = -T(0,0,n,U_0,U_2,\mu,0), \tag{4.132}$$

$$\begin{aligned} B(n,U_0,U_2,\mu) &= F(0,0,n,U_0,U_2,\mu,0) \\ &= G(0,0,n,U_0,U_2,\mu,0), \end{aligned}$$

$$= 2R(0,0,n,U_0,U_2,\mu,0)$$
$$= 2Q(0,0,n,U_0,U_2,\mu,0). \tag{4.133}$$

- **Superfluid state with an odd number of atoms**

Similarly, the fourth order perturbation energy for an odd number of atoms

$$\begin{aligned} E_G^{(4)}(\mathbf{\Psi}) &= K(S,S,n,U_0,U_2,\mu,\eta)\left|\Psi_1\right|^4 + Q(S,S,n,U_0,U_2,\mu,\eta)\left|\Psi_{-1}\right|^4 + V(S,S,n,U_0,U_2,\mu,\eta)\left|\Psi_0\right|^4 \\ &+ 4W(S,S,n,U_0,U_2,\mu,\eta)\left|\Psi_1\right|^2\left|\Psi_{-1}\right|^2 + 4X(S,S,n,U_0,U_2,\mu,\eta)\left|\Psi_1\right|^2\left|\Psi_0\right|^2 \\ &+ 4Y(S,S,n,U_0,U_2,\mu,\eta)\left|\Psi_{-1}\right|^2\left|\Psi_0\right|^2 + 2Z(S,S,n,U_0,U_2,\mu,\eta)\left(\Psi_0^*\Psi_0^*\Psi_1\Psi_{-1} + \Psi_1^*\Psi_{-1}^*\Psi_0\Psi_0\right), \end{aligned} \tag{4.134}$$

where the coefficients read

$$K(S,S,n,U_0,U_2,\mu,\eta) = a_4^{\mathrm{MF}}(1,0;1,0|1,0;1,0), \tag{4.135}$$

$$Q(S,S,n,U_0,U_2,\mu,\eta) = a_4^{\mathrm{MF}}(-1,0;-1,0|-1,0;-1,0), \tag{4.136}$$

$$V(S,S,n,U_0,U_2,\mu,\eta) = a_4^{\mathrm{MF}}(0,0;0,0|0,0;0,0), \tag{4.137}$$

$$\begin{aligned} W(S,S,n,U_0,U_2,\mu,\eta) &= a_4^{\mathrm{MF}}(1,0;-1,0|1,0;-1,0) \\ &= a_4^{\mathrm{MF}}(1,0;-1,0|-1,0;1,0) \\ &= a_4^{\mathrm{MF}}(-1,0;1,0|1,0;-1,0) \\ &= a_4^{\mathrm{MF}}(-1,0;1,0|-1,0;1,0), \end{aligned} \tag{4.138}$$

$$\begin{aligned} X(S,S,n,U_0,U_2,\mu,\eta) &= a_4^{\mathrm{MF}}(1,0;0,0|1,0;0,0) \\ &= a_4^{\mathrm{MF}}(1,0;0,0|0,0;1,0) \\ &= a_4^{\mathrm{MF}}(0,0;1,0|1,0;0,0) \\ &= a_4^{\mathrm{MF}}(0,0;1,0|0,0;1,0), \end{aligned} \tag{4.139}$$

$$\begin{aligned} Y(S,S,n,U_0,U_2,\mu,\eta) &= a_4^{\mathrm{MF}}(-1,0;0,0|-1,0;0,0) \\ &= a_4^{\mathrm{MF}}(-1,0;0,0|0,0;-1,0) \\ &= a_4^{\mathrm{MF}}(0,0;-1,0|-1,0;0,0) \\ &= a_4^{\mathrm{MF}}(0,0;-1,0|0,0;-1,0), \end{aligned} \tag{4.140}$$

$$\begin{aligned} Z(S,S,n,U_0,U_2,\mu,\eta) &= a_4^{\mathrm{MF}}(0,0;0,0|1,0;-1,0) \\ &= a_4^{\mathrm{MF}}(0,0;0,0|-1,0;1,0) \end{aligned}$$

$$= a_4^{\mathrm{MF}}(-1,0;1,0|0,0;0,0)$$
$$= a_4^{\mathrm{MF}}(1,0;-1,0|0,0;0,0). \tag{4.141}$$

Similarly, the relations between the coefficients with and without magnetization are given by

$$C(n,U_0,U_2,\mu) = -Z(1,1,n,U_0,U_2,\mu,0), \tag{4.142}$$

$$D(n,U_0,U_2,\mu) = 2X(1,1,n,U_0,U_2,\mu,0) = 2Y(1,1,n,U_0,U_2,\mu,0), \tag{4.143}$$

$$E(n,U_0,U_2,\mu) = V(1,1,n,U_0,U_2,\mu,0) - Z(1,1,n,U_0,U_2,\mu,0) - 2W(1,1,n,U_0,U_2,\mu,0), \tag{4.144}$$

$$H(n,U_0,U_2,\mu) = V(1,1,n,U_0,U_2,\mu,0) + Z(1,1,n,U_0,U_2,\mu,0) - 2X(1,1,n,U_0,U_2,\mu,0). \tag{4.145}$$

In principle, we could now find the different superfluid phases by using all the coefficients in Subsection 4.8.3. But we will not do this as we will find out in the next chapter that the range of validity of the mean-field theory is smaller than that of the Ginzburg-Landau theory. Therefore, we expect that the effective action approach gives better results for the superfluid phases and, thus, we perform the extremization procedure explicitly only for the Ginzburg-Landau theory.

5. Effective Action

In the previous chapter we have calculated the grand-canonical free energy up to the first order in the tunneling parameter by using the diagrammatic representation. With this we determine in this chapter the Ginzburg-Landau expansion of the effective action up to first order in the hopping term. Afterwards we show that, in particular at zero temperature, our Ginzburg-Landau theory can distinguish within its range of validity between various ferromagnetic and anti-ferromagnetic superfluid phases for an anti-ferromagnetic interaction and a non-vanishing external magnetic field [84, 85]. Furthermore, we show for a vanishing external magnetic field that the superfluid phase is a polar state, where all the atoms condense in the spin-0 state [81]. In addition, we study whether the superfluid-Mott insulator phase transition and the transitions between the various superfluid phases for a non-vanishing external magnetic field are of first or second order.

5.1. Ginzburg-Landau Action

In this section, we deduce the Ginzburg-Landau action for the spin-1 Bose-Hubbard model. To this end, we use a Legendre transformation to convert the artificially introduced symmetry-breaking currents j, j^* into the order parameter fields. In order to implement this Legendre transformation in an uncluttered way, the grand-canonical free energy (4.74) can be written in Matsubara space as follows:

$$\mathcal{F}[j,j^*] = \mathcal{F}_0 - \frac{1}{\beta}\sum_{i_1,i_2}\sum_{\alpha_1,\alpha_2}\sum_{\omega_{m1},\omega_{m2}}\Bigg\{ M_{i_1\alpha_1,i_2\alpha_2}(\omega_{m1}|\omega_{m2}) j_{i_1\alpha_1}(\omega_{m1}) j^*_{i_2\alpha_2}(\omega_{m2}) \tag{5.1}$$

$$+\sum_{i_3,i_4}\sum_{\alpha_3,\alpha_4}\sum_{\omega_{m3},\omega_{m4}} N_{i_1\alpha_1,i_2\alpha_2,i_3\alpha_3,i_4\alpha_4}(\omega_{m1};\omega_{m2}|\omega_{m3};\omega_{m4}) j_{i_1\alpha_1,}(\omega_{m1}) j_{i_2\alpha_2}(\omega_{m2}) j^*_{i_3\alpha_3}(\omega_{m3}) j^*_{i_4\alpha_4}(\omega_{m4})\Bigg\},$$

where the respective coefficients are given by

$$M_{i_1\alpha_1,i_2\alpha_2}(\omega_{m1}|\omega_{m2}) = \left[a_2^{(0)}(i_1\alpha_1,\omega_{m1})\delta_{i_1,i_2} + J_{i_1 i_2} a_2^{(0)}(i_1\alpha_1,\omega_{m1}) a_2^{(0)}(i_2\alpha_2,\omega_{m2})\right] \times \delta_{\omega_{m1},\omega_{m2}}\delta_{\alpha_1,\alpha_2} \tag{5.2}$$

and

$$N_{i_1\alpha_1,i_2\alpha_2,i_3\alpha_3,i_4\alpha_4}(\omega_{m1};\omega_{m2}|\omega_{m3};\omega_{m4}) = \frac{1}{4}\delta_{\alpha_1+\alpha_2,\alpha_3+\alpha_4}\delta_{\omega_{m1}+\omega_{m2},\omega_{m3}+\omega_{m4}}$$
$$\times a_4^{(0)}(i_1\alpha_1,\omega_{m1};i_1\alpha_2,\omega_{m2}|i_1\alpha_3,\omega_{m3};i_1\alpha_4,\omega_{m4})\Bigg\{\delta_{i_1,i_2}\delta_{i_2,i_3}\delta_{i_3,i_4}$$
$$+ 2\delta_{i_1,i_4}\left[J_{i_1 i_2} a_2^{(0)}(i_2\alpha_2,\omega_{m2})\delta_{i_1,i_3} + J_{i_1 i_3}\, a_2^{(0)}(i_3\alpha_3,\omega_{m3})\delta_{i_1,i_2}\right]\Bigg\}. \tag{5.3}$$

For this purpose, the order parameter field $\psi_{i\alpha}(\omega_m)$ is defined according to Refs. [116, 117] as

$$\Psi_{i\alpha}(\omega_m) = \langle \hat{a}_{i\alpha}(\omega_m) \rangle = \beta \frac{\delta \mathcal{F}}{\delta j^*_{i\alpha}(\omega_m)}, \qquad \Psi^*_{i\alpha}(\omega_m) = \left\langle \hat{a}^\dagger_{i\alpha}(\omega_m) \right\rangle = \beta \frac{\delta \mathcal{F}}{\delta j_{i\alpha}(\omega_m)}. \tag{5.4}$$

Equation (5.4) motivates to perform a Legendre transformation up to first order in the tunneling parameter J. At first, we insert (5.1) in (5.4) and find that the order parameter field is given by

$$\begin{aligned} \Psi_{i\alpha}(\omega_m) = -\sum_p \sum_{\alpha_1} \sum_{\omega_{m1}} \Bigg[& M_{p\alpha,i\alpha_1}(\omega_{m1}|\omega_m) j_{p\alpha}(\omega_{m1}) \\ & - 2 \sum_{i_2,i_3} \sum_{\omega_{m2},\omega_{m3}} \sum_{\alpha_2,\alpha_3} N_{p\alpha,i_2\alpha_2,i_3\alpha_3,i_1\alpha_1}(\omega_{m1};\omega_{m2}|\omega_{m3};\omega_m) j_{p\alpha}(\omega_{m1}) j_{i_2\alpha_2}(\omega_{m2}) j^*_{i_3\alpha_3}(\omega_{m3}) \Bigg]. \end{aligned} \tag{5.5}$$

Using Eq. (5.4) the Ginzburg-Landau action Γ has the following form

$$\Gamma\left[\Psi_{i\alpha}(\omega_m), \Psi^*_{i\alpha}(\omega_m)\right] = \mathcal{F}\left[j, j^*\right] - \frac{1}{\beta} \sum_i \sum_{\omega_m} \sum_\alpha \left[\Psi_{i\alpha}(\omega_m) j^*_{i\alpha}(\omega_m) + \Psi^*_{i\alpha}(\omega_m) j_{i\alpha}(\omega_m)\right], \tag{5.6}$$

where Ψ, $\Psi^*$and j^*, j are conjugate variables which satisfy the Legendre relations

$$j_{i\alpha}(\omega_m) = -\beta \frac{\delta \Gamma}{\delta \Psi^*_{i\alpha}(\omega_m)}, \qquad j^*_{i\alpha}(\omega_m) = -\beta \frac{\delta \Gamma}{\delta \Psi_{i\alpha}(\omega_m)}. \tag{5.7}$$

In order to recover the interesting physical situation the artificially currents j^*, j should vanish. Therefore, we obtain from (5.7) the equations of motion as follows

$$\left.\frac{\delta \Gamma}{\delta \Psi^*_{i\alpha}(\omega_m)}\right|_{\Psi^* = \Psi_{\mathrm{eq}}} = 0, \qquad \left.\frac{\delta \Gamma}{\delta \Psi_{i\alpha}(\omega_m)}\right|_{\Psi = \Psi_{\mathrm{eq}}} = 0. \tag{5.8}$$

Hence, the effective action is stationary with respect to fluctuations around the equilibrium order parameter field Ψ_{eq}. Additionally, we read off from Eq. (5.6) that the physical grand-canonical free energy in the case of the vanishing currents j^*, j is equal to evaluating the effective action at the equilibrium order parameter field Ψ_{eq}:

$$\Gamma\left[\Psi = \Psi_{\mathrm{eq}}, \Psi^* = \Psi_{\mathrm{eq}}\right] = \mathcal{F}\left[j^* = 0, j = 0\right] = \mathcal{F}. \tag{5.9}$$

To determine the explicit form of the effective action as a functional of the order parameter, we have to calculate the currents as a functionals of the Ginzburg-Landau order parameter field. To do this, we invert relation (5.5) up to first order in the tunneling parameter J and calculate the inverse matrix of $M_{p\alpha,i\alpha_1}(\omega_{m1}|\omega_m)$. At first we calculate the inverse of Eq. (5.2) by the ansatz

$$M^{-1}_{i_1\alpha_1,i_2\alpha_2}(\omega_{m1}|\omega_{m2}) = m^{(0)}_{i_1\alpha_1,i_2\alpha_2}(\omega_{m1}|\omega_{m2}) + J_{i_1 i_2}\, m^{(1)}_{i_1\alpha_1,i_2\alpha_2}(\omega_{m1}|\omega_{m2}), \tag{5.10}$$

and require that the following relation has to be satisfied

$$\sum_{\omega_{m3}}\sum_{\alpha_3}\sum_{i_3} M_{i_1\alpha_1,i_3\alpha_3}(\omega_{m1}|\omega_{m3})M^{-1}_{i_3\alpha_3,i_2\alpha_2}(\omega_{m3}|\omega_{m2}) = \delta_{i_1,i_2}\delta_{\alpha_1,\alpha_2}\delta_{\omega_{m1},\omega_{m2}}. \tag{5.11}$$

Inserting Eqs. (5.2) and (5.10) in (5.11), we obtain the following two conditions

$$m^{(0)}_{i_1\alpha_1,i_2\alpha_2}(\omega_{m1}|\omega_{m2}) = \frac{\delta_{i_1,i_2}\delta_{\alpha_1,\alpha_2}\delta_{\omega_{m1},\omega_{m2}}}{a_2^{(0)}(i_1\alpha_1,\omega_{m1})} \tag{5.12}$$

and

$$m^{(1)}_{i_1\alpha_1,i_2\alpha_2}(\omega_{m1}|\omega_{m2}) = -\frac{a_2^{(0)}(i_2\alpha_2,\omega_{m2})}{a_2^{(0)}(i_1\alpha_1,\omega_{m1})}\delta_{\omega_{m1},\omega_{m2}}\delta_{\alpha_1,\alpha_2}. \tag{5.13}$$

Substituting Eq. (5.12) and (5.13) into (5.10), yields

$$M^{-1}_{i_1\alpha_1,i_2\alpha_2}(\omega_{m1}|\omega_{m2}) = \frac{\delta_{\alpha_1,\alpha_2}\delta_{\omega_{m1},\omega_{m2}}}{a_2^{(0)}(i_1\alpha_1,\omega_{m1})}\left[\delta_{i_1,i_2} - J_{i_1i_2}\, a_2^{(0)}(i_2\alpha_2,\omega_{m2})\right]. \tag{5.14}$$

Multiplying Eq. (5.5) by the inverse matrix M^{-1}, then leads to

$$\begin{aligned} j_{i\alpha}(\omega_m) = -\sum_{p}\sum_{\alpha_1}\sum_{\omega_{m1}} M^{-1}_{i_1\alpha_1,p\alpha}(\omega_m|\omega_{m1})\Big\{&\Psi_{p\alpha}(\omega_{m1}) \\ -2\sum_{q,i_2,i_3}\sum_{\omega_{m2},\omega_{m3}}\sum_{\alpha_2,\alpha_3} &N_{q\alpha_1,i_2\alpha_2,i_3\alpha_3,p\alpha}(\omega_{m1};\omega_{m2}|\omega_{m3};\omega_m)t_{q\alpha_1}(\omega_{m1})t_{i_2\alpha_2}(\omega_{m2})t^*_{i_3\alpha_3}(\omega_{m3})\Big\}, \end{aligned} \tag{5.15}$$

with the abbreviation

$$t_{i\alpha}(\omega_m) = -\sum_{\alpha_1}\sum_{p,\omega_{m1}} M^{-1}_{p\alpha_1,i\alpha}(\omega_{m1}|\omega_m)\Psi_{p\alpha}(\omega_{m1}). \tag{5.16}$$

Inserting Eqs. (5.15) and (5.1) into Eq. (5.6) up to the first order in the tunneling parameter, we get

$$\begin{aligned} \Gamma\left[\Psi_{i\alpha}(\omega_m),\Psi^*_{i\alpha}(\omega_m)\right] = \mathcal{F}_0 + \frac{1}{\beta}\sum_i\Bigg\{&\sum_\alpha\sum_{\omega_m}\left[\frac{|\Psi_{i\alpha}(\omega_m)|^2}{a_2^{(0)}(i\alpha,\omega_m)} - \sum_j J_{ij}\Psi_{i\alpha}(\omega_m)\Psi^*_{j\alpha}(\omega_m)\right] \\ -\sum_{\alpha_1,\alpha_2,\alpha_3,\alpha_4}\sum_{\omega_{m1},\omega_{m2},\omega_{m3},\omega_{m4}} &\frac{1}{4a_2^{(0)}(i\alpha_1,\omega_{m1})a_2^{(0)}(i\alpha_2,\omega_{m2})a_2^{(0)}(i\alpha_3,\omega_{m3})a_2^{(0)}(i\alpha_4,\omega_{m4})} \\ \times a_4^{(0)}(i\alpha_1,\omega_{m1};i\alpha_2,\omega_{m2}|i\alpha_3,\omega_{m3};i\alpha_4,\omega_{m4})&\Psi_{i\alpha_1}(\omega_{m1})\Psi_{i\alpha_2}(\omega_{m2})\Psi^*_{i\alpha_3}(\omega_{m3})\Psi^*_{i\alpha_4}(\omega_{m4})\Bigg\}. \end{aligned} \tag{5.17}$$

We note that the coefficient $a_4^{(1)}$ of the free energy (5.1), (5.3) is no longer present in the Ginzburg-Landau action (5.17). The reason is that the free energy, which represents a sum over all connected diagrams, yields via the Legendre transformation an effective action which represents a sum over all one-particle irreducible diagrams [86, 123]. For obtaining physical results from Eq. (5.17), we insert

Eq. (5.17) into the equations of motion (5.8) as follows:

$$0 = \left[\frac{1}{a_2^{(0)}(i\alpha,\omega_m)} - \sum_j J_{ij}\right]\Psi^{\mathrm{eq}}_{j\alpha}(\omega_m) \tag{5.18}$$
$$- \sum_{\alpha_1,\alpha_2,\alpha_3}\sum_{\omega_{m1},\omega_{m2},\omega_{m3}} \frac{a_4^{(0)}(i\alpha_1,\omega_{m1};i\alpha_2,\omega_{m2}|i\alpha_3,\omega_{m3};i\alpha,\omega_m)\Psi^{\mathrm{eq}}_{i\alpha_1}(\omega_{m1})\Psi^{\mathrm{eq}}_{i\alpha_2}(\omega_{m2})\Psi^{\mathrm{eq}*}_{i\alpha_3}(\omega_{m3})}{2a_2^{(0)}(i\alpha_1,\omega_{m1})a_2^{(0)}(i\alpha_2,\omega_{m2})a_2^{(0)}(i\alpha_3,\omega_{m3})a_2^{(0)}(i\alpha,\omega_m)}\Bigg\}.$$

From these equations of motions we will determine in the following the quantum phase transition and the possible superfluid phases of the considered system

5.2. Ginzburg-Landau Phase Boundary

In this section, we calculate the phase boundary between the Mott insulator and the superfluid phase at zero temperature. To do this, we specialize the effective action (5.17) for a stationary equilibrium which is site-independent due to homogeneity:

$$\Psi_{i\alpha}(\omega_m) = \Psi_\alpha\sqrt{\beta}\,\delta_{m,0}\ ,\ \ \Psi^*_{i\alpha}(\omega_m) = \Psi^*_\alpha\sqrt{\beta}\,\delta_{m,0}. \tag{5.19}$$

Therefore, the effective action (5.17) reduces with (4.37) to the effective potential

$$\begin{aligned}\Gamma =& \mathcal{F}_0 + N_s\Bigg\{\sum_\alpha\left[\frac{|\Psi_\alpha|^2}{a_2^{(0)}(\alpha,0)} - zJ\,|\Psi_\alpha|^2\right]\\ &- \sum_{\alpha_1,\alpha_2,\alpha_3,\alpha_4}\frac{\beta a_4^{(0)}(\alpha_1,0;\alpha_2,0|\alpha_3,0;\alpha_4,0)\Psi_{\alpha_1}\Psi_{\alpha_2}\Psi^*_{\alpha_3}\Psi^*_{\alpha_4}}{4a_2^{(0)}(\alpha_1,0)a_2^{(0)}(\alpha_2,0)a_2^{(0)}(\alpha_3,0)a_2^{(0)}(\alpha_4,0)}\Bigg\},\end{aligned} \tag{5.20}$$

where N_s is the total number of lattices sites and $z = 2D$ denotes the coordination number of a D dimensional hypercubic lattice. Note that we neglect from now on the site dependence of the coefficients $a_2^{(0)}$ and $a_4^{(0)}$ due to Eqs. (4.95) and (4.109). In order to obtain the quantum phase transition according to the Landau theory, the equilibrium order parameter should vanish. To this end, we read off from Eq. (5.20)

$$0 = \frac{1}{a_2^{(0)}(\alpha,0)} - zJ, \tag{5.21}$$

which yields with Eq. (4.95)

$$\begin{aligned}zJ_{c,\alpha} = \Bigg[&\frac{M^2_{\alpha,S,m,n}}{E^{(0)}_{S,m,n} - E^{(0)}_{S+1,m+\alpha,n+1}} + \frac{N^2_{\alpha,S,m,n}}{E^{(0)}_{S,m,n} - E^{(0)}_{S-1,m+\alpha,n+1}} + \frac{O^2_{\alpha,S,m,n}}{E^{(0)}_{S,m,n} - E^{(0)}_{S+1,m-\alpha,n-1}}\\ &+ \frac{P^2_{\alpha,S,m,n}}{E^{(0)}_{S,m,n} - E^{(0)}_{S-1,m-\alpha,n-1}}\Bigg]^{-1}.\end{aligned} \tag{5.22}$$

We find that the Ginzburg-Landau phase boundary (5.22) is identical to the mean-field phase boundary which is given by Eq. (3.31). The corresponding same result was obtained for the scalar Bose-Hubbard model in Ref. [86].

5.3. Possible Superfluid Phases

In order to determine the respective superfluid phases, we rewrite the on-site effective potential (5.20) according to

$$\Gamma\left(\Psi_\alpha, \Psi_\alpha^*\right) = \mathcal{F}_0 + \sum_\alpha B_\alpha \left|\Psi_\alpha\right|^2 + \sum_{\alpha_1,\alpha_2,\alpha_3,\alpha_4} A_{\alpha_1\alpha_2\alpha_3\alpha_4} \Psi_{\alpha_1}^* \Psi_{\alpha_2}^* \Psi_{\alpha_3} \Psi_{\alpha_4}, \tag{5.23}$$

where we have introduced the coefficients

$$B_\alpha = \frac{1}{a_2^{(0)}(\alpha, 0)} - zJ \tag{5.24}$$

$$A_{\alpha_1\alpha_2\alpha_3\alpha_4} = -\frac{\beta a_4^{(0)}(\alpha_1, 0; \alpha_2, 0 | \alpha_3, 0; \alpha_4, 0)}{4 a_2^{(0)}(\alpha_1, 0) a_2^{(0)}(\alpha_2, 0) a_2^{(0)}(\alpha_3, 0) a_2^{(0)}(\alpha_4, 0)}, \tag{5.25}$$

where the symmetries

$$A_{\alpha_1\alpha_2\alpha_3\alpha_4} = A_{\alpha_2\alpha_1\alpha_3\alpha_4} = A_{\alpha_1\alpha_2\alpha_4\alpha_3} = A_{\alpha_2\alpha_1\alpha_4\alpha_3} \tag{5.26}$$

follow from (4.95) and (5.25). Using (5.26), Eq. (5.23) reads explicitly

$$\begin{aligned}\Gamma\left(\Psi_\alpha, \Psi_\alpha^*\right) =& B_1 \left|\Psi_1\right|^2 + B_0 \left|\Psi_0\right|^2 + B_{-1} \left|\Psi_{-1}\right|^2 + A_{1111} \left|\Psi_1\right|^4 + A_{0000} \left|\Psi_0\right|^4 \\ &+ A_{-1-1-1-1} \left|\Psi_{-1}\right|^4 + 4A_{1001} \left|\Psi_1\right|^2 \left|\Psi_0\right|^2 + 4A_{-100-1} \left|\Psi_{-1}\right|^2 \left|\Psi_0\right|^2 \\ &+ 4A_{1-11-1} \left|\Psi_{-1}\right|^2 \left|\Psi_1\right|^2 + 2A_{001-1} \Psi_0^* \Psi_0^* \Psi_1 \Psi_{-1} + 2A_{1-100} \Psi_1^* \Psi_{-1}^* \Psi_0 \Psi_0. \end{aligned} \tag{5.27}$$

As the effective potential Γ must be extremized with respect to the order parameter Ψ_α, we obtain the following self-consistency equations

$$\left(B_1 + 2A_{1111} \left|\Psi_1\right|^2 + 4A_{1001} \left|\Psi_0\right|^2 + 4A_{1-11-1} \left|\Psi_{-1}\right|^2\right) \Psi_1 + 2A_{1-100} \left|\Psi_0\right|^2 \Psi_{-1}^* = 0, \tag{5.28}$$

$$\left(B_{-1} + 2A_{-1-1-1-1} \left|\Psi_{-1}\right|^2 + 4A_{-100-1} \left|\Psi_0\right|^2 + 4A_{1-11-1} \left|\Psi_1\right|^2\right) \Psi_{-1} + 2A_{1-100} \left|\Psi_0\right|^2 \Psi_1^* = 0, \tag{5.29}$$

$$\left(B_0 + 2A_{0000} \left|\Psi_0\right|^2 + 4A_{1001} \left|\Psi_1\right|^2 + 4A_{-100-1} \left|\Psi_{-1}\right|^2\right) \Psi_0 + 2A_{001-1} \Psi_1 \Psi_{-1} \Psi_0^* = 0. \tag{5.30}$$

If there is more than one solution, we must take the one which minimizes the effective potential for some system parameter. In this way we are able to find the different superfluid phases above both the even and the odd Mott lobes.

Now we list all possible superfluid phases which could follow from solving Eqs. (5.28)–(5.30) without or with magnetization. To this end, we calculate the condensate densities for all these cases:

1. $\Psi_1 \neq 0,\ \Psi_{-1} = \Psi_0 = 0$ yields with Eq. (5.28)

$$|\Psi_1|^2 = -\frac{B_1}{2A_{1111}}. \tag{5.31}$$

Substituting into (5.27), the corresponding effective potential is

$$\Gamma = -\frac{B_1^2}{4A_{1111}}. \tag{5.32}$$

2. $\Psi_{-1} \neq 0,\ \Psi_1 = \Psi_0 = 0$ yields from Eq. (5.29)

$$|\Psi_{-1}|^2 = -\frac{B_{-1}}{2A_{-1-1-1-1}}, \tag{5.33}$$

so Eq. (5.27) becomes

$$\Gamma = -\frac{B_{-1}^2}{4A_{-1-1-1-1}}. \tag{5.34}$$

3. $\Psi_0 \neq 0,\ \Psi_1 = \Psi_1 = 0$ reduces Eq. (5.30) to

$$|\Psi_0|^2 = -\frac{B_0}{2A_{0000}} \tag{5.35}$$

and the corresponding effective potential (5.27) is

$$\Gamma = -\frac{B_0^2}{4A_{0000}}. \tag{5.36}$$

4. $\Psi_1 \neq 0,\ \Psi_{-1} \neq 0,\ \Psi_0 = 0$ yields from (5.28) and (5.29)

$$|\Psi_1|^2 = \frac{4A_{1-11-1}B_{-1} - 2A_{-1-1-1-1}B_1}{4A_{1111}A_{-1-1-1-1} - 16A_{1-11-1}^2}, \tag{5.37}$$

$$|\Psi_{-1}|^2 = \frac{4A_{1-11-1}B_1 - 2A_{1111}B_{-1}}{4A_{1111}A_{-1-1-1-1} - 16A_{1-11-1}^2}. \tag{5.38}$$

Here, Eq. (5.27) reduces to

$$\begin{aligned}\Gamma =& \frac{1}{4A_{1111}A_{-1-1-1-1} - 16A_{1-11-1}^2}\Big\{ B_1\left(4A_{1-11-1}B_{-1} - 2A_{-1-1-1-1}B_1\right) \\ &+ B_{-1}\left(4A_{1-11-1}B_1 - 2A_{1111}B_{-1}\right) + \frac{1}{4A_{1111}A_{-1-1-1-1} - 16A_{1-11-1}^2} \\ &\times \Big[A_{1111}\left(4A_{1-11-1}B_{-1} - 2A_{-1-1-1-1}B_1\right)^2 + A_{-1-1-1-1}\left(4A_{1-11-1}B_1 - 2A_{1111}B_{-1}\right)^2 \\ &+ 4A_{1-11-1}\left(4A_{1-11-1}B_{-1} - 2A_{-1-1-1-1}B_1\right)^2\left(4A_{1-11-1}B_1 - 2A_{1111}B_{-1}\right)^2 \Big] \Big\}. \end{aligned} \tag{5.39}$$

5. $\Psi_1 \neq 0$, $\Psi_0 \neq 0$, $\Psi_{-1} = 0$ yields from (5.28) and (5.30)

$$|\Psi_1|^2 = \frac{4A_{1001}B_0 - 2A_{0000}B_1}{4A_{1111}A_{0000} - 16A_{1001}^2}, \tag{5.40}$$

$$|\Psi_0|^2 = \frac{4A_{1001}B_1 - 2A_{1111}B_0}{4A_{1111}A_{0000} - 16A_{1001}^2}. \tag{5.41}$$

So, Eq. (5.27) reads

$$\begin{aligned}\Gamma =& \frac{1}{4A_{1111}A_{0000} - 16A_{1001}^2}\Bigg\{ B_1\left(4A_{1001}B_0 - 2A_{0000}B_1\right) \\ &+ B_0\left(4A_{1001}B_1 - 2A_{1111}B_0\right) + \frac{1}{4A_{1111}A_{0000} - 16A_{1001}^2} \\ &\times \Bigg[A_{1111}\Big(4A_{1001}B_0 - 2A_{0000}B_1\Big)^2 + A_{0000}\Big(4A_{1001}B_1 - 2A_{1111}B_0\Big)^2 \\ &+ 4A_{1001}\Big(4A_{1001}B_0 - 2A_{0000}B_1\Big)^2\Big(4A_{1001}B_1 - 2A_{1111}B_0\Big)^2\Bigg]\Bigg\}. \end{aligned} \tag{5.42}$$

6. $\Psi_{-1} \neq 0$, $\Psi_0 \neq 0$, $\Psi_1 = 0$ yields from (5.29) and (5.30)

$$|\Psi_{-1}|^2 = \frac{4A_{-100-1}B_0 - 2A_{0000}B_{-1}}{4A_{-1-1-1-1}A_{0000} - 16A_{-100-1}^2}, \tag{5.43}$$

$$|\Psi_0|^2 = \frac{4A_{-100-1}B_{-1} - 2A_{-1-1-1-1}B_0}{4A_{-1-1-1-1}A_{0000} - 16A_{-100-1}^2}, \tag{5.44}$$

so here, Eq. (5.27) is

$$\begin{aligned}\Gamma =& \frac{1}{4A_{-1-1-1-1}A_{0000} - 16A_{-100-1}^2}\Bigg\{ B_{-1}\left(4A_{-100-1}B_0 - 2A_{0000}B_{-1}\right) \\ &+ B_0\left(4A_{-100-1}B_{-1} - 2A_{-1-1-1-1}B_0\right) + \frac{1}{4A_{-1-1-1-1}A_{0000} - 16A_{-100-1}^2} \\ &\times \Bigg[A_{-1-1-1-1}\Big(4A_{-100-1}B_0 - 2A_{0000}B_{-1}\Big)^2 + A_{0000}\Big(4A_{-100-1}B_{-1} - 2A_{-1-1-1-1}B_0\Big)^2 \\ &+ 4A_{-100-1}\Big(4A_{-100-1}B_0 - 2A_{0000}B_{-1}\Big)^2\Big(4A_{-100-1}B_{-1} - 2A_{-1-1-1-1}B_0\Big)^2\Bigg]\Bigg\}. \end{aligned} \tag{5.45}$$

7. In the general case $\Psi_1 \neq 0$, $\Psi_{-1} \neq 0$, $\Psi_0 \neq 0$ it is not possible to solve (5.28)–(5.30) analytically, so this has to be done numerically. From a numerical evaluation we find that approximately the solution is given by either $\Psi_1 \neq 0$, $\Psi_0 \neq 0$, $\Psi_{-1} = 0$ with a small Ψ_{-1} in comparison with Ψ_1 and Ψ_0 or by $\Psi_{-1} \neq 0$, $\Psi_0 \neq 0$, $\Psi_1 = 0$ when Ψ_1 is small in comparison with Ψ_{-1} and Ψ_0, which coincides with the above cases 5 and 6, respectively.

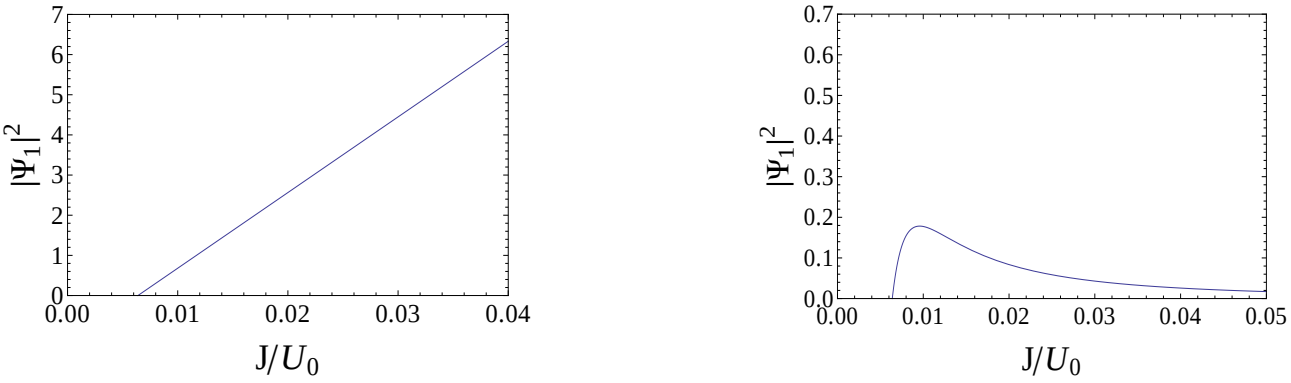

(a) (b)

Figure 5.1.: The condensate density as a function of the tunneling parameter J/U in the ferromagnetic case for both the effective action theory (left) and the mean-field theory (right) with $\mu/U = 0.92$ at zero temperature.

5.4. Validity Range of Ginzburg-Landau Theory

Calculating the condensate density in the superfluid phase reveals that it increases quite fast and that it even diverges between the even and odd lobes. This means physically that the Ginzburg-Landau theory has a limited range of validity in the superfluid phase. In order to investigate this delicate issue in more detail, we focus in this section on the scalar Bose-Hubbard model, which is recovered from our spin-1 theory in the ferromagnetic case, i.e. $\Psi_1 \neq 0$, $\Psi_{-1} = \Psi_0 = 0$, where we have $\eta = 0$ and $S = m = n$ as well as perform the identification $U_2 + U_0 = U$. Thus, we can specialize the matrix elements according to (3.33)–(3.37). The Landau coefficients Eq. (4.95) and Eq (4.109) reduce at zero temperature to

$$a_2^{(0)}(1,0) = \frac{n+1}{E^{(0)}_{n+1,n+1,n+1} - E^{(0)}_{n,n,n}} - \frac{n}{E^{(0)}_{n,n,n} - E^{(0)}_{n-1,n-1,n-1}}, \tag{5.46}$$

and

$$\begin{aligned}\beta a_4^{(0)}(1,0;1,0|1,0;1,0) =& 2\left\{ \frac{2n\,(n-1)}{(\triangle E^{(0)}_{n-1,n-1,n-1})^2 \triangle E^{(0)}_{n-2,n-2,n-2}} + \frac{2\,(n+1)\,(n+2)}{(\triangle E^{(0)}_{n+1,n+1,n+1})^2 \triangle E^{(0)}_{n+2,n+2,n+2}} \right. \\ &+ n^2 \left[-\frac{2}{(\triangle E^{(0)}_{n-1,n-1,n-1})^3} \right] - (n+1)^2 \left[\frac{2}{(\triangle E^{(0)}_{n+1,n+1,n+1})^3} \right] \\ &\left. -n\,(n+1) \left[\frac{2\left(\triangle E^{(0)}_{n+1,n+1,n+1} + \triangle E^{(0)}_{n-1,n-1,n-1}\right)}{\left(\triangle E^{(0)}_{n-1,n-1,n-1}\right)^2 \left(\triangle E^{(0)}_{n+1,n+1,n+1}\right)^2} \right] \right\}. \end{aligned} \tag{5.47}$$

Similarly, the condensate density (5.31) becomes together with (5.24), (5.25)

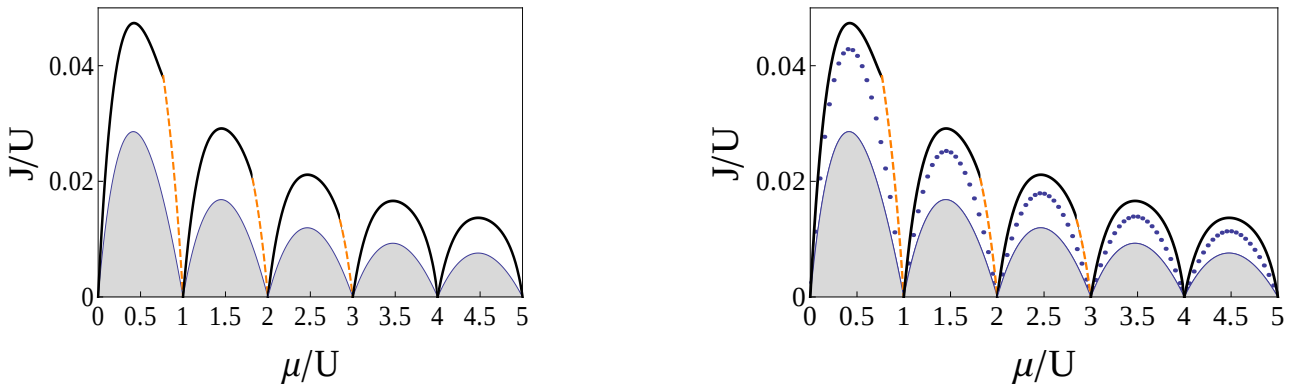

Figure 5.2.: Validity range of Ginzburg-Landau theory and mean-field theory for scalar Bose-Hubbard model in ferromagnetic case at zero temperature. (a) Range of validity of our theory where the black line depicts the condition that the average particle number equals the condensate density, i.e. $\langle n \rangle = |\Psi_1|^2$ and the dashed orange line corresponds to the situation that the condensate density is given by $n+1$. (b) Comparison of the validity ranges of Ginzburg-Landau theory (orange line) and mean-field theory (blue dots).

$$|\Psi_1|^2 = \frac{2(a_2^{(0)}(1,0))^3 \left(1 - zJa_2^{(0)}(1,0)\right)}{\beta a_4(1,0;1,0|1,0;1,0)}, \tag{5.48}$$

and the particle density is given by

$$\langle n \rangle = -\frac{1}{N_s}\frac{\partial \Gamma}{\partial \mu}\bigg|_{\Psi=\Psi_{\mathrm{eq}}}. \tag{5.49}$$

Calculating the condensate in the superfluid phase above the first Mott lobe shows, indeed, a sharp increase, see Fig. 5.1 and Ref. [86]. Thus, the condensate density (5.48) can not be valid deep in the superfluid phase. In order to determine the corresponding range of validity of the Ginzburg-Landau theory, we remark that we can not have more particles in the condensate than we have in the lattice. This leads to the condition

$$|\Psi_1|^2 \quad = \quad \langle n \rangle \,, \tag{5.50}$$

which is shown in Fig. 5.2 as a black line. For Mott lobes with $n \geq 4$ this condition is completely sufficient to characterize the range of validity. But we read off from Fig. 5.2 that condition (5.50) breaks down at the end of the Mott lobes $n = 1, 2, 3$. There we have to use an additional criterion to obtain a finite range of validity. To this end we complement condition (5.50) by the additional ad-hoc restriction that above n Mott lobe the condensate density can not be larger than $n+1$, yielding the boundary

$$|\Psi_1|^2 \quad = \quad n+1, \tag{5.51}$$

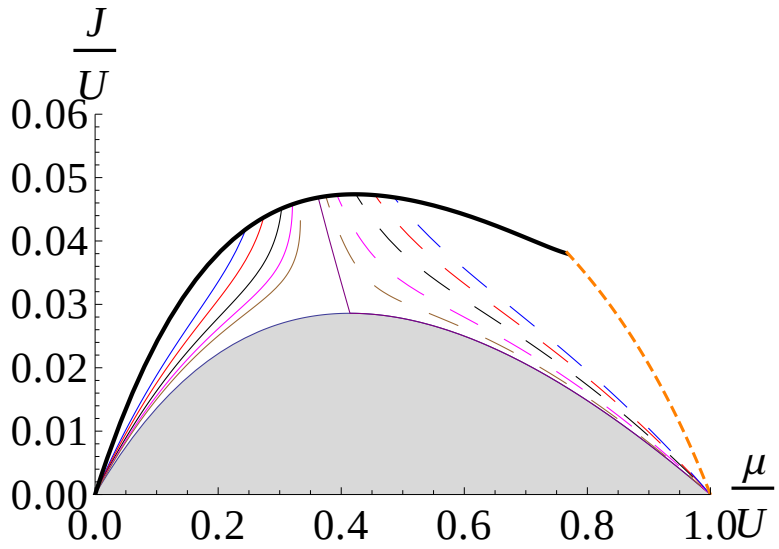

Figure 5.3.: Lines of average particle number $\langle n \rangle$ in the superfluid phase for the scalar Bose-Hubbard model for the first lobe in the ferromagnetic case at zero temperature within the range of validity of the Ginzburg-Landau theory. The predictions of the effective action theory are determined by the purple, brown (dashed), magneto (dashed), black (dashed) red (dashed), and blue (dashed) lines which are defined by $\langle n \rangle$ =1, 0.95 (1.02), 0.93 (1.05), 0.9 (1.1), 0.85 (1.15), 0.8 (1.2), respectively. The dashed orange line corresponds to the ad-hoe restriction (5.51) that the condensate density is given by $n + 1$.

which is depicted in Fig. 5.2 as a dashed orange line. When we compare the range of validity of Ginzburg-Landau with the corresponding one of mean-field theory from Section 4.8, we find that the Ginzburg-Landau theory has a larger range of validity than that of mean-field theory as shown in Fig. 5.2. In Fig. 5.3 we show for the zero temperature ferromagnetic case the lines of the average particle number $\langle n \rangle$ with both $\langle n \rangle < 1$ and $\langle n \rangle > 1$. Furthermore, we observe that the average particle number $\langle n \rangle$ increases with increasing chemical potential μ in the superfluid phase. In the following, we determine in an analogous way the range of validity of the Ginzburg-Landau theory for the spin-1 Bose-Hubbard model. In the next sections, we will discuss the resulting superfluid phases without and with magnetization only within this range of validity.

5.5. Ferromagnetic and Anti-ferromagnetic Superfluid Phases

In this section, we show that in particular at zero temperature, our Ginzburg-Landau theory distinguishes between various ferromagnetic and anti-ferromagnetic superfluid phases for a ferromagnetic and anti-ferromagnetic interaction without and with magnetization [84, 85].

5.5.1. Without Zeeman Effect

In this subsection we check the mean-field result which states that the superfluid phase is a polar state for zero-magnetic field, i.e. $\eta = 0$ [81]. According to Subsection 5.3 such a vanishing magnetization could occur in the third, fourth, and seventh case. However, a detailed analysis shows that only the third case is physically realized irrespective of the value of the chemical potential because it always

turns out to have the minimal energy. This means that the superfluid phase is a polar state which is characterized by $\Psi_0 \neq 0$, $\Psi_{-1} = \Psi_1 = 0$. On the other hand, for ferromagnetic case the superfluid phase is a ferromagnetic state which is determined by $\Psi_1 \neq 0$, $\Psi_{-1} = \Psi_0 = 0$ because the ground state $|n, n, n\rangle$ is the state with maximum spin for a given n.

5.5.2. With Zeeman Effect

For ferromagnetic interaction the superfluid phase becomes $\Psi_1 \neq 0$, $\Psi_{-1} = \Psi_0 = 0$ where the ground state $|n, n, n\rangle$ is the state with maximum spin for a given n. For an anti-ferromagnetic interaction the situation is more complicated for a non-vanishing magnetic field due to the appearance of different superfluid phases. Furthermore, we can not put $\Psi_1 = \Psi_{-1}$ because of a non-vanishing η. Unfortunately, the Ginzburg-Landau theory is only valid partially in the superfluid phase since the condensate density increases there quite fast. Thus, we calculate the different SF phases only within the parameter range where the theory is valid. All these SF phases are treated both analytically and numerically by solving the self-consistency equations (5.28)–(5.30). These phases correspond to the first, second, fourth, and seventh cases which are shown in Subsection 5.3.

5.5.3. With Fixed Spin-Dependent Interaction and Varying Magnetic Field

In this subsection, we study the predictions of the Ginzburg-Landau theory in view of an effect of the magnetic field upon the superfluid phases in the case of an anti-ferromagnetic interaction, i.e. $U_2 > 0$ as in ^{23}Na. To this end we show the resulting phase diagrams before and after the external magnetic field η reaches one of the critical values which have been discussed in Subsection 3.4.2 as shown in Fig. 5.4. If η is small compared to U_2, spin pairs are produced to get the minimal energy. Therefore, the Mott ground state becomes $|0, 0, n\rangle$ for an even n and $|1, 1, n\rangle$ for an odd n as shown in Fig. 5.4a. Thus, the magnetic field is not able to align all spins. Therefore, both spin-1 and spin-(-1) affect the phase boundary between Mott insulator and superfluid phases. The phases $\Psi_1 \neq 0$, $\Psi_{-1} \neq 0$, $\Psi_0 = 0$; $\Psi_{-1} \neq 0$, $\Psi_1 = \Psi_0 = 0$ and $\Psi_1 \neq 0$, $\Psi_{-1} = \Psi_0 = 0$ appear in the SF phase for the odd lobes with $n \geq 3$ and the phases $\Psi_1 \neq 0$, $\Psi_{-1} \neq 0$, $\Psi_0 \neq 0$; $\Psi_{-1} \neq 0$, $\Psi_1 = \Psi_0 = 0$; $\Psi_0 \neq 0$, $\Psi_1 = \Psi_{-1} = 0$ and $\Psi_1 \neq 0$, $\Psi_{-1} = \Psi_0 = 0$ for the even lobes. When η is increased above the first critical value $\eta^{(1)}_{\text{even}} = 0.06\, U_0$ from $0.05\ U_0$ to $0.07\ U_0$, both the spin S and the magnetic quantum number m change from $|0, 0, n\rangle$ to $|2, 2, n\rangle$ for even Mott lobes as shown in Fig. 5.4b. Correspondingly, the MI phases for the even lobes are decreased. The phases $\Psi_{-1} \neq 0$, $\Psi_1 = \Psi_0 = 0$ and $\Psi_1 \neq 0$, $\Psi_{-1} = \Psi_0 = 0$ appear in the SF phase for the even lobes and the phase $\Psi_{-1} \neq 0$, $\Psi_1 = \Psi_0 = 0$ is seen in the SF phase at the beginning of the odd lobes. We note that the phase $\Psi_{-1} \neq 0$, $\Psi_1 \neq 0$, $\Psi_0 \neq 0$ no longer appears as a stronger magnetic field leads to a preferred alignment of spins in z-direction.

Beyond the critical value $\eta^{(1)}_{\text{odd}} = 0.1\, U_0$ the quantum number S and m for the odd lobes change from $|1, 1, n\rangle$ to $|3, 3, n\rangle$ as shown in Fig. 5.4c. The left phase $\Psi_1 \neq 0$, $\Psi_{-1} \neq 0$, $\Psi_0 = 0$ in the odd lobes $n \geq 3$ has disappeared because increasing the magnetic field η results in a stronger alignment of the spins, but it is still not enough to align all the spins. The increase of η is enough to align all the spins for the second Mott lobe and its SF phase is $\Psi_1 \neq 0$, $\Psi_{-1} = \Psi_0 = 0$, but the SF phases for the fourth Mott lobe are $\Psi_1 \neq 0$, $\Psi_{-1} = \Psi_0 = 0$; $\Psi_{-1} \neq 0$, $\Psi_1 = \Psi_0 = 0$ and $\Psi_1 \neq 0$, $\Psi_{-1} \neq 0, \Psi_0 = 0$. The phase $\Psi_{-1} \neq 0$, $\Psi_1 = \Psi_0 = 0$ appears now only at the end of the odd lobes. After $\eta^{(2)}_{\text{even}} = 0.14\, U_0$ the

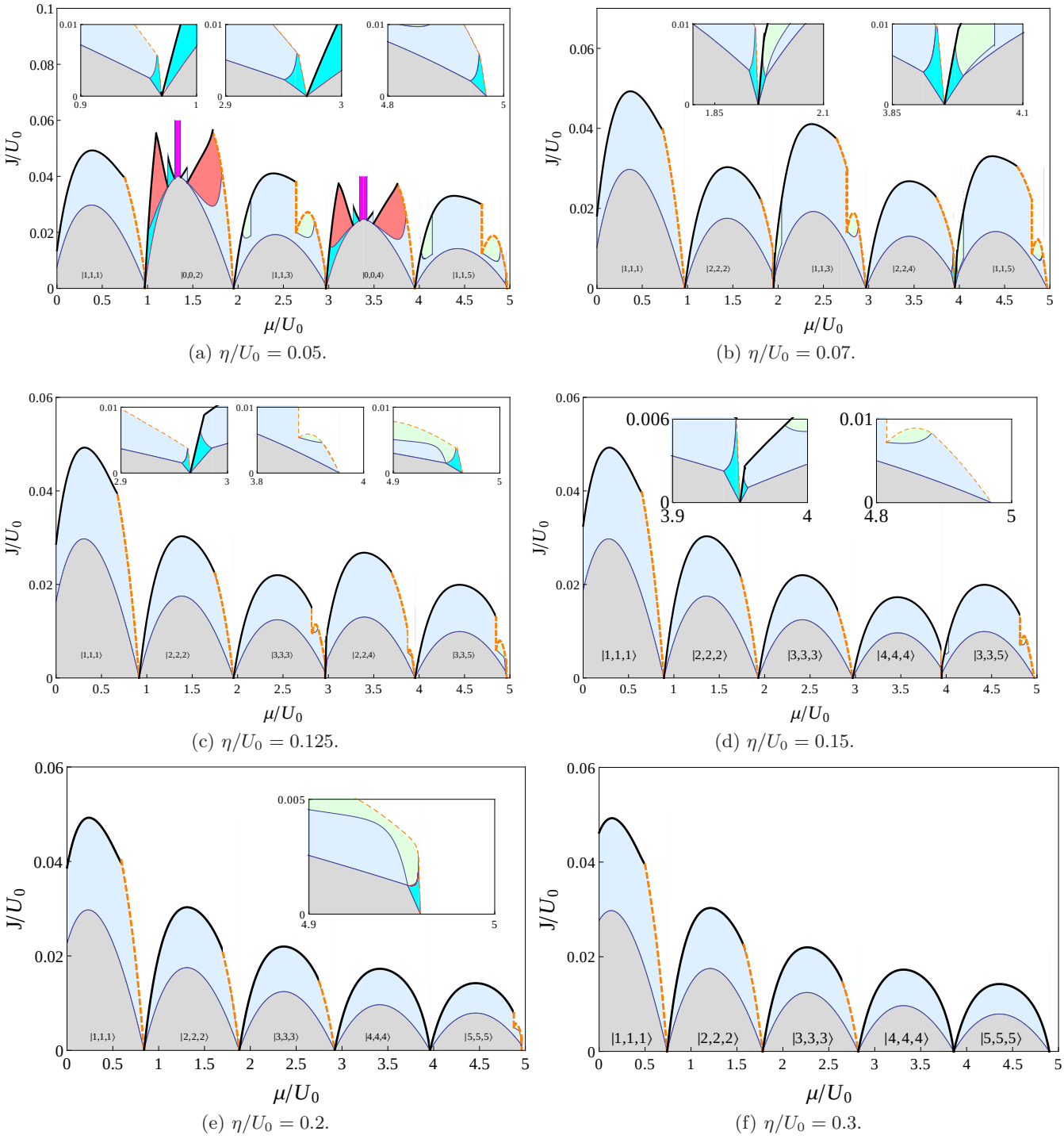

(a) $\eta/U_0 = 0.05$. (b) $\eta/U_0 = 0.07$.

(c) $\eta/U_0 = 0.125$. (d) $\eta/U_0 = 0.15$.

(e) $\eta/U_0 = 0.2$. (f) $\eta/U_0 = 0.3$.

Figure 5.4.: Superfluid phases with different external magnetic field with $U_2/U_0 = 0.04$. $\Psi_1 \neq 0$, $\Psi_0 = \Psi_{-1} = 0$ (blue); $\Psi_0 \neq 0$, $\Psi_1 \neq 0$, $\Psi_{-1} \neq 0$ (red); $\Psi_{-1} \neq 0$, $\Psi_0 = \Psi_1 = 0$ (cyan); $\Psi_0 \neq 0$, $\Psi_1 = \Psi_{-1} = 0$ (magenta); and $\Psi_1 \neq 0$, $\Psi_{-1} \neq 0$, $\Psi_0 = 0$ (green), whereas, the solid black and dashed orange lines correspond to the validity ranges (5.50) and (5.51), respectively. Moreover, Mott lobes are characterized by gray color.

quantum numbers S and m for the even lobes change from $|2,2,n\rangle$ to $|4,4,n\rangle$ as shown in Fig. 5.4d. This increase of the magnetic field is not enough to align all the spins of the fourth Mott lobe, but it is enough to align them for the third Mott lobe. Similarly, the phase $\Psi_{-1} \neq 0$, $\Psi_1 = \Psi_0 = 0$ appears in the SF phase at the contact point between the fourth and the fifth Mott lobe.

Beyond the critical value $\eta^{(2)}_{\text{odd}} = 0.18\,U_0$ the quantum numbers S and m for the even lobes change from $|3,3,n\rangle$ to $|5,5,n\rangle$ as shown in Fig. 5.4e. This increase in the magnetic field is not enough to align all the spins for the fifth Mott lobe, but it is enough to align them for the fourth Mott lobe. Similarly, the phase $\Psi_{-1} \neq 0$, $\Psi_1 = \Psi_0 = 0$ appears in the SF phase at the end of the fifth Mott lobe. As happened in the third Mott lobe, the left phase $\Psi_1 \neq 0$, $\Psi_{-1} \neq 0$, $\Psi_0 = 0$ appears once in the fifth Mott lobe. If η increases to 0.3 U_0 after the critical value $\eta^{(3)}_{\text{even}} = 0.22\,U_0$ and $\eta^{(3)}_{\text{odd}} = 0.26\,U_0$, S and m change from $|4,4,n\rangle$ to $|6,6,n\rangle$ for the even lobes and from $|5,5,n\rangle$ to $|7,7,n\rangle$ for the odd lobes as shown in Fig. 5.4e, So all seven lobes have $S = m = n$. Therefore, we have now a full spin alignment in the shown quantum phase diagram, where only the phase $\Psi_1 \neq 0$, $\Psi_{-1} = \Psi_0 = 0$ exists in the SF phase.

5.5.4. With Fixed Magnetic Field and Varying Spin-Dependent Interaction

In this subsection, we study the predictions of the Ginzburg-Landau theory in view of an effect of the spin-dependent interaction on the superfluid phases with a fixed magnetic field. Similarly, we show the phase diagrams which result before and after the spin-dependent interaction U_2 reaches one of the critical values which have been explained in Subsection 3.4.2 as shown in Fig. 5.5.

When U_2/U_0 is 0.02, the superfluid phase becomes $\Psi_1 \neq 0$, $\Psi_{-1} = \Psi_0 = 0$ where the ground state $|n,n,n\rangle$ is the state with maximum spin for all six lobes as shown in Fig. 5.5a. Above the first critical value $U^{(1)}_{2\text{even}}/U_0 = 0.036$ both the spin S and the magnetic m quantum numbers change from $|6,6,n\rangle$ to $|4,4,n\rangle$ for even lobes as shown in Fig. 5.5b. We remark that if the spin-dependent interaction increases, the effect of the external magnetic field decreases, so the Mott lobes increase. The phases $\Psi_1 \neq 0$, $\Psi_{-1} \neq 0$, $\Psi_0 = 0$ and $\Psi_{-1} \neq 0$, $\Psi_1 = \Psi_0 = 0$ appear in the SF phase for the fifth and sixth lobes. We note that the phase $\Psi_1 \neq 0$, $\Psi_{-1} \neq 0$, $\Psi_0 = 0$ appears twice in the sixth lobe. The right phase in the sixth lobe results from the change of S and m for the seventh lobe from $|7,7,7\rangle$ to $|5,5,7\rangle$, which happens at the critical value $U^{(1)}_{2\text{odd}}/U_0 = 0.0308$.

Beyond the critical value $U^{(2)}_{2\text{odd}}/U_0 = 0.044$ the values of S and m for the odd lobes change from $|5,5,n\rangle$ to $|3,3,n\rangle$ as shown in Fig. 5.5c. Similarly, the phases $\Psi_1 \neq 0$, $\Psi_{-1} \neq 0$, $\Psi_0 = 0$ and $\Psi_{-1} \neq 0$, $\Psi_1 = \Psi_0 = 0$ appear in the SF phase for the fourth and fifth lobe and the phase $\Psi_1 \neq 0$, $\Psi_{-1} \neq 0$, $\Psi_0 = 0$ increases in the sixth lobe. After the critical value $U^{(2)}_{2\text{even}}/U_0 = 0.05714$, the ground states for the even lobes change from $|4,4,n\rangle$ to $|2,2,n\rangle$ as shown in Fig. 5.5d. By the same way the phases $\Psi_1 \neq 0$, $\Psi_{-1} \neq 0$, $\Psi_0 = 0$ and $\Psi_{-1} \neq 0$, $\Psi_1 = \Psi_0 = 0$ are seen in the SF phase for the third and fourth lobe.

When U_2 increases beyond the critical value $U^{(3)}_{2\text{odd}}/U_0 = 0.08$, the ground states for the odd lobes change from $|3,3,n\rangle$ to $|1,1,n\rangle$ as shown in Fig. 5.5e. The phases $\Psi_1 \neq 0$, $\Psi_{-1} \neq 0$, $\Psi_0 = 0$ and $\Psi_{-1} \neq 0$, $\Psi_1 = \Psi_0 = 0$ appear in the SF phase for the even and odd lobes. After the critical value $U^{(3)}_{2\text{even}}/U_0 = 0.133$, S and m change from $|2,2,n\rangle$ to $|0,0,n\rangle$ for the even lobes as shown in Fig. 5.5f. Furthermore, the effect of magnetic field becomes quite weak because the value of η is close to U_2.

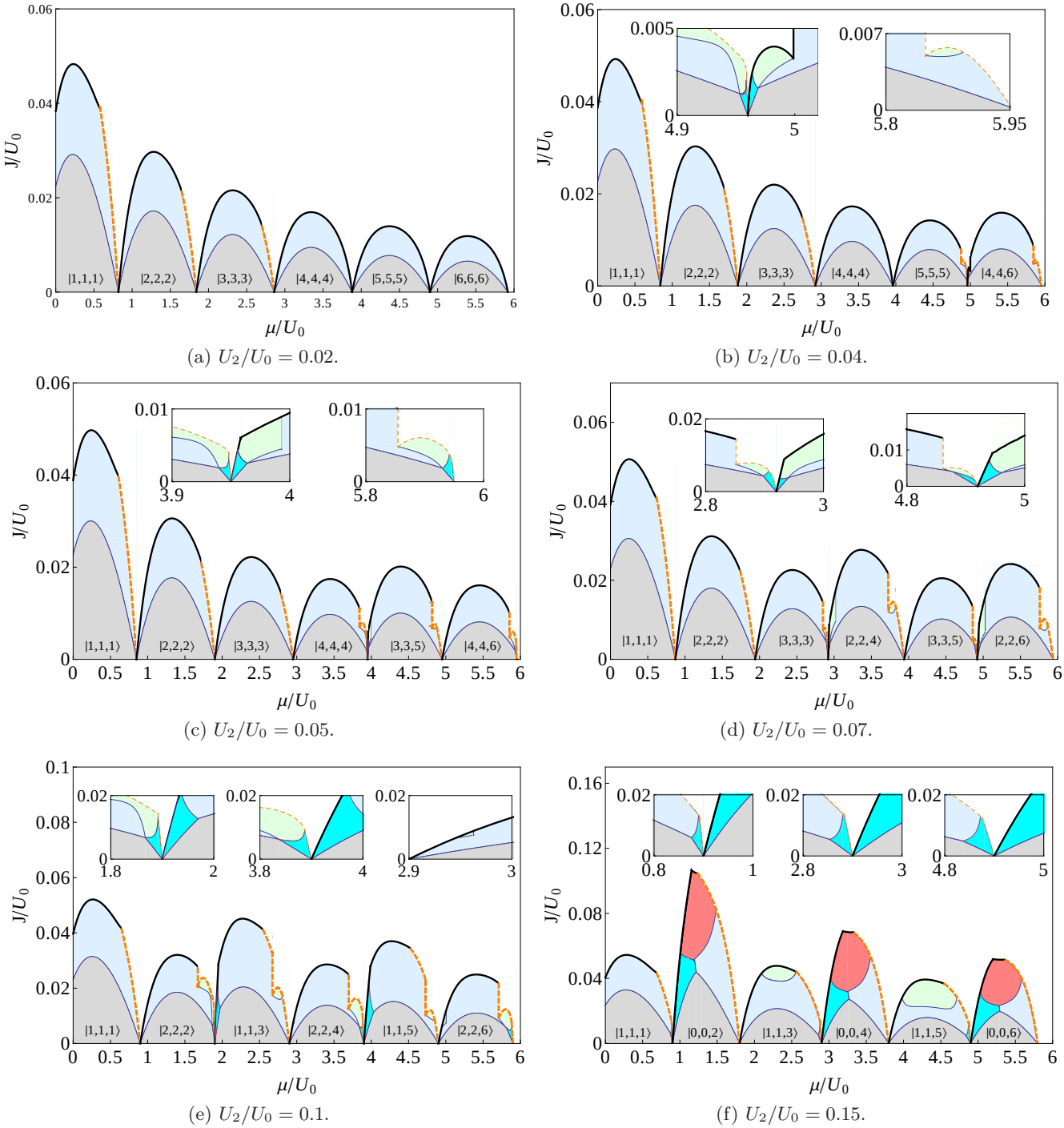

(a) $U_2/U_0 = 0.02$.

(b) $U_2/U_0 = 0.04$.

(c) $U_2/U_0 = 0.05$.

(d) $U_2/U_0 = 0.07$.

(e) $U_2/U_0 = 0.1$.

(f) $U_2/U_0 = 0.15$.

Figure 5.5.: Superfluid phases with different spin-dependent interactions strengths with $\eta/U_0 = 0.2$. $\Psi_1 \neq 0$, $\Psi_0 = \Psi_{-1} = 0$ (blue); $\Psi_0 \neq 0$, $\Psi_1 \neq 0$, $\Psi_{-1} \neq 0$ (red); $\Psi_{-1} \neq 0$, $\Psi_0 = \Psi_1 = 0$ (cyan); $\Psi_1 \neq 0$, $\Psi_0 \neq 0$, $\Psi_{-1} \neq 0$ (pink); and $\Psi_1 \neq 0$, $\Psi_{-1} \neq 0$, $\Psi_0 = 0$ (green). The validity ranges (5.50) and (5.51) correspond to the solid black and dashed orange lines, respectively. Moreover, Mott lobes are characterized by gray color.

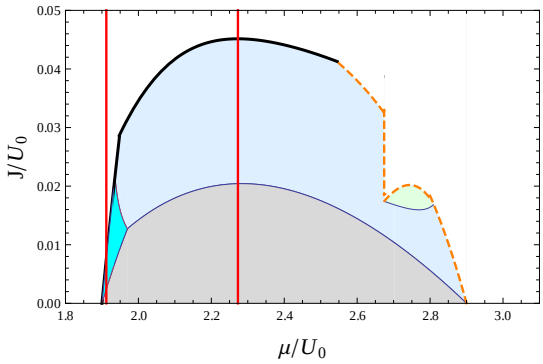

Figure 5.6.: Third Mott lobe with $\eta = 0.2\,U_0$ and $U_2 = 0.1\,U_0$.

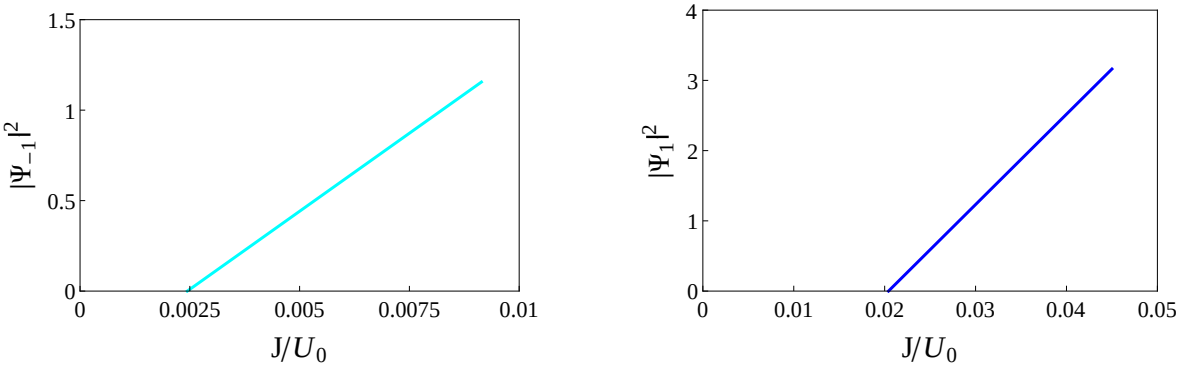

(a) $\mu = 1.912\,U_0$ (b) $\mu = 2.273\,U_0$

Figure 5.7.: Condensate density for the phases $\Psi_{-1} \neq 0$, $\Psi_0 = \Psi_1 = 0$ and $\Psi_1 \neq 0$, $\Psi_{-1} = \Psi_0 = 0$ as a function of the tunneling parameter J/U_0 of spin-1 Bose-Hubbard model in the antiferromagnetic case with $\eta = 0.2\,U_0$ and $U_2 = 0.1\,U_0$ at zero temperature.

Additionally, spin pairs are produced to get the minimal energy and, thus, the ground state becomes $|0, 0, n\rangle$ for an even n, and $|1, 1, n\rangle$ for an odd n and we find the new phase $\Psi_1 \neq 0$, $\Psi_{-1} \neq 0$, $\Psi_0 \neq 0$ in the even lobes.

5.6. Order of Phase Transition

In this section, we study which kind of order occurs for the quantum phase transition from the Mott insulator to the superfluid phase and for the transitions between the respective superfluid phases of spin-1 bosons in a three-dimensional cubic optical lattice under the effect of the external magnetic field at zero temperature.

5.6.1. Quantum Phase Transition

It is known that for spinless bosons the superfluid-Mott insulator phase transition of the Bose-Hubbard model in three dimensions is of second order [65]. In order to determine the kind of the order of the quantum phase transition for the spin-1 Bose-Hubbard model, we focus at first on the transition from the Mott insulator to a superfluid phase at a fixed chemical potential μ around an external magnetic field η and spin-dependent interaction U_2 as shown in Fig. 5.6. In Fig. 5.7 the corresponding condensate

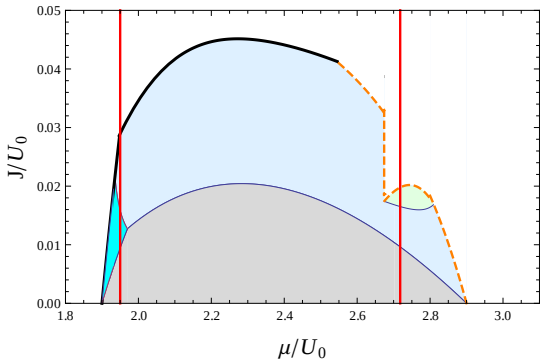

Figure 5.8.: Third Mott lobe with $\eta = 0.2\,U_0$ and $U_2 = 0.1\,U_0$.

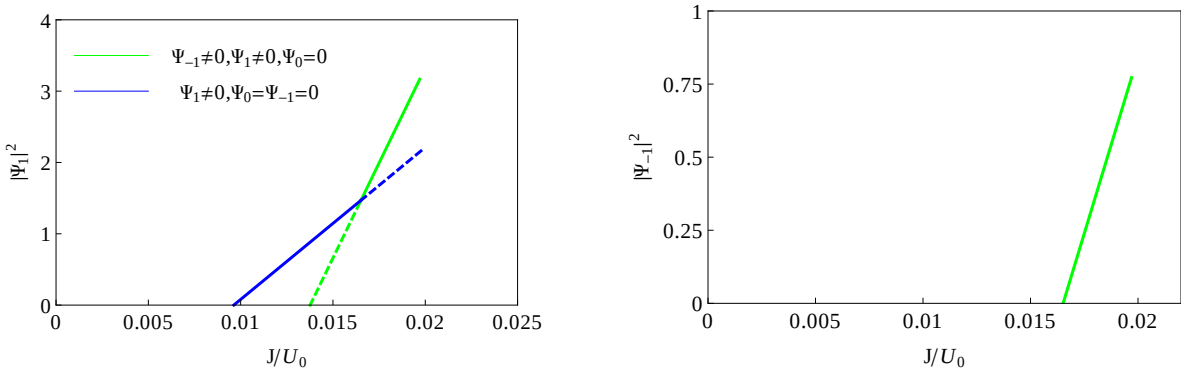

Figure 5.9.: Condensate density for two spin components as a function of the tunneling parameter J/U_0 of the spin-1 Bose-Hubbard model in the anti-ferromagnetic case with $\eta = 0.2\,U_0$, $U_2 = 0.1\,U_0$ and $\mu = 2.718\,U_0$ at zero temperature. Solid (dashed) lines correspond to solutions of minimal (not minimal) energy, compare with Fig. 5.10.

density is shown as a function of the hopping parameter J at fixed chemical and external magnetic field values for the third lobe. We note that the condensate density for the two phases $\Psi_{-1} \neq 0$, $\Psi_0 = \Psi_1 = 0$ and $\Psi_1 \neq 0$, $\Psi_{-1} = \Psi_0 = 0$ increases linearly with J until the validity range of Ginzburg-Landau theory is reached where the critical J values, calculated from (5.33) and (5.31), are 0.00244 U_0 and 0.02042 U_0, respectively. From this we read off that the superfluid-Mott insulator phase transition is of second order.

5.6.2. Transitions between Superfluid Phases

The effect of the external magnetic field on spin-1 bosons with anti-ferromagnetic interaction leads to the appearance of different phases in the superfluid phase as discussed in detail in Section 5.5.2. In order to determine the order of the transitions between the phases in the superfluid region, we focus on the transition from the $\Psi_1 \neq 0$, $\Psi_0 = \Psi_{-1} = 0$ to the $\Psi_1 \neq 0$, $\Psi_{-1} \neq 0$, $\Psi_0 = 0$ phase at a fixed chemical potential $\mu = 2.718\,U_0$ around an external magnetic field η and spin-dependent interaction U_2 for the third lobe as shown in Fig. 5.8. We find that the condensate density $|\Psi_1|^2$ continuously increases from the $\Psi_1 \neq 0$, $\Psi_0 = \Psi_{-1} = 0$ to the $\Psi_1 \neq 0$, $\Psi_{-1} \neq 0$, $\Psi_0 = 0$ phase as shown in Fig. 5.9a. Fig. 5.9b shows that the condensate density $|\Psi_{-1}|^2$ continuously increases with increasing the hopping

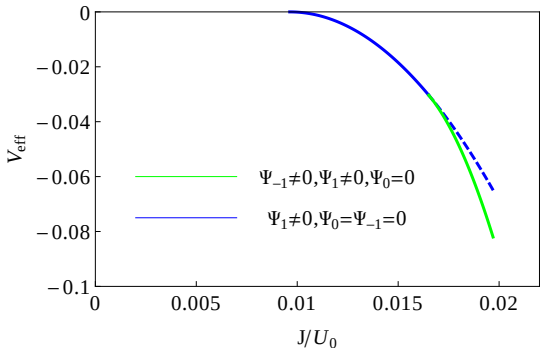

Figure 5.10.: Effective potential for the phases $\Psi_1 \neq 0$, $\Psi_{-1} = 0$, $\Psi_0 = 0$ and $\Psi_1 \neq 0$, $\Psi_{-1} = \Psi_0 = 0$ phases as a function of the tunneling parameter J/U_0 of spin-1 Bose-Hubbard model in the anti-ferromagnetic case with $\eta = 0.2\,U_0$, $U_2 = 0.1\,U_0$ and $\mu = 2.718\,U_0$ at zero temperature.

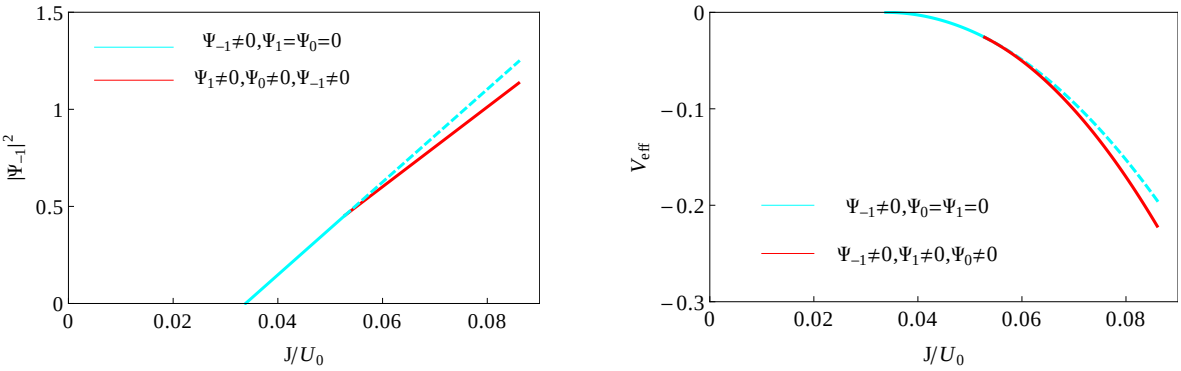

Figure 5.11.: (a) Condensate density and (b) effective potential for the phases as a function of the tunneling parameter J/U_0 of spin-1 Bose-Hubbard model in the anti-ferromagnetic case with $\eta = 0.2\,U_0$, $U_2 = 0.15\,U_0$ and $\mu = 1.095\,U_0$ at zero temperature.

parameter J. Furthermore, this condensate density starts at the critical hopping point J which marks the boundary between the phases $\Psi_1 \neq 0$, $\Psi_0 = \Psi_{-1} = 0$ to $\Psi_1 \neq 0$, $\Psi_{-1} \neq 0$, $\Psi_0 = 0$. In addition, this point is the same point where the two solutions for Ψ_1 intersect in Fig. 5.10. Therefore, the transition between these two phases is of second order.

Similarly, the transition at $\mu = 1.095\,U_0$ from $\Psi_1 \neq 0$, $\Psi_0 = \Psi_{-1} = 0$ or $\Psi_{-1} \neq 0$, $\Psi_0 = \Psi_1 = 0$ to $\Psi_1 \neq 0$, $\Psi_{-1} \neq 0$, $\Psi_0 = 0$ or $\Psi_1 \neq 0$, $\Psi_{-1} \neq 0$, $\Psi_0 \neq 0$ will be of second order as shown in Fig. 5.11.

A different situation occurs when we study the transition from $\Psi_1 \neq 0$, $\Psi_0 = \Psi_{-1} = 0$ to $\Psi_{-1} \neq 0$, $\Psi_1 = \Psi_0 = 0$ or vice versa. To this end, we focus on the transition from the $\Psi_{-1} \neq 0$, $\Psi_0 = \Psi_1 = 0$ to the $\Psi_1 \neq 0$, $\Psi_{-1} = \Psi_0 = 0$ phase at a fixed $\mu = 1.95\,U_0$ with $\eta = 0.2\,U_0$ and $U_2 = 0.1\,U_0$ for the third lobe as seen in Fig. 5.12a. We note that the $\Psi_1 \neq 0$, $\Psi_{-1} = \Psi_0 = 0$ phase jumps at the intersect point which is 0.01585 U_0 according to Fig. 5.12b. Furthermore, the dashed line in Fig. 5.12b means that we can not take this phase due to the minimal energy. Therefore, the transition between the $\Psi_{-1} \neq 0$, $\Psi_0 = \Psi_1 = 0$ and $\Psi_1 \neq 0$, $\Psi_{-1} = \Psi_0 = 0$ phases is of first order.

Finally, we conclude that the transition between the phases $\Psi_1 \neq 0$, $\Psi_0 = \Psi_{-1} = 0$ to $\Psi_1 \neq 0$, $\Psi_{-1} \neq 0$, $\Psi_0 = 0$ is of second order and the transition between the phases $\Psi_{-1} \neq 0$, $\Psi_0 = \Psi_1 = 0$

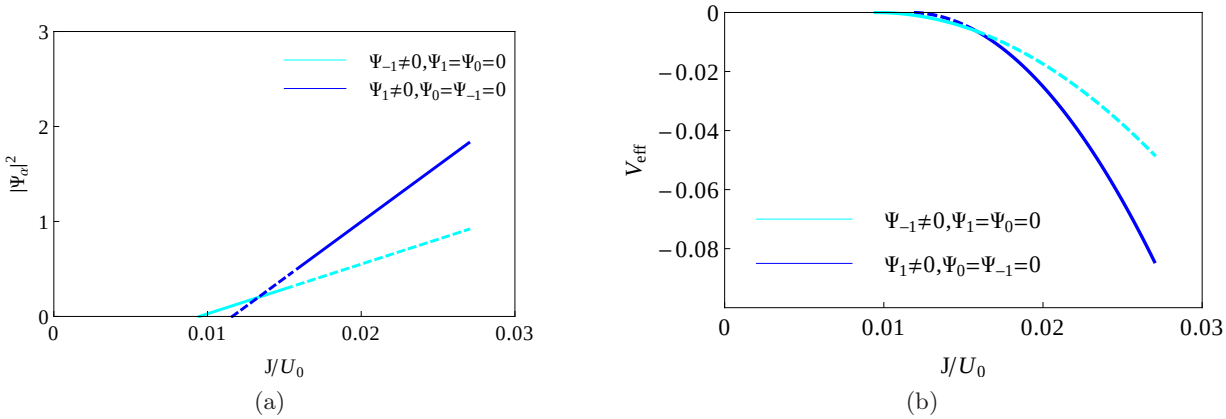

Figure 5.12.: (a) Condensate density and (b) effective potential for the phases $\Psi_{-1} \neq 0$, $\Psi_0 = \Psi_1 = 0$ and $\Psi_1 \neq 0$, $\Psi_{-1} = \Psi_0 = 0$ as a function of the tunneling parameter J/U_0 of spin-1 Bose-Hubbard model in the anti-ferromagnetic case with $\eta = 0.2\,U_0$ and $U_2 = 0.1\,U_0$ and $\mu = 1.95\,U_0$ at zero temperature.

and $\Psi_1 \neq 0$, $\Psi_{-1} = \Psi_0 = 0$ is of first order at a fixed value of chemical potential $\mu = 1.95\,U_0$ around an external magnetic field $\eta = 0.2\,U_0$ and spin-dependent interaction $U_2 = 0.1\,U_0$ in the third lobe, see Fig. 5.8. Therefore, it is very interesting to observe that both the first- and second-order phase transition occurs above the same Mott lobe in the superfluid phase.

6. Summary and Outlook

Spin-1 bosons in a three-dimensional cubic optical lattice represent a challenging quantum many-body system. A first theoretical investigation was performed in Refs. [80, 81], where, in case of the anti-ferromagnetic interaction of ^{23}Na, the location of the SF-MI transition and several properties for SF and MI phases for spin-1 bosons were determined without external magnetic field at zero temperature. In particular, it was found that the superfluid transition occurs into a polar spin-0 state [81], i.e. the SF phase represents a polar state with zero spin expectation value. The effect of a non-vanishing external magnetic field upon the SF-MI transition was determined within a mean-field approximation in Ref. [82, 83]. In addition, it was also shown in Ref. [82, 83] that the superfluid transition occurs into a polar spin-1 or spin-(-1) state, but it was not investigated which magnetic properties emerge deep in the superfluid phase.

In our thesis, we followed Refs. [84, 85] and showed that new magnetic superfluid phases can emerge due to the delicate interplay of the anti-ferromagnetic interaction of spin-1 bosons and the linear Zeemann effect in a three-dimensional cubic optical lattice at zero temperature. To this end, our thesis begun with **Chapter 1**, where we briefly discussed the experimental and theoretical description of Bose-Einstein condensation in general and the physics of lattice systems in particular.

In **Chapter 2** we discussed at first the spinor interaction potential between two atoms. Then, we derived a generalization of the Bose-Hubbard model for spin-1 atoms in a cubic optical lattice by using a tight-binding approximation, where the resulting Hamiltonian was given in Eq. (2.23). Whereas in the literature the discussion of Mott insulator phases for the spin-1 Bose-Hubbard model had been restricted to a vanishing external magnetic field [102, 103], we studied the impact of the linear Zeeman effect on these Mott phases. To this end we used the degeneracy (2.52), where two states have the same energy with equal particle number but different total spin [82, 104], and obtained the phase diagram for both ferromagnetic and anti-ferromagnetic interactions as shown in Fig. 2.4 and explained in Subsection 2.4.2.

Chapter 3 provided a general introduction to critical phenomena as well as first- and second-order phase transitions. In particular, the symmetry breaking mechanism and the role of the order parameter were discussed. Special attention was made in the context of spin-1 Bose gas in a cubic optical lattice in order to discuss the quantum phase transition between Mott insulator and superfluid phases by using the perturbative mean-field theory with the main result (3.31), which applies recursion relations for the matrix elements of particle creation and annihilation operators in Appendix A. Within the framework of Refs. [82, 83, 100, 101, 104] we studied then the effect of an external magnetic field on the quantum MI-SF phase transition by taking into account the degeneracy (2.52) with a fixed spin-dependent interaction strength as shown in Fig. 3.5 and explained in Section 3.5. In addition, we studied the effect of spin-dependent interaction strength and linear Zeeman effect on the quantum phase transition, which is shown in Fig. 3.6 and explained in Section 3.6. Our work agreed with

Refs. [82, 83, 100, 101, 104] where the superfluid transition occurs from the Mott insulating phase into either a spin-1 or spin-(-1) state.

In **Chapter 4** we developed an alternative field-theoretic approach to determine the quantum phase boundary in terms of a Ginzburg-Landau theory. To this end we extended the Ginzburg-Landau theory developed in Refs. [86,87] from the spin-0 to the spin-1 Bose-Hubbard model. At first we added additional source currents to the Bose-Hubbard model in order to break the global $U(1)$ symmetry. Using the linked-cluster theorem [120] we obtained then a diagrammatic expansion of the grand-canonical free energy in first order of the hopping parameter and in fourth order of the symmetry-breaking currents. Thus, the grand-canonical free energy is a sum over cumulants which are only represented by the connected Green functions because the disconnected diagrams of the thermal Green functions are cancelled due to the expansion of the logarithm of the partition function. We used diagrammatic rules as they yield a much simpler calculation for the perturbative contributions of the free energy. In order to simplify our calculation the Matsubara transformation was introduced, where similar diagrammatic rules could be applied for imaginary time by using the transformations (4.79) and (4.81). Additionally, we started to investigate the implications of this theoretical approach by evaluating the resulting physical stability conditions for a static equilibrium order parameter field. We found up to the calculated level of accuracy that the mean-field free energy is reproduced. Afterwards, we found that, when the chemical potential μ is fixed, the mean-field condensate density with spin-1 is not monotonically increasing with the hopping as is shown in Fig. 4.1 and also in Ref. [86]. Thus, the mean-field prediction for the condensate density is not physical provided that the hopping is too large. We used this circumstance to our advantage and defined a validity range of the mean-field theory as shown in in Fig. 4.2. In order to check our calculation we determined the fourth-order perturbation correction for an even number of atoms with no magnetization in the anti-ferromagnetic case. Our finding (4.118) agreed with Ref. [81] and then we calculated this perturbation for both an even and odd number of atoms with external magnetic field in the anti-ferromagnetic case.

In **Chapter 5** we applied a Legendre transformation to the free energy by mapping the unphysical symmetry-breaking currents onto physical time-, space-, and spin-dependent order parameter fields, thus the effective Ginzburg-Landau action was obtained. Then, we calculated the condensate in the superfluid phase above the Mott lobes and found a sharp increase, see Fig. 5.7 and Ref. [86]. Thus, the condensate density (5.48) could not be valid deep in the superfluid phase. Therefore, the range of validity of the Ginzburg-Landau theory was obtained in Fig. 5.2 and explained in Section 5.4. From this we found that the Ginzburg-Landau theory has a larger range of validity than that of mean-field theory. In particular at zero temperature, our theory can distinguish between different magnetic superfluid phases for a ferromagnetic and anti-ferromagnetic interaction with and without magnetization. Then, depending on the particle number, the spin-dependent interaction and the value of the magnetic field we found superfluid phases with a macroscopic occupation of the two spin states ± 1 or even of all three spin states $0, \pm 1$. This is qualitatively different from the mean-field approximation, which only predicted two superfluid phases with spin-1 or spin-(-1) with external magnetic field [70, 101]. Furthermore, inspecting the energies of the respective phases in the vicinity of their boundaries allowed to determine the respective order of the quantum phase transition. We found that this quantum phase transition from the Mott insulator to a superfluid phase is always

of second order at fixed chemical potential. Thus, our finding disagrees with Kimura et al. [100], where a first-order SF-MI phase transition was found at a part of the phase boundary by using the Gutzwiller variational approach. Finally, we observed that the transitions between different superfluid phases can be of both first and second order above the same Mott lobe. For instance, the transition from $\Psi_1 \neq 0$, $\Psi_0 = \Psi_{-1} = 0$ to $\Psi_{-1} \neq 0$, $\Psi_1 = \Psi_0 = 0$ or vice versa is of first order as shown in Fig. 5.12a and explained in Subsection 5.6.2, whereas the transition from $\Psi_1 \neq 0$, $\Psi_0 = \Psi_{-1} = 0$ to $\Psi_1 \neq 0$, $\Psi_{-1} \neq 0$, $\Psi_0 = 0$ or $\Psi_1 \neq 0$, $\Psi_{-1} \neq 0$, $\Psi_0 \neq 0$ phases or vice versa is of second order as shown in Figs. 5.9–5.11.

In conclusion, we worked out a Ginzburg-Landau theory for spin-1 bosons in a cubic optical lattice within its range of validity and investigated at zero temperature the resulting different superfluid phases for an anti-ferromagnetic interaction in the presence of an external magnetic field. Inspecting the energies of the respective phases in the vicinity of their boundaries allowed to determine the order of the quantum phase transition. With this we found that the quantum phase transition from the Mott insulator to the superfluid phase is of second order for spin-1 bosons in a cubic optical lattice under the effect of the magnetic field. Furthermore, depending on the particle number, the spin-dependent interaction and the value of the magnetic field, we found new magnetic superfluid phases with a macroscopic occupation of the two spin states ± 1 or even of all three spin states $0, \pm 1$. This is different from the mean-field approximation, which only predicts two superfluid phases with spins aligned or opposite to the field direction [82,83]. Finally, we found that both a first- and a second-order phase transition can occur above the same Mott lobe in the superfluid phase depending on whether the respective macroscopic occupation of hyperfine spin states changes discontinuously or continuously.

In this thesis we restricted ourselves to apply the Ginzburg-Landau theory for studying the emergence of different magnetic Mott insulator and superfluid phases. However, we note that this theory would also allow, in principle, to study the effect of a finite temperature on the quantum phase transition and superfluid phases and to investigate time-of-flight absorption pictures as well as the collective excitations of all these different phases. In Ref. [126] already the corresponding spin-0 case was treated, where particle- and hole excitations characterize the Mott insulator phase, whereas the superfluid phase yields both a Goldstone and a Higgs mode [127–129].

Certainly, it would be interesting to study also in detail how all these results would change for more general spinor Bose gas systems, for instance, in a superlattice [130, 131]. One example is provided by the competition between the linear Zeeman effect, considered here, and its quadratic counterpart (see, for instance, Refs. [132, 133]), another one would be substituting the nonfrustrated cubic by a frustrated triangular optical lattice [79]. Finally, one can expect even more complex magnetic Mott insulator and superfluid phases for spin-2 or spin-3 bosons, which could be realized with ^{87}Rb [78] and ^{52}Cr atoms [134].

A. Matrix Elements

The Matrix elements M, N, O and P from Eqs. (3.23), (3.24) represent mathematical backbone for analyzing spin-1 bosons in a lattice. Initially, they were calculated individually in a stepwise procedure in Refs. [81, 83]. In this appendix, however, we follow Ref. [104] and determine these matrix elements by a recursive procedure. In particular at finite temperature, when many of these matrix elements have to be evaluated in (4.95) and (4.109), this recursive approach turns out to be more efficient than the original stepwise procedure.

We start with characterizing the ground state of the on-site Hamiltonian (2.23) via [93]

$$|S,S,n\rangle = \frac{1}{\sqrt{f(n,S)}} \hat{a}_1^{\dagger S} \left(\hat{\Theta}^\dagger\right)^{(n-S)/2} |0\rangle\,, \tag{A.1}$$

where the normalization factor is given by

$$f(n,S) = S! \left(\frac{n-S}{2}\right)! \, 2^{(n-S)/2} \, \frac{(n+S+1)!!}{(2S+1)!!}, \tag{A.2}$$

and $\hat{\Theta}^\dagger = \hat{a}_0^{\dagger 2} - 2\hat{a}_1^\dagger \hat{a}_{-1}^\dagger$ represents the creation operator of a spin singlet pair. By applying the ladder operators $\hat{S}_+ = \sqrt{2}(\hat{a}_1^\dagger \hat{a}_0 + \hat{a}_0^\dagger \hat{a}_{-1})$ and $\hat{S}_- = \sqrt{2}(\hat{a}_0^\dagger \hat{a}_1 + \hat{a}_{-1}^\dagger \hat{a}_0)$ on the ground state $|S,S,n\rangle$, we get the excited states $|S,m,n\rangle$ with $m < S$.

Now, we turn to calculate the matrix elements M, N, O and P in Eqs. (3.23), (3.24). The first substantial consideration declares that no state $|S,m,n\rangle$ with $m > S$ does exist, so we have

$$N_{1,S,S,n} = N_{0,S,S,n} = P_{0,S,S,n} = P_{-1,S,S,n} = 0, \tag{A.3}$$

and

$$\hat{a}_1^\dagger \, |S,S,n\rangle = M_{1,S,S,n} \, |S+1,S+1,n+1\rangle\,. \tag{A.4}$$

On the other hand we conclude from (A.1) and (A.2)

$$\hat{a}_1^\dagger \, |S,S,n\rangle = \sqrt{\frac{(S+1)(n+S+3)}{2S+3}} \, |S+1,S+1,n+1\rangle\,, \tag{A.5}$$

so, comparing (A.4) and (A.5) yields

$$M_{1,S,S,n} = \sqrt{\frac{(S+1)(n+S+3)}{2S+3}}. \tag{A.6}$$

In this manner, we put our hands on the first matrix element with $m = S$. In order to calculate

recursively $M_{1,S,m,n}$ with $m < S$, we apply $\hat{S}_+$on Eq. (3.23) and obtain

$$M_{1,S,m,n} = \sqrt{\frac{S(S+1) - m(m+1)}{(S+1)(S+2) - (m+1)(m+2)}} M_{1,S,m+1,n}. \tag{A.7}$$

This recursion relation is useful to calculate $M_{1,S,m-1,n}$ from $M_{1,S,m,n}$. We can use the same procedure to calculate the matrix element with $\alpha = 0$

$$\begin{aligned} M_{0,S,m,n} = &\sqrt{\frac{S(S+1) - m(m+1)}{(S+1)(S+2) - m(m+1)}} M_{0,S,m+1,n} \\ &+ \sqrt{\frac{2}{(S+1)(S+2) - m(m+1)}} M_{1,S,m,n}. \end{aligned} \tag{A.8}$$

and also with $\alpha = -1$

$$\begin{aligned} M_{-1,S,m,n} = &\sqrt{\frac{S(S+1) - m(m+1)}{(S+1)(S+2) - m(m-1)}} M_{-1,S,m+1,n} \\ &+ \sqrt{\frac{2}{(S+1)(S+2) - m(m-1)}} M_{0,S,m,n}. \end{aligned} \tag{A.9}$$

Specializing $m = S$ yields finally

$$M_{-1,S,S,n} = \sqrt{\frac{n+S+3}{(2S+3)(2S+1)}}. \tag{A.10}$$

Now we come to the evaluation of the Matrix elements $N_{\alpha,S,m,n}$. The particle number can be written as

$$\begin{aligned} n =& \langle S, S, n \mid \hat{n} \mid S, S, n \rangle \\ =& \sum_\alpha \left\langle S, S, n \mid \hat{a}_\alpha \hat{a}_\alpha^+ \mid S, S, n \right\rangle - 3, \end{aligned} \tag{A.11}$$

thus, we obtain with (3.23) and (3.24)

$$N_{-1,S,S,n} \;=\; -\sqrt{3 + n - \sum_\alpha M^2_{\alpha,S,S,n}}. \tag{A.12}$$

Matrix elements $N_{\alpha,S,m,n}$ with $m < S$ can be derived as above, yielding

$$N_{-1,S,m,n} = \sqrt{\frac{S(S+1) - m(m-1)}{S(S-1) - (m-1)(m-2)}} N_{-1,S,m-1,n}. \tag{A.13}$$

$$N_{0,S,m,n} = \sqrt{\frac{S(S+1)-m(m-1)}{S(S-1)-m(m-1)}} N_{0,S,m-1,n} + \sqrt{\frac{2}{S(S-1)-m(m-1)}} N_{-1,S,m,n}. \tag{A.14}$$

and also

$$N_{1,S,m,n} = \sqrt{\frac{S(S+1)-m(m-1)}{S(S-1)-m(m+1)}} N_{1,S,m-1,n} + \sqrt{\frac{2}{S(S+1)-m(m-1)}} N_{0,S,m,n}, \tag{A.15}$$

Thus, with this all matrix element of the creation operators $\hat{a}_\alpha^+$ in (3.23) can be calculated. Therefore, we turn now to the calculation of the matrix element of the annihilation operators $\hat{a}_\alpha$ in (3.24) by the identical method. In order to calculate $O_{-1,S,m,n}$. We apply the operator $\hat{a}_{-1}$ to (A.1), yielding

$$O_{-1,S,S,n} = -\sqrt{\frac{(n-S)(S+1)}{2S+3}}. \tag{A.16}$$

Applying $\hat{S}_+$ on (3.24) , we get

$$O_{-1,S,m,n} = \sqrt{\frac{S(S+1)-m(m+1)}{(S+1)(S+2)-(m+1)(m+2)}} O_{-1,S,m+1,n}. \tag{A.17}$$

Similarly, we obtain the recursion relations

$$O_{0,S,m,n} = \sqrt{\frac{S(S+1)-m(m+1)}{(S+1)(S+2)-m(m+1)}} O_{0,S,m+1,n} - \sqrt{\frac{2}{(S+1)(S+2)-m(m+1)}} O_{-1,S,m,n}, \tag{A.18}$$

and

$$O_{1,S,m,n} = \sqrt{\frac{S(S+1)-m(m+1)}{(S+1)(S+2)-m(m-1)}} O_{1,S,m+1,n} - \sqrt{\frac{2}{(S+1)(S+2)-m(m-1)}} O_{0,S,m,n}. \tag{A.19}$$

In order to determine $P_{1,S,S,n}$, the particle number $n = \sum_\alpha \langle S,S,n \mid \hat{a}_\alpha^+ \hat{a}_\alpha \mid S,S,n \rangle$ operator reduces with ((3.24)) to

$$P_{1,S,S,n} = \sqrt{n - \sum_\alpha O_{\alpha,S,S,n}^2}. \tag{A.20}$$

Applying $\hat{S}_-$ on (3.24) we get

$$P_{1,S,m,n} = \sqrt{\frac{S(S+1)-m(m-1)}{S(S-1)-(m-1)(m-2)}}P_{1,S,m-1,n}, \tag{A.21}$$

$$\begin{aligned} P_{0,S,m,n} =& \sqrt{\frac{S(S+1)-m(m-1)}{S(S-1)-m(m-1)}}P_{0,S,m-1,n} \\ & - \sqrt{\frac{2}{S(S-1)-m(m-1)}}P_{1,S,m,n}, \end{aligned} \tag{A.22}$$

and

$$\begin{aligned} P_{-1,S,m,n} =& \sqrt{\frac{S(S+1)-m(m-1)}{S(S-1)-m(m+1)}}P_{-1,S,m-1,n} \\ & - \sqrt{\frac{2}{S(S-1)-m(m+1)}}P_{0,S,m,n}. \end{aligned} \tag{A.23}$$

Finally, we drive useful relations between these creation and annihilation matrix elements. Using (1.2) we get

$$\left\langle S,m,n \mid \hat{a}^+_\alpha \mid S-1,m-\alpha,n-1 \right\rangle = M_{\alpha,S-1,m-\alpha,n-1}. \tag{A.24}$$

Taking into account (3.24) we obtain

$$\left\langle S,m,n \mid \hat{a}^+_\alpha \mid S-1,m-\alpha,n-1 \right\rangle = P_{\alpha,S,m,n}. \tag{A.25}$$

Thus, we conclude

$$M_{\alpha,S-1,m-\alpha,n-1} = P_{\alpha,S,m,n}. \tag{A.26}$$

In a similar way we also obtain

$$P_{\alpha,S+1,m+\alpha,n+1} = M_{\alpha,S,m,n}, \tag{A.27}$$

$$N_{\alpha,S+1,m-\alpha,n-1} = O_{\alpha,S,m,n}, \tag{A.28}$$

and

$$O_{\alpha,S-1,m+\alpha,n+1} = N_{\alpha,S,m,n}. \tag{A.29}$$

Note that we have used the minus sign in (A.12) and the positive sign in (A.20) in order to satisfy the

Table A.1.: Matrix element of creation operators

S	m	$M_{1,S,m,n}$	$M_{0,S,m,n}$	$M_{-1,S,m,n}$	$N_{1,S,m,n}$	$N_{0,S,m,n}$	$N_{-1,S,m,n}$
0	0	$\sqrt{\frac{n+3}{3}}$	$\sqrt{\frac{n+3}{3}}$	$\sqrt{\frac{n+3}{3}}$	0	0	0
1	1	$\sqrt{\frac{2(n+4)}{5}}$	$\sqrt{\frac{n+4}{5}}$	$\sqrt{\frac{n+4}{15}}$	0	0	$-\sqrt{\frac{n+1}{3}}$
1	0	$\sqrt{\frac{n+4}{5}}$	$2\sqrt{\frac{n+4}{15}}$	$\sqrt{\frac{n+4}{5}}$	0	$\sqrt{\frac{n+1}{3}}$	0
1	-1	$\sqrt{\frac{n+4}{15}}$	$\sqrt{\frac{n+4}{5}}$	$\sqrt{\frac{2(n+4)}{5}}$	$-\sqrt{\frac{n+1}{3}}$	0	0
2	2	$\sqrt{\frac{3(n+5)}{7}}$	$\sqrt{\frac{n+5}{7}}$	$\sqrt{\frac{3(n+5)}{105}}$	0	0	$-\sqrt{\frac{2n}{5}}$
2	1	$\sqrt{\frac{2(n+5)}{7}}$	$2\sqrt{\frac{6(n+5)}{105}}$	$3\sqrt{\frac{n+5}{105}}$	0	$\sqrt{\frac{n}{5}}$	$-\sqrt{\frac{n}{5}}$
2	0	$3\sqrt{\frac{2(n+5)}{105}}$	$3\sqrt{\frac{3(n+5)}{105}}$	$3\sqrt{\frac{2(n+5)}{105}}$	$-\sqrt{\frac{n}{15}}$	$2\sqrt{\frac{n}{15}}$	$-\sqrt{\frac{n}{15}}$
2	-1	$3\sqrt{\frac{n+5}{105}}$	$2\sqrt{\frac{6(n+5)}{105}}$	$\sqrt{\frac{2(n+5)}{7}}$	$-\sqrt{\frac{n}{5}}$	$\sqrt{\frac{n}{5}}$	0
2	-2	$\sqrt{\frac{3(n+5)}{105}}$	$\sqrt{\frac{n+5}{7}}$	$\sqrt{\frac{3(n+5)}{7}}$	$-\sqrt{\frac{2n}{5}}$	0	0
3	3	$\frac{2}{3}\sqrt{n+6}$	$\sqrt{\frac{n+6}{9}}$	$\sqrt{\frac{n+6}{63}}$	0	0	$-\sqrt{\frac{3(n-1)}{7}}$
3	2	$\sqrt{\frac{n+6}{3}}$	$2\sqrt{\frac{n+6}{21}}$	$\sqrt{\frac{n+6}{21}}$	0	$\sqrt{\frac{n-1}{7}}$	$-\sqrt{\frac{2(n-1)}{7}}$
3	1	$\sqrt{\frac{5(n+6)}{21}}$	$\sqrt{\frac{5(n+6)}{21}}$	$\sqrt{\frac{2(n+6)}{21}}$	$-\sqrt{\frac{n-1}{35}}$	$2\sqrt{\frac{2(n-1)}{35}}$	$-\sqrt{\frac{6(n-1)}{35}}$
3	0	$\sqrt{\frac{10(n+6)}{63}}$	$\frac{4}{3}\sqrt{\frac{n+6}{7}}$	$\sqrt{\frac{10(n+6)}{63}}$	$-\sqrt{\frac{3(n-1)}{35}}$	$3\sqrt{\frac{n-1}{35}}$	$-\sqrt{\frac{3(n-1)}{35}}$
3	-1	$\sqrt{\frac{2(n+6)}{21}}$	$\sqrt{\frac{5(n+6)}{21}}$	$\sqrt{\frac{5(n+6)}{21}}$	$-\sqrt{\frac{6(n-1)}{35}}$	$2\sqrt{\frac{2(n-1)}{35}}$	$-\sqrt{\frac{n-1}{35}}$
3	-2	$\sqrt{\frac{n+6}{21}}$	$2\sqrt{\frac{n+6}{21}}$	$\sqrt{\frac{n+6}{3}}$	$-\sqrt{\frac{2(n-1)}{7}}$	$\sqrt{\frac{n-1}{7}}$	0
3	-3	$\sqrt{\frac{n+6}{63}}$	$\sqrt{\frac{n+6}{9}}$	$\frac{2}{3}\sqrt{n+6}$	$-\sqrt{\frac{3(n-1)}{7}}$	0	0

relations (A.26)–(A.29). The resulting matrix elements of the creation and annihilation operators for the states with lowest spin quantum numbers are listed in Table A.1 and Table A.2, respectively, and coincide with the findings in Refs. [81, 83, 104].

Table A.2.: Matrix element of annihilation operators

S	m	$O_{1,S,m,n}$	$O_{0,S,m,n}$	$O_{-1,S,m,n}$	$P_{1,S,m,n}$	$P_{0,S,m,n}$	$P_{-1,S,m,n}$
0	0	$-\sqrt{\frac{n}{3}}$	$\sqrt{\frac{n}{3}}$	$-\sqrt{\frac{n}{3}}$	0	0	0
1	1	$-\sqrt{\frac{n-1}{15}}$	$\sqrt{\frac{n-1}{5}}$	$-\sqrt{\frac{2(n-1)}{5}}$	$\sqrt{\frac{n+2}{3}}$	0	0
1	0	$-\sqrt{\frac{n-1}{5}}$	$2\sqrt{\frac{n-1}{15}}$	$-\sqrt{\frac{n-1}{5}}$	0	$\sqrt{\frac{n+2}{3}}$	0
1	-1	$-\sqrt{\frac{2(n-1)}{5}}$	$\sqrt{\frac{n-1}{5}}$	$-\sqrt{\frac{n-1}{15}}$	0	0	$\sqrt{\frac{n+2}{3}}$
2	2	$-\sqrt{\frac{3(n-2)}{105}}$	$\sqrt{\frac{n-2}{7}}$	$-\sqrt{\frac{3(n-2)}{7}}$	$\sqrt{\frac{2(n+3)}{5}}$	0	0
2	1	$-3\sqrt{\frac{n-2}{105}}$	$2\sqrt{\frac{6(n-2)}{105}}$	$-\sqrt{\frac{2(n-2)}{7}}$	$\sqrt{\frac{n+3}{5}}$	$\sqrt{\frac{n+3}{5}}$	0
2	0	$-3\sqrt{\frac{2(n-2)}{105}}$	$3\sqrt{\frac{3(n-2)}{105}}$	$-3\sqrt{\frac{2(n-2)}{105}}$	$\sqrt{\frac{n+3}{15}}$	$2\sqrt{\frac{n+3}{15}}$	$\sqrt{\frac{n+3}{15}}$
2	-1	$-\sqrt{\frac{2(n-2)}{7}}$	$2\sqrt{\frac{6(n-2)}{105}}$	$-3\sqrt{\frac{n-2}{105}}$	0	$\sqrt{\frac{n+3}{5}}$	$\sqrt{\frac{n+3}{5}}$
2	-2	$-\sqrt{\frac{3(n-2)}{7}}$	$\sqrt{\frac{n-2}{7}}$	$-\sqrt{\frac{3(n-2)}{105}}$	0	0	$\sqrt{\frac{2(n+3)}{5}}$
3	3	$-\sqrt{\frac{n-3}{63}}$	$\frac{\sqrt{n-3}}{3}$	$-\frac{2}{3}\sqrt{n-3}$	$\sqrt{\frac{3(n+4)}{7}}$	0	0
3	2	$-\sqrt{\frac{n-3}{21}}$	$2\sqrt{\frac{n-3}{21}}$	$-\sqrt{\frac{n-3}{3}}$	$\sqrt{\frac{2(n+4)}{7}}$	$\sqrt{\frac{n+4}{7}}$	0
3	1	$-\sqrt{\frac{2(n-3)}{21}}$	$\sqrt{\frac{5(n-3)}{21}}$	$-\sqrt{\frac{5(n-3)}{21}}$	$\sqrt{\frac{6(n+4)}{35}}$	$2\sqrt{\frac{2(n+4)}{35}}$	$\sqrt{\frac{n+4}{35}}$
3	0	$-\sqrt{\frac{10(n-3)}{63}}$	$\frac{4}{3}\sqrt{\frac{n-3}{7}}$	$-\sqrt{\frac{10(n-3)}{63}}$	$\sqrt{\frac{3(n+4)}{35}}$	$3\sqrt{\frac{n+4}{35}}$	$\sqrt{\frac{3(n+4)}{35}}$
3	-1	$-\sqrt{\frac{5(n-3)}{21}}$	$\sqrt{\frac{5(n-3)}{21}}$	$-\sqrt{\frac{2(n-3)}{21}}$	$\sqrt{\frac{n+4}{35}}$	$2\sqrt{\frac{2(n+4)}{35}}$	$\sqrt{\frac{6(n+4)}{35}}$
3	-2	$-\sqrt{\frac{n-3}{3}}$	$2\sqrt{\frac{n-3}{21}}$	$-\sqrt{\frac{n-3}{21}}$	0	$\sqrt{\frac{n+4}{7}}$	$\sqrt{\frac{2(n+4)}{7}}$
3	-3	$-\frac{2}{3}\sqrt{n-3}$	$\frac{\sqrt{n-3}}{3}$	$-\sqrt{\frac{n-3}{63}}$	0	0	$\sqrt{\frac{3(n+4)}{7}}$

B. Correlation Relations

This appendix contains the definition of the formulas used in Chapter 4 to simplify the calculation of fourth order in the currents. First, using Eqs. (3.23), (3.24) and (4.8), we can calculate the thermal averages (4.103)–(4.108) which yields:

$$
\begin{aligned}
&\left\langle \hat{a}_{\alpha_4}(\tau_4)\hat{a}_{\alpha_3}(\tau_3)\hat{a}^\dagger_{\alpha_1}(\tau_1)\hat{a}^\dagger_{\alpha_2}(\tau_2)\right\rangle^{(0)} = \frac{1}{\mathcal{Z}^{(0)}}\sum_{S,m,n} e^{-\beta E^{(0)}_{S,m,n}} \\
&\times \left\langle S,m,n\middle|\hat{a}_{\alpha_4}(\tau_4)\hat{a}_{\alpha_3}(\tau_3)\hat{a}^\dagger_{\alpha_1}(\tau_1)\hat{a}^\dagger_{\alpha_2}(\tau_2)\middle|S,m,n\right\rangle = \frac{1}{\mathcal{Z}^{(0)}}\sum_{S,m,n} e^{-\beta E^{(0)}_{S,m,n}} \\
&\times \left\langle S,m,n\middle|[e^{(\tau_4-\tau_2)\hat{H}^{(0)}}\hat{a}_{\alpha_4}e^{(\tau_3-\tau_4)\hat{H}^{(0)}}\hat{a}_{\alpha_3}e^{(\tau_1-\tau_3)\hat{H}^{(0)}}\hat{a}^\dagger_{\alpha_1}e^{(\tau_2-\tau_1)\hat{H}^{(0)}}\hat{a}^\dagger_{\alpha_2}\middle|S,m,n\right\rangle \\
&= \frac{\delta_{\alpha_1+\alpha_2,\alpha_3+\alpha_4}}{\mathcal{Z}^{(0)}}\sum_{S,m,n} e^{-\beta E^{(0)}_{S,m,n}}e^{(\tau_4-\tau_2)E^{(0)}_{S,m,n}}\Big[M_{\alpha_4,S,m,n}M_{\alpha_3,S,m,n}M_{\alpha_1,S,m,n}M_{\alpha_2,S,m,n} \\
&\times e^{(\tau_2-\tau_1)E^{(0)}_{S+1,m+\alpha_2,n+1}}e^{(\tau_1-\tau_3)E^{(0)}_{S+2,m+\alpha_2+\alpha_1,n+2}}e^{(\tau_3-\tau_4)E^{(0)}_{S+1,m+\alpha_4,n+1}} + M_{\alpha_4,S,m,n}M_{\alpha_2,S,m,n} \\
&\times N_{\alpha_3,S+1,m+\alpha_4,n+1}N_{\alpha_1,S+1,m+\alpha_2,n+1}e^{(\tau_2-\tau_1)E^{(0)}_{S+1,m+\alpha_2,n+1}}e^{(\tau_1-\tau_3)E^{(0)}_{S,m+\alpha_3+\alpha_4,n+2}}e^{(\tau_3-\tau_4)E^{(0)}_{S+1,m+\alpha_4,n+1}} \\
&+ M_{\alpha_4,S,m,n}N_{\alpha_2,S,m,n}N_{\alpha_3,S+1,m+\alpha_4,n+1}M_{\alpha_1,S-1,m+\alpha_2,n+1}e^{(\tau_2-\tau_1)E^{(0)}_{S-1,m+\alpha_2,n+1}}e^{(\tau_1-\tau_3)E^{(0)}_{S,m+\alpha_3+\alpha_4,n+2}} \\
&\times e^{(\tau_3-\tau_4)E^{(0)}_{S+1,m+\alpha_4,n+1}} + N_{\alpha_4,S,m,n}M_{\alpha_2,S,m,n}M_{\alpha_3,S-1,m+\alpha_4,n+1}N_{\alpha_1,S+1,m+\alpha_2,n+1}e^{(\tau_2-\tau_1)E^{(0)}_{S+1,m+\alpha_2,n+1}} \\
&\times e^{(\tau_1-\tau_3)E^{(0)}_{S,m+\alpha_3+\alpha_4,n+2}}e^{(\tau_3-\tau_4)E^{(0)}_{S-1,m+\alpha_4,n+1}} + N_{\alpha_4,S,m,n}N_{\alpha_2,S,m,n}M_{\alpha_3,S-1,m+\alpha_4,n+1}M_{\alpha_1,S-1,m+\alpha_2,n+1} \\
&\times e^{(\tau_2-\tau_1)E^{(0)}_{S-1,m+\alpha_2,n+1}}e^{(\tau_1-\tau_3)E^{(0)}_{S,m+\alpha_3+\alpha_4,n+2}}e^{(\tau_3-\tau_4)E^{(0)}_{S-1,m+\alpha_4,n+1}} + N_{\alpha_3,S-1,m+\alpha_4,n+1}N_{\alpha_4,S,m,n} \\
&\times N_{\alpha_1,S-1,m+\alpha_2,n+1}N_{\alpha_2,S,m,n}e^{(\tau_2-\tau_1)E^{(0)}_{S-1,m+\alpha_2,n+1}}e^{(\tau_1-\tau_3)E^{(0)}_{S-2,m+\alpha_3+\alpha_4,n+2}}e^{(\tau_3-\tau_4)E^{(0)}_{S-1,m+\alpha_4,n+1}}\Big].
\end{aligned}
\tag{B.1}
$$

Similarly

$$
\begin{aligned}
&\left\langle \hat{a}_{\alpha_4}(\tau_4)\hat{a}^\dagger_{\alpha_1}(\tau_1)\hat{a}_{\alpha_3}(\tau_3)\hat{a}^\dagger_{\alpha_2}(\tau_2)\right\rangle^{(0)} = \frac{\delta_{\alpha_1+\alpha_2,\alpha_3+\alpha_4}}{\mathcal{Z}^{(0)}}\sum_{S,m,n} e^{-\beta E^{(0)}_{S,m,n}}e^{(\tau_4-\tau_2)E^{(0)}_{S,m,n}}\Big[M_{\alpha_4,S,m,n}M_{\alpha_2,S,m,n} \\
&\times O_{\alpha_3,S+1,m+\alpha_2,n+1}O_{\alpha_1,S+1,m+\alpha_4,n+1}\, e^{(\tau_2-\tau_3)E^{(0)}_{S+1,m+\alpha_2,n+1}}e^{(\tau_3-\tau_1)E^{(0)}_{S+2,m+\alpha_4-\alpha_1,n+2}}e^{(\tau_1-\tau_4)E^{(0)}_{S+1,m+\alpha_4,n+1}} \\
&+ M_{\alpha_4,S,m,n}M_{\alpha_2,S,m,n}P_{\alpha_1,S+1,m+\alpha_4,n+1}P_{\alpha_3,S+1,m+\alpha_2,n+1}e^{(\tau_2-\tau_3)E^{(0)}_{S+1,m+\alpha_2,n+1}}e^{(\tau_3-\tau_1)E^{(0)}_{S,m+\alpha_4-\alpha_1,n}} \\
&\times e^{(\tau_1-\tau_4)E^{(0)}_{S+1,m+\alpha_4,n+1}} + M_{\alpha_4,S,m,n}N_{\alpha_2,S,m,n}O_{\alpha_3,S-1,m+\alpha_2,n+1}P_{\alpha_1,S+1,m+\alpha_4,n+1}e^{(\tau_2-\tau_3)E^{(0)}_{S-1,m+\alpha_2,n+1}} \\
&\times e^{(\tau_3-\tau_1)E^{(0)}_{S,m+\alpha_4-\alpha_1,n}}e^{(\tau_1-\tau_4)E^{(0)}_{S+1,m+\alpha_4,n+1}} + N_{\alpha_4,S,m,n}M_{\alpha_2,S,m,n}P_{\alpha_3,S+1,m+\alpha_2,n+1}O_{\alpha_1,S-1,m+\alpha_4,n+1}
\end{aligned}
$$

$$\times e^{(\tau_2-\tau_3)E^{(0)}_{S+1,m+\alpha_1,n+1}}e^{(\tau_3-\tau_1)E^{(0)}_{S,m+\alpha_4-\alpha_1,n}}e^{(\tau_1-\tau_4)E^{(0)}_{S-1,m+\alpha_4,n+1}} + N_{\alpha_4,S,m,n}N_{\alpha_2,S,m,n}O_{\alpha_3,S-1,m+\alpha_2,n+1}$$
$$\times O_{\alpha_1,S-1,m+\alpha_4,n+1}e^{(\tau_2-\tau_3)E^{(0)}_{S-1,m+\alpha_2,n+1}}e^{(\tau_3-\tau_1)E^{(0)}_{S,m+\alpha_4-\alpha_1,n}}\ e^{(\tau_1-\tau_4)E^{(0)}_{S-1,m+\alpha_4,n+1}} + N_{\alpha_4,S,m,n}N_{\alpha_2,S,m,n}$$
$$\times P_{\alpha_3,S-1,m+\alpha_1,n+1}P_{\alpha_1,S-1,m+\alpha_4,n+1}e^{(\tau_2-\tau_3)E^{(0)}_{S-1,m+\alpha_2,n+1}}e^{(\tau_3-\tau_1)E^{(0)}_{S-2,m+\alpha_4-\alpha_1,n}}e^{(\tau_1-\tau_4)E^{(0)}_{S-1,m+\alpha_4,n+1}}\Bigg], \tag{B.2}$$

$$\left\langle \hat{a}_{\alpha_4}(\tau_4)\hat{a}^\dagger_{\alpha_1}(\tau_1)\hat{a}^\dagger_{\alpha_2}(\tau_2)\hat{a}_{\alpha_3}(\tau_3)\right\rangle^{(0)} = \frac{\delta_{\alpha_1+\alpha_2,\alpha_3+\alpha_4}}{\mathcal{Z}^{(0)}}\sum_{S,m,n} e^{-\beta E^{(0)}_{S,m,n}}e^{(\tau_4-\tau_3)E^{(0)}_{S,m,n}}\Bigg[M_{\alpha_4,S,m,n}O_{\alpha_3,S,m,n}$$
$$\times O_{\alpha_1,S+1,m+\alpha_4,n+1}M_{\alpha_2,S+1,m-\alpha_3,n+1}\,e^{(\tau_3-\tau_2)E^{(0)}_{S+1,m-\alpha_3,n-1}}e^{(\tau_2-\tau_1)E^{(0)}_{S+2,m+\alpha_4-\alpha_1,n}}e^{(\tau_1-\tau_4)E^{(0)}_{S+1,m+\alpha_4,n+1}}$$
$$+ M_{\alpha_4,S,m,n}O_{\alpha_3,S,m,n}P_{\alpha_1,S+1,m+\alpha_4,n+1}N_{\alpha_2,S+1,m-\alpha_3,n-1}e^{(\tau_3-\tau_2)E^{(0)}_{S+1,m-\alpha_3,n-1}}e^{(\tau_2-\tau_1)E^{(0)}_{S,m+\alpha_4-\alpha_1,n}}$$
$$\times e^{(\tau_1-\tau_4)E^{(0)}_{S+1,m+\alpha_4,n+1}} + M_{\alpha_4,S,m,n}P_{\alpha_3,S,m,n}M_{\alpha_2,S-1,m-\alpha_3,n-1}P_{\alpha_1,S+1,m+\alpha_4,n+1}e^{(\tau_3-\tau_2)E^{(0)}_{S-1,m-\alpha_3,n-1}}$$
$$\times e^{(\tau_2-\tau_1)E^{(0)}_{S,m+\alpha_4-\alpha_1,n}}e^{(\tau_1-\tau_4)E^{(0)}_{S+1,m+\alpha_4,n+1}} + N_{\alpha_4,S,m,n}O_{\alpha_3,S,m,n}N_{\alpha_2,S+1,m-\alpha_3,n-1}O_{\alpha_1,S-1,m+\alpha_4,n+1}$$
$$\times e^{(\tau_3-\tau_2)E^{(0)}_{S+1,m-\alpha_3,n-1}}e^{(\tau_2-\tau_1)E^{(0)}_{S,m+\alpha_4-\alpha_1,n}}e^{(\tau_1-\tau_4)E^{(0)}_{S-1,m+\alpha_4,n+1}} + N_{\alpha_4,S,m,n}P_{\alpha_3,S,m,n}M_{\alpha_2,S-1,m-\alpha_3,n-1}$$
$$\times O_{\alpha_1,S-1,m+\alpha_4,n+1}e^{(\tau_3-\tau_2)E^{(0)}_{S-1,m-\alpha_3,n-1}}e^{(\tau_2-\tau_1)E^{(0)}_{S,m+\alpha_4-\alpha_1,n}}\ e^{(\tau_1-\tau_4)E^{(0)}_{S-1,m+\alpha_4,n+1}}$$
$$+ N_{\alpha_4,S,m,n}P_{\alpha_3,S,m,n}N_{\alpha_2,S-1,m-\alpha_3,n-1}P_{\alpha_1,S-1,m+\alpha_4,n+1}e^{(\tau_3-\tau_2)E^{(0)}_{S-1,m-\alpha_3,n-1}}e^{(\tau_2-\tau_1)E^{(0)}_{S-2,m+\alpha_4-\alpha_1,n}}$$
$$\times e^{(\tau_1-\tau_4)E^{(0)}_{S-1,m+\alpha_4,n+1}}\Bigg], \tag{B.3}$$

$$\left\langle \hat{a}^\dagger_{\alpha_1}(\tau_1)\hat{a}^\dagger_{\alpha_2}(\tau_2)\hat{a}_{\alpha_3}(\tau_3)\hat{a}_{\alpha_4}(\tau_4)\right\rangle^{(0)} = \frac{\delta_{\alpha_1+\alpha_2,\alpha_3+\alpha_4}}{\mathcal{Z}^{(0)}}\sum_{S,m,n} e^{-\beta E^{(0)}_{S,m,n}}e^{(\tau_1-\tau_4)E^{(0)}_{S,m,n}}\Bigg[O_{\alpha_4,S,m,n}O_{\alpha_1,S,m,n}$$
$$\times O_{\alpha_3,S+1,m-\alpha_4,n-1}O_{\alpha_2,S+1,m-\alpha_1,n-1}\,e^{(\tau_4-\tau_3)E^{(0)}_{S+1,m-\alpha_4,n-1}}e^{(\tau_3-\tau_2)E^{(0)}_{S+2,m-\alpha_2-\alpha_1,n-2}}e^{(\tau_2-\tau_1)E^{(0)}_{S+1,m-\alpha_1,n-1}}$$
$$+ O_{\alpha_4,S,m,n}P_{\alpha_3,S+1,m-\alpha_4,n-1}O_{\alpha_1,S,m,n}P_{\alpha_2,S+1,m-\alpha_1,n-1}e^{(\tau_4-\tau_3)E^{(0)}_{S+1,m-\alpha_4,n-1}}e^{(\tau_3-\tau_2)E^{(0)}_{S+2,m-\alpha_2-\alpha_1,n-2}}$$
$$\times e^{(\tau_2-\tau_1)E^{(0)}_{S+1,m-\alpha_1,n-1}} + P_{\alpha_4,S,m,n}O_{\alpha_3,S-1,m-\alpha_4,n-1}O_{\alpha_1,S,m,n}P_{\alpha_2,S+1,m-\alpha_1,n-1}e^{(\tau_4-\tau_3)E^{(0)}_{S-1,m-\alpha_4,n-1}}$$
$$\times e^{(\tau_3-\tau_2)E^{(0)}_{S,m-\alpha_2-\alpha_1,n-2}}e^{(\tau_2-\tau_1)E^{(0)}_{S+1,m-\alpha_1,n-1}} + O_{\alpha_4,S,m,n}P_{\alpha_3,S+1,m-\alpha_4,n-1}P_{\alpha_1,S,m,n}O_{\alpha_2,S-1,m-\alpha_1,n-1}$$
$$\times e^{(\tau_4-\tau_3)E^{(0)}_{S+1,m-\alpha_4,n-1}}e^{(\tau_3-\tau_2)E^{(0)}_{S,m-\alpha_2-\alpha_1,n-2}}e^{(\tau_2-\tau_1)E^{(0)}_{S-1,m-\alpha_1,n-1}} + P_{\alpha_4,S,m,n}O_{\alpha_3,S-1,m-\alpha_4,n-1}P_{\alpha_1,S,m,n}$$
$$\times O_{\alpha_2,S-1,m-\alpha_1,n-1}\,e^{(\tau_4-\tau_3)E^{(0)}_{S-1,m-\alpha_4,n-1}}e^{(\tau_3-\tau_2)E^{(0)}_{S,m-\alpha_2-\alpha_1,n-2}}\ e^{(\tau_2-\tau_1)E^{(0)}_{S-1,m-\alpha_1,n-1}} + P_{\alpha_4,S,m,n}$$
$$\times P_{\alpha_3,S-1,m-\alpha_4,n-1}P_{\alpha_1,S,m,n}P_{\alpha_2,S-1,m-\alpha_1,n-1}e^{(\tau_4-\tau_3)E^{(0)}_{S-1,m-\alpha_4,n-1}}e^{(\tau_3-\tau_2)E^{(0)}_{S-2,m-\alpha_2-\alpha_1,n-2}}$$
$$\times e^{(\tau_2-\tau_1)E^{(0)}_{S-1,m-\alpha_1,n-1}}\Bigg], \tag{B.4}$$

$$\left\langle \hat{a}^\dagger_{\alpha_1}(\tau_1)\hat{a}_{\alpha_3}(\tau_3)\hat{a}^\dagger_{\alpha_2}(\tau_2)\hat{a}_{\alpha_4}(\tau_4)\right\rangle^{(0)} = \frac{\delta_{\alpha_1+\alpha_2,\alpha_3+\alpha_4}}{\mathcal{Z}^{(0)}}\sum_{S,m,n} e^{-\beta E^{(0)}_{S,m,n}}e^{(\tau_1-\tau_4)E^{(0)}_{S,m,n}}\Bigg[O_{\alpha_4,S,m,n}O_{\alpha_1,S,m,n}$$

$$\times M_{\alpha_3,S+1,m-\alpha_1,n-1}M_{\alpha_2,S+1,m-\alpha_4,n-1}\,e^{(\tau_4-\tau_2)E^{(0)}_{S+1,m-\alpha_4,n-1}}e^{(\tau_2-\tau_3)E^{(0)}_{S+2,m-\alpha_1+\alpha_3,n}}e^{(\tau_3-\tau_1)E^{(0)}_{S+1,m-\alpha_1,n-1}}$$
$$+\,O_{\alpha_4,S,m,n}N_{\alpha_3,S+1,m-\alpha_1,n-1}O_{\alpha_1,S,m,n}N_{\alpha_2,S+1,m-\alpha_4,n-1}e^{(\tau_4-\tau_2)E^{(0)}_{S+1,m-\alpha_4,n-1}}e^{(\tau_2-\tau_3)E^{(0)}_{S,m-\alpha_1+\alpha_3,n}}$$
$$\times e^{(\tau_3-\tau_1)E^{(0)}_{S+1,m-\alpha_1,n-1}}+P_{\alpha_4,S,m,n}N_{\alpha_3,S+1,m-\alpha_1,n-1}O_{\alpha_1,S,m,n}M_{\alpha_2,S-1,m-\alpha_4,n-1}e^{(\tau_4-\tau_2)E^{(0)}_{S-1,m-\alpha_4,n-1}}$$
$$\times e^{(\tau_2-\tau_3)E^{(0)}_{S,m-\alpha_1+\alpha_3,n}}e^{(\tau_3-\tau_1)E^{(0)}_{S+1,m-\alpha_1,n-1}}+O_{\alpha_4,S,m,n}M_{\alpha_3,S-1,m-\alpha_1,n-1}P_{\alpha_1,S,m,n}N_{\alpha_2,S+1,m-\alpha_4,n-1}$$
$$\times e^{(\tau_4-\tau_2)E^{(0)}_{S+1,m-\alpha_4,n-1}}e^{(\tau_2-\tau_3)E^{(0)}_{S,m-\alpha_1+\alpha_3,n}}e^{(\tau_3-\tau_1)E^{(0)}_{S-1,m-\alpha_1,n-1}}+P_{\alpha_4,S,m,n}M_{\alpha_3,S-1,m-\alpha_1,n-1}P_{\alpha_1,S,m,n}$$
$$\times M_{\alpha_2,S-1,m-\alpha_4,n-1}e^{(\tau_4-\tau_2)E^{(0)}_{S-1,m-\alpha_4,n-1}}e^{(\tau_2-\tau_3)E^{(0)}_{S,m-\alpha_1+\alpha_3,n}}e^{(\tau_3-\tau_1)E^{(0)}_{S-1,m-\alpha_1,n-1}}+P_{\alpha_4,S,m,n}$$
$$\times N_{\alpha_3,S-1,m-\alpha_1,n-1}P_{\alpha_1,S,m,n}N_{\alpha_2,S-1,m-\alpha_4,n-1}e^{(\tau_4-\tau_2)E^{(0)}_{S-1,m-\alpha_4,n-1}}e^{(\tau_2-\tau_3)E^{(0)}_{S-2,m-\alpha_1+\alpha_3,n}}$$
$$\times e^{(\tau_3-\tau_1)E^{(0)}_{S-1,m-\alpha_1,n-1}}\Bigg], \tag{B.5}$$

$$\left\langle \hat{a}^\dagger_{\alpha_1}(\tau_1)\hat{a}_{\alpha_4}(\tau_4)\hat{a}_{\alpha_3}(\tau_3)\hat{a}^\dagger_{\alpha_2}(\tau_2)\right\rangle^{(0)}=\frac{\delta_{\alpha_1+\alpha_2,\alpha_3+\alpha_4}}{\mathcal{Z}^{(0)}}\sum_{S,m,n}e^{-\beta E^{(0)}_{S,m,n}}e^{(\tau_1-\tau_2)E^{(0)}_{S,m,n}}\Bigg[M_{\alpha_2,S,m,n}O_{\alpha_1,S,m,n}$$
$$\times M_{\alpha_4,S+1,m-\alpha_1,n-1}O_{\alpha_3,S+1,m+\alpha_2,n+1}\,e^{(\tau_2-\tau_3)E^{(0)}_{S+1,m+\alpha_2,n+1}}e^{(\tau_3-\tau_4)E^{(0)}_{S+2,m-\alpha_1+\alpha_4,n}}e^{(\tau_4-\tau_1)E^{(0)}_{S+1,m-\alpha_1,n-1}}$$
$$+\,M_{\alpha_2,S,m,n}N_{\alpha_4,S+1,m-\alpha_1,n-1}O_{\alpha_1,S,m,n}P_{\alpha_3,S+1,m+\alpha_2,n+1}e^{(\tau_2-\tau_3)E^{(0)}_{S+1,m+\alpha_2,n+1}}e^{(\tau_3-\tau_4)E^{(0)}_{S,m-\alpha_1+\alpha_4,n}}$$
$$\times e^{(\tau_4-\tau_1)E^{(0)}_{S+1,m-\alpha_1,n-1}}+N_{\alpha_2,S,m,n}N_{\alpha_4,S+1,m-\alpha_1,n-1}O_{\alpha_1,S,m,n}O_{\alpha_3,S-1,m+\alpha_2,n+1}\,e^{(\tau_2-\tau_3)E^{(0)}_{S-1,m+\alpha_2,n+1}}$$
$$\times e^{(\tau_3-\tau_4)E^{(0)}_{S,m-\alpha_1+\alpha_4,n}}e^{(\tau_4-\tau_1)E^{(0)}_{S+1,m-\alpha_1,n-1}}+M_{\alpha_2,S,m,n}M_{\alpha_4,S-1,m-\alpha_1,n-1}P_{\alpha_1,S,m,n}P_{\alpha_3,S+1,m+\alpha_2,n+1}$$
$$\times e^{(\tau_2-\tau_3)E^{(0)}_{S+1,m+\alpha_2,n+1}}e^{(\tau_3-\tau_4)E^{(0)}_{S,m-\alpha_1+\alpha_4,n}}e^{(\tau_4-\tau_1)E^{(0)}_{S-1,m-\alpha_1,n-1}}+N_{\alpha_2,S,m,n}M_{\alpha_4,S-1,m-\alpha_1,n-1}P_{\alpha_1,S,m,n}$$
$$O_{\alpha_3,S-1,m+\alpha_2,n+1}e^{(\tau_2-\tau_3)E^{(0)}_{S-1,m+\alpha_2,n+1}}e^{(\tau_3-\tau_4)E^{(0)}_{S,m-\alpha_1+\alpha_4,n}}e^{(\tau_4-\tau_1)E^{(0)}_{S-1,m-\alpha_1,n-1}}+N_{\alpha_2,S,m,n}P_{\alpha_1,S,m,n}$$
$$\times N_{\alpha_4,S-1,m-\alpha_1,n-1}P_{\alpha_3,S-1,m+\alpha_2,n+1}e^{(\tau_2-\tau_3)E^{(0)}_{S-1,m+\alpha_2,n+1}}e^{(\tau_3-\tau_4)E^{(0)}_{S-2,m-\alpha_1+\alpha_4,n}}e^{(\tau_4-\tau_1)E^{(0)}_{S-1,m-\alpha_1,n-1}}\Bigg]. \tag{B.6}$$

Following the same procedure as for the second-order expansion coefficient and using Matsubara transformation (4.79) yields the following integral of the form

$$\begin{aligned}
\mathcal{I}&=\kappa\int_0^\beta d\tau_1e^{a\tau_1}\int_0^{\tau_1}d\tau_2e^{b\tau_2}\int_0^{\tau_2}d\tau_3e^{b\tau_3}\int_0^{\tau_3}d\tau_4e^{d\tau_4}\\
&=\kappa\int_0^\beta d\tau_1e^{a\tau_1}\int_0^{\tau_1}d\tau_2e^{b\tau_2}\int_0^{\tau_2}d\tau_3e^{b\tau_3}\left[\frac{e^{d\tau_3}-1}{d}\right]\\
&=\kappa\int_0^\beta d\tau_1e^{a\tau_1}\int_0^{\tau_1}d\tau_2e^{b\tau_2}\left[\frac{e^{(c+d)\tau_2}-1}{(c+d)\,d}-\frac{e^{c\tau_2}-1}{cd}\right]\\
&=\kappa\int_0^\beta d\tau_1e^{a\tau_1}\left[\frac{e^{(b+c+d)\tau_1}-1}{(b+c+d)\,(c+d)\,d}-\frac{e^{b\tau_1}-1}{b\,(c+d)\,d}-\frac{e^{(c+b)\tau_1}-1}{(c+b)\,cd}+\frac{e^{b\tau_1}-1}{bcd}\right]\\
&=\kappa\Bigg[\frac{e^{(a+b+c+d)\beta}-1}{(a+b+c+d)\,(b+c+d)\,(c+d)\,d}-\frac{e^{a\beta}-1}{a\,(b+c+d)\,(c+d)\,d}-\frac{e^{(a+b)\beta}-1}{b\,(a+b)\,(c+d)\,d}
\end{aligned}$$

$$- \frac{e^{(a+b+c)\beta} - 1}{(a+b+c)(b+c)cd} + \frac{e^{a\beta} - 1}{ab(c+d)d} + \frac{e^{(a+b)\beta} - 1}{(a+b)bcd} - \frac{e^{a\beta} - 1}{abcd} + \frac{e^{a\beta} - 1}{a(b+c)cd} \Bigg]. \tag{B.7}$$

In the case of $a + b + c + d = 0$, we need

$$\lim_{a+b+c+d\to 0} \frac{e^{(a+b+c+d)\beta} - 1}{(a+b+c+d)(b+c+d)(c+d)d} = \frac{\beta}{(a+b+c+d)(b+c+d)(c+d)d}. \tag{B.8}$$

If $b + c = 0$, so

$$\lim_{b+c\to 0} \left(\frac{e^{a\beta} - 1}{a(b+c)cd} - \frac{e^{(a+b+c)\beta} - 1}{(a+b+c)(b+c)cd} \right) = \frac{e^{a\beta} - 1}{a^2cd} - \frac{\beta e^{a\beta}}{acd}. \tag{B.9}$$

Similarly, when $c + d \to 0$ and $a + b \to 0$, we get

$$\lim_{\substack{c+d\to 0 \\ a+b\to 0}} \left(\frac{e^{(a+b+c+d)\beta} - 1}{(a+b+c+d)(b+c+d)(c+d)d} - \frac{e^{(a+b)\beta} - 1}{b(a+b)(c+d)d} \right). \tag{B.10}$$

$$= -\frac{\beta}{b^2d} - \frac{a\beta^2}{2(b^2d)}. \tag{B.11}$$

C. Coefficients of Mean-Field Theory

In this appendix, we show the coefficients of the fourth order perturbation energy (4.123) at zero-temperature in the case of anti-ferromagnetic interaction with an odd number of atoms without Zeeman Effect

$$E_G^{(4)}(\mathbf{\Psi}) = C(n,U_0,U_2,\mu)\left||\Psi_0|^2 - 2|\Psi_1||\Psi_{-1}|\right|^2 + D(n,U_0,U_2,\mu)(\mathbf{\Psi}^\dagger\cdot\mathbf{\Psi})^2 + E(n,U_0,U_2,\mu)\left[|\Psi_1|^2 - |\Psi_{-1}|^2\right]^2 + H(n,U_0,U_2,\mu)\left[(\Psi_0^*\Psi_0)^2 + 2\left(\Psi_1^*\Psi_{-1}\right)^2\right], \tag{C.1}$$

where

$$\begin{aligned} C(n,U_0,U_2,\mu) =& \frac{1}{\left(\triangle E^{(0)}_{2,2n+2}\right)^2}\left[\frac{490+336n+56n^2}{175\triangle E^{(0)}_{3,2n+3}} - \frac{210n+84n^2}{175\triangle E^{(0)}_{3,2n+1}} - \frac{330+462n+396n^2}{225\triangle E^{(0)}_{1,2n+3}}\right] \\ & - \frac{1}{\left(\triangle E^{(0)}_{2,2n}\right)^2}\left[\frac{56n-56n^2}{175\triangle E^{(0)}_{3,2n}} + \frac{210n+84n^2}{175\triangle E^{(0)}_{3,2n+1}} + \frac{198n+132n^2}{225\triangle E^{(0)}_{0,2n-1}}\right] \\ & - 2\frac{30+42n+12n^2}{45\triangle E^{(0)}_{2,2n+2}\triangle E^{(0)}_{1,2n+3}\triangle E^{(0)}_{0,2n+2}} - 2\frac{210n+84n^2}{175\triangle E^{(0)}_{2,2n+2}\triangle E^{(0)}_{3,2n+1}\triangle E^{(0)}_{2,2n}} \\ & - 2\frac{6n+4n^2}{15\triangle E^{(0)}_{1,2n-1}\triangle E^{(0)}_{0,2n}\triangle E^{(0)}_{2,2n}}, \end{aligned} \tag{C.2}$$

$$\begin{aligned} E(n,U_0,U_2,\mu) =& -\frac{1}{\left(\triangle E^{(0)}_{2,2n+2}\right)^2}\left[-\frac{325+260n+52n^2}{225\triangle E^{(0)}_{2,2n+2}} + \frac{20+28n+8n^2}{45\triangle E^{(0)}_{0,2n+2}} - \frac{45+48n+12n^2}{45\triangle E^{(0)}_{0,2n}} \right. \\ & \left. + \frac{120n+48n^2}{225\triangle E^{(0)}_{2,2n}}\right] - \frac{1}{\left(\triangle E^{(0)}_{2,2n}\right)^2}\left[\frac{120n+48n^2}{225\triangle E^{(0)}_{2,2n+2}} - \frac{12n+12n^2}{45\triangle E^{(0)}_{0,2n+2}} - \frac{52n^2}{225\triangle E^{(0)}_{2,2n}}\right] \\ & - \frac{1}{\left(\triangle E^{(0)}_{0,2n+2}\right)^2}\left[\frac{20+28n+8n^2}{45\triangle E^{(0)}_{2,2n+2}} - \frac{12n+12n^2}{45\triangle E^{(0)}_{2,2n}}\right] \\ & - \frac{1}{\left(\triangle E^{(0)}_{0,2n}\right)^2}\left[-\frac{45+48n+12n^2}{45\triangle E^{(0)}_{2,2n+2}} + \frac{12n+8n^2}{45\triangle E^{(0)}_{2,2n}}\right], \end{aligned} \tag{C.3}$$

$$
\begin{aligned}
D(n,U_0,U_2,\mu) = &-\frac{1}{\left(\triangle E^{(0)}_{2,2n+2}\right)^2}\left[\frac{1470+1008n+168n^2}{175\triangle E^{(0)}_{3,2n+3}}+\frac{70n+28n^2}{175\triangle E^{(0)}_{3,2n+1}}+\frac{10+14n+4n^2}{225\triangle E^{(0)}_{1,2n+3}}\right.\\
&\left.-\frac{825+660n+132n^2}{225\triangle E^{(0)}_{2,2n+2}}-\frac{45+48n+12n^2}{45\triangle E^{(0)}_{0,2n}}-\frac{330n+132n^2}{225\triangle E^{(0)}_{2,2n}}-\frac{30+42n+12n^2}{45\triangle E^{(0)}_{0,2n+2}}\right]\\
&-\frac{1}{\left(\triangle E^{(0)}_{2,2n}\right)^2}\left[\frac{-168n+168n^2}{175\triangle E^{(0)}_{3,2n-1}}+\frac{70n+28n^2}{175\triangle E^{(0)}_{3,2n+1}}+\frac{6n+4n^2}{225\triangle E^{(0)}_{1,2n-1}}\right.\\
&\left.-\frac{330n+132n^2}{225\triangle E^{(0)}_{2,2n+2}}-\frac{18n+12n^2}{45\triangle E^{(0)}_{0,2n}}-\frac{132n^2}{225\triangle E^{(0)}_{2,2n}}-\frac{12n+12n^2}{45\triangle E^{(0)}_{0,2n+2}}\right]\\
&-\frac{1}{\left(\triangle E^{(0)}_{0,2n+2}\right)^2}\left[\frac{10+14n+4n^2}{9\triangle E^{(0)}_{1,2n+3}}-\frac{30+42n+12n^2}{45\triangle E^{(0)}_{2,2n+2}}-\frac{12n+12n^2}{45\triangle E^{(0)}_{2,2n}}\right]\\
&-\frac{1}{\left(\triangle E^{(0)}_{0,2n}\right)^2}\left[\frac{6n+4n^2}{9\triangle E^{(0)}_{1,2n-1}}-\frac{45+48n+12n^2}{45\triangle E^{(0)}_{2,2n+2}}-\frac{18n+12n^2}{45\triangle E^{(0)}_{2,2n}}\right]\\
&-2\frac{10+14n+4n^2}{45\triangle E^{(0)}_{2,2n+2}\triangle E^{(0)}_{1,2n+3}\triangle E^{(0)}_{0,2n+2}}-2\frac{70n+28n^2}{175\triangle E^{(0)}_{2,2n+2}\triangle E^{(0)}_{3,2n+1}\triangle E^{(0)}_{2,2n}}\\
&-2\frac{6n+4n^2}{15\triangle E^{(0)}_{1,2n-1}\triangle E^{(0)}_{0,2n}\triangle E^{(0)}_{2,2n}},
\end{aligned}
\tag{C.4}
$$

$$
\begin{aligned}
H(n,U_0,U_2,\mu) = &-\frac{1}{\left(\triangle E^{(0)}_{2,2n+2}\right)^2}\left[-\frac{25+20n+4n^2}{225\triangle E^{(0)}_{2,2n+2}}-\frac{10+14n+4n^2}{45\triangle E^{(0)}_{0,2n+2}}-\frac{15+16n+4n^2}{45\triangle E^{(0)}_{0,2n}}\right.\\
&\left.-\frac{10n+4n^2}{225\triangle E^{(0)}_{2,2n}}\right]-\frac{1}{\left(\triangle E^{(0)}_{0,2n+2}\right)^2}\left[-\frac{10+14n+4n^2}{225\triangle E^{(0)}_{2,2n+2}}-\frac{6+10n+4n^2}{9\triangle E^{(0)}_{0,2n}}\right.\\
&\left.-\frac{4n+4n^2}{45\triangle E^{(0)}_{2,2n}}-\frac{4+8n+4n^2}{9\triangle E^{(0)}_{0,2n+2}}\right]-\frac{1}{\left(\triangle E^{(0)}_{2,2n}\right)^2}\left[\frac{10n+4n^2}{225\triangle E^{(0)}_{2,2n+2}}-\frac{4n+4n^2}{45\triangle E^{(0)}_{0,2n+2}}\right.\\
&\left.-\frac{4n^2}{225\triangle E^{(0)}_{2,2n}}-\frac{6n+4n^2}{45\triangle E^{(0)}_{0,2n}}\right]-\frac{1}{\left(\triangle E^{(0)}_{0,2n}\right)^2}\left[\frac{15+16n+4n^2}{45\triangle E^{(0)}_{2,2n+2}}-\frac{6+10n+4n^2}{9\triangle E^{(0)}_{0,2n+2}}\right.\\
&\left.-\frac{9+12n+4n^2}{9\triangle E^{(0)}_{0,2n}}-\frac{6n+4n^2}{45\triangle E^{(0)}_{2,2n}}\right].
\end{aligned}
\tag{C.5}
$$

where $\triangle E^{(0)}_{S',n'} = E^{(0)}_{S',n'} - E^{(0)}_{1,n}$

Bibliography

[1] A. Einstein, Sitzber. Kgl. Preuss. Akad. Wiss., page 3 (1925).

[2] S. N. Bose, Planck's law and light quantum hypothesis, *Z. Phys.* **26**, 178 (1924).

[3] W. Ketterle, D. S. Durfee, and D. M. Stamper-Kurn, *Making, probing and understanding Bose-Einstein condensates.* In *Bose-Einstein Condensation in Atomic Gases*, Proceedings of the International School of Physics "Enrico Fermi", Course CXL (ed. M. Inguscio, S. Stringari, and C. E. Wieman), p. 67, IOS Press, Amsterdam (1999).

[4] P. L. Kapitza, Viscosity of liquid helium below the lambda-point, *Nature* **141**, 74 (1938).

[5] J. F. Allen and A. D. Miesner, Flow of liquid helium II, *Nature* **141**, 75 (1938).

[6] F. London, The phenomenon of liquid helium and the Bose-Einstein degeneracy, *Nature* **141**, 643 (1938).

[7] L. Tisza, Transport phenomena in helium II, *Nature* **141**, 913 (1938).

[8] L. D. Landau, The theory of superfluidity of helium II, *J. Phys. USSR* **5**, 71 (1941).

[9] N. N. Bogoliubov, On the theory of superfluidity, *J. Phys. USSR* **11**, 23 (1947).

[10] O. Penrose and L. Onsager, Bose-Einstein condensation and liquid helium*, Phys. Rev.* **104**, 576 (1956).

[11] E. P. Gross, Structure of a quantized vortex in boson systems, *Nuovo Cimento* **20**, 454 (1961).

[12] L. P. Pitaevskii, Vortex lines in an imperfect Bose gas*, Zh. Eksp. Teor. Fiz.* **40**, 646 (1961).

[13] K. B. Davis, M.-O. Mewes, M. R. Andrews, N. J. van Druten, D. S. Durfee, D. M. Kurn, and W. Ketterle, Bose-Einstein condensation in a gas of sodium atoms, *Phys. Rev. Lett.* **75**, 3969 (1995).

[14] T. Hänsch and A. Schawlow, Cooling of gases by laser radiation, *Opt. Comm.* **13**, 68 (1975).

[15] O. J. Luiten, M. W. Reynolds, and J. T. M. Walraven, Kinetic theory of the evaporative cooling of a trapped gas, *Phys. Rev. A* **53**, 381 (1996).

[16] D. G. Fried, T. C. Killian, L. Willmann, D. Landhuis, S. C. Moss, D. Kleppner, and T. J. Greytak, Bose-Einstein condensation of atomic hydrogen, *Phys. Rev. Lett.* **81**, 3811 (1998).

[17] C. C. Bradley, C. A. Sackett, and R. G. Hulet, Bose-Einstein condensation of lithium: observation of limited condensate number, *Phys. Rev. Lett.* **78**, 985 (1997).

[18] G. Modugno, G. Ferrari, G. Roati, R. J. Brecha, A. Simoni, and M. Inguscio, Bose-Einstein condensation of potassium atoms by sympathetic cooling, *Science* **294**, 1320 (2001).

[19] S. L. Cornish, N. R. Claussen, J. L. Roberts, E. A. Cornell, and C. E. Wieman, Stable ^{85}Rb Bose-Einstein condensates with widely tunable interactions, *Phys. Rev. Lett.* **85**, 1795 (2000).

[20] M. H. Anderson, J. R. Ensher, M. R. Matthews, C. E. Wieman, and E. A. Cornell, Observation of Bose-Einstein condensation in a dilute atomic vapor, *Science* **269**, 198 (1995).

[21] T. Weber, J. Herbig, M. Mark, H.-C. Nägerl, and R. Grimm, Bose-Einstein condensation of cesium, *Science* **299**, 232 (2003).

[22] Y. Takasu, K. Maki, K. Komori, T. Takano, K. Honda, M. Kumakura, T. Yabuzaki, and Y. Takahashi, Spin-singlet Bose-Einstein condensation of two-electron atoms, *Phys. Rev. Lett.* **91**, 040404 (2003).

[23] S. Kraft, F. Vogt, O. Appel, F. Riehle, and U. Sterr, Bose-Einstein condensation of alkaline earth atoms: ^{40}Ca, *Phys. Rev. Lett.* **103**, 120401 (2009).

[24] S. Stellmer, M. K. Tey, B. Huang, R. Grimm, and F. Schreck, Bose-Einstein condensation of strontium, *Phys. Rev. Lett.* **103**, 200401 (2009).

[25] Y. N. Martinez de Escobar, P. G. Mickelson, M. Yan, B. J. DeSalvo, S. B. Nagel, and T. C. Killian, Bose-Einstein condensation of ^{84}Sr. *Phys. Rev. Lett.* **103**, 200402 (2009).

[26] A. Robert, O. Sirjean, A. Browaeys, J. Poupard, S. Nowak, D. Boiron, C. I. Westbrook, and A. Aspect, A Bose-Einstein condensate of metastable atoms, *Science* **292**, 461 (2001).

[27] F. P. Dos Santos, J. Leonard, J. Wang, C. J. Barrelet, F. Perales, E. Rasel, C. S. Unnikrishnan, M. Leduc, and C. Cohen-Tannoudji, Bose-Einstein condensation of metastable helium, *Phys. Rev. Lett.* **86**, 3459 (2001).

[28] A. Griesmaier, J. Werner, S. Hensler, J. Stuhler, and T. Pfau, Bose-Einstein condensation of chromium, *Phys. Rev. Lett.* **94**, 160401 (2005).

[29] K. Aikawa, A. Frisch, M. Mark, S. Baier, A. Rietzler, R. Grimm, and F. Ferlaino, Bose-Einstein condensation of erbium, *Phys. Rev. Lett.* **108**, 210401 (2012).

[30] M. Lu, N. Q. Burdick, S. H. Youn, and B. L. Lev, Strongly dipolar Bose-Einstein condensate of dysprosium, *Phys. Rev. Lett.* **107**, 190401 (2011).

[31] M. Lewenstein, A. Sanpera, and V. Ahufinger, *Ultracold Atoms in Optical Lattices, Simulating Quantum Many-Body Systems*, Oxford University Press (2012).

[32] T.-L. Ho, Spinor Bose condensates in optical traps, Phys. *Rev. Lett.* **81**, 742 (1998).

[33] T. Ohmi and K. Machida, Bose-Einstein condensation with internal degrees of freedom in alkali atom gases, *J. Phys. Soc. Jpn.* **67**, 1822 (1998).

[34] J. Stenger, S. Inouye, D. M. Stamper-Kurn, H.-J. Miesner, A. P. Chikkatur, and W. Ketterle, Spin domains in ground state spinor Bose-Einstein condensates, *Nature* **396**, 345 (1999).

[35] D. M. Stamper-Kurn, M. R. Andrews, A. P. Chikkatur, S. Inouye, H. J. Miesner, J. Stenger, and W. Ketterle, Optical confinement of a Bose-Einstein condensate, *Phys. Rev. Lett.* **80**, 2027 (1998).

[36] R. Grimm, M. Weidemüuller, and Y. B. Ovchinnikov, Optical dipole trap for neutral atoms, *Adv. At. Mol. Opt. Phys.* **42**, 95 (2000).

[37] M.-S. Chang, C. D. Hamley, M. D. Barrett, J. A. Sauer, K. M. Fortier, W. Zhang, L. You, and M. S. Chapman, Observation of spinor dynamics in optically trapped ^{87}Rb Bose-Einstein condensates, *Phys. Rev. Lett.* **92**, 140403 (2004).

[38] H. Schmaljohann, M. Erhard, J. Kronjäger, M. Kottke, S. van Staa, L. Cacciapuoti, J. J. Arlt, K. Bongs, and K. Sengstock, Dynamics of $F = 2$ spinor Bose-Einstein condensates, *Phys. Rev. Lett.* **92**, 040402 (2004).

[39] T. Kuwamoto, K. Araki, T. Eno, and T. Hirano, Magnetic field dependence of the dynamics of ^{87}Rb spin-2 Bose-Einstein condensates, *Phys. Rev. A* **69**, 063604 (2004).

[40] Y. Kawaguchia and M. Ueda, Spinor Bose–Einstein condensates, *Phys. Rep.* **520**, 253 (2012).

[41] J. M. McGuirk, H. J. Lewandowski, D. M. Harber, T. Nikuni, J. E. Williams, and E. A. Cornell, Spatial resolution of spin waves in an ultracold gas, *Phys. Rev. Lett.* **89**, 090402 (2002).

[42] Q. Gu, K. Bongs, and K. Sengstock, Spin waves in ferromagnetically coupled spinor Bose gases, *Phys. Rev. A* **70**, 063609 (2004).

[43] C. K. Law, H. Pu, and N. P. Bigelow, Quantum spins mixing in spinor Bose-Einstein condensates, *Phys. Rev. Lett.* **81**, 5257 (1998).

[44] H. Pu, C. K. Law, S. Raghavan, J. H. Eberly, and N. P. Bigelow, Spin-mixing dynamics of a spinor Bose-Einstein condensate, *Phys. Rev. A* **60**, 1463 (1999).

[45] P. L. Gould, G. A. Ruff, and D. E. Pritchard, Diffraction of atoms by light: The near-resonant Kapitza-Dirac effect, *Phys. Rev. Lett.* **56**, 827 (1986).

[46] P. J. Martin, B. G. Oldaker, A. H. Miklich, and D. E. Pritchard, Bragg scattering of atoms from a standing light wave, *Phys. Rev. Lett.* **60**, 515 (1988).

[47] A. Hemmerich and T. W. Hänsch, Two-dimensional atomic crystal bound by light, *Phys. Rev. Lett.* **70**, 410 (1993).

[48] A. Hemmerich, M. Weidemüller, T. Esslinger, C. Zimmermann, and T. W. Hänsch, Trapping atoms in a dark optical lattice, *Phys. Rev. Lett.* **75**, 37 (1995).

[49] M. Weidemüller, A. Hemmerich, A. Görlitz, T. Esslinger, and T. W. Hänsch, Bragg diffraction in an atomic lattice bound by light, *Phys. Rev. Lett.* **75**, 4583 (1995).

[50] G. Grynberg, B. Lounis, P. Verkerk, J. Y. Courtois, and C. Salomon, Quantized motion of cold cesium atoms in two- and three-dimensional optical potentials, *Phys. Rev. Lett.* **70**, 2249 (1993).

[51] Q. Niu, X. G. Zhao, G. A. Georgakis, and M. G. Raizen, Atomic Landau-Zener tunneling and Wannier-Stark ladders in optical potentials, *Phys. Rev. Lett.* **76**, 4504 (1996).

[52] B. M. Dahan, E. Peik, J. Reichel, Y. Castin, and C. Salomon, Bloch oscillations of atoms in an optical potential, *Phys. Rev. Lett.* **76**, 4508 (1996).

[53] B. Anderson and M. Kasevich, Macroscopic quantum interference from atomic tunnel arrays, *Science* **282**, 1686 (1998).

[54] F. S. Cataliotti, S. Burger, C. Fort, P. Maddaloni, F. Minardi, A. Trombettoni, A. Smerzi and M. Inguscio, Josephson junction arrays with Bose-Einstein condensates, *Science* **293**, 843 (2001).

[55] I. Bloch, Ultracold quantum gases in optical lattices, *Nature Phys.* **1**, 23 (2005).

[56] H. Feshbach, A unified theory of nuclear reactions II, *Ann. Phys. (New York)* **19**, 287 (1962).

[57] D. Jaksch, C. Bruder, J. I. Cirac, C. W. Gardiner, and P. Zoller, Cold bosonic atoms in optical lattices, Phys. *Rev. Lett.* **81**, 3108 (1998).

[58] W. Krauth, M. Caffarel, and J.-P. Bouchaud, Gutzwiller wave function for a model of strongly interacting bosons, *Phys. Rev. B* **45**, 3137 (1992).

[59] K. Sheshadri, H. R. Krishnamurthy, R. Pandit, and T. V. Ramakrishnan, Superfluid and insulating phases in an interacting-Boson Model: mean-field theory and the RPA, *Europhys. Lett.* **22**, 257 (1993).

[60] D. van Oosten, P. van der Straten, and H. T. C. Stoof, Quantum phases in an optical lattice, *Phys. Rev. A* **63**, 053601 (2001).

[61] G. G. Batrouni, R. T. Scalettar, and G. T. Zimanyi, Quantum critical phenomena in one-dimensional Bose systems, *Phys. Rev. Lett.* **65**, 1765 (1990).

[62] R. T. Scalettar, G. G. Batrouni, and G. T. Zimanyi, Localization in interacting, disordered, Bose systems, *Phys. Rev. Lett.* **66**, 3144 (1991).

[63] P. Niyaz, R. T. Scalettar, and C. Y. Fong, Ground-state phase diagram of an interacting Bose model with near-neighbor repulsion, *Phys. Rev. B* **44**, 7143 (1991).

[64] G. G. Batrouni, V. Rousseau, R. T. Scalettar, M. Rigol, A. Muramatsu, P. J. H. Denteneer, and M. Troyer, Mott domains of bosons confined on optical lattices, *Phys. Rev. Lett.* **89**, 117203 (2002).

[65] M. P. A. Fisher, P. B. Weichman, G. Grinstein, and D. S. Fisher, Boson localization and the superfluid-insulator transition, *Phys. Rev. B* **40**, 546 (1989).

[66] M. Greiner, O. Mandel, T. Esslinger, T. W. Hänsch, and I. Bloch, Quantum phase transition from a superfluid to a Mott insulator in a gas of ultracold atoms, *Nature* **415**, 39 (2002).

[67] T. Wang, X.-F. Zhang, S. Eggert, and A. Pelster, Generalized effective-potential Landau theory for bosonic quadratic superlattices, *Phys. Rev. A* **87**, 063615 (2013).

[68] G. Modugno, F. Ferlaino, R. Heidemann, G. Roati, M. Inguscio, Production of a Fermi gas of atoms in an optical lattice, *Phys. Rev. A* **68**, 011601(R) (2003).

[69] A. Albus, F. Illuminati, and J. Eisert, Mixtures of bosonic and fermionic atoms in optical lattices, *Phys. Rev. A* **68**, 023606 (2003).

[70] H. P. Büchler, and G. Blatter, Supersolid versus phase separation in atomic Bose-Fermi mixtures, *Phys. Rev. Lett.* **91**, 130404 (2003).

[71] M. Lewenstein, L. Santos, M. A. Baranov, and H. Fehrmann, Atomic Bose-Fermi mixtures in an optical lattice, *Phys. Rev. Lett.* **92**, 050401 (2004).

[72] I. Bloch, Quantum coherence and entanglement with ultracold atoms in optical lattices, *Nature* **453**, 1016 (2008).

[73] M. Lewenstein, A. Sanpera, and V. Ahufinger, *Ultracold Atoms in Optical Lattices, Simulating Quantum Many-Body Systems*, Oxford University Press (2012).

[74] K.V. Krutitsky, A. Pelster, and R. Graham, Mean-field phase diagram of disordered bosons in a lattice at nonzero temperature, *New J. Phys.* **8**, 187 (2006).

[75] G. Roati, C. D'Errico, L. Fallani, M. Fattori, C. Fort, M. Zaccanti, G. Modugno, M. Modugno, and M. Inguscio, Anderson localization of a non-interacting Bose–Einstein condensate, *Nature* **453**, 895 (2008).

[76] M. Barrett, J. Sauer, and M. S. Chapman, All-Optical Formation of an Atomic Bose-Einstein Condensate, *Phys. Rev. Lett.* **87**, 010404 (2001).

[77] A. Widera, F. Gerbier, S. Fölling, T. Gericke, O. Mandel, and I. Bloch, Coherent collisional spin dynamics in optical lattices , *Phys. Rev. Lett.* **95**, 190405 (2005).

[78] A. Widera, F. Gerbier, S. Fölling, T. Gericke, O. Mandel, and I. Bloch, Precision measurement of spin-dependent interaction strengths for spin-1 and spin-2 ^{87}Rb atoms, *New J. Phys.* **8**, 152 (2006).

[79] C. Becker, P. Soltan-Panahi, J. Kronjäger, S. Dörscher, K. Bongs, and K. Sengstock, Ultracold quantum gases in triangular optical lattices , *New J. Phys.* **12**, 065025 (2010).

[80] E. Demler and F. Zhou, Spinor bosonic atoms in optical lattices: Symmetry breaking and fractionalization, *Phys. Rev. Lett.* **88**, 163001 (2002).

[81] S. Tsuchiya, S. Kurihara, and T. Kimura, Superfluid–Mott insulator transition of spin-1 bosons in an optical lattice, *Phys. Rev. A.* **70**, 043628 (2004).

[82] N. Uesugi, and M. Wadati, Superfluid–Mott insulator transition of spinor gases with external magnetic fields, *J. Phys. Soc. Japan* **72**, 1041 (2003).

[83] A. A. Svidzinsky and S. T. Chui, Insulator-superfluid transition of spin-1 bosons in an optical lattice in magnetic field, *Phys. Rev. A* **68**, 043612 (2003).

[84] M. Mobarak and A. Pelster, Superfluid phases of spin-1 bosons in cubic optical lattice, *Laser Phys. Lett.* **10**, 115501 (2013).

[85] M. Mobarak and A. Pelster, Tuning superfluid phases of spin-1 bosons in cubic optical lattice with linear Zeeman effect, `arXiv:1310.0600`.

[86] B. Bradlyn, F. E. A. dos Santos, and A. Pelster, Effective action approach for quantum phase transitions in bosonic lattices, *Phys. Rev. A* **79**, 013615 (2009).

[87] F. E. A. dos Santos and A. Pelster, Quantum phase diagram of bosons in optical lattices, *Phys. Rev. A* **79**, 013614 (2009).

[88] F. Dalfovo, S. Giorgini, L. P. Pitaevskii, and S. Stringari, Theory of Bose-Einstein condensation in trapped gases, *Rev. Mod. Phys.* **71**, 463 (1999).

[89] K. Huang and C. N. Yang, Quantum-mechanical many-body problem with hard sphere interaction, *Phys. Rev.* **105**, 767 (1957).

[90] K. Huang, *Statistical Mechanics*, Second Edition, John Wiley & Sons, New York (1987).

[91] M. S. Chang, *Coherent Spin Dynamics of a Spin-1 Bose-Einstein Condensate*, PhD thesis, Georgia University (2006).

[92] C. J. Pethick and H. Smith, *Bose-Einstein Condensation in Dilute Gases,* Cambridge University Press, Cambridge, 2nd edition (2008).

[93] T.-L. Ho and S. K. Yip, Fragmented and single condensate ground states of spin-1 Bose gas, *Phys. Rev. Lett.* **84**, 4031 (2000).

[94] M. Snoek and F. Zhou, Microscopic wave functions of spin-singlet and nematic Mott states of spin-one bosons in high-dimensional bipartite lattices, *Phys. Rev. B* **69**, 09441 (2004).

[95] A. Imambekov, M. Lukin, and E. Demler, Spin-exchange interactions of spin-one bosons in optical lattices: Singlet, nematic, and dimerized phases, *Phys. Rev. A* **68**, 063602 (2003).

[96] J. P. Burke, C. H. Greene, and J. L. Bohn, Multichannel cold collisions: Simple dependences on energy and magnetic field, *Phys. Rev. Lett.* **81**, 3355 (1998).

[97] P. B. Blakie and C. W. Clark, Wannier states and Bose-Hubbard parameters for 2D optical lattices, *J. Phys. B* **37**, 1391 (2004).

[98] F. Schwabl, *Statistical Mechanics*, Springer, 3rd Edition (2002).

[99] P. Soltan-Panahi, *Spinor Bose-Einstein Condensation*, Diploma thesis, Freie Universität Berlin (2006).

[100] T. Kimura, S. Tsuchiya, and S. Kurihara, Possibility of a first-order superfluid-Mott insulator transition of spinor Bosons in an optical lattice, *Phys. Rev. Lett.* **94**, 110403 (2005).

[101] T. Kimura, S. Tsuchiya, M. Yamashita, and S. Kurihara, Superfluid–Mott insulator transition of spin-1 bosons in optical lattice under magnetic field, *J. Phys. Soc. Japan* **75**, 074601 (2006).

[102] M. Łącki, S. Paganelli, V. Ahufinger, A. Sanpera, and J. Zakrzewski, Disordered spinor Bose-Hubbard model, *Phys. Rev. A* **83**, 013605 (2011).

[103] S. Paganelli, M. Łącki, V. Ahufinger, J. Zakrzewski, and A. Sanpera, Spin effect in Bose-Glass phases, *J. Low Temp. Phys.* **165**, 227 (2011).

[104] M. Ohliger, *Thermodynamic Properties of Spinor Bosons in Optical Lattices*, Diploma thesis, Freie Universität Berlin (2008).

[105] L. E. Reichl, *A Modern Course in Statistical Physics*, John Wiley & Sons, Inc (1998).

[106] S. Sachdev, *Quantum Phase Transitions*, Cambridge University Press, 2nd edition (2001).

[107] A. Rapp, *Quantum Phase Transitions in Correlated Systems*, PhD. thesis, Budapest University of Technology and Economics (2008).

[108] W. S. Bakr, *Microscopic Studies of Quantum Phase Transitions in Optical Lattices*, PhD thesis, Harvard University Cambridge, Massachusetts (2011).

[109] L. D. Landau and E. M. Lifshitz, *Statistical Physics Part I*, Pergamon Press (1980).

[110] E. M. Lifshitz and L. P. Pitaevskii, *Statistical Physics Part II*, Pergamon Press (1980).

[111] B. Capogrosso-Sansone, N. Prokofev, and B. Svistunov, Phase diagram and thermodynamics of the three-dimensional Bose-Hubbard model, *Phys. Rev. B* **75**, 134302 (2007).

[112] J. K. Freericks and H. Monien, Strong-Coupling expansions for the pure and disordered Bose-Hubbard model, Phys. Rev. *B* **53**, 2691 (1996).

[113] D. Hinrichs, *Critical Properties of the Bose-Hubbard Model*, PhD thesis, Carl von Ossietzky Universität Oldenburg (2012).

[114] D. Hinrichs, A. Pelster, and M. Holthaus, Perturbative calculation of critical exponents for the Bose-Hubbard model, *Appl. Phys. B* **113**, 57 (2013).

[115] G. G. Batrouni, V. G. Rousseau, and R. T. Scalettar, Magnetic and superfluid transition in the one-dimensional spin-1 boson Hubbard model, *Phys. Rev. Lett.* **102**, 140402 (2009).

[116] C. J. Gorter and H. G. B. Casimir, Thermodynamics to superconducting state, *Z. Tech. Phys.* **15**, 539 (1934).

[117] J. Zinn-Justin, *Quantum Field Theory and Critical Phenomena*, Fourth Edition, Oxford University Press (2002).

[118] L. P. Kadanoff, and G. Baym, *Quantum Statistical Mechanics: Green's Function Methods in Equilibrium and Non-Equilibrium Problems*, W. A. Benjamin, New York(1962).

[119] C. J. Gorter and H. G. B. Casimir, On superconductivity, *Phys. Z.* **35**, 963 (1934).

[120] W. Metzner, Linked-cluster expansion around the atomic limit of the hubbard-model, *Phys. Rev. B* **43**, 8549 (1991).

[121] H. Kleinert, and V. Schulte-Frohlinde, *Critical Properties of* Φ^4*- Theories*, World Scientific, Singapore (2001).

[122] J. W. Negele and H. Orland, *Quantum many-particle systems,* Westview Press (1998).

[123] C. Nietner, *Quantum Phase Transition of Light in the Jaynes-Cummings Lattices*, Diploma thesis, Freie Universität Berlin (2010).

[124] T. D. Graß, *Real-Time Ginzburg-Landau Theory for Bosonic Gases in Optical Lattice*, Diploma thesis, Freie Universität Berlin (2009).

[125] W. X. Zhang, S. Yi, and L. You, Mean-field ground state of a spin-1 condensate in a magnetic field, *New J. Phys.* **5**, 77 (2003).

[126] T. D. Graß, F. E. A. dos Santos, and A. Pelster, Excitation spectra of bosons in optical lattices from the Schwinger-Keldysh calculation, *Phys. Rev. A* **8**4, 013613 (2011).

[127] P. T. Ernst, S. Götze, J. S. Krauser, K. Pyka, D.-S. Lühmann, D. Pfannkuche, and K. Sengstock, Probing superfluids in optical lattices by momentum-resolved Bragg spectroscopy, *Nature Phys.* **6**, 56 (2010).

[128] U. Bissbort, S. Götze, Y. Li, J. Heinze, J. S. Krauser, M. Weinberg, C. Becker, K. Sengstock, and W. Hofstetter, Detecting the Amplitude Mode of Strongly Interacting Lattice Bosons by Bragg Scattering, *Phys. Rev. Lett.* **106**, 205303 (2011).

[129] M. Endres, T. Fukuhara, D. Pekker, M. Cheneau, P. Schauß, C. Gross, E. Demler, S. Kuhr, and I. Bloch, The 'Higgs' amplitude mode at the two-dimensional superfluid/Mott insulator transition, *Nature* **487**, 454 (2012).

[130] A. Wagner, C. Bruder, and E. Demler, Spin-1 atoms in optical superlattices: single-atom tunneling and entanglement, *Phys. Rev. A* **84**, 063636 (2011).

[131] A. Wagner, A. Nunnenkamp, and C. Bruder, Mean-field analysis of spinor bosons in optical superlattices, *Phys. Rev. A* **86**, 023624 (2012).

[132] L. Santos, M. Fattori, J. Stuhler, and T. Pfau, Spinor condensates with a laser-induced quadratic Zeeman effect, *Phys. Rev. A* **75**, 053606 (2007).

[133] N. T. Phuc, Y. Kawaguchi, and M. Ueda, Effects of thermal and quantum fluctuations on the phase diagram of a spin-1 ^{87}Rb Bose-Einstein condensate, *Phys. Rev. A* **84**, 043645 (2011).

[134] A. Griesmaier, J. Werner, S. Hensler, J. Stuhler, and T. Pfau, Bose-Einstein condensation of Chromium, *Phys. Rev. Lett.* **94**, 160401 (2005).

[135] T.-L. Ho and S. K. Yip, Fragmented and single condensate ground states of spin-1 Bose gas, *Phys. Rev. Lett.* **84**, 4031 (2000).

List of Publications

1. M. Mobarak and A. Pelster: *Superfluid phases of spin-1 bosons in cubic optical lattice;* Laser Phys. Lett. **10**, 115501 (2013).

2. M. Mobarak and A. Pelster: *Tuning superfluid phases of spin-1 bosons in cubic optical lattice with linear Zeeman effect*; arXiv:1310.0600.

Acknowledgement

First and foremost, I am grateful to **God** for completing this thesis, which is the result of four years of research work at the institute of theoretical physics of the free university of Berlin.

I would like to express my sincere gratitude to the head of our group, Prof. Dr. Dr. h.c. mult. Hagen Kleinert, for allowing me to prepare my thesis under his supervision and within his research group that covers different topics of physics. His scientific insights have led to so many moments of enlightenment. His almost inexhaustible knowledge coupled with motivating discussion appetite has significantly contributed to the success of this dissertation.

Special thanks also goes to my supervisor during my research years, Priv-Doz. Dr. Axel Pelster, for his continuous support, guidance, cooperation, encouragement and for facilitating all the needed requirements. He integrated me into the work group and introduced me into this subject. Furthermore, from him I learned innumerable mathematical tricks being extremely valuable for solving many physical problems. His diligence, comments and thirst for knowledge have enriched me and the discussions with him have always been very instructive. Also I am deeply indebted to him for his occasional directional corrections and constructive criticism in the preparation of this script.

I would like to acknowledge the financial support from the Egyptian Government. A special thanks to my colleagues at the free university of Berlin, Mathias Ohliger, Christian Nietner, Antun Balaz, Jürgen Dietel, Aristeu Lima, Victor Bezerra, Ednilson Santos, Tobias Graß, Hamid Al-Jibbouri, Mahmoud Ghabour, Tama Khelil, Christine Gruber, Javed Akram, Mathias Hayn, Falk Wächtler, Mathias May, Marek Schiffer, Tobias Rexin, Nathalie Pfitzinger, and Branko Nikolic.

My sincere thanks goes to my parents for their endless love, unconditional support, and encouragement, which have always been my strength. In particular, their patience and sacrifice will remain my inspiration, which is sufficient to overcome the challenges of life. Unfortunately, my father passed away. I would like also to express my sincere gratitude to my aunt Nawal, who is not only an aunt but also a close friend, for her continous encouragement and support over the years.

I would like to thank my lovely wife, who inspired me, for her support, encouragement, quiet patience and unwavering love during the past twelve years of my life. She was always helping me and stood by my side during difficult times. In addition, my heartfelt thanks to my wife's mother for her kindness and moral support. My heartfelt regards goes to my children, Omar and Salma, for giving me happiness through my studies.

Finally, and most importantly, I dedicate this thesis to my father's soul. *I miss you*!